V. P. Mestcheryakov

Explosive erosion of high-current contacts and electrodes

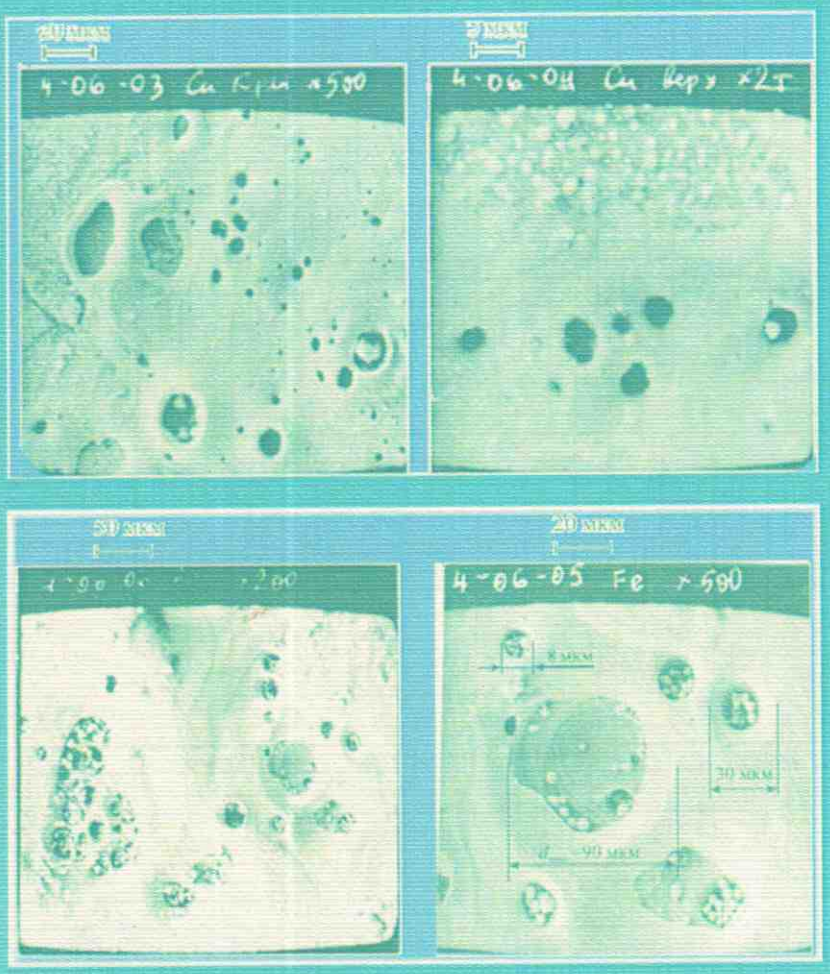

Ulyanovsk 2012

V.P. Mestcheryakov

Explosive erosion

of high-current contacts and electrodes

Translated from Russian by S.A. Akachev

Ulyanovsk

2012

Mestcheryakov V.P.

Explosive erosion of high-current contacts and electrodes. Ulyanovsk: 2012. – 189 p.

The results of experimental and theoretical researches of erosion of opening contacts and deion plates of arc chamber at interrupting of short-circuit currents by low-voltage automatic breakers are stated in the book.

The book is intended for high readership and foremost for engineers concerned with practical studies of designs of the breakers, their tests and researches.

Revised and enlarged edition.

List of contents

The preface

Brought to attention of the reader the book is actually a book continuation «Electric arc of the high power in circuit breakers», published in two parts by Joint Stock Company "Kontaktor" (Ulyanovsk) in 2006 and 2008. In the present work physical processes on opening argentiferous composite contacts at switching-off of short-circuit currents by low-voltage circuit breakers are considered in more details. In the book «Electric arc of the high power in circuit breakers» in practical engineering calculations of erosion of contacts the power density q_{bs}, coming on cathodic and anode spots of arc, was taken to be equal. Therefore the cathode and the anode by such calculation methods were exposed to erosion equally. The total mass of contacts erosion composed the sum of masses of erosion of the cathode and the anode.

In the present work the differentiated estimation of erosion of the cathode and the anode is accepted at switching-off of short-circuit currents. As a result of the differentiated approach to an estimation of erosion of the cathode and the anode with use of experimental data a number of the new physical phenomena on base spots of low-voltage arc of high power was been revealed. As an example on base spots of arc with a discrete core we will make mention of formation of microplasmoids in which currents of ectons proceed.

The author expresses deep gratitude and sincere gratitude for translation of the present book to Stanislav Akachev.

V.P. Mestcheryakov
2012

Introduction

It was more than 200 years to the day since discovery of luminous electric arc discharge by V.V. Petrov in 1802. Electric arc discharges play an important role in human life and founded wide application in the welding technics and metal arc cutting, electrometallurgy, electrospark processing of metals, light engineering, electric current transformation.

Characteristics of arc discharges change in very wide limits. So, for example, values of a current intensity are changed from several amperes to hundreds of kiloamperes and voltage - from a dozen of volts to hundreds of kilovolts. Arc discharges represent complicated electro- and thermophysical the phenomena in which non-stationary and non-quilibrium thermodynamic processes proceed. Investigations of arc discharges are interfaced to great experimental and theoretical difficulties. Therefore, investigation of all variety of forms of arc discharges is not possible organizational and economically. Thereby investigations are conducted in concrete directions.

Despite intensive domestic and foreign investigations of arc discharges our knowledge appears insufficient and, sometimes, doubtful and inconsistent.

Results of investigations of arc discharges have great value in the electrical engineering. Almost all produced electric energy is consumed in power equipment and used for management of technological processes. Here it is necessary to specify energy production, metalcutting, mining and consumer good industries, transport, metallurgy, agriculture, research installations, a military technology and household devices. Distribution of electric energy and management of technological processes are carried out by high-voltage, low-voltage and vacuum circuit breakers. At switching-off of electric circuit electric arc on contacts of breakers arise. At that it is necessary to extinguish electric arc effectively.

At switching-off of electric circuit on contacts of switches an electric arc is drawn which must be extinguished effectively. Importance of investigations of processes of extinguishing of arc in circuit breakers (for example, at low voltage ($\leq$1000V)) is underlined by that 75 % of all produced electric energy are consumed at low voltage. Various types of devices are intended for work at certain modes. In particular, automatic circuit breakers carry out distribution of energy and protection of electric circuits and installations from abnormal overload currents and short-circuit currents.

It is widely known that short-circuit currents as a result of large mechanical forces arising between current conductors and thermal influences of arc lead to destruction of expensive equipment and quite often to fires and human victims.

For maintenance of required operating modes of control switches for electric drives and automatic circuit breakers it is necessary to create designs of their contact systems and arc chambers such as they could extinguish arc effectively.

Also it is necessary to provide long operational service life of circuit breakers which can be reached only at rather low electric wear of contacts and arc chambers.

The book [1.1] which is intended for engineers-designers provides a number of the recommendations which allow designing contact systems and arc chutes of optimum designs.

Brought to attention of the reader this work is continuation of experimental and theoretical investigations of arc of high power in the low-voltage circuit breakers stated in [1.1]. The basic attention in work will be given electric erosion of a cathode and an anode on argentiferous contacts and steel deion plates of arc chute under influence of electric arc at switching-off of short-circuit currents.

Chapter 1
Initiation of arc discharge at switching-off of short-circuit currents

An arc discharge is one of kinds of the electric discharges burning in the gas environment. Atmospheric air under normal conditions represents good enough insulator. At the temperature exceeding 6000 K, atoms of oxygen and nitrogen, making up air, as a result of intensive chaotic thermal movement mutually face, lose negatively charged electrons and form positively charged ions. If to put external electric field to volume of thermally ionised gas then electrons and ions will get the directed movement which it is accepted to name electric current.

Steams of metals have the same properties, as usual gases. However, their ionisation occurs at smaller values of temperature than gases. For example, ionisation of steams Ag and Cu begins at temperature 4000 K practically.

There are minimum values of current intensity and voltage at which arc discharge is formed. For example, on electrodes made from Ag at voltage 25 V arc strikes at current intensity equal 1,7 A.

Current density j in ionised steams of metals and gases characterizes transfer of charges quantitatively and can be defined from the formula:

$$j = 3{,}34 \cdot 10^{-10} \cdot e \cdot (n_e \cdot \nu_e + n_i \cdot \nu_i) A/cm^2,$$

where $e = 4{,}8 \cdot 10^{-10}$ – electron charge, CGS unit, n_e and n_i – density of electrons and ions, cm^{-3}, ν_e and ν_i – average speed of the directed movement of electrons and ions, cm/s. In quasi-neutral plasma: $n_e = n_i$.

In low-voltage arc of interruption directed speed of electrons is $\sim 10^8$ cm/s, and ions $\sim 10^6$ cm/s. As ν_i is two orders less ν_e it is considered to be that electrons are a basic carrier of a current in electric discharges. Therefore for a decision of practical engineering problems at definition of current density in low-voltage arc of interruption it is possible to use the formula:

$$j_e = 3{,}34 \cdot 10^{-10} \cdot e \cdot n_e \cdot \nu_e, \; A/cm^2.$$

For analysis of the physical phenomena in arc discharge at switching-off of nominal currents and short-circuit currents by circuit breakers the given formula defining current density will be quite sufficient.

Physical processes of formation of arc discharges and their characteristics essentially depend upon current intensity, material of electrodes, distance between them and ways of their initiation by:

- contact opening;
- blowing of plasma into interelectrode gap;
- electric discharge;
- burning of wire;
- laser irradiation and etc.

Depending on a current intensity, a material of electrodes, distance between them and a way of initiation of the arc discharge the structure of its plasma will be various and therefore its electrophysical properties will be different too.

Sufficient information about thermo- and electrophysical properties of air and steams of metals for engineering practice is given in [1.1, part I].

1.1. Initiation of arc discharge by contact opening

At contact opening of circuit breaker in the process of switching-off of electric circuit which is under current load an arc discharge is drawn between the contacts. However before initiation of arc a bridge from liquid metal of the contacts is formed during their disconnection. At the further opening of the contacts a length of the bridge, its volume, mass and lifetime depend on current intensity, metal of contacts, speed of their opening, contact force and external magnetic field intensity in an area of the bridge. The liquid metal bridge can be broken by elongation and quiet evaporation, or electric (thermal) explosion, or pulse magnetic (mechanical) explosion. The form of destruction of the liquid bridge depends on quantity and speed of introduction of energy from an electric network in mass of its body.

There are very many works about investigations of bridge stage of erosion of opening contacts and their results are published both in foreign and in the domestic lit-

erature. Absolute majority of the investigations of bridge erosion have been carried out at relatively low values of current intensity and basically in a range of rated currents of relay equipment.

In the present work the processes of initiation of arc discharges on the argentiferous sintered-metal arcing contacts of automatic low-voltage circuit breakers rated currents from 1000 to 6300 A in a range of short-circuit currents from 6,3 to 60 κA *(r.m.s.)* are considered.

In a number of the works in which the results are very in details stated in [1.2], physical processes of erosion of contacts and electrodes and methods of its calculations are considered. In [1.2] erosion of contacts is considered at currents reaching tens and even hundreds of kiloamperes. But in this work the basic attention has been given processes on the fixed electrodes with different gaps between them.

In [1.3] the results of investigations of destruction of liquid metal bridges in a range of currents 5÷5000 A in the conditions of vacuum and atmospheric air are given. As contact materials the tungsten and sintered-metal contacts NiW with content of nickel 6,7 % have been used. As a result of investigations it was been established that the form of destruction of the bridges depends on current intensity. For the characteristic of the form of destruction of the bridge a mode of change of voltage on the opening contacts was been assumed. On the tungsten contacts at current 700 A the normal form of destruction of the bridge was observed at which pressure on the bridge during $\sim 0{,}5 \cdot 10^{-3} s$ raised smoothly and the bridge was broken by expansion and its steady evaporation.

At current 1800 A a voltage on the bridge smoothly raised in the beginning, and then there was its "splash". Therefore this form of destruction of the bridge has received the name "splash". At last, at current 5000 A voltage on the bridge instantly changed abruptly. At such abnormal change of voltage it has been recognised that the bridge broke as a result of electric explosion.

However on the contacts consisting of metal-sintered compositions NiW, at current 5000 A the explosive form of destruction of the bridge was not observed. In that case probably the form of destruction of the bridge is defined by thermo- and electrophysical properties of Ni which greatly differ from thermo - and electrophysical properties of W (see table 1.1).

In [1.4, p. 277] a voltage oscillogram on opening contacts was given. At the moment of time of their opening this voltage reaches an arcing voltage. «We consider

that in this situation arc initiation occurs at electric explosion of the metal bridges between the cathode and the anode» [1.4, p. 277].

In work [1.5] investigations of contact erosion at "bridge" stage in air were been conducted at currents to 40 *кА* and voltage 5 V. In fig. 1.1 there are photos of destruction of bridges made from Ag, Cu and Fe at switching-off of current 16 *кА*, borrowed of [1.3, p. 38]. According to the authors at destruction of the bridge made from Ag in the area of current constriction the metal evaporates completely and expansion of the limited quantity of macroparticles is observed. At switching-off of a current by contacts from Cu and Fe there is an intensive disorder of macroparticles. It means that at electric explosion of bridges from Cu and Fe their particles will not have time to evaporate completely.

In the works [1.3, 1.4 and 1.5] there are not calculating formulas and quantitative estimations of thermo- and electrophysical parametres at which the explosive form of destruction of liquid-metal the bridge can proceed at switching-off of short-circuit currents.

Formation and destruction of the liquid bridge between opening contacts represent a complex physical phenomenon in which nonequilibrium non-stationary thermodynamic processes, chemical reactions and phase transitions of states of matter proceed simultaneously.

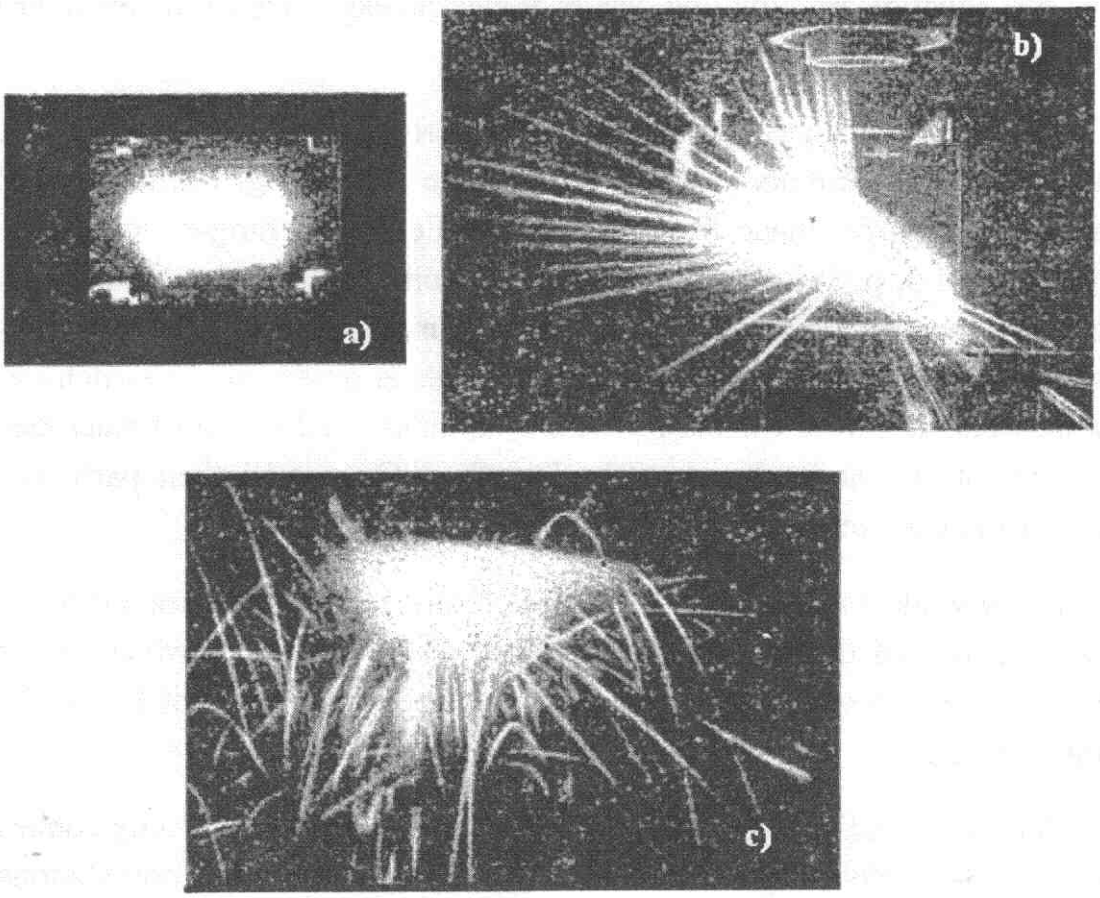

Fig. 1.1 [1.5]. The moments of destruction of bridges from the various materials arising at switching-off of a current 16 кА: a) silver, brightly shone cloud of metal steam and insignificant quantity of scattering particles; b) copper, more weak luminescence of yellow-green colour, many particles scattering almost rectilinearly; c) iron, weak luminescence, very many particles scattering on curvilinear trajectories

Character of destruction of the bridge depends on a complex of properties of materials of electrodes and power capacity of a disconnected circuit. Character of thermodynamic processes in the metal-liquid bridge is defined by instability of a condition of its substance, in which weight can not completely absorb energy brought to it.

In table 1.1 the thermo- and electrophysical properties of some contact materials are given. In table 1.1 the contact materials are located in ascending order of their arc resistance [1.2, p. 224]. From results of the investigations given in works [1.3 and 1.5], it follows that the order of contact materials with the greatest propensity to

course of the explosive form of destruction of bridges at switching-off of short-circuit currents has reverse sequence, than it is specified in table 1.1.

Table 1.1. The thermo- and electrophysical properties of some contact materials

Metal	Ag	Cu	Ni	Fe	W
T_{melt}, K	1235	1356	1728	1808	3863
T_{boil}, K	2485	2840	3003	3027	5933
ρ_{sol}, g/cm^3	10,5	9,02	8,9	7,82	19,3
ρ_{melt}, g/cm^3	9,32	8,29	-	7,2	-
ρ_{boil}, g/cm^3	9,0	7,73	-	6,86	-
C, $cal/g \cdot K$, sol.	0,0544	0,0931	0,106	0,117	0,0321
C, $cal/g \cdot K$, liq.	0,0656	0,11	0,142	-	-
λ, $W/m \cdot K$, sol.	429	401	91	80	174
a, cm^2/s, sol.	1,74	1,17	0,23	0,23	0,64
a, cm^2/s, liq.	0,55	0,42	0,12	0,07	0,14
ρ, 10^{-6}, $Ohm \cdot cm$	1,63	1,73	7,2	9,98	13,5
W_{ev}, J/g	2360	5280	7030	7030	4690
m_o, 10^{-24}, g	179,1	105,1	97,5	92,7	305,2

For example, due to higher electrical resistivity of W than Ni the liquid-metal bridge made from W can faster save up energy sufficient for its electric explosion. Obviously this energy should exceed energy of sublimation: specific energy of evaporation (sublimation) of W lower than energy of Ni:

$$W_{sub}^{W} = 4620 J/g < 7030 J/g = W_{sub}^{Ni}.$$

Therefore, it is possible to accept that additive Ni in the metal-sintered contact on the basis of W reduces probability of bridge`s destruction by electric explosion.

If to compare effects of destruction of bridges from Ag and Cu, shown in fig. 1.1 it is necessary to notice that, apart from practical equality of their electrical resistivity and thermal conductivity coefficients, the liquid bridge from Ag can faster evaporate than from Cu. Temperature of boiling of Ag and, especially, specific energy of evaporation is lower than Cu:

$$T_{boil}^{Ag} = 2485 K < 2840 K = T_{boil}^{Cu};$$

$$W_{sub}^{Ag} = 2360 J/g < 5280 J/g = W_{sub}^{Cu}.$$

In [1.4] one can see data of numerous investigaions of electric breakdowns and initiation of spark and arc discharges in the conditions of vacuum which are accompanied by explosions of microasperities on a surface of electrodes. Explosive processes at flow of electric current were investigated at electric breakdown on an edge and initiation of the spark discharge by a current of autoelectronic emission, on blowing up wires, by means of influence of a laser beam on a surface of metals etc. As a result of the researches it was been established a number of conditions at which electric explosions on a surface of base spots of electric discharges could be taken place.

One of the main reasons of microexplosions at electric breakdown of a vacuum interelectrode interval is Joule heating-up of microasperities on a surface of the cathode due to a current of autoelectronic emission. Current density can reach $10^8 \div 10^9$ A/cm^2. Electric explosion of microasperities leads to emission of blow-out of plasma jet. Also explosive electron emission can be caused by thermionic emission due to overheat of microasperities which explode finally. The portion of electrons, thrown out as a result of explosive electron emission, is named *ecton* (EC - the first letters of English words explosion centre, translation: «the explosion centre») by the author [1.4].

As a result of microasperitie`s explosion an emission of the drops occurs. Their velocity is $(2 \div 4) \cdot 10^4$ *cm/s*. This velocity is caused by high pressure of a thrown up plasma jet on liquid metal. The pressure can reach $10^8 \div 10^9$ *Pa*. Under influence of this pressure the forward front of a plasma jet gets velocity $(1 \div 2) \cdot 10^6$ *cm/s*.

At laser irradiation of metal on its surface melting, evaporation or explosion can take place depending on a value of power coming on unit of area of laser spot. In Table 1.2 physical phenomenon in spot of laser irradiation on titanium target depending on power density are given [1.4, p. 64].

Table 1.2

Proccess	Power density, W/cm^2
Melting	10^5
Evaporation	$10^6 \div 10^8$
Explosion	$>10^8$

In [1.2] it is shown that intense evaporation of Zn, Cu and W takes place at power density close to 10^8 W/cm^2.

Therefore explosive process on the metal surface can take place at power density $\geq 10^8$ W/cm^2 coming on it.

Explosion of some volume of metal can occur, if the specific energy transfered in its weight, will reach certain critical value. According to [1.4], explosion of microasperities can occur, if specific energy of their metal exceeds specific energy of sublimation in 2÷3 times. In a condition of nonideal dense plasma its specific energy can reach values 10^5 J/g. During sublimation metal passes from a solid phase in the gaseous one. At electric explosion of metal it is exposed to transformation from solid phase to liquid one, then it occurs a phase transition of its substance in the agragate condition representing association of several atoms and molecules, gas and plasma formation.

The probability of course of explosive destruction of substance is influenced essentially also by speed of entering of energy in it. In case of arc discharges speed of entering of energy in mass of metal, in which the current flows, can serve as speed of its increase.

From the point of view which is stated in [1.4], rate of current rise, leading to explosion of microasperities on the copper cathode of vacuum arc discharges, can reach values $\frac{di}{dt} \sim 10^8$ A/s. At $\frac{di}{dt} > 10^8$ A/s on the cathode there are qualitative changes which lead to change of a spectrum of radiation of plasma, occurrence of new cells, sharp rise of speed of spots moving etc.

The given review of investigations of explosive mechanisms of destruction of microasperities on base spots of arc discharges of explosive wires which can be model for researches of destructions of metal-liquid bridges, and on a surface of spots of a laser irradiation, and also the established critical parametres at which explosive processes of metals proceed, applications of the last for an estimation of probability of course of explosive processes of metal-liquid bridges on opening contacts at switching-off of short-circuit currents.

1.2. Destruction of the bridge by Joule heat

Investigations of distinguishing of high-power arc in low-voltage breakers have shown that opening of argentiferous metal-sintered contacts at switching-off of short-circuit currents can proceed either quietly or with a burst [1.1, part I, p. 196; part II, p. 14].

In fig. 1.2 oscillograms of a current and voltage of arc at switching-off of current in a test loop at phase voltage U_{ph}=420 *V* and *cos* φ = 0,2: and - I=6,4 *кА*; - I=16,0 *кА* are given.

From oscillograms in fig. 1.2 it can be seen that contacts opened in the first case at a current 7,5 *кА*, and in the second - at a current 13 *кА*.

Fig. 1.3 shows the oscillograms of arc voltage on opening argentiferous contacts and a photo of shots 2 - high-speed filming of arc from the same tests. The oscillograms of the same tests are shown in fig. 1.2.

From fig. 1.3 it can be seen that at instantaneous current equal 7,5 *кА* the metal-liquid bridge has collapsed quietly and at the current 13,0 *кА* plasma jet blow-out from the contact gap. At currents not exceeding 12,0 *кА* on argentiferous contacts, as a rule, the arc discharge is drawn in (0,5÷1,0) *ms* after the moment of time of contact opening as a result of quiet destruction of the bridge. In that case voltage on the contacts is increased smoothly from voltage drop across the resistance of closed contacts to arcing voltage. It is possible to accept a value of arcing voltage on argentiferous contacts equal 20 *V*.

In fig. 1.4 the quiet form of destruction of the metal-liquid bridge is schematically shown. As a result of extension of the bridge, action of the electromagnetic pressure compressing its channel and surface tension forces, it gets the form of a body of rotation with the reduced section in its average part.

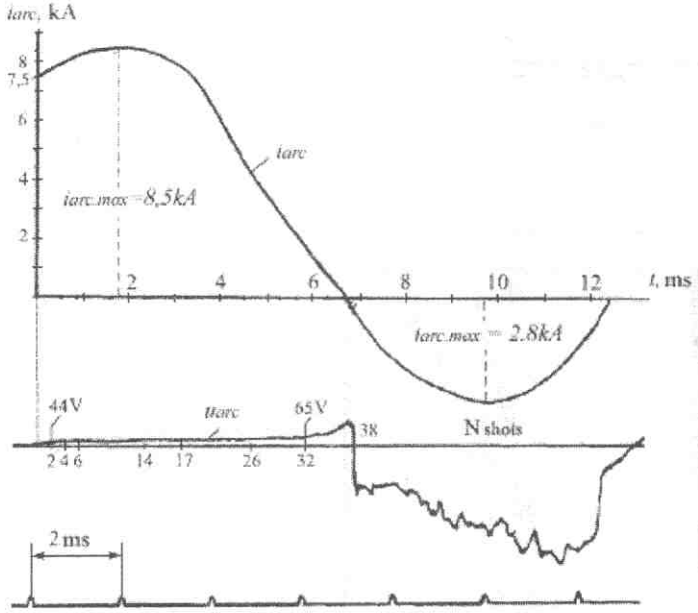

a)

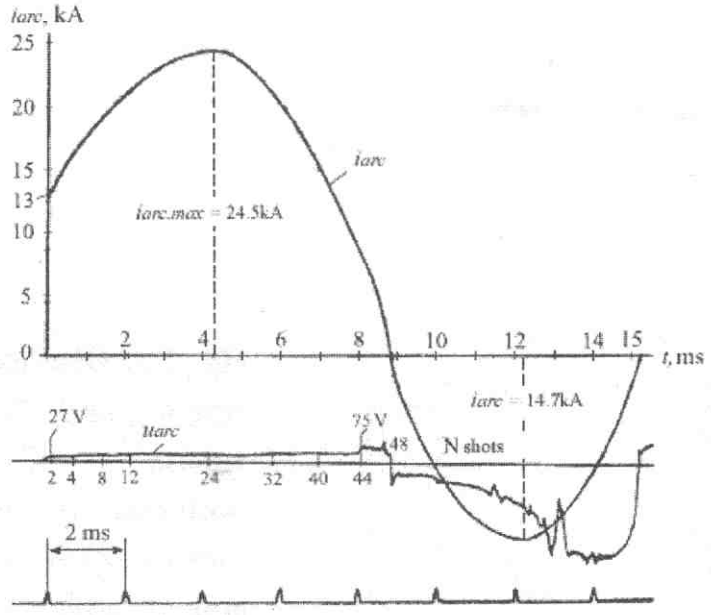

b)

Fig. 1.2 Oscillograms of a current and voltage of arc at switching-off of current in loop at phase voltage U_{ph}=420 *V* and *cosφ*=0,2: a) *I*=6,4 *κA*; b) *I*=16,0 *κA*

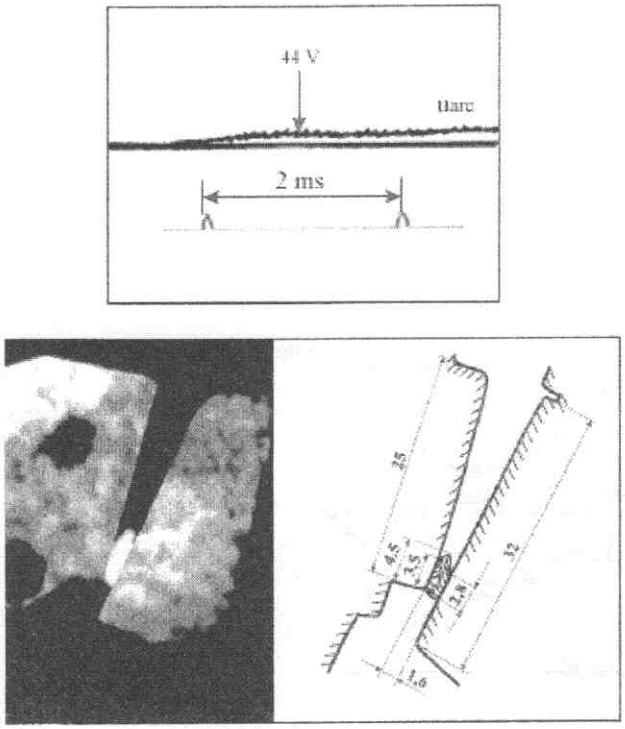

a)

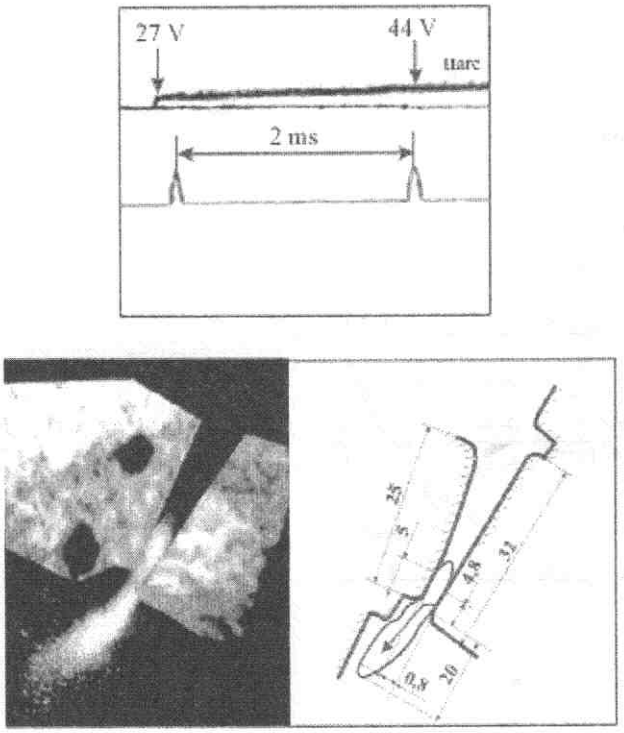

b)

Fig. 1.3. Oscillograms of voltage u_{arc} and photos of arc on opening silver-containing contacts. At the moment of contact opening time instantaneous current was: *a* – i_{arc} = 7,5 *кА;b* – i_{arc} = *13,0 кА;*
arc time t_{arc} = 0,334 *ms*, exposure time of one shot Δt = 0,167 *ms.*
Sizes are given in *mm.*

At enough high values of current intensity under influence of electrodynamic forces constriction and break of the metal-liquid bridge can occur. At the moment of time of break of the bridge the arc discharge is drawn. The rest of liquid melt on base spots of arc gets the form of cones under influence of surface tension forces and drops form on their tops. As a result of current flow in an isthmus, connecting a cone of liquid melt with a drop, electrodynamic force appears which try to tear off a drop from the isthmus. This force can be defined from the formula:

$$f = 1{,}02 \cdot 10^{-8} \cdot i^2 \cdot \ln \frac{r_{drop}}{r_{ist}},$$

where i – instantaneous current, A; r_{drop} and r_{ist} – radiuses of the drop and the isthmus correspondingly, *cm*. If to accept the ratio $\frac{r_{drop}}{r_{ist}} = 5$, then at the current $7{,}5 \cdot 10^3$ A a value of tearing force of drop is:

$$f = 1{,}02 \cdot 10^{-8} \cdot (7{,}5 \cdot 10^3\ A)^2 \cdot \ln 5 = 0{,}918\ kgf\ .$$

The drops on both electrodes under influence of such high forces tear off the cones of liquid melt and direct towards each other. At collision the drops merge and form one drop. The drop being in the arc channel can either evaporate or split up or be squeezed out from the arc channel.

Let us try to estimate, at least roughly, destiny of a drop in this specific experiment.

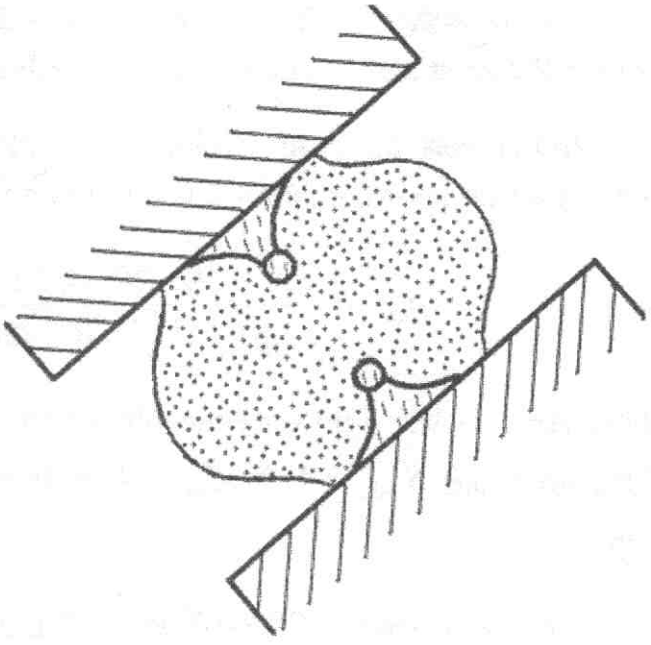

Fig. 1.4. Quiet form of destruction of the bridge

In [1.1, part II, p. 69-70] it is shown that the range of the sizes of drops in arc chambers of low-voltage automatic circuit breakers at switching-off of short-circuit

currents changes from partes of micrometers to units of millimetres. In the gap between contacts δ =1,6 *mm* (fig. 1.3, a) a drop can settle with diameter up to 1,0 *mm*.

According to [1.1, part II, p. 69-70] the current can flow through a drop, if

$$\Delta U > (U_c + U_a),$$

where $\Delta U = E d_{drop}$ – voltage of plasma on stage length equal to diameter of the drop and (U_c+U_a) =20*V* - average value of the sum of electrode voltage drops on electrodes from *Ag*. If to accept that a value of field density *E V/cm* in arc plasma equal to its average value:

$$E_{av} = \frac{u_{arc}}{\delta} = \frac{20\ V}{0{,}16\ cm} = 125\ V/cm,$$

then:

$$\Delta U = E_{av} \cdot d_{drop} = 125\ V/cm \cdot 0{,}1\ cm = 12{,}5\ V.$$

As far as ΔU = 12,5 *V* < (U_c+U_a) = 20 *V*, therefore, the current can not flow through the drop and it will not heat up by Joule heat.

In that case the drop will heat up by means of power density coming on its surface. As a first approximation it is possible to accept power density equal:

$$q_{drop} = \frac{\Delta P}{S_{drop}} = \frac{7{,}5 \cdot 10^3\ A \cdot 12{,}5\ V}{3{,}14 \cdot 10^{-2}\ cm^2} = 29{,}9 \cdot 10^5\ W/cm^2,$$

where $\Delta P = i \cdot \Delta U$ – power concentrated in arc plasma in the area of an arrangement of the drop and $S_{drop} = 4 \cdot \pi \cdot r_{drop}^2 = 4 \cdot \pi \cdot (0{,}05\ cm)^2 == 3{,}14 \cdot 10^{-2}\ cm^2$ – an area of a drop surface.

At power density $29{,}9 \cdot 10^5\ W/cm^2$ the drop *Ag* can exist in molten state only. In order that a drop could evaporate intensively, power density should be not less than $10^7\ W/cm^2$. Therefore the drop *Ag* with diameter 1,0 *mm* can not evaporate completely in the arc channel in which a current is 7,5 *кА*.

In [1.1, part II, p. 82] it is shown that drops *Ag* in the channel of arc under influence of a thermal flux can be split up for smaller parts. In this case the minimum (critical) radius of a drop from *Ag* after its split will equal to:

$$r_{drop.cr} \sim 122\sqrt{\frac{1}{q_{drop}}} = 122 \cdot \sqrt{\frac{1}{29{,}9 \cdot 10^{12}\ erg/(s \cdot cm^2)}} = 0{,}18 \cdot 10^{-4}\ cm,$$

where q_{drop} – power density coming on the drop, $erg/(s \cdot cm^2)$.

The drops, having radius $r_{drop} < r_{drop.cr}$, will not blow up. The drops, having radius on two orders more critical radius, can not blow up also.

Thus, at opening of argentiferous contacts at a current 7,5 κA and quiet destruction of liquid-metal bridge the drops with diameter ~ 1,0 mm which are formed of its liquid melt and being in the channel of arc cannot blow up. But such rather large drops can either drop out of the channel of arc under the influence of gravity or be squeezed out by the electromagnetic pressure compressing a channel of arc.

The drops having diameter less $36 \cdot 10^{-4}\ cm$ will be intensively split up for smaller parts under the influence of thermal fluxes.

Suspension of relatively the small drops having diameter about a fraction of micrometeres, as a part of ionised steams of contact metal at the initial stage of their opening, forms nonideal plasma of the arc discharge.

Mass of the drops formed from liquid melt of the bridge and splintered and have been thrown out from the arc channel make contact erosion on the bridge stage of contact opening.

At value of current $7{,}5 \cdot 10^3\ A$ and voltage drop on the bridge, u_{br}=16 V during time of its coexistence $t_{br} = 0{,}5 \cdot 10^{-3}\ s$ the following quantity of energy can be evolved:

$$\Delta W_{br} = i \cdot u_{br} \cdot t_{br} = 7{,}5 \cdot 10^3\ A \cdot 16\ V \cdot 0{,}5 \cdot 10^{-3}\ s = 60\ W \cdot s.$$

According to fig. 1.3,a it is possible to accept volume of the bridge equal to:

$$V_{br} = \delta \cdot S_{br.av} = 0{,}16\ cm \cdot 0{,}079\ cm^2 = 0{,}0126\ cm^3,$$

where δ=0,16 cm – length of the bridge equal to contact gap and $S_{br.av}$= 0,079 cm^2 – average value of its sectional area

$$(S_{br.av} = \frac{S_{brc} + S_{br.a}}{2} = \frac{\pi}{8} \cdot (d_{br.c}^2 + d_{br.a}^2) = \frac{\pi}{8} \cdot [(0{,}35\ cm)^2 + (0{,}28\ cm)^2] = 0{,}079\ cm^2).$$

Mass of the bridge from liquid Ag at its melting temperature is equal to:

$$m_{br} = \rho_{Ag} \cdot V_{br} = 9{,}32\ g/cm^3 \cdot 0{,}0126\ cm^3 = 0{,}117\ g\ .$$

In that case the specific contribution of energy to mass of the bridge is:

$$\Delta\omega_{br} = \frac{\Delta W_{br}}{m_{br}} = \frac{60\ W \cdot s}{0{,}117\ g} = 513\ W \cdot s/g\ .$$

Current density in the bridge is:

$$j_{br} = \frac{i}{S_{br.av}} = \frac{7{,}5 \cdot 10^3\ A}{0{,}079\ cm^2} = 9{,}5 \cdot 10^4\ A/cm^2\ .$$

Electromagnetic pressure in the bridge channel is:

$$P_{br} = P_{atm} + 9{,}87 \cdot 10^{-9} \cdot i \cdot j_{br}\ atm =$$
$$= 1{,}0\ atm + 9{,}87 \cdot 10^{-9} \cdot 7{,}5 \cdot 10^3\ A \cdot 9{,}5 \cdot 10^4\ A/cm^2 = 8{,}0\ atm.$$

Growth rate of a current in the bridge is equal to:

$$\frac{i}{t_{br}} = \frac{7{,}5 \cdot 10^3\ A}{0{,}5 \cdot 10^{-3}\ s} = 1{,}5 \cdot 10^7\ A/s\ .$$

Let us compare the received results of calculations of the parametres characterising the mechanism of destruction of the metal-liquid bridge with critical parametres at which it occurs an explosion of metals at flowing current through them:

- $\Delta\omega_{br}^{Ag} = 513\ \frac{J}{g} << 2360\ \frac{J}{g} = W_{ev}^{Ag}$;
- $j_{br} = 9{,}5 \cdot 10^4\ \frac{A}{cm^2} << (10^8 \div 10^9)\ \frac{A}{cm^2}$
- $P_{br} = 8{,}0\ atm = 8 \cdot 10^5\ Pa << (10^8 \div 10^9)\ Pa$
- $\frac{i}{t_{br}} = 1{,}5 \cdot 10^7\ \frac{A}{s} < 10^8\ A/s$.

From the mentioned comparison of parametres unequivocally it follows that opening of argentiferous contacts at current $7{,}5 \cdot 10^3$ *À* really should proceed at quiet destruction of the metal-liquid bridge.

On fig. 1.3,b one can see that at instantaneous current 13,0 *кА* a voltage on the contacts abruptly reaches value 27 *V* at the moment of time of their opening which is quite sufficient for initiation of the arc discharge. In 0,334 *ms* after the moment of time of contacts opening a plasma jet is pulled out the arc channel. Because of the fact that voltage on contacts at their opening has reached arcing values adruptly and the plasma jet blows out from arc channel, an assumption about explosive form of destruction of the metal-liquid bridge is occurred. In this case we will estimate bridge parameters.

At average value of a current 13,0 *кА* and voltage 27 *V* during $t = 0{,}334 \cdot 10^{-3}\ s$ in contacts gap the following quantity of energy was evolved:

$$\Delta W = i \cdot u \cdot t = 13 \cdot 10^3\ A \cdot 27\ V \cdot 0{,}334 \cdot 10^{-3}\ s = 117\ W \cdot s\,.$$

According to fig. 1.3,b it would be possible to assume that volume of the metal-liquid bridge was equal to:

$$V_{br} = \delta \cdot S_{br.av} = 0{,}08\ cm \cdot 0{,}188\ cm^2 = 0{,}015\ cm^3\,,$$

where δ=0,08 *cm* – bridge length and $S_{br.av}$=0,188 cm^2 – average value of the sectional area of the bridge:

$$S_{br.av} = \frac{S_{br.c} + S_{br.a}}{2} = \frac{\pi}{8} \cdot (d_{br.c}^2 + d_{br.a}^2) = \frac{\pi}{8} \cdot [(0{,}5\ cm)^2 + (0{,}48\ cm)^2] = 0{,}188\ cm^2\,.$$

At melting temperature of *Ag* a mass of the metal-liquid bridge is:

$$m_{br} = \rho_{Ag} \cdot V_{br} = 9{,}32\ g/cm^3 \cdot 0{,}015\ cm^3 = 0{,}14\ g\,.$$

In this case the specific energy entered into mass of the bridge is equal:

$$\Delta\omega_{br} = \frac{\Delta W}{m_{br}} = \frac{117\ W \cdot s}{0{,}14\ g} = 836\ W \cdot s/g\,.$$

This value of the specific energy entered in the metal-liquid bridge from *Ag* is much lower than its energy of sublimation:

$$\Delta\omega_{br} = 836\ J/g << 2360\ J/g = W_{sub}^{Ag}.$$

Therefore it is possible to make a conclusion that at a current equal 13,0 κA the opening of contacts can not be attended with the explosive form of destruction of the bridge.

During the initial moment of time of formation of the bridge the average density of a current is:

$$j_{br} = \frac{i}{S_{br.av}} = \frac{13 \cdot 10^3\ A}{0{,}188\ cm^2} = 6{,}9 \cdot 10^4\ A/cm^2.$$

That is during the initial moment of time of formation of the bridge a current density equaled $6{,}9 \cdot 10^4\ À/ñì^2$ can not lead to its electric explosion. However the bridge under the influence of electrodynamic forces is exposed constriction. If to admit that at the last moment of time of coexistence of the bridge the minimum sectional section will equal to $S_{br.min}$=0,01 cm^2 then in the bottleneck of the bridge the current density can be equal:

$$j_{br.max} = \frac{i}{S_{br.min}} = \frac{13 \cdot 10^3\ A}{0{,}01\ cm^2} = 1{,}3 \cdot 10^6\ A/cm^2.$$

In that case superfluous electromagnetic pressure in the bottleneck of the bridge will get values:

$$P_{br.max} = 9{,}87 \cdot 10^{-9} \cdot i \cdot j_{br.max} =$$

$$= 9{,}87 \cdot 10^{-9} \cdot 13{,}0 \cdot 10^3\ A \cdot 1{,}3 \cdot 10^6\ A/cm^2 = 167\ atm = 1{,}67 \cdot 10^7\ Pa.$$

Therefore the metal-liquid bridge from Ag even in the end of time of the coexistence at current $13 \cdot 10^3\ A$ could not blow up, as both the current density and pressure in the bridge are significantly below critical values at which electric explosion of metals can occure:

- $j_{br.max} = 1{,}3 \cdot 10^6\ A/cm^2 << 10^8\ A/cm^2$;
- $P_{br.max} = 1{,}67 \cdot 10^7\ Pa < 10^8\ Pa$.

Let us notice that at a current 16,0 κA opening of contacts from *Ag,* shown in fig. 1.1, was occurred without electric explosion also.

At the same time in fig. 1.3 it is seen that voltage on opening contacts adruptly reaches arcing values and the plasma jet is pulled out from contact gap. We will explain both specified facts.

Scanning speed of registration of the voltage with help of a cathodic oscillograph was 10 *m/s*. That is time duration 100 μs kept within 1,0 *mm* on the oscillogram. It is possible to assume that the metal-liquid bridge between the contacts at a current 13,0 κA co-existed about 100 μs. It was not possible to observe the valid course of voltage changing on the bridge. Therefore on the length less than 1,0 *mm* on the oscillogram a voltage changing on the bridge looks like jump. At investigation of bridge stage of erosion of contacts the time permission of a data-acquisition equipment should be $\leq 10^{-6}$ s obviously.

For an explanation of the reasons of eruption of plasma jet from contact gap at the initial stage of their opening we are reversed to fig. 1.5 on which it is schematically shown an eruption of plasma jet from contact gap.

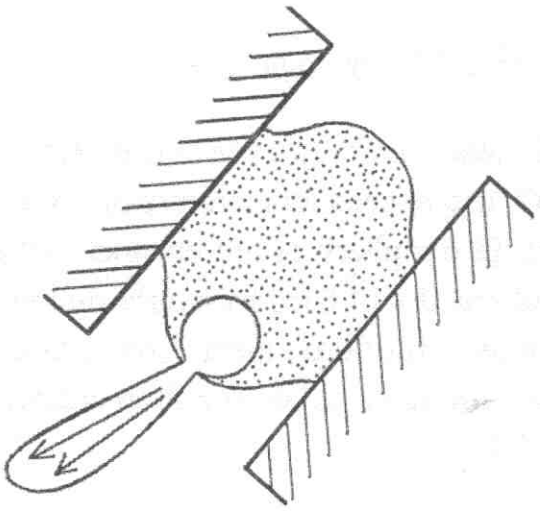

Fig. 1.5. The schematic image of eruption of a plasma jet from a drop breaking through its cover

Earlier it was shown a formation of the drop in arc channel after quiet destruction of the metal-liquid bridge. The drop in arc channel is subjected to pressure:

$$P_{drop} = P_{ch} + \frac{2 \cdot \sigma}{r_{drop}},$$

where $P_{ch} = (9{,}87 \cdot 10^{-9} \cdot i\,A \cdot j_{ch}\,A/см^2 atm) \cdot 1{,}01 \cdot 10^{-6}\ dyne/cm^2$ – pressure in arc channel; $2 \cdot \sigma / r_{br}$ - Laplace pressure in the drop by means of surface tension forces [1.6], σ = 980 *dyne/cm* – surface tension coefficient *Ag* in liquid state and $r_{drop} = 0{,}15 \cdot 10^{-4}\ cm$ – drop radius.

The current density in the arc channel is equal to:

$$j_{ch} = \frac{i_{arc}}{S_{ch}} = \frac{13 \cdot 10^3\ A}{0{,}28\ cm^2} = 4{,}6 \cdot 10^4\ A/cm^2,$$

where $S_{ch} = \pi \cdot r_{ch}^2 = \pi \cdot (0{,}3\ cm)^2 = 0{,}28\ cm^2$ – sectional area of arc channel (fig. 1.3, b).

In that case a pressure in the drop will be:

$$P_{drop} = (9{,}87 \cdot 10^{-9} \cdot 13 \cdot 10^3\ A \cdot 4{,}6 \cdot 10^4\ A/cm^2) \cdot 1{,}01^6\ dyne/cm^2 + \frac{2 \cdot 980\ dyne/cm}{0{,}15 \cdot 10^{-4}\ cm} =$$

$$= 6 \cdot 10^6\ dyne/cm^2 + 1{,}3 \cdot 10^6\ dyne/cm^2 = 7{,}3 \cdot 10^6\ dyne/cm^2.$$

As a result of excess of pressure of liquid metal in a drop over normal atmospheric pressure, the temperature of its boiling will also exceed temperature of boiling of metal at normal pressure. If the drop appears on periphery of arc channel and it will adjoin to ambiant environment then its liquid metal will become overheated and it will tempestuously boil. As a result of phase transition of drop metal from a liquid state to gaseous state the formed steams can break through a cover of a drop and will expire in an environment in the form of a plasma jet.

According to [1.7] at pressure of 8,0 atmospheres the temperature of saturated steams *Ag* is T_{sat}=3020 *K*. It is possible to define density of saturated vapor *Ag* in a drop from the formula:

$$\rho = m_0 \cdot n_0,$$

where $m_0 = 179{,}1 \cdot 10^{-24}\ g$ – mass of atom *Ag* and n_0 – vapor concentration *Ag*, cm^{-3}, which can be define by the formula:

$$Ð = n_0 \cdot k \cdot Ò,$$

where P – vapor pressure, *dyne/cm*^{2}, $k = 1{,}38 \cdot 10^{-16}\ erg/K$ – Boltzmann constant, T – vapor temperature, K. In a considered example for estimated calculations it is possible to accept that in a mouth of the expiration of a stream from the drop concentration of saturated steam is equal to:

$$n_0 = \frac{P_{drop}}{k \cdot T_{sat}} = \frac{7{,}3 \cdot 10^6\ dyne/cm^2}{1{,}38 \cdot 10^{-16}\ erg/K \cdot 3020\ K} = 1{,}75 \cdot 10^{19}\ cm^{-3}.$$

Density of steams expiring from the drop:

$$\rho_{ev} = m_0 \cdot n_0 = 179{,}1 \cdot 10^{-24}\ g \cdot 1{,}75 \cdot 10^{19}\ cm^{-3} = 31{,}3 \cdot 10^{-4}\ g/cm^3.$$

Speed of the expiration of steam Ag in a drop mouth can be:

$$\upsilon_{ev} = \left(\frac{2 \cdot P_{drop}}{\rho_{ev}} \right)^{1/2} = \left(\frac{2 \cdot 7{,}3 \cdot 10^6\ dyne/cm^2}{31{,}3 \cdot 10^{-4}\ g/cm^3} \right)^{1/2} = 6{,}83 \cdot 10^4\ cm/s.$$

Speed of forward front of the shone jet, shown on fig. 1.3,b, according to experimental data [1, part II, p. 34] is 27 *m/s*. Decreasing of speed of a current of forward front of a plasma jet from a mouth of its expiration occurs by means of aerodynamic resistance which renders it environment air.

Results of estimated calculations of parametres of a plasma jet expiring from the floating drop of liquid metal in powerful arc channel explain possibility of its expiration convincingly enough. However the expiration of plasma jet from an contact gap occurs not at the moment of time of contact opening but after the moment of time of initiation of the arc discharge.

In fig. 1.6 a photo of the first shot of high-speed filming of contact opening and the oscillogram of the current and voltage of arc are given.

At the moment of time of contact opening the instantaneous current was equal to 52 *кА* and voltage on the contacts has reached 33 *V* adruptly. The photo shows that contact opening has obviously explosive form. During shooting of the first shot it was allocated energy in the contact gap:

$$\Delta W = i_{arc} \cdot u_{arc} \cdot \Delta t = 52 \cdot 10^3\ A \cdot 33\ V \cdot 0{,}25 \cdot 10^{-3}\ s = 429\ W \cdot s.$$

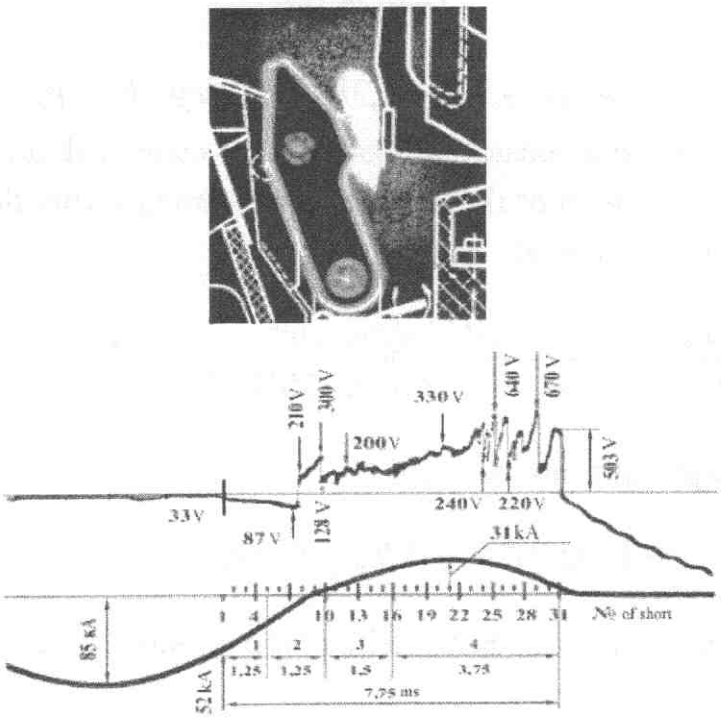

Fig. 1.6. Explosive process of contact opening at instantaneous current equal 52 *κA*. Exposition time of one shot is 0,25 *ms*

On the photo in fig. 1.6 it is impossible to define sizes of the bridge. Therefore we will define volume and weight of the bridge by means of calculation. For settlement model of the bridge we will accept model of a jet of the liquid metal formed on the cathode of a vacuum arc (see fig. 1.7) [1.4, p. 237]. Metal-liquid bridge can be presented in the form of two jets of liquid metal directed towards each other. The jets of liquid metal on the cathode are exposed to explosion [1.4, p. 289]. On the place of the blown up jet the crater is formed. It is accepted [1.4, p. 338] that crater expansion stops «when Joule diameter is compared to diameter of heat conductivity». From fig. 1.7 we can see that diameter of a crater is equal to diameter of the basis of the jet of liquid metal.

In fig. 1.8 [1.4, p. 338] the diagram of dependence of crater diameter on the copper cathode from value of current intensity is shown. At a current intensity exceeding 50 A dependence $d_{cr}(i)$ becomes linear. Diameter of the crater is defined by the formula [1.4, p. 339]:

$$d_{cr} = \frac{i}{2 \cdot \pi \cdot \left(a \cdot \bar{h}\right)^{1/2}},$$

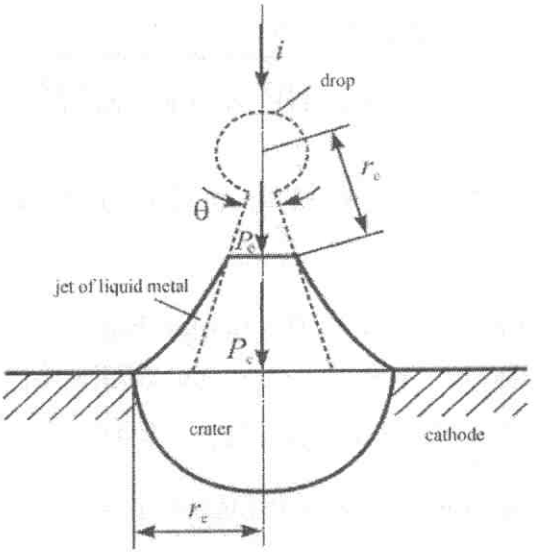

Fig. 1.7. [1.4]. Jet of liquid metal, r_c - radius of a area of the melt metal, P_c - pressure of plasma upon liquid metal, i - current

where a – temperature conductivity coefficient and $\bar{h}$ – specific action for explosion of liquid metal jet.

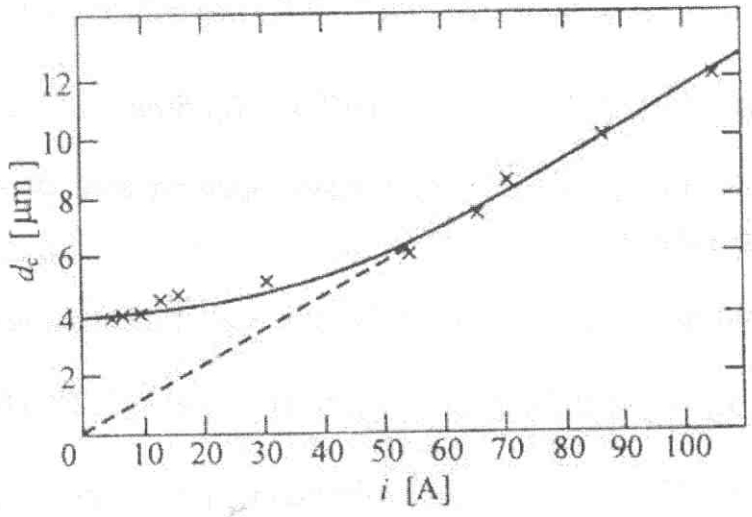

Fig. 1.8 [1.4]. Dependence of the most probable diameter of a crater on a cathodic current for a vacuum arc with the copper cathode, having an individual cathodic spot

If to apply the resulted formula for rough estimation of diameter of the bridge basis at switching-off of short-circuit current we will have in a considered example:

$$d_{br} = \frac{i_{arc}}{2 \cdot \pi \cdot \left(a \cdot \bar{h}\right)^{1/2}} =$$

$$= \frac{52 \cdot 10^3\ A}{2 \cdot \pi \cdot \left(0{,}55\ cm^2/s \cdot 2 \cdot 10^9\ A^2 \cdot s/cm^4\right)^{1/2}} \cong 0{,}25\ cm,$$

where for liquid Ag $a = 0{,}55\ cm^2/s$ [1.4, p.123] and $\bar{h} = 2 \cdot 10^9\ A^2 \cdot s/cm^4$ [1.4, p.109].

The received value of diameter of the bridge basis is comparable with values of diameters of the bridge bases at switching-off of currents equal $7{,}5 \cdot 10^3\ A$ $(d_{br} = 0{,}35\ cm)$ and $13 \cdot 10^3\ A$ $(d_{br} = 0{,}48\ cm)$. However it is necessary to notice that mass of liquid metal of the bridge at current $52 \cdot 10^3\ A$, at which there is its explosion, probably it should be less than at currents $7{,}5 \cdot 10^3\ A$ and $13 \cdot 10^3\ A$ at which bridges evaporate. We will be convinced that the bridge at current $52 \cdot 10^3\ A$ really blows up.

If to accept volume of the bridge for cylinder it will equal to:

$$V_{br} = \pi \cdot r_{br}^2 \cdot \delta = \pi \cdot \left(0{,}125\ cm\right)^2 \cdot 0{,}05\ cm = 2{,}45 \cdot 10^{-3}\ cm^3,$$

where $\delta = \upsilon_c \cdot \Delta t = 2 \cdot 10^2\ cm/s \cdot 0{,}25 \cdot 10^{-3}\ s = 0{,}05\ cm$ – length of bridge, $\upsilon_c = 2 \cdot 10^2\ cm/s$ – average velocity of contact opening and $\Delta t = 0{,}25 \cdot 10^{-3}\ s$ – exposure time of one shot at filming.

Mass of liquid Ag composing the bridge is equal at its melting temperature:

$$m_{br} = \rho_{liq} \cdot V_{br} = 9{,}32\ g/cm^3 \cdot 2{,}45 \cdot 10^{-3}\ cm^3 = 2{,}28 \cdot 10^{-2}\ g.$$

In this case specific energy of bridge liquid metal will equal to:

$$\Delta\omega_{br} = \frac{\Delta W}{m_{br}} = \frac{429\ J}{2{,}28 \cdot 10^{-2}\ g} = 1{,}88 \cdot 10^4\ J/g.$$

A value $\Delta\omega_{br} = 1{,}88 \cdot 10^4\ J/g$ is considerably superior to specific energy of sublimation Ag:

$$\Delta\omega_{br} = 1{,}88 \cdot 10^4\ J/g >> 2{,}36 \cdot 10^3\ J/g = \Delta W_{ev}^{Ag}.$$

Therefore, metal-liquid bridge Ag at the current $52 \cdot 10^3\ A$ really must be blown up.

Current density in the bridge can reach a value:

$$j_{br} = \frac{i}{S_{br}} = \frac{52 \cdot 10^3\ A}{4{,}9 \cdot 10^{-2}\ cm^2} = 1{,}06 \cdot 10^6\ A/cm^2,$$

where $S_{br} = \pi \cdot r_{br}^2 = \pi \cdot (0{,}125\ cm)^2 = 4{,}9 \cdot 10^{-2}\ cm^2$.

In that case a pressure in arc channel may have a value:

$$P_{br} = 9{,}87 \cdot 10^{-9} \cdot j_{br}\ \frac{A}{cm^2} \cdot i\ A =$$

$$= 9{,}87 \cdot 10^{-9} \cdot 1{,}06 \cdot 10^6\ \frac{A}{cm^2} \cdot 52 \cdot 10^3\ A = 5{,}44 \cdot 10^2\ atm = 5{,}44 \cdot 10^7\ Pa.$$

Value of current intensity equal $1{,}06 \cdot 10^6\ A/cm^2$ is less two orders of current density ($10^8\ A/cm^2$) and pressure $5{,}44 \cdot 10^7\ Pa$ is less one order times ($10^8\ Pa$) at which electric explosions of metals occur. However it is necessary to consider that high pressure in the metal-liquid bridge leads to its constriction and rupture. If in process of constriction the bridge its cross-section in the narrowest part decreases to $0{,}01\ cm^2$ than a current intensity and pressure will be equal:

$$j_{br.max} = \frac{i}{S_{br.min}} = \frac{52 \cdot 10^3\ A}{0{,}01\ cm^2} = 5{,}2 \cdot 10^6\ A/cm^2;$$

$$P_{br.max} = 9{,}87 \cdot 10^{-9} \cdot j_{br.max} \cdot i =$$

$$= 9{,}87 \cdot 10^{-9} \cdot 5{,}2 \cdot 10^6\ \frac{A}{cm^2} \cdot 52 \cdot 10^3\ A = 2{,}7 \cdot 10^3\ atm = 2{,}7 \cdot 10^8\ Pa.$$

The pressure equal $2{,}7 \cdot 10^8\ Pa$, is quite enough for initiation of the explosive form of destruction of the metal-liquid bridge.

Here it is expedient to estimate growth rate of a current in the bridge arising at contact opening. To define exact time of destruction of the bridge with help of oscillogram in fig. 1.6 it is not obviously possible. Therefore we will accept that this time is equal to time of exposition of one shot of high-speed filming. Then growth rate of a current in the bridge will equal to:

$$\frac{i}{\Delta t} = \frac{52 \cdot 10^3\ A}{0{,}25 \cdot 10^{-3}\ s} = 2{,}08 \cdot 10^8\ A/s\ .$$

According to a point of view stated in [1.4], at $di/dt > 10^8\ A/s$ on the cathode there are qualitative changes which lead to change of a spectrum of radiation of plasma, occurrence of new cells, sharp increase of speed of moving of spots etc.

At investigations of arc of high power [1.1] ceramic-metal argentiferous contacts on the basis of nickel were used. Energies of sublimation *Cu, Ag, Ni,* and *Fe* according to [1.7] are:

$$Ag - 2{,}36 \cdot 10^3 \frac{J}{g};\ Cu - 5{,}28 \cdot 10^3 \frac{J}{g};\ Ni\ and\ Fe - 7{,}03 \cdot 10^3 \frac{J}{g}\ .$$

Hence, for explosion *Ag* it is required less specific energy than for explosion *Cu* and for *Ni* still less. Therefore in the argentiferous contacts in which composition consists of 70 % *Ag* and 30 % *Ni*, basically *Ag* is subjected to explosion. Proceeding from the stated it follows that growth rate of a current in the bridge on the argentiferous contacts equal $2{,}08 \cdot 10^8\ A/s$ leads to the explosive mechanism of formation of arc discharge and on its base spots it is necessary to expect course of rather rapid processes.

Let us notice that in a considered example a speed of input of Joule heat in the metal-liquid bridge is equal:

$$\frac{\Delta W}{\Delta t} = \frac{429\ J}{0{,}25 \cdot 10^{-3}\ s} = 1{,}72 \cdot 10^6\ J/s\ .$$

Introduction of parameter of growth rate of Joule heat is proved by that at contact opening growth rate of voltage takes place also. At quiet destruction of the bridge a voltage on the opening contacts grows smoothly. At explosive destruction of the bridge a voltage on contacts at the moment of time of their opening increases adruptly and can reach different values. Due to influence of voltage value on opening contacts on probability of destruction of the bridge by explosion it is expedient to take into account a speed of input of energy in the bridge. Growth rate of the energy entered into the bridge is equal $1{,}7 \cdot 10^6\ J/s$. It is possible to accept this value as a critical value which leads to explosive destruction of the metal-liquid bridge from *Ag*.

1.3. Destruction of the metal-liquid bridge on opening contacts by pulsed magnetic field

Low-voltage automatic circuit breakers are intended for distribution of electric energy to industrial facilities, can conduct rated current in continuous service, repeatedly disconnect electric circuits without current load and with nominal current load. A limited number of times they can automatically disconnect emergency currents of an overload and short-circuit currents in a mode O-CO-CO. In cascade circuits of power supply of industrial facilities the circuit breakers should possess ability selectively to disconnect separate consumers on which emergency currents arise.

In the past decades designs of contact breakers were not subjected to fundamental changes. Designs of contact systems, arc chambers, mechanisms of trip and trip-free are still built on known principles. Development engineering of new designs of breakers go by the way of perfection of separate units and in a greater degree their arrangement for the purpose of decrease of dimensions of breakers.

Application of contactless devices and their hybrids with contact breakers in power supply systems of industrial facilities is limited yet. It is connected with technical parametres of semi-conductor devices and with requirements of safety rules of maintenance personnel (contactless devices do not provide a galvanic isolation of switched circuits).

Nonselective breakers, which it is commonly supposed that they are opened "instantly", have own time of switching-off, that is time from moment of fault inception till moment of opening of contacts is from 30 to 70 *ms*.

Selective breakers, which have a special adjustable delay of switching-off during time of short-circuit current, can open in a range from 0,1 to 0,7 *s*.

In table 1.3 we can see quantity of energy which is generated by arc in place of short-circuit depending on its duration.

Table 1.3. Quantity of energy generated in place of short-circuit depending on its duration at I_{cu}=80 *кА*, U_{arc}=60 *V*, $W_{sc}= I_{cu} \cdot U_{arc} \cdot t_{sc}$.

T_{sc}, ms	1,0	12	25	100	250	500	1000
W_{sc}, kJ	5	58	120	480	1200	2400	4800

In case of switching-off of short-circuit current, for example, equal 80 кА (r.m.s.) during time not exceeding several units of milliseconds, an energy generated by arc in place of short-circuit, does not bear considerable mechanical and thermal damage to an electric equipment and a housing in which these equipment are estab-

lished. In case of switching-off of short-circuit current by nonselective or selective breakers: place of short-circuit is subjected to considerable mechanical and thermal damage. Accordingly it can lead to occurrence of a fire and injuries of maintenance personnel, including to human victims. Special hazard is causes by short-circuit in the cable lines. Under influence of high temperature of arc discharge their isolation instantly dissolves that leads to its ignition and then aluminium conductors. Caloric content of cables isolation is equal 5000 *kcal/kg* and aluminium - 7900 *kcal/kg*. Therefore to extinguish ignition of cables is very difficult.

According to catalogues of foreign companies rated currents of high-speed current-limiting circuit-breakers, as a rule, do not exceed 2000 A. Development of high-speed breakers of high rated currents (above 2000A) is interfaced to considerable technical difficulties.

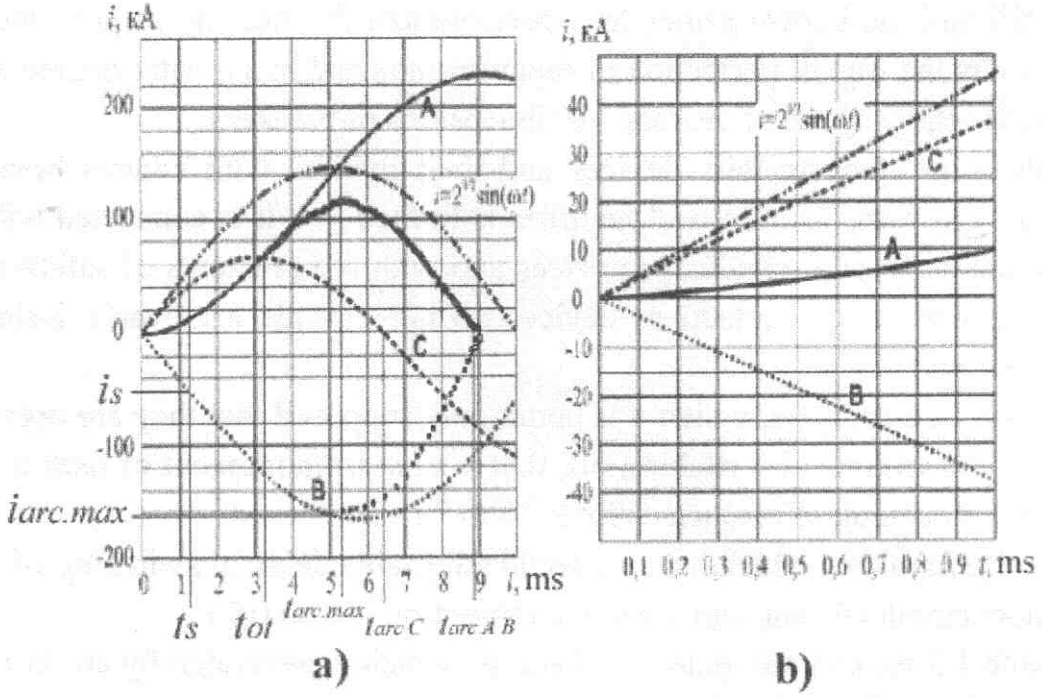

Fig.1.9. Change of a current in three-phase system: a) during 10 *ms* from beginning of short-circuit; b) during 1,0 *ms*.

In Fig. 1.9 change of short-circuit current equal 100 кА (r.m.s.) in three-phase system is shown:

- i_s – setting current of short-circuit clearing;
- t_s – time to setting current of short-circuit clearing;
- t_{ot} – opening time of breaker;
- $i_{arc\ max}$ – maximal instantaneous current of arc;

- $t_{arc\ max}$ – time of maximal instantaneous current of arc $i_{arc\ max}$;
- $t_{arc\ C}$ – time point of arc extinguishing in phase C;
- $t_{arc\ A\ B}$ - time point of arc extinguishing in phases A and B.

Three periods are distinguished in a switching-off total time t_{arc} current of short-circuit by high-speed breakers. Duration of the first period before achievement of a setting current of a breaker i_s by short-circuit current is equal t_s. Time t_{ot} - opening time of breaker is a basic indicator characterising speed of breaker. In electric circuit with frequency of a current 50 *Hz*, steepness of increase of short-circuit current is rather considerable, and delay in some milliseconds is accompanied by large increase of current in protected circuit. Obviously, for maximum limitation of short-circuit current, this component of tripping time should be probably smaller.

In this work the third stage of switching-off of short-circuits by high-speed breaker will be considered. Immovability time of metal-liquid bridge and arc arising on opening contacts enter into this stage.

Contacts opening of breakers at switching-off of any values of a current intensity in electric circuits containing inductance is accompanied by formation of metal-liquid bridge from a liquid-melt in a spot of contacting where current constriction takes place. Forming mechanism of a bridge and its destruction is various at different values of a current intensity. Destruction mechanism of bridge has the features at switching-off of short-circuit currents [1.1, 1.3]. Existence time of a bridge is equal to 0,5 *ms* at switching-off of short-circuit currents by argentiferous contacts. Velocity of contacts opening of automatic switches, as a rule, does not exceed 2,0 *m/s*. At such velocity of contacts opening during time equal 0,5 *ms* a gap between them will become about 1,0 *mm*. In these conditions depending on value of a current intensity a bridge can or easy evaporate or can be subjected to damage by electric (thermal) explosion. However a bridge can be destroyed mechanically by means of a pulse magnetic field.

For more intensive arc extinguishing in some designs of contactors and actuators the magnetic blasting is applied. It is created by series coils in a combination with ferromagnetic systems. In [1.8] it is shown that intensity of a field of the magnetic blasting created by series coils in devices with rated current up to 1000 *A*, can reach several hundreds of oersted. Because of design features of devices of magnetic blasting in their magnetic systems at enough great values of current intensity there comes saturation and magnetic field dispersion.

A motive power setting an arc in motion is force of interaction of a current I with external magnetic field H. This force per unit length of the arc channel is de-

fined by the formula [1.8]

$$f = 1{,}02 \cdot I \cdot H \cdot 10^{-4}\ g/cm,$$

where I – arc current, A and H – external magnetic field intensity, Oe. Let us underline that key parametre defining motive power influencing arc is defined by product of $I \cdot H$. As the field intensity equal 1,0 Oe corresponds numerical to magnetic induction B=1,0 Gs further for an estimation of the force influencing arc parameter $I \cdot \hat{A}$, $A \cdot Gs$ will be used.

According to [1.8] arc on parallel electrodes with gap between them 10 mm at $I \cdot B = 10^3\ A \cdot 10^3\ Gs = 10^6\ A \cdot Gs$ can move with velocity 145 m/s. At gaps between electrodes in a range of 1,0-2,0 mm and $I \cdot B = 400A \cdot 930Gs = 3{,}72 \cdot 10^5\ A \cdot Gs$ arc can move with velocity 90-100 m/s. However at current $7 \cdot 10^3 A$ between copper electrodes at distance between them 1,0 mm and iron electrodes 2,0 mm there was liquid-drop crosspiece which remained motionless.

At a current 400 A the metal-liquid bridge arose at gap between electrodes 0,3 mm. At $I \cdot B = 3{,}72 \cdot 10^5\ A \cdot Gs$ this bridge could move on electrodes with velocity ~3 m/s. If to present that the metal-liquid bridge has arisen on the opening contacts at their length 20 mm than at speed of its movement of 3,0 m/s the bridge can leave contact gap in time:

$$t_{br} = \frac{l}{v_{br}} = \frac{20 \cdot 10^{-3} m}{3{,}0 m/s} = 6{,}67 ms.$$

Average time of arc immovability at switching-off of short-circuit currentsat at velocity of contact opening 2,0 m/s is 5,45 ms according to data [1.1, part II, p. 54]. In this time alternating short-circuit current in electric circuit will grow and can reach almost maximum value. For current-limiting circuit-breaker it is inadmissible.

It is experimentally established that at switching-off of short-circuit currents arc starts to move on contacts when contact gap is not less (8-10) mm. Velocity of opening contacts in automatic circuit breakers of domestic and foreign manufacture, as a rule, is no more than 2,0 m/s. The gap equal δ=10 mm, at speed of disconnection of contacts υ=2,0 m/s will be reached in time

$$t = \frac{\delta}{\upsilon} = \frac{10 \cdot 10^{-3} m}{2{,}0 m/s} = 5{,}0 \cdot 10^{-3} s = 5{,}0 ms.$$

Moreover, a voltage on motionless arc between contacts does not exceed 60 *V* and it is much more below peak value of phase voltage of test loop making 341 *V* or 592 *V* depending on circuit rated voltage [1.1, part II, p. 241].

At such proportion of arc voltage and phase voltage arc current cannot be limited considerably in relation to expected short-circuit current. For these two reasons short-circuit current will grow after opening of contacts during ~5,0 *ms*.

If to give velocity of opening contacts ~ (6-8) *m/s* than rise time of short-circuit current will be equal [1.1. part II, p. 119]:

$$t_{arc.\max} = \frac{l}{\upsilon} = \frac{10 \cdot 10^{-3} m}{(6 \div 8) m/\mathrm{s}} = (1{,}67 \div 1{,}25) \cdot 10^{-3} s.$$

Time (1,67-1,25) *ms* appears also long enough as during this time not only short-circuit current continues to grow but also contacts are exposed to the maximum erosion [1.1, part II, p.129]. Therefore at contact opening it is necessary to put to arc an external pulsed magnetic field which would throw out arc from the contact gap equal (1,0-2,0) *mm*. Under the specified conditions time of a arc delay on the contacts and rise of short-circuit current will be:

$$t_{arc.\max} = \frac{l}{\upsilon} = \frac{2{,}0 \cdot 10^{-3} m}{(6 \div 8) m/\mathrm{s}} = (0{,}33 \div 0{,}25) \cdot 10^{-3} s.$$

As time $t_{arc.max}$ = (0,33-0,25) *ms* is less than existence time of the metal-liquid bridge arising at the moment of contact opening which on experimental data is ~0,5 *ms* than at performance of the above-stated conditions, rise of arc curren practically will stop "instantly" and the metal-liquid bridge will collapse in advance. Both specified circumstances, in turn, will increase operational service life of a breaker.

For acknowledgement of possibility of split of the metal-liquid bridge and drops of metals by means of pulsed magnetic fields the breadboard model (fig. 1.9.1) was produced, consisting of electrodes (1) and the coils (2) connected on series and between themselves and electrodes.

Under the arrangement with manager of electrophysical laboratory of Belarus Academy of Science M.K. Mitckevich (Doctor of Engineering Science) and its employee A.I. Bushik (Candidate of Physical and Mathematical Sciences), experiments were carried out with help of the equipment of the specified laboratory equipped with enough powerful condenser installation with charge voltage upto 600 *V* and ultra-

rapid film camera SFR. Between electrodes with gap 1 *mm* a copper wire in diameter

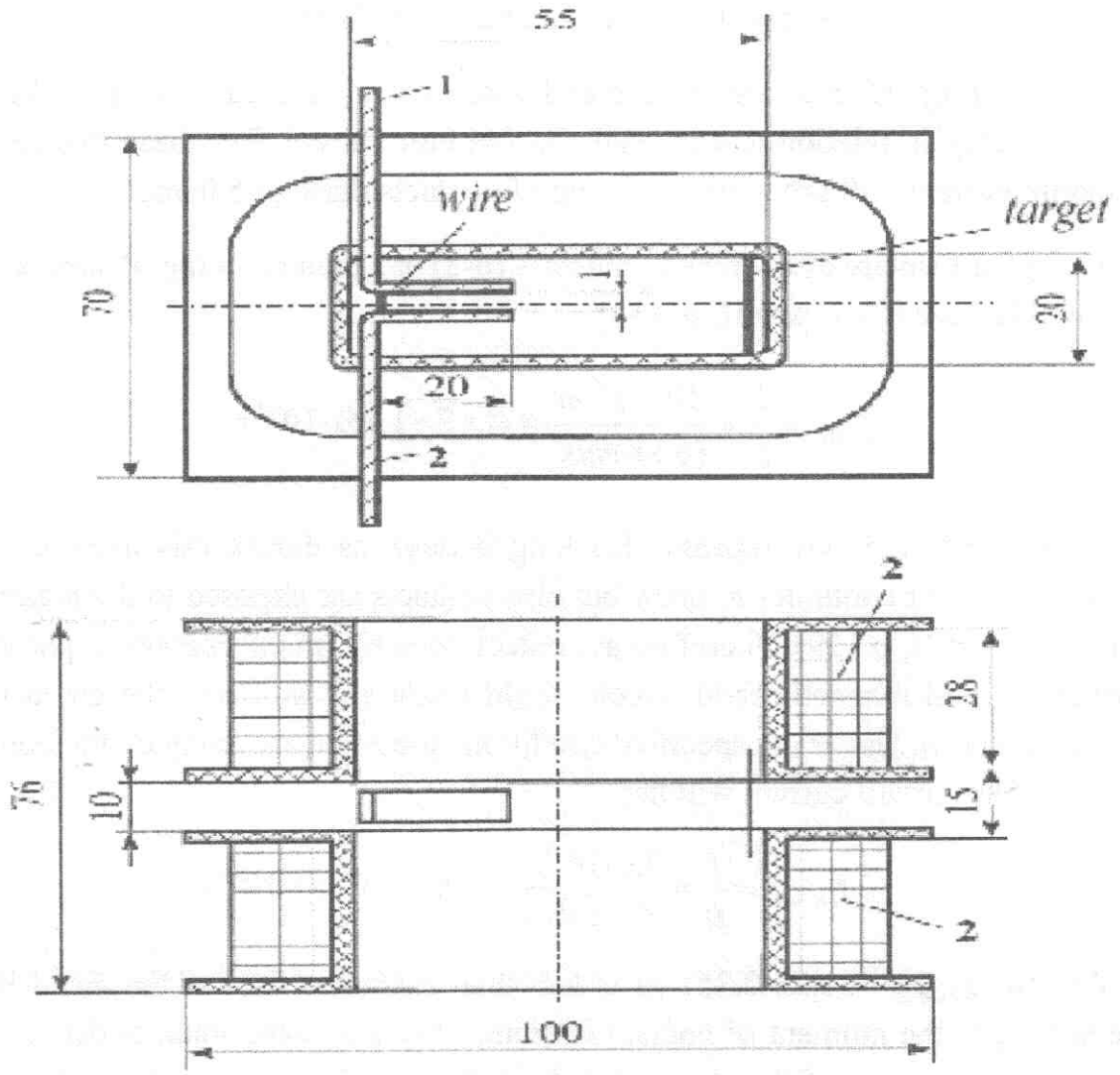

Fig. 1.9.1. The scheme of a breadboard model for investigation of magnetic explosion of a copper wire between electrodes

of 0,35 *mm* was established. Synchronously with discharge the camera was started. Speed of filming was 250000 *shorts/s*. On distance approximately 40 *mm* from electrodes in a direction of emission of plasma flow the glass target which should catch drops was established. After each test it was taken pictures of the rests of the fused wire on surfaces of electrodes, the traces left basic spots of arc at its movement, and the drops which have settled on a target. On a place of the blown up wire an arc was raised. The drops formed as a result of explosion of a delay represent its splinters.

With help of records of ultra-rapid filming the form and length of plasma flow, speed of distribution of front of flow and arc movement on electrodes were defined.

In the absence of external magnetic field, due to burn-out of copper wire arc at the maximum instant value of current intensity 2150 *A* was displaced on edge of electrodes and left considerable melting. On electrodes the fused rests of a wire (fig. 1.10, a) were observed. On the target the drops were absent.

In the presence of pulsed field with the maximum induction about 3000 *Gs* and a current 2150 *A* on a place of explosion of a copper wire the insignificant its melted rests were observed. Arc traces on electrodes were rather wide (their greatest size was 6 *mm*) and occupied a surface of electrodes on all their length from the location of the wire to their forward edge. On electrodes the melting traces were absent (fig. 1.10, b). Distribution velosity of front of plasma flow in a direction of action of a magnetic field was more than 400 *m/s*. On a target there was a set of drops of metal with the sizes upto 200 *μm*.

At application of pulsed magnetic field with the maximum magnetic induction of 12700 *Gs* on electrodes there were weak traces in the form of a path with width of 3 *mm* without melting and tracks of movement of very small droplets of liquid copper (fig. 1.10, c).

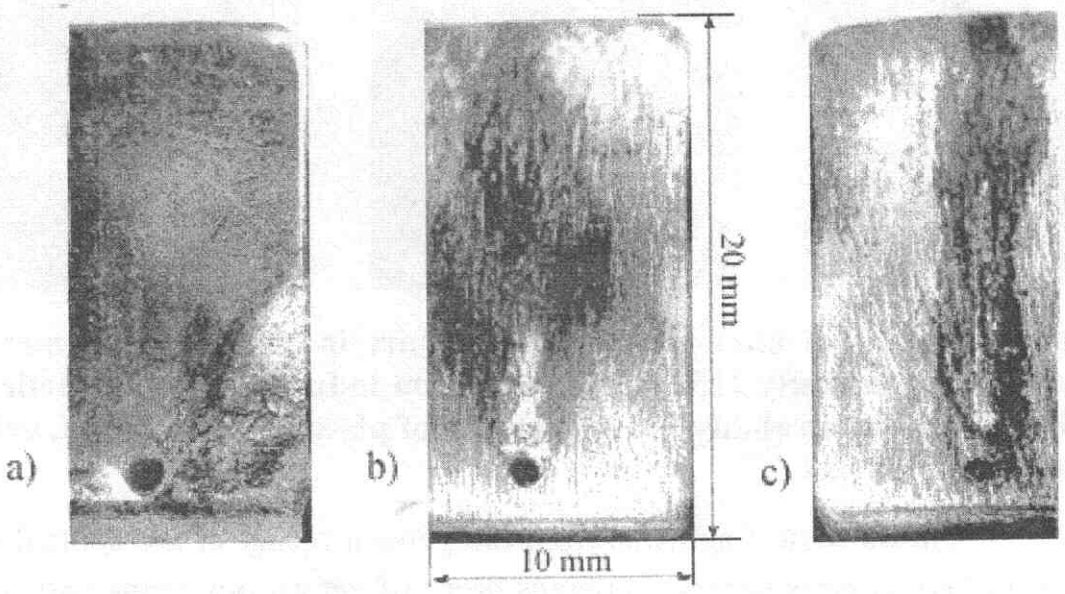

Fig. 1.10. A kind of a surface of electrodes as a result burn-out of copper wire with diameter 0,35 *mm* in electrodes gap equal 1,0 *mm*. The maximum instant value of a current is 2150 *A*. a) Arc traces on electrodes in case of absence of external magnetic field, b) Arc traces on electrodes at influence of pulsed magnetic field with induction of 3000 *Gs*, c) Arc traces on electrodes at influence of pulse magnetic field with induction 12700 *Gs*

In fig. 1.11 consecutive shots of ultra-rapid filming of burn-out of wire, emission of arc and plasma flow from contact gap 1 *mm* by pulsed magnetic field with induction B = 12700 *Gs* are shown. In this case, time of arc immobility was 130 μs. This time includes time of burn-out of wire also. Velocity of movement of plasma flow front was 720 *m/s*, and velocity of movement of arc was 158 *m/s*. The magnetic field blows from contact gap and plasma in the form of torches and arc simultaneously. But velocity of movement of plasma flow front is considerably above velocity of movement of arc. The powerful pulsed magnetic field together with emission of plasma in the form of torches clears a contact gap from the rests of the blown up wire and metal steams.

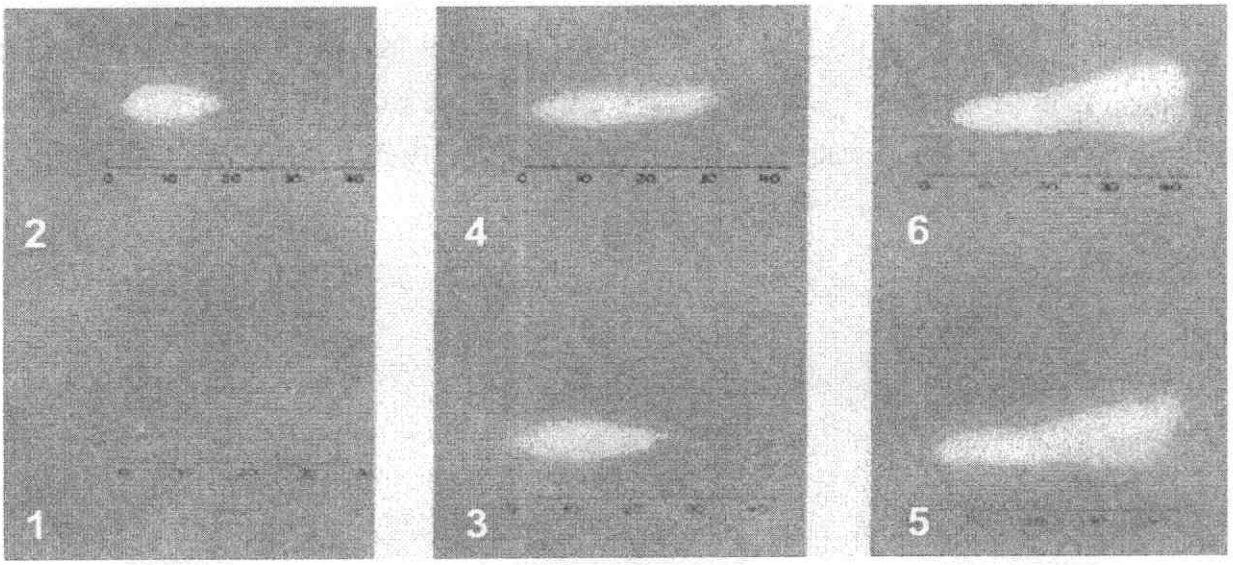

Fig. 1.11. Shots of ultra-rapid filming of arc in contact gap 1 *mm*. The maximum current intensity 2150 *A*, the maximum induction of a magnetic field 1,27 *T*, time of arc immovability 130 μs, velocity of plasma front 720 *m/s*, velocity of arc movement 158 *m/s*

Fig. 1.12 shows some fragments from the general plenty of the splitted drops which have settled on glass targets. In photos drops of the various forms with a wide spectrum of their sizes are well visible. Liquid drops at flight as a result of influence of forces of aerodynamic pressure get the form of flat disks in which there are breaks, and further there is their splitting (fig. 1.12, a and b).

Let us especially notice the interesting fact, consisting that on targets there were many families of drops, at which in the centre of absolutely correct circle formed by small drops there is rather large drop (fig. 1.12, c). At flight large drops are not simply split up, and from their surface more small drops fall down which dissipate on a

cone with a corner in top ~ 20'. At impact of drops with a surface of a target they get a little extended form in a radial direction from the circle centre. In some cases small drops have tails in the form of thin threads which show a direction of flight of drops.

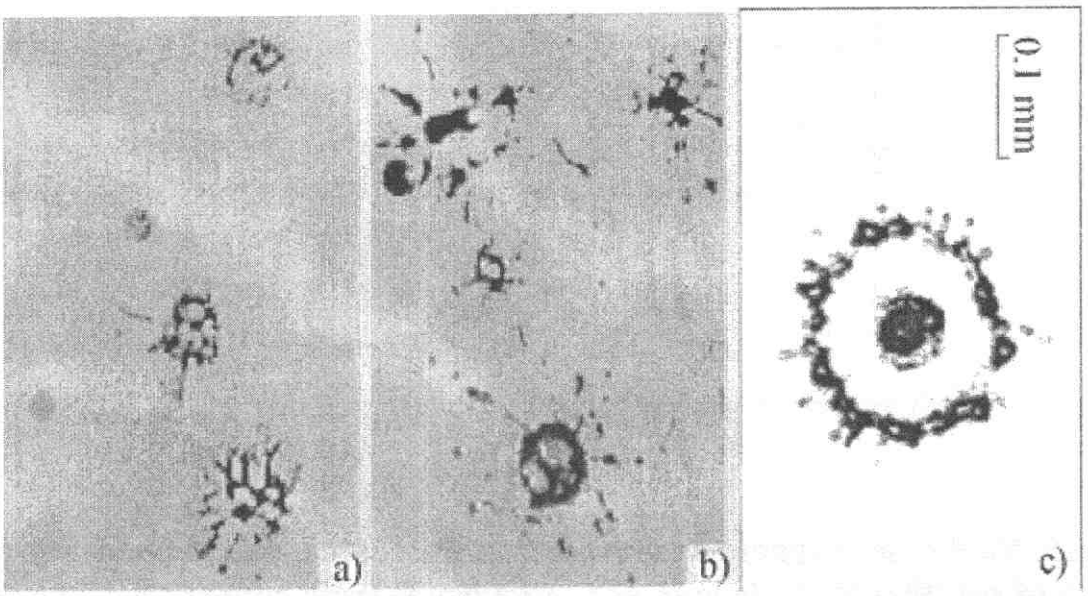

Fig. 1.12. Separate fragments of the splitted drops which are the rests of the blow-out wire settled on targets

At last, it is possible to draw a conclusion that arc at speed of movement 100-150 *m/s* and length of contacts of 20 *mm* can leave contact gap 1 *mm* during 0,15-0,2 *ms*. So that arc has begun movement on contacts, the front of plasma stream should move with a speed not less than 250 *m/s* at which rather large drops will be split up [1.1, part II, p. 74].

According to experimental data, for maintenance of splitting of the bridge and drops, product of value of a current intensity of arc i_∂ and magnetic field induction B in gap between contacts should be not less:

$$I_{arc} \cdot B = 2150\ A \cdot 3000\ Gs = 6{,}5 \cdot 10^6\ A \cdot Gs$$

Fig. 1.13 shows a plot of minimum magnetic induction B in the gap between the contacts, necessary for maintenance of arc movement and splitting of the bridge and large drops from copper, depending on instant value of a current intensity i_{arc}. Necessary value of magnetic induction in contact gap should be provided or for the account of circuit of contact system or external electromagnetic devices. We will notice that such conditions would allow extinguishing arc successfully and at switching-off of small critical currents and of rated currents repeatedly.

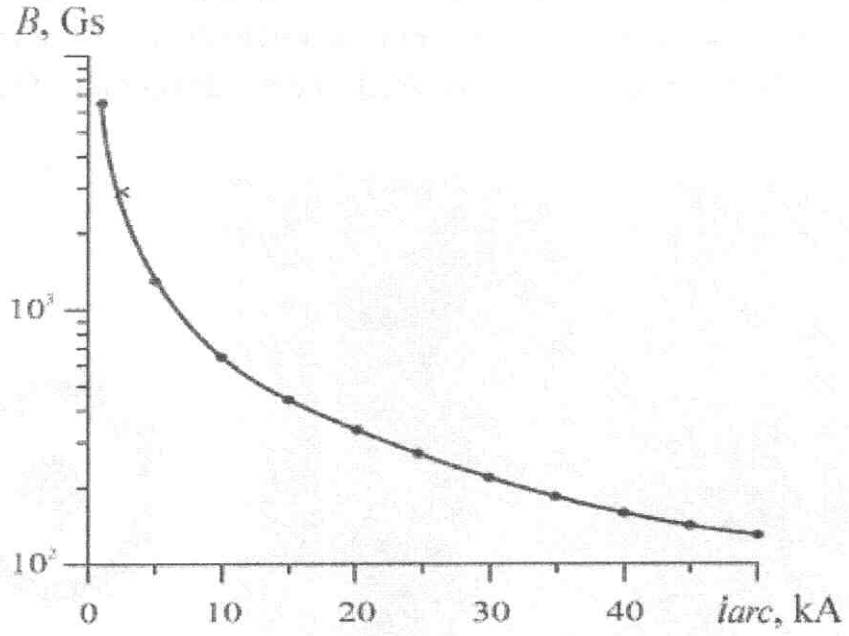

Fig. 1.13. Minimum magnetic induction *B* in the contact gap necessary for maintenance of splitting of the bridge and large drops from copper wire and start of arc motion depending on instant value of current intensity $i_{arc.}$

For fast-speed current-limiting circuit breaker rated current 6300 *A* and rated voltage of circuit 660 *V* it was been developed an original design of series coil of the magnetic blasting, combined with a design of fixed arcing contact without application of the ferromagnetic system shown in fig. 1.14 [1.9].

Fixed arcing contact established on upper current lead of circuit breaker represents series electromagnetic coil consisting of two parallel coils connected by a crosspiece on which ceramic-metal contact (CMC) is soldered. Opening contacts are disposed between two coils in their window. The similar relative positioning of opening contacts and coil windows provide maximum influence of a magnetic field of the coil on the electric arc arising at switching-off both small critical and rated currents, and overload and short-circuit currents. The series coil should provide minimum time of arc immovability on the contacts at their opening.For estimation of influence of magnetic blasting on the metal-liquid bridge and arc in an area of their occurrence there were been calculated the form of magnetic fields (Fig. 1.15) and numerical values of magnetic induction at values of currents 63 and 630 *A* corresponding to small critical currents for automatic circuit breakers and at rated current 6300 *A*. The results of calculations are given in table 1.3.1. Calculations have been executed for contact gap 2,0 *mm*, that is length of arc is equal 2,0 *mm* and its diameter has been accepted equal 2,0 *mm*.

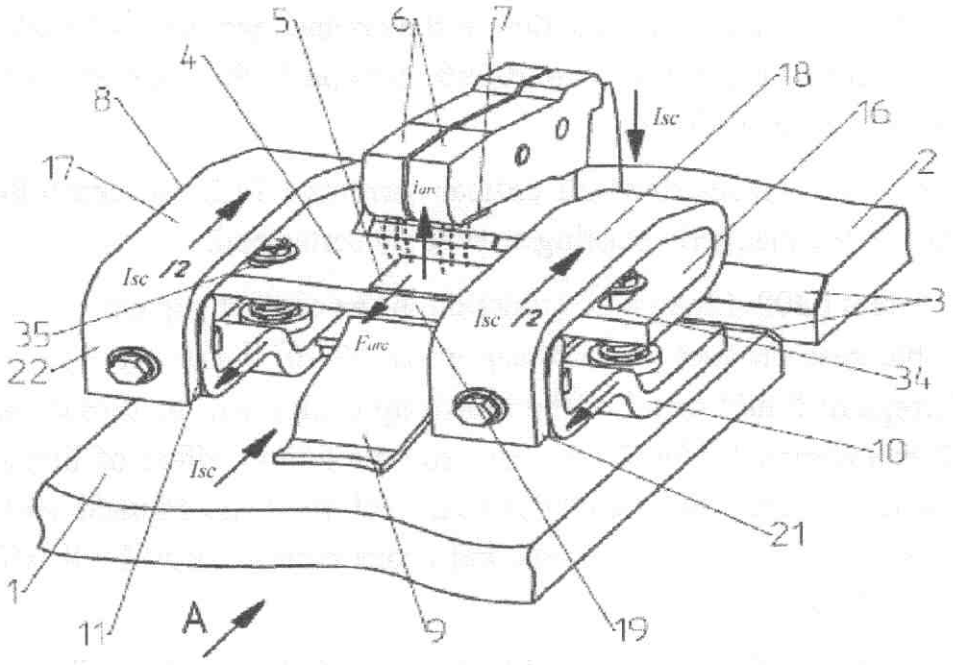

Fig. 1.14. The contact system combined with series coil of magnetic blasting

At a current in the loop 63 *A* magnetic induction in the area of contact opening from series coil can make (8-11) *Gs*, according to [1.8] velocity of arc movement will be not less than 10 *m/s* and it will be extinguished in time less than 0,1 *s*.

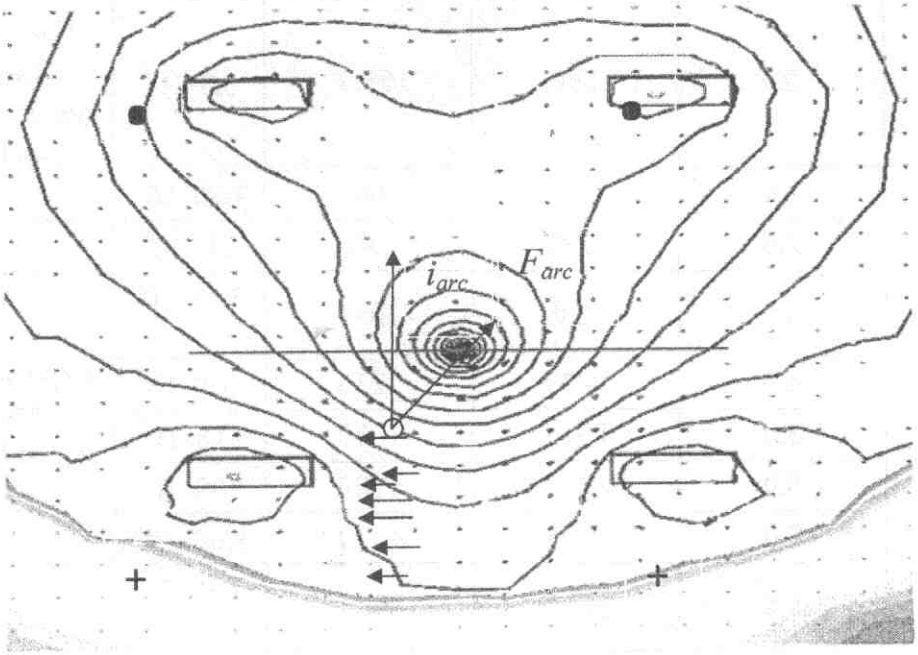

Fig. 1.15. The form of magnetic field created by series coil in an area of arc initiation

At a current 630 *A* magnetic induction in the contact gap can make 60 *Gs*, and velocity of arc movement is not less than 20 *m/s* and and in this case time of arc extinguishingc does not exceed 10 *ms*.

Hence, arc at any values of small critical currents will be successfully extinguished by means of the magnetic blasting created by series coil.

At rated current 6300 *A* magnetic induction in the contact gap can exceed value of 1000 *Gs*. In that case product of $I \cdot \hat{A}$ can make $\geq 7 \cdot 10^6\ A \cdot Gs$. At $I \cdot \hat{A} \geq 6{,}5 \cdot 10^6\ A \cdot Gs$ arc and drops of liquid metal of the blown up bridge will be thrown out from contact gap 1,0 *mm* during 0,15-0,2 *ms*. Thus the maximum effect of limitation of growth of short-circuit current will be reached. Arc will move on contacts with velocity $\geq$ 100 *m/s*, the forward front of plasma and drops carried away by it will move with velocity upto 400 *m/s*.

Table 1.3.1. Parametres of the magnetic blasting created by series coil

Current of test loop, *A*	Time of contact opening, *ms*	Instant value of arc current, *A*	Total value of induction, *Gs*	$I \cdot \hat{A}$, $A \cdot Gs$	Remark
63	5,0	89	11,0	980	$v_{arc} = 10 m/s$ arc will be extinguished
630	5,0	890	65,0	$5{,}8 \cdot 10^4$	$v_{arc} = 20 - -30 m/s$ arc will be extinguished
6300	1,0	2753	386	$1{,}06 \cdot 10^6$	
	2,0	5237	743	$3{,}9 \cdot 10^6$	
	3,0	7208	1037	$7{,}47 \cdot 10^6$	Explosion of a bridge $v_{arc} = 150 m/s$
	4,0	8473	1236	$1{,}05 \cdot 10^7$	
	5,0	8910	1320	$1{,}18 \cdot 10^7$	
	6,0	8473	1280	$1{,}09 \cdot 10^7$	
	7,0	7208	1120	$8{,}08 \cdot 10^6$	
	8,0	5237	855	$4{,}48 \cdot 10^6$	
	9,0	2753	509	$1{,}4 \cdot 10^6$	

At such velocity of movement the drops from Ag, Cu and Ni will be split up for small parts that will allow arc to move freely between contacts and behind their limits [1.2, part II, p. 74, fig. 4.38]. The surface of contacts practically will not be exposed melting and their wear will be insignificant, and operational service life of a circuit breaker will essentially increase.

Breadboard model has been made for a purpose of confirmation operational efficiency of contact system with magnetic blasting [1.9] in a form of series coil combined with fixed contact of breaker. In the breadboard model a lamina has been rigidly fixed instead of mobile contact. A gap between contacts was constant and equal 2,0 *mm*. In intercontact gap a copper wire with diameter 1,0 *mm* was fixed.

As a power supply a special facility of direct current with maximal value 8000 A served. Voltage was equal to some units of volts. Thus, at fusion of wire a drop of liquid metal was formed which shorted both contacts. Under influence of force arising at interaction of a current, flowing through a drop, and magnetic field, a drop takes off from a contact gap. A current interrupts and arc discharge is not initiated because of a low voltage. Its value was less value of arcing voltage.

In Fig. 1.15.1 one can see oscillograms of current, flowing through a wire and a drop of liquid metal, and voltage drops on melting wire and a drop of liquid metal.

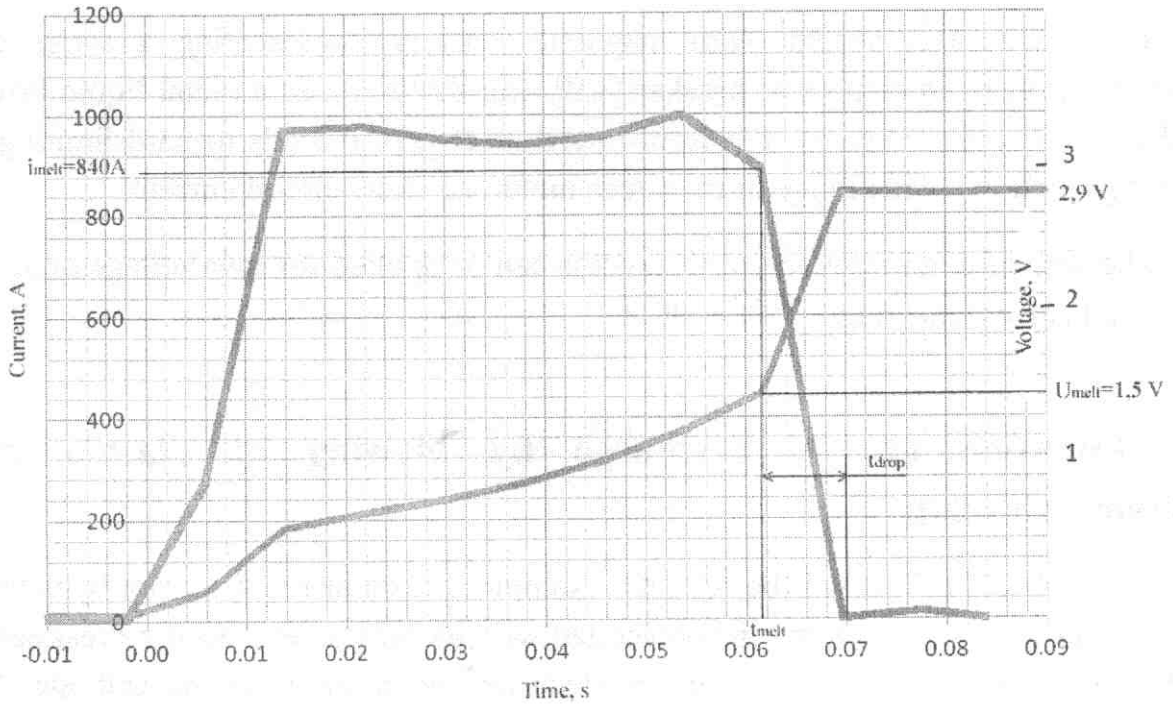

Fig. 1.15.1 Change of a current and voltage on melting wire and a drop of liquid metal located in intercontact gap equal 2,0 *mm*.

From the oscillogram it is visible that the current through wire has not exceeded

1000 A. It is possible to receive a value of current equal to more than 1000 *A* only by opening of contacts. The wire has fused at the moment of time t_{melt} at current intensity equal i_{melt}=840 *A* and voltage U_{melt}=1,5 *V*. At the moment of time t_{drop} a drop took off from intercontact gap and a current in a circuit interrupted.

A glass was established on distance of 10 *cm* from a forward edge of contacts for catching of drops. At the moment of time of current interruption a specific click of hit of a drop in glass was sounded. Then glass have been removed and a drop had flown on distance more than 3,0 *m*.

As a result of numerical integration a potential energy of a drop has been equal W_{drop}=7,39 *W·s*, at taking-off of a drop from intercontact gap a potential energy converses in kinetic one:

$$W_{drop} = \frac{m_{drop} \cdot V_{drop}^2}{2},$$

where m_{drop}=34,6·10^{-3} *g* – mass of a drop from liquid copper with diameter 2,0 *mm*.

From here initial velocity of flight of a drop is equal to:

$$V_{drop} = \left(\frac{2 \cdot W_{drop}}{m_{drop}} \right)^{1/2} = \left(\frac{7{,}39 \cdot 10^7 erg \cdot 2}{34{,}6 \cdot 10^{-3} g} \right)^{1/2} = 6{,}5 \cdot 10^4 \frac{cm}{s} = 650 \frac{m}{s}.$$

Thus, a contact system with magnetic blasting, representing a series coil combined with fixed contact of breaker [1.9], can throw out as a metal-liquid bridge as electric arc effectively enough from intercontact gap. It leads to hard limiting of current growth in a wide range of its values including short-circuit current.

The similar contact system with success can be applied for low-voltage breakers with rated current in a range 250÷6300 *A*.

1.4. Initiation of arc discharge by blowing of plasma into interelectrode gap

In [1.10, p. 137] it will be seen the example of excitation of arc not by contact opening but blowing of plasma in contact gap with its subsequent electric breakdown. In that case arc was started due to autoelectronic emission from the cathode. Arc starting can be achieved by blowing into contact gap in which it will start due to thermoionic emission. As an example in fig. 1.16 some shots of high-speed filming of arc starting in arc chamber with deion plates due to blowing of plasma.

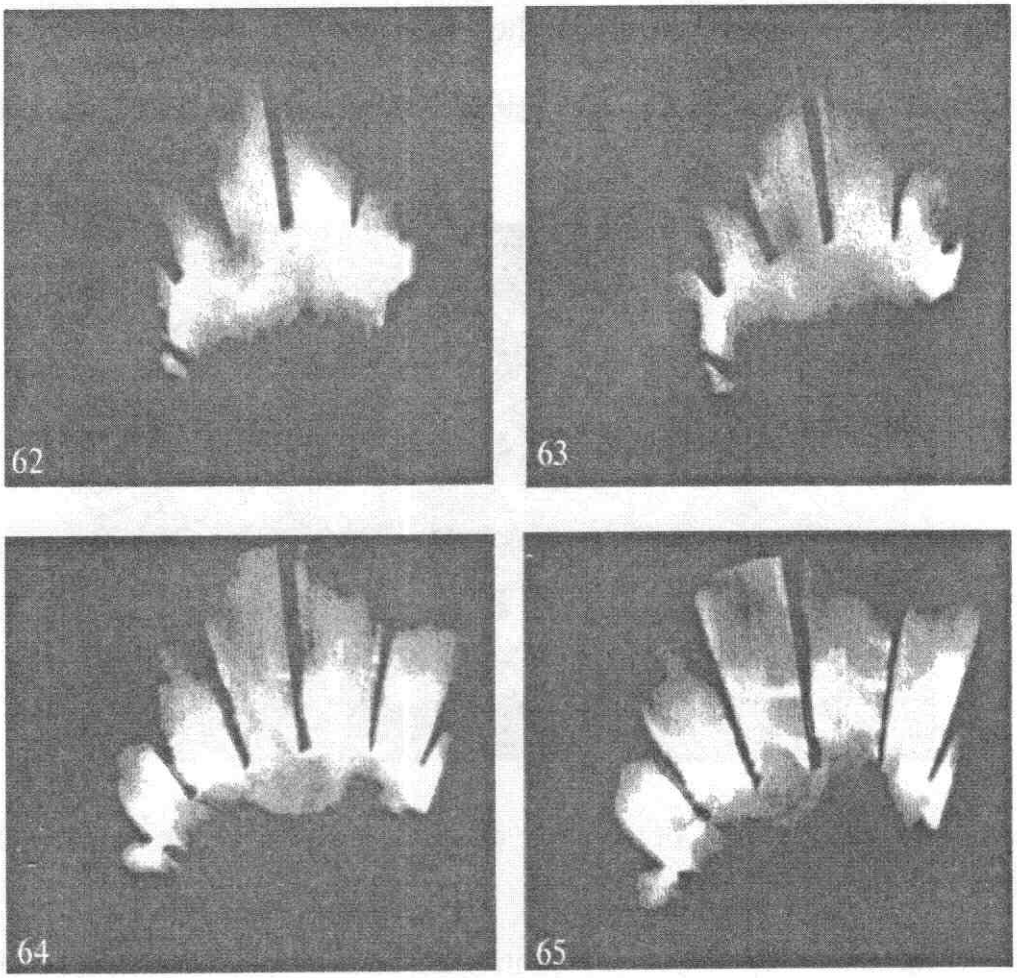

Fig. 1.16. Arc starting between deion plates of arc chamber due to inflowing of plasma at $i_{arc.max}$=2,5 *кА*;exposition of one shot 0,167 *ms*

Maximum instant value of a arc current was $i_{arc.max}$ =2,5 *кА* at phase voltage 420*V*. Distance between the bottom edges of plates is equal 24 *mm*. Plasma of diffuse arc gradually envelops a surface of the plates. Their temperature is equal to an ambient temperature. In 0,7 *ms* glowing points were appeared on cathodic and anodic sides of the plates after contact of plasma with their surface. From these points the discrete jets of the plasma. Hereafter these jets formed arc discharge with the split core between deion plates. In this case due to thermionic emission arc was started between electrodes which preliminary were cold.

According to oscillogram given in [1.1, part II, p. 292, fig. 6.20], it is seen a direction of potentials on deion plates at the moment of time of contact opening at switching-off of electric circuit. It occurred long before the moment of time of the beginning of inflowing of plasma in the gaps between deion plates. As at direction of potentials on deion plates their surfaces had got certain polarity than at inflowing of

plasma in arc chamber electrons direct to the anode and ions - to the cathode.

There are microroughnesses on a surface of copper-coated deion plates (see fig. 1.17).

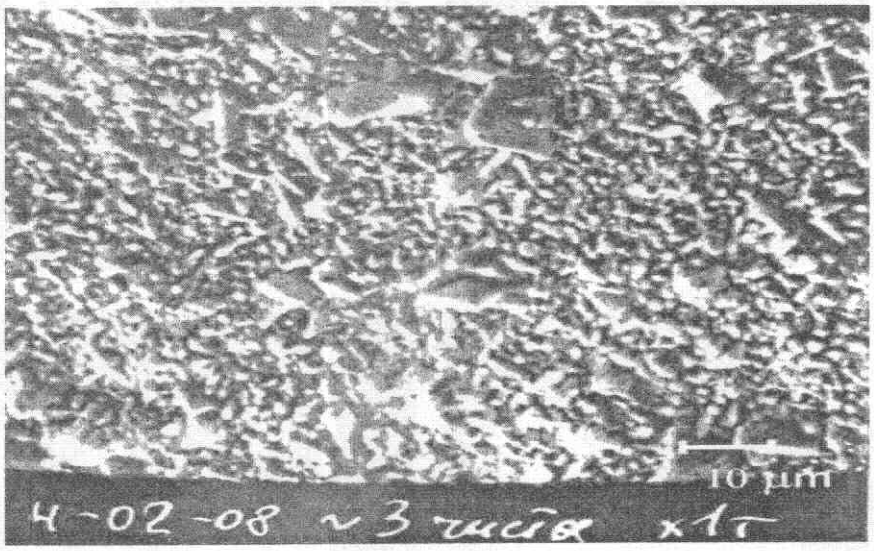

Fig 1.17. Non-erodable area of surface of electrolytic copper coating of deion plate (zoom x1000)

Such microstructures can be the centres of concentration of charges on which power lines of electric field concentrate. Under influence of this field the centres of concentration of charges are exposed to electrone and ion bombardment which causes formation of microjets of plasma.

In [1.1, fig. 21, p. 40] it is shown arc chamber of breakers rated currents 4000 and 6300 *A*, short-circuit breaking capacity at rated voltage 380 *V* is 65 and 115 *кA* (r.m.s.) respectively. In fig. 1.18 there is oscillogram of current and voltage at switching-off of circuit current 65 *кA* during operation O. Maximum instant value of arc current was in phase B and was equal $i_{arc.max}$=79,4 *кA*.

In fig. 1.19 the deion plates are shown after switching-off of a current 65 *кA* in a mode O-CO-CO. The distance between deion plates in the arc chute was 17 *mm*. The arc completely entered into a chute and got diffusse form with the splitted core. Discrete erosive traces of arc distributed in regular intervals on all area of plates. Erosion of plates has appeared superficial and insignificant, practically without loss of its weight.

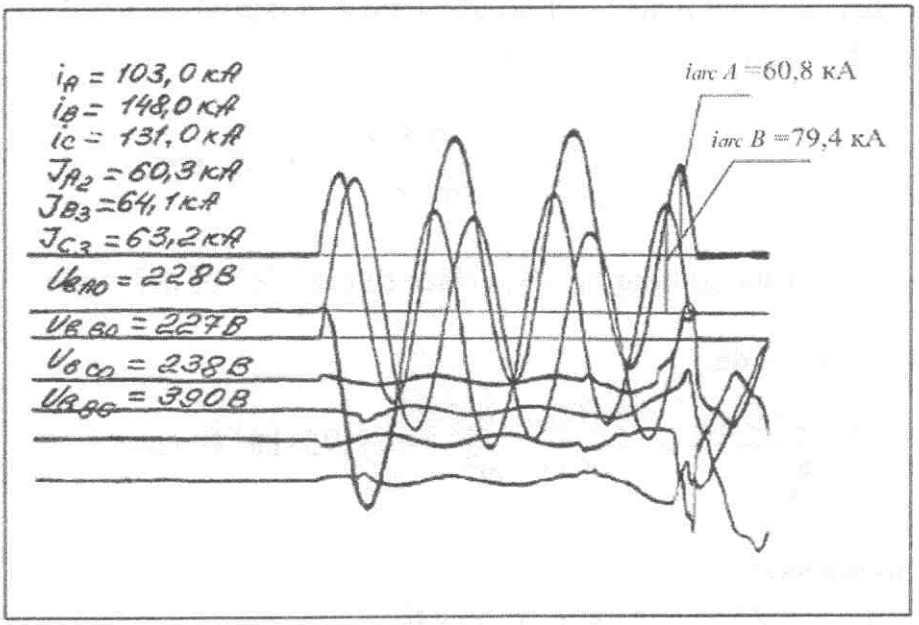

Fig. 1.18. The oscillogram of current and voltage arc at current switching-off of current in the loop 65 *кА* by the circuit breaker in operation "O"

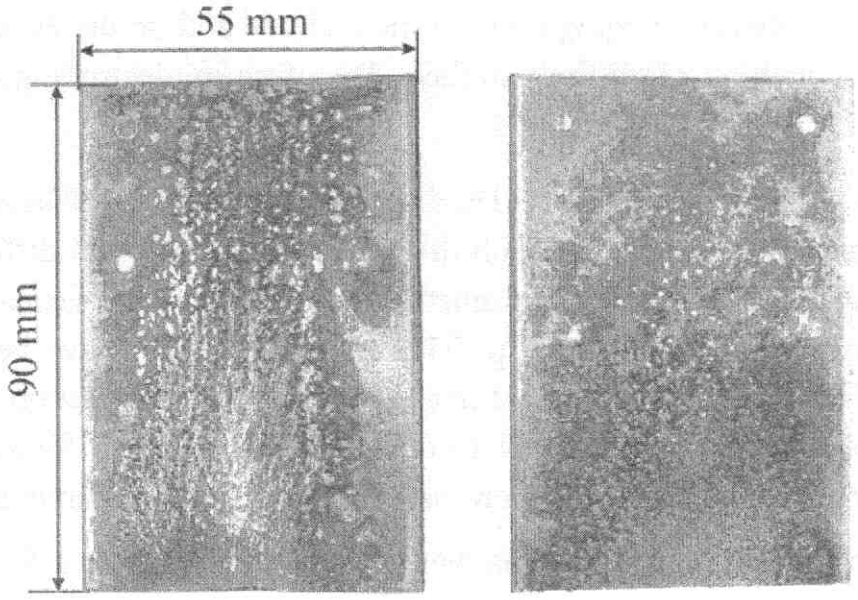

anode **cathode**

Fig. 1.19. Erosive traces of arc with the split vore on the cathodic and anodic parties of deion plates after switching-off of current 65 *кА* in a mode O-CO-CO

An average current intensity of arc dispersed in regular intervals on all area the deion plate which is equal $S_{d.pl} = 49{,}5\ cm^2$:

$$j_{av.arc.den} = \frac{i_{arc.\max}}{S_{d.pl}} = \frac{79400\ A}{4950\ mm^2} = 16\ A/mm^2.$$

The power density coming on all surface of one side of deion plate is:

- on the cathodic side:

$$q_{c.d.pl} = \frac{i_{arc.\max} \cdot U_{ef.c}}{S_{d.pl}} = \frac{79400\ A \cdot 6{,}2\ V}{49{,}5\ cm^2} = 9{,}95 \cdot 10^3\ W/cm^2;$$

- on the anode side:

$$q_{a.d.pl} = \frac{i_{arc.\max} \cdot U_{ef.a}}{S_{d.pl}} = \frac{79400\ A \cdot 13{,}8\ V}{49{,}5\ cm^2} = 2{,}21 \cdot 10^4\ W/cm^2.$$

Here $U_{ef.c} = 6{,}2\ V$ - cathodic and $U_{ef.a} = 13{,}8\ V$ - anode effective potentials on copper electrodes according to [1.11].

The power density coming both on the cathode and on the anode is obviously insufficient for melting of all their surface. Therefore in electrode gap of length 17 *mm* a diffuse arc with split core forms.

On the photos given in fig. 1.19, definition of the sizes of basic spots of discrete jets of plasma of diffuse arc with the split core causes great difficulties. Therefore, for estimated calculations of parametres of discrete jets of plasma it is reversible to the data resulted in [1.1, part I, p. 258, table 3.4] which have been received at switching-off of circuit current 50 *кА (r.m.s.)* by arc chute with copper-coated deion plates with gaps between them equal 16 *mm*. That is conditions for switching-off of short-circuit currents in both tests were practically equal. The maximum diameter of anode spots of discrete jets of plasma was 0,15 *cm,* and their area $S_{bs.dj} = 1{,}77 \cdot 10^{-2}\ cm^2$.

The quantity of relatively large base spots of discrete jets of plasma on the anode can be accepted $n_{dj} \sim 115$ for one switching-off of short-circuit current according to fig. 1.19. In the given test an average value of current of a discrete jet of plasma can be equal:

$$i_{dj} = \frac{i_{arc.\max}}{n_{dj}} = \frac{79400\ A}{115} = 690\ A.$$

This value of a current equals to maximum average value of a current of discrete jets of plasma (683 A) given in [1.1, part I, p. 258].

Power density coming on a base spot of discrete jet of plasma on the anode equals:

$$q_{bs.dj} = \frac{i_{dj.av} \cdot U_{ef.a}}{S_{bs.dj}} = \frac{690\ A \cdot 13{,}8\ V}{1{,}77 \cdot 10^{-2}\ cm^2} = 5{,}38 \cdot 10^5\ W/cm^2.$$

At density of power $\geq 10^5\ W/cm^2$ all metal on the area of a base spot of discrete jet of plasma will be in melted condition.

Under the influence of power density $5{,}38 \cdot 10^{12} erg/(s \cdot cm^2)$ time of warming up of a surface of base spot of discrete jet of plasma from ambient temperature T_0=313 K (40^{0}C standard specified temperature) to melted temperature Cu T_{melt}=1356 K equals [1.13, p. 54]:

$$\tau_{bs.melt} = \frac{\pi\lambda c\rho(T_{melt} - T_0)^2}{4q_{bs.dj}^2} = \frac{\pi \cdot 352 \cdot 10^5 \frac{erg}{s \cdot cm \cdot K} \cdot 0{,}461 \cdot 10^7 \frac{erg}{g \cdot K}}{4(5{,}38 \cdot 10^{12} \frac{erg}{s \cdot cm^2})^2} \times$$

$$\times 8{,}29 g/cm^3 \cdot (1356K - 313K)^2 = 4{,}0 \cdot 10^{-5} s.$$

Here $\lambda = 352 \cdot 10^5 \frac{erg}{s \cdot cm \cdot K}$ – heat conductivity Cu at temperature 1200 K, $c = 0{,}461 \cdot 10^7 \frac{erg}{g \cdot K}$ – specific thermal capacity Cu at temperature 1300 K, $\rho = 8{,}29 g/cm^3$ – density Cu at melting temperature T_{melt} = 1356 K [1.1, table 1.8, p. 69].

Time of warming up of a surface of base spot of discrete jet of plasma from melting temperature to boiling temperature Cu T_{boil} = 2840 K:

$$\tau_{bs.boil} = \frac{\pi\lambda c\rho(T_{boil} - T_{melt})^2}{4q_{bs.dj}^2} = \frac{\pi \cdot 352 \cdot 10^5 \frac{erg}{s \cdot cm \cdot K} \cdot 0{,}62 \cdot 10^7 \frac{erg}{g \cdot K}}{4(5{,}38 \cdot 10^{12} \frac{erg}{s \cdot cm^2})^2} \times$$

$$\times 7{,}73 g/cm^3 \cdot (2840K - 1356K)^2 = 1{,}0 \cdot 10^{-4} s,$$

where $\rho = 7{,}73\ g/cm^3$ – density Cu at boiling temperature T_{boil}, $c = 0{,}62 \cdot 10^7 \frac{erg}{g \cdot K}$ – specific thermal capacity of copper at temperature 1800 K [1.1, part I, p. 106].

Total time of achievement of boiling temperature by a surface of base spot of discrete jet of plasma on copper under influence of power density $q_{bs.dj} = 5{,}38 \cdot 10^5\ W/cm^2$ is:

$$\tau_{boil} = \tau_{bs.melt} + \tau_{bs.boil} = (0{,}4 + 1{,}0) \cdot 10^{-4}\ s = 1{,}4 \cdot 10^{-4}\ s.$$

According to experimental data of investigations of arc extinguishing of high power in the breakers [1.1] time of existence of discrete jets of plasma equals from 0,2 to 2,8 *ms*. That is on a base spot of discrete jet of plasma liquid melt is formed. During its existence its temperature can reach boiling temperature of electrode metal.

For comparison of time of fixing of arc base spots to deion plates with coating Cu6 and Ni6 we will accept power density coming on base spot of discrete jet of plasma of diffuse arc with split core equals $5{,}38 \cdot 10^5\ W/cm^2$.

Time of warming up of a surface of base spot of discrete jet of plasma by power density $5{,}38 \cdot 10^{12} \frac{erg}{s \cdot cm^2}$ from ambient temperature T_0=313 K to melting temperature Ni T_{melt}= 1728 K equals:

$$\tau_{bs.melt} = \frac{\pi\lambda c\rho(T_{melt} - T_0)^2}{4q_{bs.dj}^2} = \frac{\pi \cdot 72 \cdot 10^5 \frac{erg}{s \cdot cm \cdot K} \cdot 0{,}595 \cdot 10^7 \frac{erg}{g \cdot K} \cdot}{4(5{,}38 \cdot 10^{12} \frac{erg}{s \cdot cm^2})^2} \times$$

$$\times 7{,}764 g/cm^3 \cdot (1728K - 313K)^2 = 1{,}82 \cdot 10^{-5} s.$$

Here $\lambda = 72 \cdot 10^5 \frac{erg}{s \cdot cm \cdot K}$ – heat conductivity Ni at temperature 1000 K,

$c = 0{,}595 \cdot 10^7 \frac{erg}{g \cdot K}$ – specific thermal capacity Ni at temperature 1100 K,

$\rho = 7{,}764\ g/cm^3$ – density of liquid Ni at temperature 1773 K [1.1, table 1.8, p. 69].

Time of warming up of a surface of base spot of discrete jet of plasma from melting temperature to boiling temperature of Ni $T_{boil} = 3003\ K$:

$$\tau_{bs.boil} = \frac{\pi\lambda c\rho(T_{boil} - T_{melt})^2}{4q_{bs.dj}^2} = \frac{\pi \cdot 72 \cdot 10^5 \frac{erg}{s \cdot cm \cdot K} \cdot 0{,}595 \cdot 10^7 \frac{erg}{g \cdot K}}{4(5{,}38 \cdot 10^{12} \frac{erg}{s \cdot cm^2})^2} \times$$

$$\times 7{,}714 g/cm^3 \cdot (3003K - 1728K)^2 = 1{,}47 \cdot 10^{-5} s.$$

Total time of achievement of boiling temperature by a surface of base spot of discrete jet of plasma on nickel under influence of power density $5{,}38 \cdot 10^5\ W/cm^2$ is:

$$\tau_{boil} = \tau_{bs.melt} + \tau_{bs.boil} = (1{,}82 + 1{,}47) \cdot 10^{-5}\ s = 3{,}29 \cdot 10^{-5}\ s.$$

Let us estimate time of a fixing of base spots of discrete jets of plasma to the deion plates made of steel 08 without coating under influence of power density $5{,}38 \cdot 10^5\ W/cm^2$. In that case time of warming up of a surface of base spot of discrete jet of plasma from ambient temperature T_0=313 K to melting temperature of steel 08 T_{melt}= 1808 K is:

$$\tau_{bs.melt} = \frac{\pi\lambda c\rho(T_{melt} - T_0)^2}{4q_{bs.dj}^2} = \frac{\pi \cdot 29 \cdot 10^5 \frac{erg}{s \cdot cm \cdot K} \cdot 0{,}666 \cdot 10^7 \frac{erg}{g \cdot K}}{4(5{,}38 \cdot 10^{12} \frac{erg}{s \cdot cm^2})^2} \times$$

$$\times 7{,}3 g/cm^3 \cdot (1808K - 313K)^2 = 8{,}64 \cdot 10^{-6} s.$$

here $\lambda = 29 \cdot 10^5 \frac{erg}{c \cdot cm \cdot K}$ – heat conductivity of steel 08 at temperature 1200 K,

$c = 0{,}666 \cdot 10^7 \frac{erg}{g \cdot K}$ – specific thermal capacity of steel 08 at temperature 1300 K,

$\rho \sim 7{,}3\ g/cm^{-3}$ – density of Fe at temperature 1808 K [1.1, table 1.8, p. 69].

Time of warming up of a surface of base spot of discrete jet of plasma from melting temperature to boiling temperature of steel 08 T_{boil}= 3023 K.

$$\tau_{bs.boil} = \frac{\pi\lambda c\rho(T_{boil} - T_{melt})^2}{4q_{bs.dj}^2} = \frac{\pi \cdot 29 \cdot 10^5 \frac{erg}{s \cdot cm \cdot K} \cdot 0{,}666 \cdot 10^7 \frac{erg}{g \cdot K}}{4(5{,}38 \cdot 10^{12} \frac{erg}{s \cdot cm^2})^2} \times$$

$$\times 6{,}86 g/cm^3 \cdot (3023K - 1808K)^2 = 5{,}3 \cdot 10^{-6} s,$$

where $\rho = 6{,}86 g/cm^3$ – density of Fe at boiling temperature $T_{boil.}$

Total time of achievement of boiling temperature by a surface of base spot of discrete jet of plasma on steel 08 under influence of power density $5{,}38 \cdot 10^5 W/cm^2$ is:

$$\tau_{boil} = \tau_{bs.melt} + \tau_{bs.boil} = (8{,}64 + 5{,}3) \cdot 10^{-6} s = 1{,}39 \cdot 10^{-5} s.$$

Thus, time of fixing of base spots of arc to electrodes at the same power density depends on their material:

$$\tau_{boil}^{Cu} = 1{,}4 \cdot 10^{-4} s > 3{,}29 \cdot 10^{-5} s = \tau_{boil}^{Ni} > 1{,}39 \cdot 10^{-5} c = \tau_{boil}^{Fe}.$$

However especially it is necessary to pay attention to expediency of coating of deion plates with protective oxide films (for example, black oxide treatment). In a case of black oxide treatment of deion plates time of fixing of base spots of arc at its entering arc chute will be minimum. In a case of diffuse arc with split core numerous base spots of discrete jets of plasma will have the minimum cross-section sizes. These spots will regularly cover all surface of deion plates without their appreciable erosion [1.1, part I, p. 233, fig. 3.37, p. 235], and also see [1.1, part II, fig. 5.23 (colour insert)].

It is necessary to notice also that time of fixing of base spots of arc to electrodes depends on its current intensity. At $i_{arc.max}$=79,4 κA power density coming on base spot of discrete jet of plasma in diffuse arc with split core was equaled $5{,}38 \cdot 10^5 W/cm^2$, and time of fixing of arc to the electrode made of steel 08 was equaled $1{,}39 \cdot 10^{-5} s$. In [1.1] it is shown that at current in test loop 5,9 κA power density coming on base spot of discrete jet of plasma was equaled $4{,}16 \cdot 10^4 W/cm^2$.

Time of fixing of discrete jet of plasma to the electrode made of steel 08 at power density $4{,}16 \cdot 10^4\ W/cm^2$ was equaled $2{,}32 \cdot 10^{-3}\ s$ [1.1, part II, p. 195].

Average value of current density in base spot of discrete jet of plasma is:

$$j_{bs.dj} = \frac{i_{dj.av}}{S_{bs.dj}} = \frac{690\,A}{1{,}17 \cdot 10^{-2}\,cm^2} = 3{,}9 \cdot 10^4\ A/cm^2.$$

Pressure in anode region of discrete jet of plasma:

$$P_{dj} = P_{atm} + 9{,}87 \cdot 10^{-9} \cdot j_{bs.dj} \cdot i_{dj.av} = 1{,}0 atm + 9{,}87 \cdot 10^{-9} \times$$
$$\times 3{,}9 \cdot 10^4\ A/cm^2 \cdot 690\,A = 1{,}27 atm.$$

The effective temperature of plasma of a discrete jet can be defined from the formula:

$$q_{rad} = 5{,}6 \cdot 10^3 \cdot \beta \cdot \left(\frac{T_{ef}}{100}\right)^4 \frac{erg}{s \cdot cm^2},$$

[1.1, part II, p. 365], if to accept that all energy of plasma from the jet`s channel is lost by radiation in environment. Such assumption can be comprehensible, if the effective temperature of plasma is enough high [1.1, part II, p. 115, fig. 4.60 and p. 118, fig. 4.62].

$$T_{ef.dj} = 10^2 \left(\frac{q_{rad}}{5{,}6 \cdot 10^3 \cdot \beta}\right)^{1/4} = 10^2 \left(\frac{5{,}38 \cdot 10^{12}\ \frac{erg}{s \cdot cm^2}}{5{,}6 \cdot 10^3 \cdot 0{,}6}\right)^{1/4} = 2 \cdot 10^4\ K.$$

here β=0,6 – emissivity factor for plasma of arc burning in steams of metals [1.12].

Really, effective temperature of a discrete jet of plasma has appeared enough high, therefore the accepted assumption is quite pertinent.

Concentration of one-nuclear steams Cu at $T_{ef} = 2{,}0 \cdot 10^4\ K$ and pressure ~ 1,0 *atm* equals [1.1, part I, p. 69, table 1.7]:

$$n_0 = n_{boil} \cdot \frac{T_{boil}}{T_{ef}} = 1{,}6 \cdot 10^{18}\ cm^{-3}\ \frac{2840 K}{20000 K} = 0{,}227 \cdot 10^{18}\ cm^{-3}.$$

Degree of ionisation of steams Cu at $T_{ef} = 2{,}0 \cdot 10^4\ K$ and pressure ~ 1,0 *atm* can be accepted equal x_e~1,0 [1.1, p. 327]. In such plasma concentration of electrons is equal to:

$$n_e = n_0 \cdot \frac{\mathrm{x}_e}{1+\mathrm{x}_e} = 0{,}227 \cdot 10^{18} cm^{-3} \cdot 0{,}5 = 0{,}114 \cdot 10^{18} cm^{-3}.$$

The directed velocity of electrons in discrete jet of plasma is equal to:

$$\upsilon_e = 0{,}593 \cdot 10^8 \cdot \sqrt{\Delta U_{arc}} = 0{,}593 \cdot 10^8 \sqrt{79V} = 5{,}27 \cdot 10^8 cm/s.$$

In fig. 1.20 it is given microelectronic photos of characteristic traces of discrete jets of plasma on the anode side of deion steel plates with coating from Cu6.

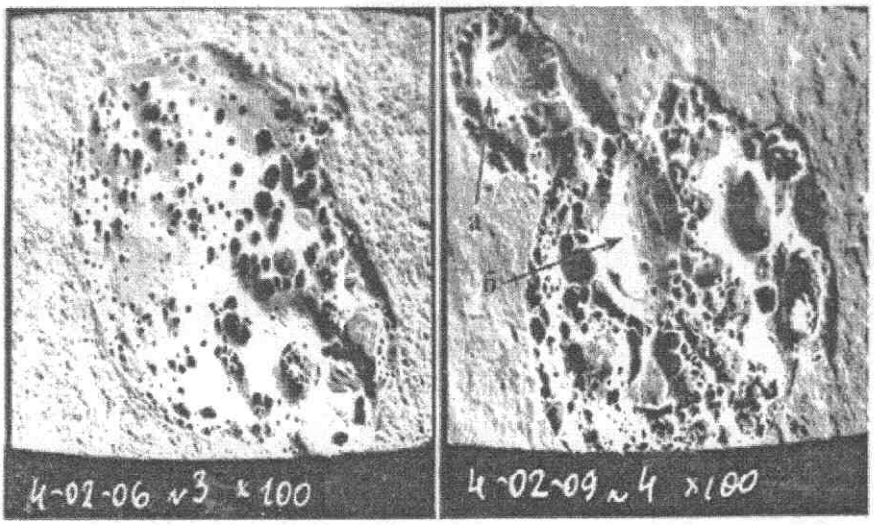

a) b)

Fig. 1.20. Traces of discrete jets of plasma on the anode side of deion plates from steel 08 covered by galvanic way Cu6:

a) $i_{arc.max}$=9,3 кА (×100); b) $i_{arc.max}$=13,7 кА (×100)

In fig. 1.21 it is shown submicroscopical photos of separate areas of erosion of deion plate shown in fig. 1.19.

Fig. 1.20 and fig. 1.21 show numerous craters from which the microjets of plasma flowed out creating a total flow of plasma of discrete jets. Diameters of craters on the copper anode change from fractions to 15 *μm*.

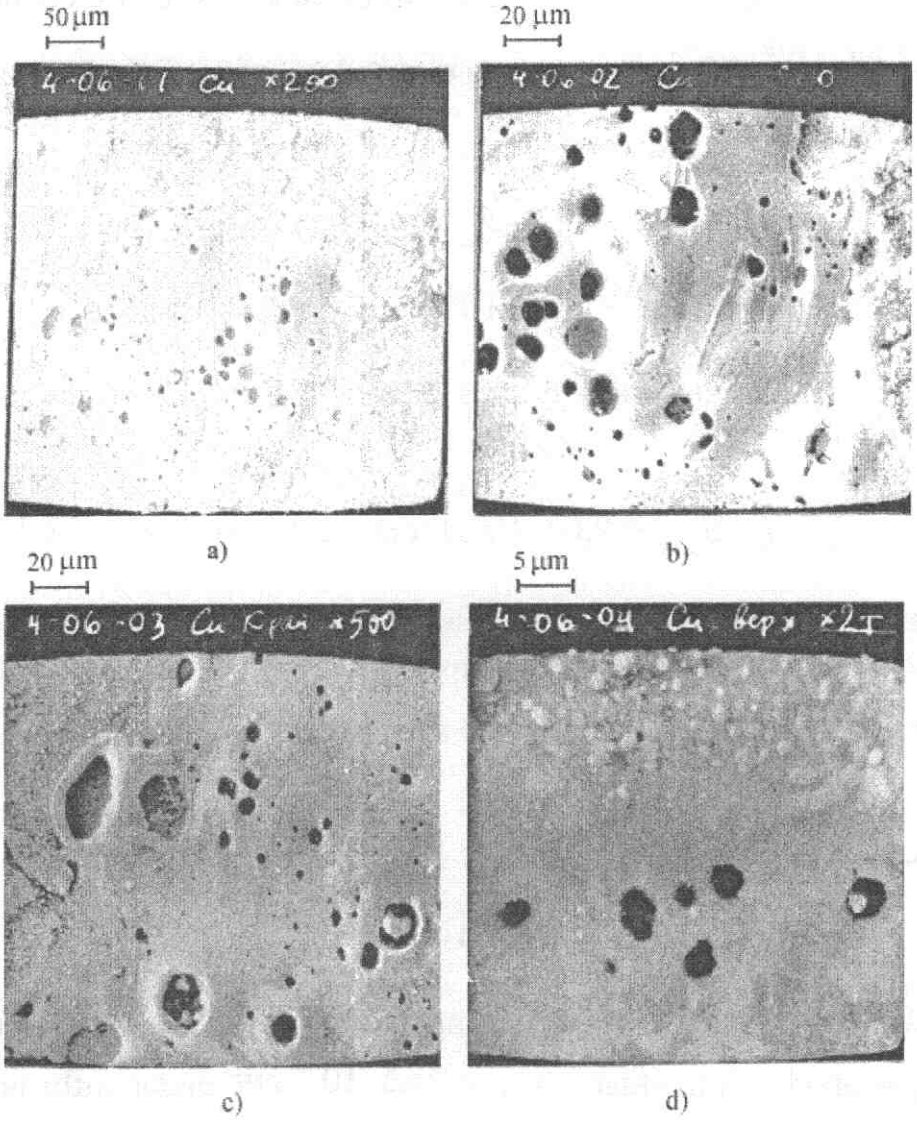

Fig. 1.21. A kind of separate areas of erosion of deion plates in fig. 1.19: a) $\times 200$; **b)** $\times 500$; **c)** $\times 500$; **d)** $\times 2000$; $i_{arc.\max} = 79{,}4\ кА$.

For estimated calculations of parametres of microjets of plasma, we will accept that average diameter of their craters on the anode is: $d_{a.av} = 7 \cdot 10^{-4}\ cm$. Average value of square of such crater is equal to:

$$S_{a.av} = \pi \cdot r_{a.av}^2 = \pi \cdot (3{,}5 \cdot 10^{-4} cm)^2 = 38{,}5 \cdot 10^{-8}\ cm^2.$$

As total flow of plasma of discrete jets is formed by flows of plasma of microjets we will accept that their effective temperature $T_{ef} = 2{,}0 \cdot 10^4\ K$ and electron concentration $n_e = 0{,}114 \cdot 10^{18}\ cm^{-3}$.

If voltage $\Delta U_{arc} \approx 79\,V$, is applied to plasma in which electron concentration $n_e = 0{,}114 \cdot 10^{18}\ cm^{-3}$, that average directed velocity of electrons will be equal to $v_e = 5{,}27 \cdot 10^8\ cm/s$ and average current density of a current:

$$j_к = 3{,}34 \cdot 10^{-10} \cdot e \cdot n_e \cdot v_e = 3{,}34 \cdot 10^{-10} \cdot 4{,}8 \cdot 10^{-10} \times$$
$$\times 0{,}114 \cdot 10^{18} cm^{-3} \cdot 5{,}27 \cdot 10^8 cm/s = 9{,}63 \cdot 10^6\ A/cm^2.$$

In that case a current intensity of a microjet of plasma on the anode will be equal to:

$$i_a = j_к \cdot S_{a.av} = 9{,}63 \cdot 10^6 A/cm^2 \cdot 38{,}5 \cdot 10^{-8} cm^2 = 3{,}7\ A.$$

Let us estimate time of initiation of a thin layer of liquid spot on the surface of copper-coated electrode having initial temperature T_0=313 K. In the case under consideration power density coming on anode spot having square $S_{a.av} = 38{,}5 \cdot 10^{-8}\ cm^2$ is equal to:

$$q_a = \frac{i_a \cdot U_{ef.a}^{Cu}}{S_{a.av}} = \frac{3{,}7A \cdot 13{,}8V}{38{,}5 \cdot 10^{-8} cm^2} = 1{,}33 \cdot 10^8\ W/cm^2.$$

Time for achievement of melting temperature and boiling temperature of a surface of copper anode with square $S_{a.av} = 38{,}5 \cdot 10^{-8}\ cm^2$ under influence of power density $q_a = 1{,}33 \cdot 10^8\ W/cm^2$ is respectively equal:

$$\tau_{a.melt} = \frac{\pi\lambda c\rho(T_{melt} - T_0)^2}{4q_a^2} = \frac{\pi \cdot 352 \cdot 10^5 \frac{erg}{s \cdot cm \cdot K} \cdot 0{,}461 \cdot 10^7 \frac{erg}{g \cdot K}}{4(1{,}33 \cdot 10^{15} \frac{erg}{s \cdot cm^2})^2} \times$$
$$\times 8{,}29 g/cm^3 \cdot (1356K - 313K)^2 = 6{,}49 \cdot 10^{-10} s.$$

$$\tau_{a.boil} = \frac{\pi\lambda c\rho(T_{boil} - T_{melt})^2}{4q_a^2} = \frac{\pi \cdot 352 \cdot 10^5 \frac{erg}{s \cdot cm \cdot K} \cdot 0{,}621 \cdot 10^7 \frac{erg}{g \cdot K}}{4(1{,}33 \cdot 10^{12} \frac{erg}{s \cdot cm^2})^2} \times$$
$$\times 7{,}79 g/cm^3 \cdot (2840K - 1356K)^2 = 1{,}66 \cdot 10^{-9} s.$$

$$\tau_{boil} = \tau_{a.melt} + \tau_{a.boil} = (0{,}649 + 1{,}66) \cdot 10^{-9}\ s = 2{,}31 \cdot 10^{-9}\ s.$$

That is under influence of power density $q_a = 1{,}33 \cdot 10^8\ W/cm^2$ formation time of liquid melt with square $S_{a.av} = 38{,}5 \cdot 10^{-8}\ cm^2$ is equal to $2{,}31 \cdot 10^{-9}\ s$, and it is on some degrees of order less than formation time of liquid melt on base spot of discrete jet of plasma with square $1{,}77 \cdot 10^{-2}\ cm^2$ under influence of power density $5{,}38 \cdot 10^5\ W/cm^2$ ($\tau_{boil}^{Cu} = 1{,}4 \cdot 10^{-4}\ s$).

According to [1.4, p. 354] it is possible to define a formation time of the crater formed by means of Joule heat of metal by currents and diffusions of heat by heat conductivity with of help of the formula:

$$t_{cr} = \frac{r_{cr}}{4 \cdot a},$$

where a – temperature conductivity coefficient of metal which depends on its temperature; r_{cr} – crater radius.

In a considered example crater formation time for a copper anode with radius $r_{a.ñð} = 3{,}5 \cdot 10^{-4}\ ñì$ is equal to:

$$t_{cr.a} = \frac{r_{a.av}^2}{4 \cdot a_{liq}} = \frac{(3{,}5 \cdot 10^{-4}\ cm)^2}{4 \cdot 0{,}42 cm^2/s} = 7{,}29 \cdot 10^{-8} s,$$

where $a_{liq} = 0{,}42 cm^2/s$ – temperature conductivity coefficient of Cu in liquid condition [1.4, p.123].

Let us pay attention to that for liquid melt Cu time of achievement of boiling temperature is slightly less than time of formation of a crater:

$$t_{a.boil} = 1{,}4 \cdot 10^{-9} s < 7{,}29 \cdot 10^{-8} s = t_{cr.a}.$$

It means that the crater is formed as a result of initiation of microbubbles. From this it follows that under influence of a thermal flow of plasma accumulating on a surface of deion plate, in the beginning in time ~10^{-9} s on the centre of concentration of charges a spot of liquid melt is formed. Then on it in time ~10^{-8} s a microbubble is

appeared which blowing up, throws up a microjet of ionised steams of metal. On the place of the blown up microbubble a crater remains.

Around discretely the arisen craters on the anode a liquid melt of Cu arises which extends gradually. Then the liquid melt merges round nearby craters. On a surface of the liquid melt a bubble boiling with blowing up microbubbles arises. On extended liquid melt a base spot of a discrete jet of plasma is formed. The great number of simultaneously functioning microjets of plasma, chaotically located on base spot, leads to formation of electromagnetic plasma whirlwind of discrete jet of plasma under influence of own magnetic field [1.1, part I, p. 246].

Obviously, excess pressure in the microjet of plasma, flowing from microbubble, equaled:

$$P_к = 9{,}87 \cdot 10^{-9} \cdot j_к \cdot i_к = 9{,}87 \cdot 10^{-9} \cdot 9{,}63 \cdot 10^{6} \frac{A}{cm^2} \cdot 3{,}7A = 0{,}35atm,$$

can not lead to high erosion of deion plates at explosion of the microbubbles.

The given results of calculations and experimental investigations of erosive traces on deion plates of arc chute of low-voltage breakers at switching-off of short-circuit currents give ground to draw a conclusion that at flowing of plasma on electrode the fundamental starting mechanism of initiation of arc discharge is singular blown up microbubble on its surface. Delay time of initiation of discrete microjet of plasma on the anode from Cu can be equal to $(10^{-9} \div 10^{-8})s$ from moment of time of beginning of flowing plasma on the centre of concentration of charges till moment of time of beginning of flowing of ionised steams of metal carring a current.

In [1.14] it is in details shown that erosive traces of arc discarges on the cathode and the anode from different materials have a different appearance, structure and geometrical dimensions. For example, on the cathode diameters of microcraters change from 0,3 to 5,0 μm. In [1.1, part I, p. 222] also a difference of forms, structures and dimensions of cathodic and anode traces on different materials of electrodes is shown at switching-off of short-circuit currents by breakers.

For estimated calculations of initiation time of microjets of plasma flowing out from the cathode we will accept that average diameter of their craters is $d_{c.av} = 2 \cdot 10^{-4} cm$. Average value of crater square is equal to:

$$S_{\kappa.av} = \pi \cdot r_{\kappa.av}^2 = \pi \cdot (1 \cdot 10^{-4} cm)^2 = 3{,}14 \cdot 10^{-8} cm^2.$$

Formation time of crater on copper liquid melt with diameter $2 \cdot 10^{-4} cm$ is equal to:

$$t_{cr.c} = \frac{r_{cr}^2}{4 \cdot a_{liq}} = \frac{(1 \cdot 10^{-4} cm)^2}{4 \cdot 0{,}42 cm^2 / s} = 6 \cdot 10^{-9} s.$$

Obviously that formation time of a crater on the cathode, in which size is less than on the anode, should be shorter than formation time of a crater on the anode. Really:

$$t_{cr.c} = 6 \cdot 10^{-9} s < 7{,}29 \cdot 10^{-8} s = t_{cr.a}.$$

That is at inflowing of plasma in electrode gap of the plasma microjets carrying a current arise on the cathode and the anode out of step. Initiation of the first microjet of plasma does not mean initiation of the self-sustained arc discharge. The self-sustained arc discharge can be initiated only when electrons from the cathode will reach the anode and will subject to its bombardment and ions - from the anode-cathode.

For estimation of initiation time of the self-sustained arc discharge it is necessary to consider flight time of electrons and ions through electrode gap.

The average distance between deion plates in the given test is equal to l=2,5 *cm*. Electrons at their average velocity of directed movement $\upsilon_e = 5{,}27 \cdot 10^8 cm/s$ will reach the anode in time:

$$t_e = \frac{l}{\upsilon_e} = \frac{2{,}5 cm}{5{,}27 \cdot 10^8 cm/s} = 4{,}74 \cdot 10^{-9} s.$$

Under influence of voltage between electrode gap $\Delta U = 79V$, velocity of directed movement of ions is equal to [1.1, part II, p. 45]:

$$\upsilon_{ion} = 0{,}134 \cdot 10^6 \sqrt{\Delta U} = 0{,}134 \cdot 10^6 \sqrt{79V} = 1{,}19 \cdot 10^6 cm/s.$$

Flight time of ions from the anode to the cathode will be equal:

$$t_{ion} = \frac{l}{\upsilon_{ion}} = \frac{2{,}5 cm}{1{,}19 \cdot 10^6 cm/s} = 2{,}1 \cdot 10^{-6} s.$$

Hence, time from a moment of beginning time of leakage a plasma flow on the centres of concentration of charges on the cathode till a moment of time of beginning of bombardment by electrons, flowing from the cathode, the anode is equal to:

$$t_{e.c} = t_{cr.c} + t_e = 6 \cdot 10^{-9} s + 4{,}74 \cdot 10^{-9} s = 1{,}07 \cdot 10^{-8} s.$$

Hence, time from a moment of beginning time of leakage a plasma flow on the centres of concentration of charges on the anode till a moment of time of beginning of bombardment by ions, flowing from the anode, the cathode, is equal to:

$$t_{i.a} = t_{cr.a} + t_i = 7{,}29 \cdot 10^{-8} s + 2{,}1 \cdot 10^{-6} s \approx 2{,}2 \cdot 10^{-6} s.$$

As $t_{i.a} = 2{,}2 \cdot 10^{-6} s >> t_{e.c} = 1{,}44 \cdot 10^{-8} s$, that initiation time $t_{\inf .arc}$ of self-sustained arc discharge from moment of time of beginning of inflowing of plasma flow in the gap between copper-coated deion plates of arc chute at switching-off of circuit current 65 кА (r.m.s.) is equal to:

$$t_{\inf .arc} = t_{i.a} = 2{,}2 \cdot 10^{-6} s.$$

After self-excitation the arc discharge will independently function as a result of physical processes on the cathode and the anode providing self-sustaining of its burning [1.4].

1.5. Forming of arc discharge

At the moment of time of breakage of bridge destroyed either by quiet evaporation or electric explosion an arc discharge arises between the contacts. At switching-off of short-circuit currents a power density coming on a surface of base spots both on the cathode and on the anode at the initial stage of existence of arc is equal to 10^5 W/cm^2. As it has been shown earlier a power density equal 10^5 W/cm^2 is capable to melt a metal surface only. In process of contacts movement and expansion of base spots of arc a power density on base spot decreases to value 10^4 W/cm^2. Power density equal 10^4 W/cm^2 is not capable to melt metal on all area of the base spot. In [1.1, part I, p.300, fig. 3.84] it is shown that because of complexity of a relief on base spots distribution of charges on their surface is very non-uniformly. On those places on which the centres of concentration of electric charges are formed, the power density can reach values $\geq 10^8$ W/cm^2. A power density, equal 10^8 W/cm^2 and more, leads to

electric explosions of microroughnesses on a surface of base spots. At that the craters are formed and plasma microjets are thrown up from them. The craters and plasma microjets are discrete on a surface of base spots and in time. It is the first such microjet of plasma leads to initiation of arc discharge between contacts.

As a result of intensive arrival of steams of contacts metals, spliting of the drops which have arisen at destruction of liquid-metal bridges and formation of microdrops at explosion of microroughnesses on base spots at the initial stage of initiation of arc it is arosen a nonideal plasma in its channel. Time of coexistence of nonideal plasma is equal to from 1,0 to 2,0 *ms* at switching-off of short-circuit currents according to experimental data.

In [1.1, part II, p. 61] it is shown that under condition $\frac{l_{arc}}{r_{bs}} \leq 1{,}0$ (l_{arc} - a length of arc which can be equal to contact gap δ, r_{bs} - radius of base spot of arc) plasma in arc channel is saturated by metal steams of contacts and drops. At value $\frac{l_{arc}}{r_{bs}} \sim$ 0,6÷0,8 plasma in arc channel starts to be saturated with environment gas. At $\frac{l_{arc}}{r_{bs}} >$ 1,0 plasma in arc channel can be accepted for ideal gas. And, the higher a plasma temperature will be, the greater degree it can be accepted for the ideal.

The structures of the base spots and arc channel, which are mutually connected, vary in process of contact opening. At $\frac{l_{arc}}{r_{bs}} \ll 1{,}0$ arc discharge can represent constricted arc with a continuous core [1.1, part II, fig. 5.17 (colour insert)]. At value $\frac{l_{arc}}{r_{bs}} < 1{,}0$ arc discharge takes a form of short constricted arc with a discrete core [1.1, part II, p. 5.18 (colour insert)]. In that case the base spot of arc on opening contacts has continuous melting which is observed on arcing contacts.

At $\frac{l_{arc}}{r_{bs}} < 1{,}0$ as it is experimentally established [1.1, part II, p. 61], arc steadily stands between contacts. At velocity of contact opening 2,0 *m/s* an average time of an

arc immovability is 5,45 *ms*. Arc gets a mobility at $\frac{l_{arc}}{r_{bs}} \geq 1{,}0$. Arc plasma is saturated with environment gas and a response rate of its mass sharply decreases.

Thus, contact opening at switching-off of relatively high current intensity is accompanied by the following consistently proceeding physical processes:

- initiation and destruction of liquid-metal bridge;
- formation of short constricted arc with a continuous core with relation $\frac{l_{arc}}{r_{bs}} << 1{,}0$ in which the channel is saturated by nonideal plasma and microdrops, possessing relatively high response rate and keeping arc in motionless position;
- formation of short constricted arc with a discrete core with relation $\frac{l_{arc}}{r_{bs}} < 1{,}0$, in its channel plasma starts to be saturated by environment gas;
- formation of constricted arc with a discrete core with relation $\frac{l_{arc}}{r_{bs}} \geq 1{,}0$, its plasma saturated by environment gas can be accepted the ideal. Arc gets mobility and leaves the contact gap.

Conclusions to chapter 1

The resulted results of experimental and theoretical investigatios of excitation of arc discharge opening argentiferous contacts and plasma inflowing in the contact gap between the arc chambers plates at switching-off of short-circuit currents by low-voltage brerakers and in the published works of authors [1.2, 1.3, 1.4, 1.8 and 1.14] give the chance to draw following conclusions:

1.1. The metal-liquid bridge arising contacts` opening can damage by either quiet evaporation or electric (thermal) explosion or pulse magnetic (mechanical) explosion.

1.2. The destruction form of metal-liquid bridge depends on a current intensity (current density), a material of contacts, the specific energy entered into its weight,

1.3. current density, pressure and velocity of increaseing of a current in its channel, and also intensity of the magnetic field influencing its body.

1.4. Electric explosion of metal-liquid bridge causes input of specific energy in mass of its body. This energy exceeds energy of sublimation of material contacts energy in 2÷3 times, current density $(10^8 \div 10^9)$ A/cm^2, pressure $(10^8 \div 10^9)$ Pa and velocity of increase of a current ~ 10^8 A/s in its channel and power density $\geq 10^8$ W/cm^2 coming on its base spot.

1.5. Electric explosion of the metal bridge at opening of argentiferous contacts at switching-off of short-circuit currents by low-voltage breakers can occur at instantaneous current not less than 50 κA.

1.6. Explosive destruction of the liquid bridge is caused by a pulse magnetic field under a condition:

$$i_{br} \cdot B \geq 6{,}5 \cdot 10^6 \ A \cdot Gs \,.$$

1.7. At the initial stage of arc discharge formation on opening contacts the power density coming on its base spots is equal of units of 10^5 W/cm^2 which is capable to melt metal on all their area. In process of opening of contacts and expansion of base spots of arc power density coming on them decreases to units of 10^4 W/cm^2 which can not provide metal melting on all area of base spots.

1.8. On microroughnesses which are formed on the surface of contacts which have a difficult relief, there are centres of concentration of charges on which power density reaches values $\geq 10^8$ W/cm^2. This leads to formation of microbubbles and their explosion.

1.9. Explosions of microbubbles lead to formation of craters and effusion of microjets of plasma which are discrete both on a surface of base spot and in time.

1.10. Initiation of arc discharge on opening contacts at switching-off of short-circuit currents a number of consistently proceeding physical processes accompany:

- formation of the liquid bridge and its destruction;
- formation of short constricted arc with the continuous core in which channel is saturated by nonideal plasma and microdrops;
- formation of short constricted arc with the discrete core in which channel is made of ideal plasma.

1.11. At inleakage of plasma of diffuse arc on surface of deion plates of arc chute in the beginning under the influence of its thermal flow on the centres of concentration of charges the spots of melts are formed in time ~ 10^{-9} *s*, and then on them the microbubbles arise in time (10^{-9}÷10^{-8}) *s* which, blowing up, effuse plasma microjets.

1.12. On a surface of the melt, on which it is arisen a bubble boiling with blowing up microbubbles and effusion of microsjets of plasma, the base spot of plasma discrete jet of arc discharge with split core is formed.

1.13. The starting mechanism of initiation of arc discharge at inleakage of plasma on electrode is singular blown up microbubbles on its surface.

1.14. Time of initiation of plasma microjets on the cathode and the anode has different values. Values of current intensity and power density coming on the centres of concentration of charges which are on the cathode have smaller value than on the anode. The sizes of craters on the cathode change from 0,3 to 5,0 *μm*, and on the anode they reach 15 *μm*. Therefore, time of formation of craters on the cathode can be equal to $6{,}0 \cdot 10^{-9}$ *s*, and on the anode - $7{,}29 \cdot 10^{-8}$ *s*.

1.15. Binding time of the base spots of diffuse arc with split core to the anode at the same current and power density coming on a base spot of discrete plasma microjets depends on a kind of a material of electrodes. For example, at a current intensity of a plasma discrete jet 690 *A* and power density coming on its base spot $5{,}38 \cdot 10^{5}$ W / cm^2 time of their binding is equal to:

$$t_{Cu} = 2{,}75 \cdot 10^{-4}\ s > 6{,}69 \cdot 10^{-5}\ s = t_{Ni} > 2{,}71 \cdot 10^{-5}\ s = t_{Fe}.$$

1.16. Binding time of the base spots of plasma discrete jets also depends on value of a current intensity of arc $i_{arc.max}$. For example, at $i_{arc.max} = 79{,}4\ кA$ binding time is equal $2{,}71 \cdot 10^{-5}$ *s*, at $i_{arc.max} = 5{,}9\ кA$ - $2{,}32 \cdot 10^{-3}$ с.

Reference index to chapter 1

1.1 *Mestcheryakov V.P.* Electric arc of high power in circuit breakers. – Ulyanovsk; part I, 2006; part II, 2008 [rus].

1.2 *Butkevich G.V., Belkin G.S., Vedeshenkov N.A., Zhavoronkov M.A.* Electric erosion of high-current of contacts and electrodes. – M.: Energy, 1978 [rus].

1.3 *Rahovski V.I., Levchenko G.V., Teodorovich O.K.* Arcing tips of electrical devices. – M.; L.: Energy, 1966 [rus].

1.4 *Mesyats G.A.* Ectons in vacuum discharge: breakdown, spark, arc. – M.: Science, 2000 [rus].

1.5 *Melchert, F.* Uber das Verhalten Kontakten bei lichtbogen freime Schalten sehr hoher Strome / F. Melchert, Diss. – TH. Braunshweig, 1957.

1.6 *Geguzin Y.E* Drop. – M.: Science, 1987 [rus].

1.7 *Gerasimov Y.I., Krestavnikov A.N., Shakhov A.S.* Chemical thermodynamics in nonferrous metallurgy. Reference manual 8 vol. Vol.2. Thermodynamics of copper, plumb, tin, silver and their compounds. – M.: Metallurgizdat, 1961. T.4. Thermodynamics of aluminium, antimony, magnesium, nickel, bismuth, cadmium and their major compauds. – M.: Metallurgizdat, 1965 [rus].

1.8 *Bron O.B.* Electric arc in control switches. – M.; L.: GEI, 1954 [rus].

1.9 Useful model patent № 95895. 24.02.2010. Contact system with magnetic blowout. Holder of patent JSC «Kontaktor». Authors: *Mestcheryakov V.P., Topchi A.S., Sindyukov O.P.*

1.10 *Bron O.B., Sushkov L.K.* Plasma fluxes in electric arc of sitching devices. – L.: Energy, 1975 [rus].

1.11 *Daalder, J. E.* Energy dissipation in the cathode of a vacuum arc. I. Phys. / J. E. Daalder. – D: Appl. Phys. – Vol. 10.1977.

1.12 *Leskov G.I.* Electric welding arc. – M.: Mashinostroenie, 1970 [rus].

1.13 *Polezhaev Y.V., Yurevich F.B.*. Thermal protection. – M.: Energy, 1976 [rus].

1.14 *Mitskevich M.K., Bushkin A.I., Bakuto I.A., Shikhov V.A., Devoino I.G.*. Electroerosion machining of metals. – Minsk: Science and technics, 1988 [rus]

Chapter 2

Form and structure of arc discharge of high power and its base spots

The form and structure of arc discharge are directly connected with the form and structure of its traces on base spots. Experimentally, by means of high-speed filming, it was observed an open-flame arc relatively of small power in which current usually did not exceed 1000 *A*. In such cases arc represents a column or a cord [2.1].

In fig. 2.1 two photos of arc in which current was 200 and 500 *A* [2.2, p. 145]. At these values of a current intensity arc really has a form of cord or column. Therefore in the technical literature traditionally schematically electric arc is shown in the form of a column. Proceeding from such representation of the form of arc its theoretical models were built also. The greatest interest of the experts was caused by simplified channel model of arc [2.3]. In such model of arc it is meant that its channel has a continuous core and its base spot - continuous melting.

However by means of high-speed filming of arc between carbon electrodes with distance between them 40 *mm*, a split core has been revealed at a current 1400 *A* [2.2, p. 39], (see fig. 2.2).

Formation of split core has been explained by splitting of a cathodic base spot of arc. "The filaments", forming a channel of arc with split core, behave dynamically: move, disappear and arise again. The spectral analysis shows that "filaments" consist of steams of a material of cathode.

Numerous tests of low-voltage automatic circuit breakers for electric wear resistance at rated current exceeding 2000 *A* and short-circuit breaking capacity at switching-off of short-circuit currents have shown two principal kinds of electric erosion of deion plates of arc chutes.

In arc chutes in which distances between deion plates is from 2,0 to 5,0 *mm*, continuous melting of surface of base spots of arc takes place. Arc chutes of such designs are subjected to considerable electric wear and have the limited operational service life.

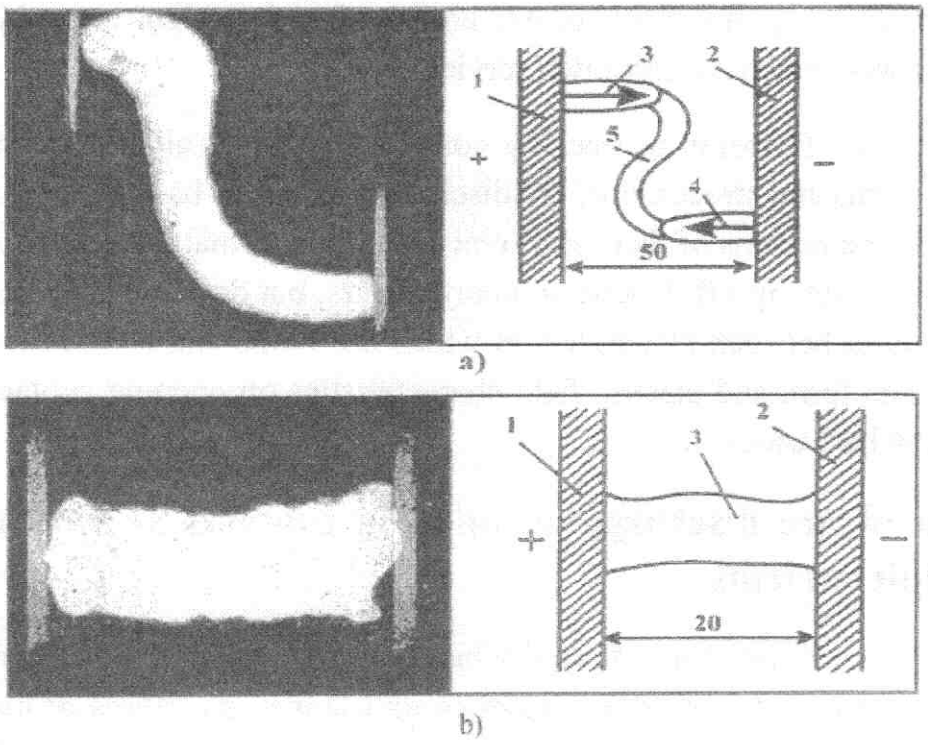

Fig. 2.1. [2.2]. Form of arc between parallel electrodes: a) I=200 A; b) I= 500 A

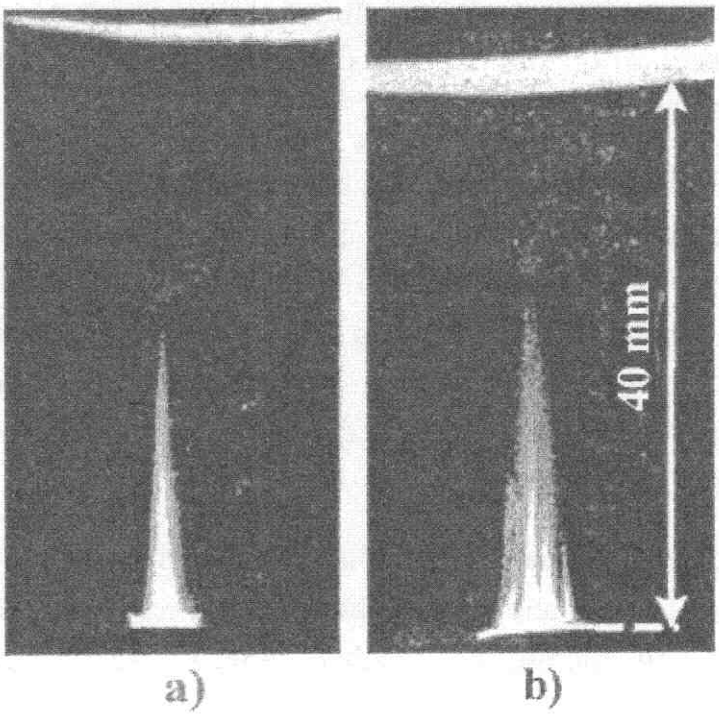

Fig. 2.2. [2.2]. Arc between carbon electrodes: a) continuous core, I=490 A; b) split core, I=1400 A

In arc chutes with distance between deion plates exceeding 8,0 *mm*, erosive traces of arc discharge are discrete. Arc chutes of such designs are subjected to dot insignificant wear and have unlimited service life.

As degree of erosion of opening contacts and fixed electrodes (deion plates) depends on forms and structures of arc discharges and their base spots then it is expedient to study the reasons of their occurrence and transformation. The form and structure of arc of switching-off depend on many factors, but determining factor is electric field distribution between electrodes on which arc burns and electric charges on its base spots. The form and electric field characteristics on opening contacts and fixed electrodes can be various.

2.1. Form of arc discharge on opening contacts at switching-off of short-circuit currents

The form and structure of arc discharge on opening contacts depend on many factors: form and electric field structures in its channel, structures of distribution of charges on base spots, current intensity, power density on base spots, ratio of area of a lateral surface of channel to sum of areas of base spots $\left(S_{lat}/\left(S_{bs.c}+S_{bs.a}\right)=l_{arc}/r_{bs}\right)$, velocity of contact opening, electro- and thermophysical characteristics of contact material and duration of location of arc on contacts. The form and arc structure on opening contacts at switching-off of short-circuit currents has a number of the features.

In process of opening of contacts the geometrical sizes and electrophysical characteristics of arc change. For analysis of changing of the form of arc and physical processes proceeding on opening contacts at switching-off of short-circuit currents we will consider a concrete example. In fig. 2.3 it is shown a current oscillogram i_{arc} and voltage u_{arc} of arc at current switching-off in test loop 16 κA (r.m.s.), phase voltage 420 V and $cos\varphi$ = 0,2. Contacts opened at the moment of time when instantaneous current was equal 13,0 κA.

From the moment of time of opening of contacts a current rised to maximum instant value $i_{arc.max}$=24,5 κA and then began to fall down. Voltage on contacts at the moment of time of their opening has reached value u_{arc}=27,0 V stepwise, sufficient for arc initiation.

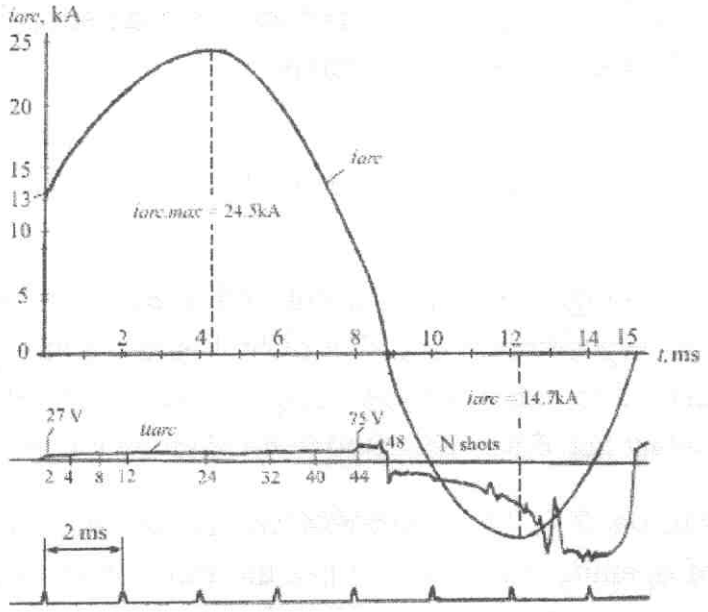

Fig. 2.3. Oscillograms of current and voltage of arc at switching-off of current in loop I=16,0 κA at phase voltage U_{ph} = 420 V and $cos\varphi$ = 0,2

In fig. 2.4 separate more typical shots of record of initiation and arc development on opening contacts are given. Arc on contacts is graphically represented in fig. 2.4 on the scale of photos. Arrows specify possible trajectories of movement of particles in the channel of arc and in plasma flows.

For the purpose of definition of the geometrical sizes of the channel of conductivity of a current of arc and its base spots by means of a photometric method of equidensites a core of arc on opening contacts has been revealed. In fig. 2.5 an original photo of motionless arc on contacts is shown. Current of arc was equal $i_{arc.max}$=24,5 κA (shot № 24 in fig. 2.4) and family of equidensites of the third step.

In fig. 2.5 a core of arc can be seen clear. We will pay attention that brightly shone area of arc in the original photo, adjoining directly to contact, and borders of base spots of arc core, received with the help of equidensites, well coincide. Therefore a border of base spots of arc on contacts was defined on area of a bright luminescence of arc adjoining directly to a surface of contacts, visible in the photo of high-speed filming.

In table 2.1 various geometrical and electrophysical characteristics of arc, including instant value of power, on opening contacts are given after the results of processing of oscillogram (fig. 2.3) and the record (fig. 2.4).

Average current density j_{bs} in base spot and average specific conductivity σ of plasma in arc channel were defined by formulas:

$$j_{bs} = \frac{i_{arc}}{S_{bs}}, \quad \sigma = \frac{i_{arc} \cdot \delta}{u_{arc} \cdot S_{bs}},$$

where i_{arc} and u_{arc} - average value of current and voltage of arc for time interval Δt=0,167 *ms*, equal to exposition of one shot of high-speed filming; S_{bs} - area of base spot, its form is accepted round, δ – contact gap. A cylinder built on base spots with length is equal to contact gap δ was accepted to conducting current of arc channel.

In the photos in fig. 2.4, 2.5, it can be seen that arc discharge on argentiferous contacts (velocity of opening was 2,0 *m/s*) has the form of short consricted arc with characteristic proportion $l_{arc}/r_{bs} < 1{,}0$. Arc on opening contacts remains motionless [2.4, part I, p. 205]. We will consider electric characteristics of short consricted arc on opening argentiferous contacts.

According to table 2.1 current-voltage characteristic of arc on opening contacts was built which is shown in fig. 2.6. According to the graph it can be seen that current-voltage characteristic of motionless arc on opening contacts has flat ascending form.

Table 2.1. Characteristics of arc on opening contacts at switching-off of current in the loop I=16,0 *кА* at phase voltage U_{ph}=420 *V* and $cos\varphi = 0{,}2$

№ of short	t_{arc}, ms	i_{arc}, kA	U_{arc}, V	P, kW	δ, cm	v_c, m/s	$d_{bs.c}$, cm	$S_{bs.c}$, cm²	$j_{bs.c}$, 10^3, A/cm²	σ, (Ohm·cm)$^{-1}$	$d_{bs.as}$, cm	$S_{bs.as}$, cm²	$j_{bs.as}$, 10^3, A/cm²
2	0.334	13.0	27	351	0.08	2.4	0.48	0.18	71.9	214	0.42	0.14	94.2
4	0.668	15.0	34	510	0.21	3.1	0.81	0.51	29.4	152	0.89	0.62	24.2
8	1.34	18.2	36	655.2	0.36	2.7	1.44	1.63	11.2	112	1.45	1.65	11.0
12	2.00	21.5	44	946	0.58	2.9	1.94	2.95	7.3	96	1.87	2.74	7.8
16	2.67	23.3	44	1020.8	0.63	2.4	2.27	4.05	5.73	82	1.96	3.02	7.7
24	4.00	24.5	44	1078	0.67	1.67	2.46	4.75	5.16	78.5	2.10	3.46	7.1
32	5.34	21.9	44	963.6	0.73	1.37	2.50	4.9	4.47	74.2	2.10	3046	6.3
40	6.68	14.6	48	700.8	0.92	1.37	2.12	3.53	4.14	72.3	1.74	2.38	6.1
44	7.35	9.0	75	675	1.00	1.36	1.70	2.27	3.96	52.9	1.88	2.75	3.3

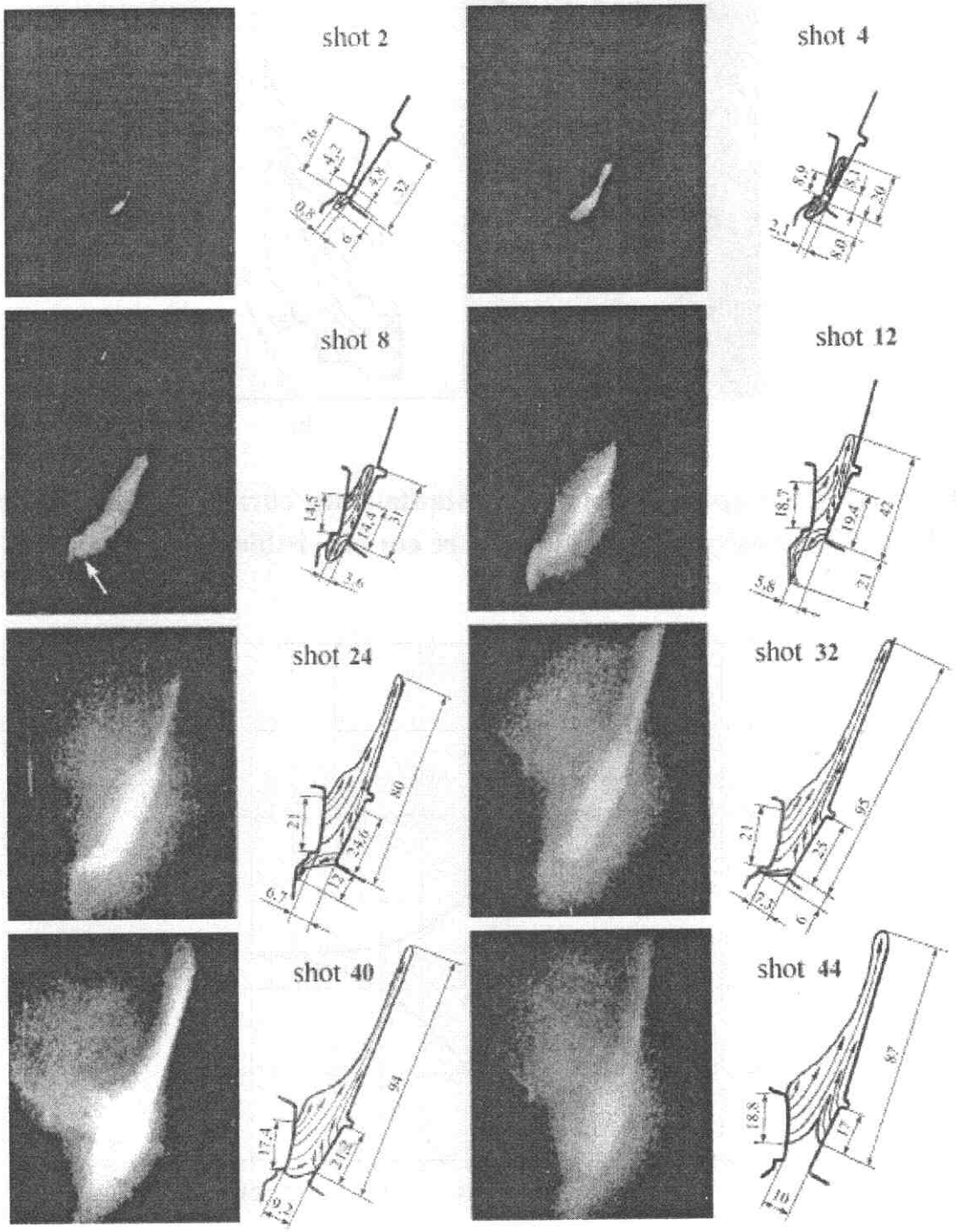

Fig. 2.4. Arc on opening contacts at switching-off of current in loop 16.0 kA, U_{ph} = 420V, cosφ=0.2: 2 – t=0.334 ms, i_{arc}=13.0 kA, u_{arc}=27V; 4 - t=0.668 ms, i_{arc}=15.0 kA, u_{arc}=34V, 8 - t=1.34 ms, i_{arc}=18.2 kA, u_{arc}=36V; 12 - t=2.0 ms, i_{arc}=21.5 kA, u_{arc}=44V; 24 - t=4.0 ms, $i_{arc.max}$=24.5 kA, u_{arc}=44V; 32 - t=5.34 ms, i_{arc}=21.9 kA, u_{arc}=44V; 40 - t=6.68 ms, i_{arc}=14.6 kA, u_{arc}=48V; 44 - t=7.35 ms, i_{arc}=9.0 kA, u_{arc}=75V.

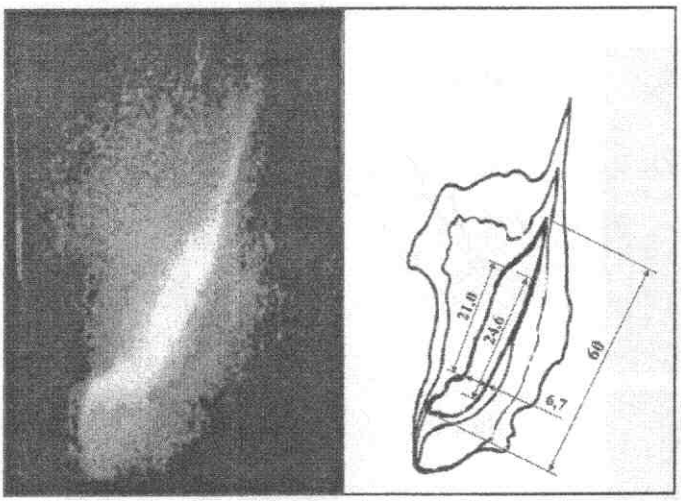

a) b)

Fig. 2.5. Arc on the opening contacts. Instantaneous current 24.5kA. a) original; b) family of equidensites of third stage. Arc core is visible clearly.

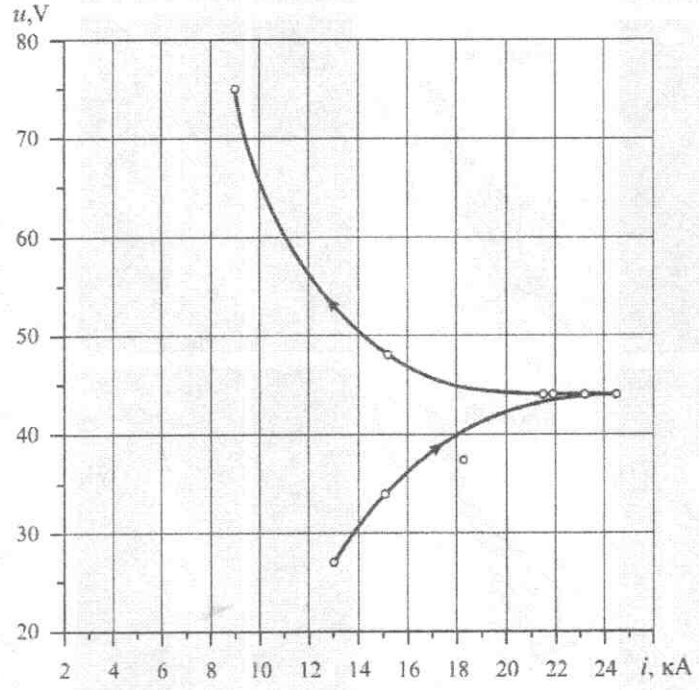

Fig. 2.6. Current-voltage characteristic of arc on opening contacts at при $I_{arc.max}$ = 24,5 кА

In table 2.2 values of average intensity of electric field E_{av} between opening contacts, calculated according to table 2.1, are given. In fig. 2.7 the graph of average intensity of electric field between opening contacts depending on a current is shown.

Average intensity of a field along the channel of arc as a function of current decreases in process of contact opening. At increase of current up to its maximum instant value roll-off of field intensity E_{av} occurs quickly. After transition of arc current through maximum a velocity of roll-off of field intensity E_{av} decreases. With start of arc motion on the contacts an average intensity of field E_{av} increases.

Table 2.2. Average intensity of electric field E_{av} and intensity E_{ch} in arc channel.

t, ms	0,334	0,668	1,34	2,0	2,67	4,0	5,34	6,68	7,35
i_{arc}, кА	13,0	15,0	18,2	21,5	23,2	24,5	21,9	14,6	9,0
U_{arc}, V	27	34	36	44	44	44	44	48	75
δ, cm	0,08	0,21	0,36	0,58	0,63	0,67	0,73	0,92	1,0
E_{av}, V/cm	337	162	100	76	70	66	60	52	75
E_{ch}, V/cm	88	67	44	41	38	36	33	30	50

It is possible to present voltage on arc in a following kind:

$$u_{arc} = (U_c + U_a) + E_{ch} \cdot l_{arc}, \qquad (*)$$

where $l_{arc} = \delta$ - length of arc equal to contact gap, E_{ch} - field intensity in arc channel on argentiferous contacts in process of their opening. Values E_{ch} have been calculated from formula (*) with using of the data of table 2.1. At definition of field intensity in arc channel E_{ch} a sum of electrode voltage drops has been subtracted from arc voltage u_{arc}. For argentiferous contacts sum is $(U_c + U_a)$=20 V.

Dependence of intensity E_{ch} from current on opening contacts is shown in fig. 2.7. With growth of arc current intensity in its channel falls quickly. At decreasing of current a falling velocity E_{ch} considerably decreases.

In fig. 2.8 the graph of electric field intensity E_{ch} in arc channel on opening contacts depending on their gap is given. Characteristic $E_{ch} = f(\delta)$ on opening contacts is falling. But with start of arc motion on contacts E_{ch} grows sharply.

In fig. 2.9 the graph of change of current density in base spots on the cathode and the anode in process of contact opening is given. This graph was built according to table 2.1.

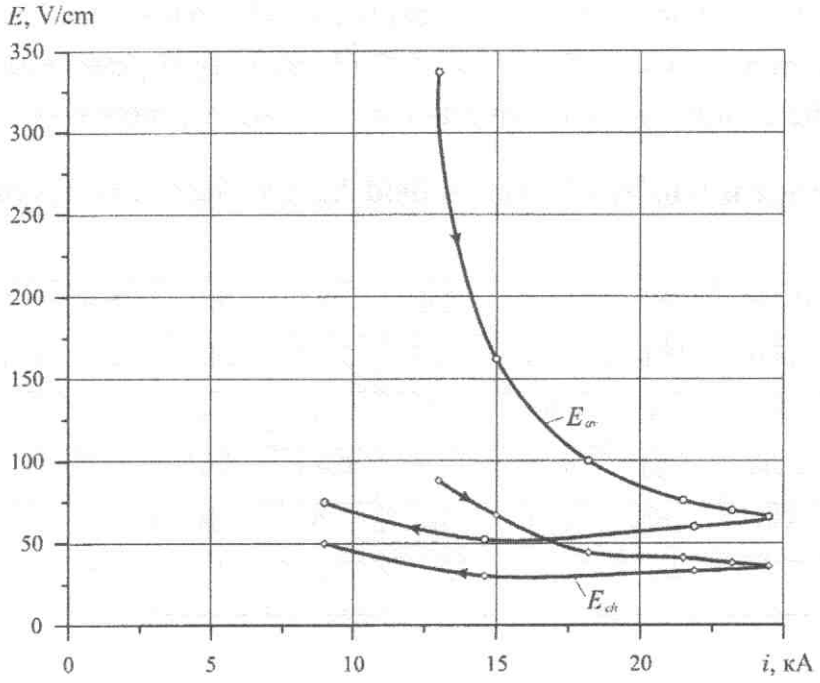

Fig. 2.7. Field intensity *E* between opening contacts

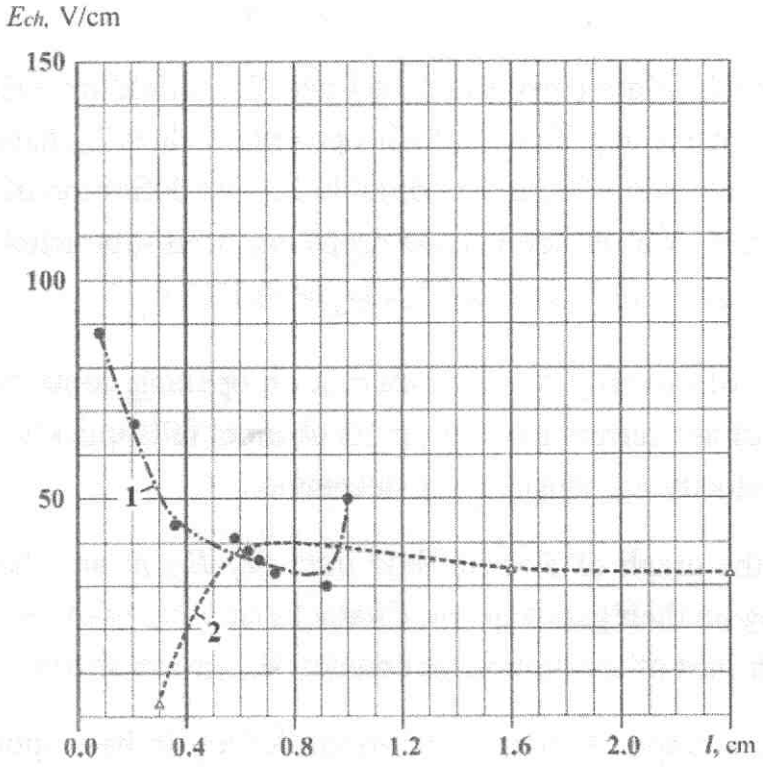

Fig. 2.8. Electric field intensity E_{ch} in arc channel: 1 – on argentiferous contacts depending on their gap at $i_{arc.max}$=24,5 *кА*; 2 - between copper-plated deion plates

in arc chute depending on distance between them in current range $i_{arc.max}$=5,9÷28,3 *кА*

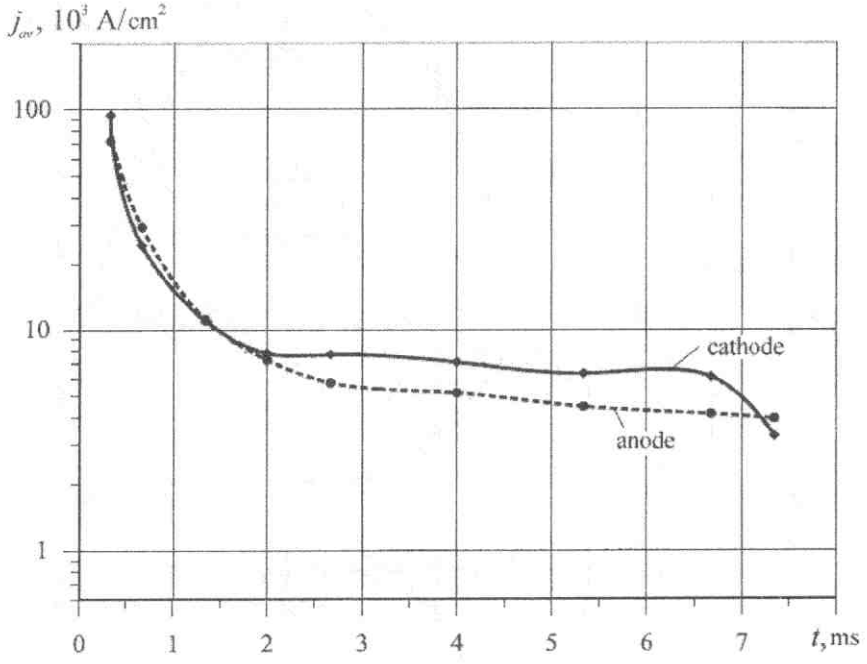

Fig. 2.9. Time change of average density of arc current in base spots of a cathode and a anode in process of argentiferous contacts opening at arc current $i_{arc.max}$=24,5 *кА*

According to the table 2.1 in fig. 2.10 there are given the graphs of changing of specific conductivity of plasma in channel of short constricted arc on opening argentiferous contacts in process of their opening.

Both characteristics: $j=f(t)$ and $\sigma = f(t)$ - are falling. At the initial stage of opening of contacts during 1,5÷2,0 *ms* the characteristics are slumping. Then, in process of the further opening of contacts, there comes rather established mode. With start of arc motion on contacts both characteristics fall sharply.

Attracts attention the general character of change of electric parametres of short constricted arc on opening contacts of low-voltage circuit breakers at switching-off of short-circuit currents. All of them, behind an exception of current-voltage characteristic, have a falling kind. For the analysis of character of change of electric parametres of short constricted arc it is reversible to its geometrical characteristics changing in process of opening of contacts. In table 2.3 numerical values of area of a lateral surface of arc and its base spots on opening contacts and their ratio $\left(S_{lat}/\left(S_{bs.c}+S_{bs.a}\right)=l_{arc}/r_{bs}\right)$ are given.

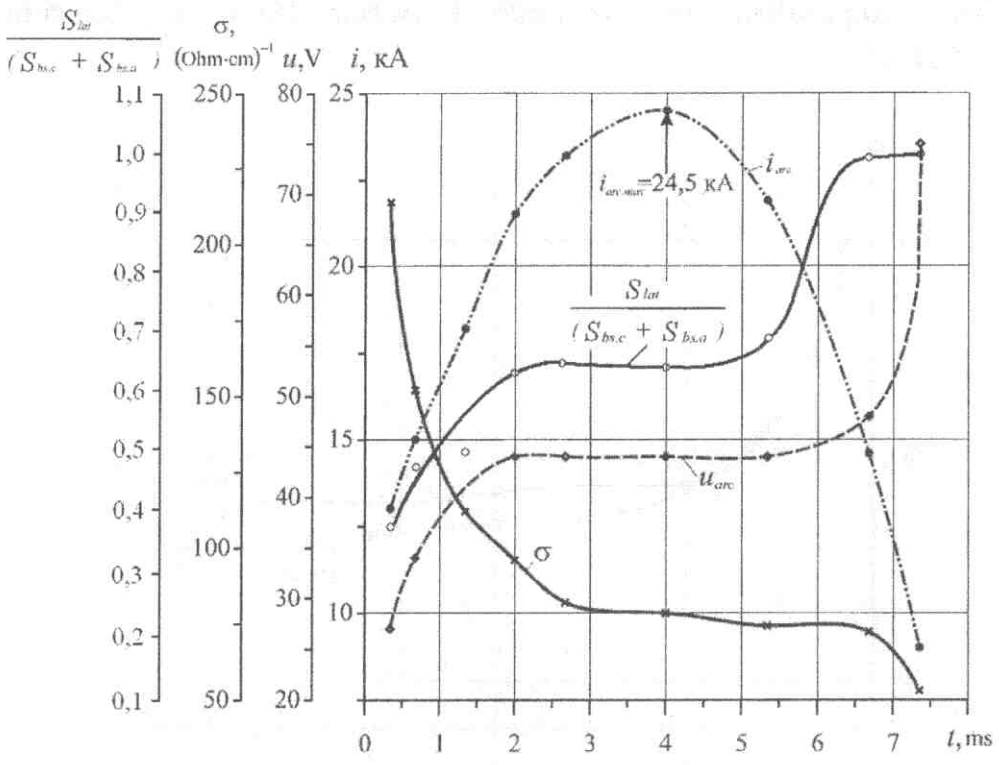

Fig. 2.10. The graphs of change of current i_{arc} and voltage u_{arc}, specific conductivity of its plasma σ on opening contacts at $i_{arc.max}$=24,5 κA, ratio of a lateral surface of the arc channel and a sum of areas of its base spots $S_{lat}/(S_{bs.c}+S_{bs.a})$

Table 2.3. Areas of base spots and an arc lateral surface on opening contacts

$I_{arc.max}$, κA	t_{arc}, ms	$S_{bs.c}, cm^2$	$S_{bs.a}, cm^2$	$S_{bs.c}+S_{bs.a}, cm^2$	S_{lat}, cm^2	$\frac{S_{lat}}{(S_{bs.c}+S_{bs.a})}$
24,5	0,334	0,18	0,14	0,32	0,12	0,375
	0,668	0,51	0,62	1,13	0,53	0,469
	1,34	1,63	1,65	3,28	1,63	0,497
	2,0	2,95	2,74	5,69	3,53	0,620
	2,67	4,05	3,02	7,07	4,49	0,635
	4,0	4,75	3,46	8,21	5,18	0,631
	5,34	4,9	3,46	8,36	5,73	0,685
	6,68	3,53	2,38	5,91	6,12	1,036
	7,35	2,27	2,75	5,02	5,34	1,064

For evident representation about an interconnection of geometry of arc and its electric characteristics a geometrical characteristic of arc $S_{lat}/(S_{bs.c}+S_{bs.a})$ is put in fig. 2.10 on which it is shown a change of arc current i_{arc}, its voltage u_{arc} on opening contacts and specific conductivity of plasma in arc channel.

It appears, despite change of arc current, geometrical characteristic of arc l_{arc}/r_{bs} and characteristic of arc voltage u_{arc} have an identical form and correspond each other in time. According to these characteristics the characteristics of specific conductivity of arc plasma and current intensity in base spots both under the form and in time change also.

From here it is possible to draw a conclusion that formation of arc and its development pass three stages. At the first stage proceeding from the moment of time of contact opening 1,5÷2,0 *ms*, arc channel is saturated by nonideal plasma consisting of ionised steams of contact metal (in this case steams of *Ag*) and having high specific conductivity. At the first stage a geometrical characteristic of arc grows but does not exceed value < 0,6. At the second stage a geometrical parametre of arc l_{arc}/r_{bs} is equal ~ 0,7.

At this stage which can proceed some milliseconds, a volume of arc channel extends synchronously in all directions at velocity of contacts opening 2,0 *m/s*. Electric parametres u_{arc}, σ and j have quasiconstant value. It is possible to accept that plasma of arc consisting of ionised steams of metal of contacts is ideal. At the third stage of development of arc on opening contacts geometrical parameter l_{arc}/r_{bs} from value 0,7 grows and can reach more than 1,0. In that case plasma of arc for the account of injection effect in electrode areas is saturated with environment gas. Specific conductivity of plasma in arc channel decreases sharply, and voltage on opening contacts grows quickly. A response rate of plasma arc mass also sharply decreases and it gets mobility [2.4, part II, p. 69, fig. 4.29].

Strictly speaking, for short constricted arc it is necessary to accept arc for which geometrical parameter l_{arc}/r_{bs} does not exceed value 0,6. In that case the arc channel consists of only ionised steams of contact metal. At l_{arc}/r_{bs} =0,6÷0,8 plasma in arc channel starts to be saturated with environment gas.

In process of increasing of geometrical parameter of arc l_{arc}/r_{bs} a composition of plasma changes. In transitive form of arc a mass of steams of contact metal in its channel decreases and mass of environment gas increases. At value $l_{arc}/r_{bs} >> 1{,}0$ a form of arc transformes from short constricted one to long constricted one. In that case it is possible to accept that arc plasma consists only of the ionised gas of environment. The given electric characteristics of arc discharge received experimentally, and its photos of high-speed filming on opening contacts provide guidance on to the

form of short constricted arc at switching-off of short-circuit currents by low-voltage breakers.

However because of the big brightness of a luminescence of plasma it is not possible to distinguish a structure of arc channel and its base spots. The experimental data-acquisition equipment, in such cases, should possess time ($\sim 10^{-9}$ *s*) and spatial ($\sim 10^{-3}$ *mm*) resolution.

However it is necessary to notice that injector effect in which result environment gas is soaked up in arc channel, can occur under a condition if it has the discrete structure consisting of set of separate jets of plasma.

2.2. Model of arc with continuous core

In the published works quite often a channel model of arc is addressed [2.3, p. 61]. In such model of arc instead of bell-shaped distributions on its section of temperature $T(r)$, current intensity $j(r)$ and specific conductivity $\sigma(r)$ their uniform distribution on all volume of its channel is accepted (fig. 2.11). Arc parametres are characterized by effective temperature T_{ef} and average values on all volume of the arc channel of current intensity j_{av} and specific conductivity its plasma σ_{av}. In such simplified model of arc it is meant that its core has continuous structure.

At the value of temperature equal to effective temperature T_{ef}, the shaded area *a* in fig. 2.11 is equal to sum of areas *b*. By analogy a value of average specific conductivity σ_{av} is defined by equality of the areas *c* и *d*. However thus diameter d_{ef} is not equal to diameter of base spot d_{bs}. The fact of the matter is that within the cylinder with basis $d_{bs} = d_{\sigma}$ plasma has specific conductivity σ_{av} which value is established at temperature T_{ef} on border of cylinder with base d_{ef}. As temperature T_{ef} is sufficient is high, outside of the cylinder with base d_{ef} plasma possesses still sufficiently great conductivity.

According to [2.3, p. 62] the effective radius of channel model of arc is equal to:

$$r_{ef} = 0{,}7 r_{arc},$$

where r_{arc} – arc radius in which limits all current pass.

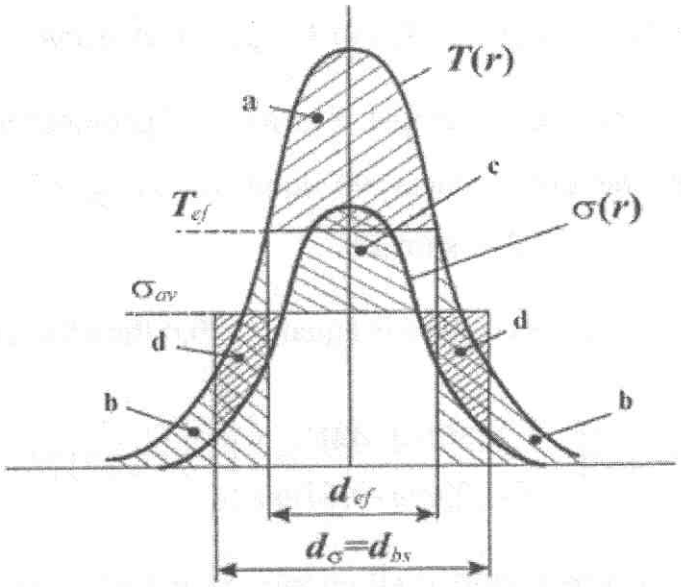

Fig. 2.11. The schematic image of graphs of distribution *T (r), σ (r) and* T_{ef}, σ_{av} in channel model of short constricted arc with a continuous core

A balance equation of power of such model of arc having area of radiation $S_{rad} = 2 \cdot \pi \cdot r_{ef} \cdot \delta = 4{,}396 \cdot r_{arc} \cdot \delta$, looks like:

$$i_{arc} \cdot u_{arc} = \sigma \cdot \beta \cdot S_{rad} \cdot T_{ef}^4,$$

where δ - length of arc channel equal to contact gap, i_{arc} and u_{arc} – average values of a current and voltage of arc for time interval Δt, $\sigma = 5{,}67 \cdot 10^{-5} erg/(s \cdot cm \cdot K^4)$ – Stefan-Boltzmann constant, β=0,5-0,7– degree of blackness for arcs burning in steams of metals.

From last expression it is possible to define effective temperature - a temperature averaged on all volume of arc channel:

$$T_{ef} = \left(\frac{i_{arc} \cdot u_{arc}}{\sigma \cdot \beta \cdot S_{rad}} \right)^{1/4}.$$

In CGS system the formula, defining effective temperature of arc, will become:

$$T_{ef} = 447 \left(\frac{i_{arc} \cdot u_{arc}}{\beta \cdot r_{arc} \cdot \delta} \right)^{1/4},$$

where T_{ef} is measured in K, i_{arc} in A, u_{arc} in V, r_{arc} and δ in cm.

Let us consider a concrete example. Electric and geometrical parametres of arc which motionless on opening contacts are equal to: $i_{arc.\max}$=24,5 κA, u_{arc}=44 V, r_{arc}=1,23 cm, δ=0,67 cm (fig. 2.4, shot 24).

If to accept that blackness degree is equal β=0,6 the effective temperature in arc channel will equal:

$$T_{ef} = 447\left(\frac{24500A \cdot 44V}{0{,}6 \cdot 1{,}23cm \cdot 0{,}67cm}\right)^{1/4} K = 17176\ K.$$

In this case it was accepted that all energy generated in arc dissipates in environment by radiation.

Let us consider the problem about ways of dissipation of energy generated in arc which will define structure of an equation of power balance of arc.

It is possible to present an equation of power balance of system "contacts-arc" during an immovability of short constricted arc on opening contacts in a following kind:

$$\Delta W_{arc} = \Delta Q_{con} + \Delta Q_{ch},$$

where ΔW_{arc} – energy generated by arc for time interval Δt, ΔQ_{con} – a part of energy of arc absorbed by contacts, ΔQ_{ch} – energy of arc channel.

Energy which is taken away in contacts, is defined by the formula:

$$\Delta Q_{con} = \Delta Q_{con.c} + \Delta Q_{con.a} = \eta \cdot \Delta W_{arc},$$

where $\Delta Q_{con.c}$ и $\Delta Q_{con.a}$ – parts of arc energy taken away in the cathode and the anode respectively, η – factor defining a part of energy absorbed by contacts.

According to [2.3, p. 135] coefficient of efficiency η for welding arcs with melted electrodes as a first approximation is accepted as the relation:

$$\eta = \frac{U_c + U_a}{u_{arc}},$$

where $U_c + U_a$ – sum of electrode voltage drops, u_{arc} – full voltage on arc.

Using last expression, we will define a part of energy of arc taken away in contacts which is spent for heating and erosion of contacts:

$$\Delta Q_{con} = \eta \cdot \Delta W_{arc} = \frac{U_c + U_a}{u_{arc}} \cdot \Delta W_{arc}.$$

Energy of channel is equal:

$$\Delta Q_{ch} = \Delta W_{arc} - \Delta Q_{con} = \Delta W_{arc} - \eta \cdot \Delta W_{arc} = (1-\eta) \cdot \Delta W_{arc}.$$

In this example $\eta = \frac{U_c + U_a}{u_{arc}} = \frac{20V}{44V} = 0{,}45$, where $U_c + U_a$ – the sum of electrode voltage drops on argentiferous contacts (for Ag $U_c = 12{,}5 \div 17\,V, U_a = 4 \div 6\,V$).

Then we will have:

$$T_{ef}^{'} = 447\left(\frac{(1-\eta) \cdot i_{arc} \cdot u_{arc}}{\beta \cdot r_{arc} \cdot \delta}\right)^{1/4} =$$

$$= 447\left(\frac{(1-0{,}45) \cdot 24500A \cdot 44V}{0{,}6 \cdot 1{,}23cm \cdot 0{,}67cm}\right)^{1/4} K = 14758\,K.$$

This value of temperature is much lower than its value at dissipation of all generated energy in arc by means of radiation:

$$T_{ef} = 17176\,K > 14758\,K = T_{ef}^{'}.$$

Energy of arc channel is spent on dissociation and gas ionisation in arc channel (ΔQ_{ion}) and taken away in environment by convective streams ($\Delta Q_{f.pl}$) and radiation (ΔQ_{rad}):

$$\Delta Q_{ch} = \Delta Q_{ion} + \Delta Q_{f.pl.} + \Delta Q_{rad}.$$

Let us estimate a part of energy which is spent for ionisation of ideal one-nuclear gas consisting of steams of silver at different values of temperature and pres-

sure $P = 1\ atm$. Energy which is necessary for spending for ionisation of steams of silver in arc channel of volume V_{arc}, can be defined by the formula:

$$\Delta Q_{ion} = q_i \cdot n_i \cdot V_{arc},$$

where $q_i = 1{,}6 \cdot 10^{-12} \cdot U_i = 12{,}06 \cdot 10^{-12} erg$ – energy of ionisation of one atom of silver, $U_i = 7{,}54\ V$ – potential of ionisation of silver atom, n_i – concentration of ions.

At the same experimental data ($i_{arc.\max} = 24{,}5\ кА$, $u_{arc} = 44\ V$, $r_{arc} = 1{,}23\ cm$, $\delta = 0{,}67 cm$) volume of arc channel is equal:

$$V_{arc} = \pi \cdot r_{ef}^2 \cdot \delta = \pi \cdot (0{,}7 \cdot r_{arc})^2 \cdot \delta =$$

$$= 3{,}14 \cdot (0{,}7 \cdot 1{,}23\ cm)^2 \cdot 0{,}67\ cm = 1{,}56\ cm^3.$$

Energy of arc channel is:

$$\Delta Q_{ch} = (1 - \eta) \cdot i_{arc} \cdot u_{arc} \cdot \Delta t =$$

$$= (1 - 0{,}45) \cdot 24500 A \cdot 44 V \cdot 0{,}167 \cdot 10^{-3} s = 99{,}0\ W \cdot s,$$

where $\Delta t = 0{,}167 \cdot 10^{-3} s$ – time of exposition of one shot of high-speed filming.

Numerical values of energy necessary for ionisation of one-nuclear steams Ag are given in table 2.4.

Table 2.4. The energy necessary for ionisation of one-nuclear steams Ag, in arc channel with volume V_δ=1,56 cm^3 depending on temperature at P=1 atm.

$T, 10^3, K$	8	9	10	11	12
$n_i, 10^{17}, cm^{-3}$	1,393	2,163	2,700	2,891	2,856
$\Delta Q_i, 10^5, erg$	26,2	40,69	50,79	54,38	53,72
$\Delta Q_i, W \cdot s$	0,262	0,4069	0,5079	0,5438	0,5372
$\Delta Q_i / \Delta Q_{ch}, \%$	0,067	0,414	0,518	0,554	0,548

From the data given in table 2.4 it is visible that in the general energy of arc channel ΔQ_{ch} a part of energy spent for ionisation of steams Ag does not exceed 1 % and in practical engineering calculations it can be neglected.

A part of energy, dissipating in environment by radiation, depends on temperature of arc channel and blackness degree. A value of temperature defined from a condition of loss of energy of arc channel only by radiation, is essentially overestimated.

Blackness degree, in turn, can change on some degrees depending on structure of arc plasma. If arc plasma consists of pure steams of metals, such as Ag, Fe, Cu or Ni for practical engineering calculations blackness degree can be accepted equal $\beta = 0{,}5 \div 0{,}7$. If in steams of these metals graphite impurity will be that $\beta = 0{,}5 \div 0{,}85$.

Degree of blackness of gas depends both on temperature and from pressure. For example, for air at pressure $P = 1\ atm$ in a range of temperatures $T = 8000 \div 12000\ K$ degree of blackness changes in the range of $\beta = 1{,}46 \cdot 10^{-3} \div 2{,}63 \cdot 10^{-2}$. At pressure of air $P = 10\ atm$ in the same range of temperatures $\beta = 4 \cdot 10^{-2} \div 1{,}4 \cdot 10^{-1}$ [2.4, part II, table 7.11, p. 370]. Therefore at similar calculations of effective temperature in arc channel it is necessary to choose a value of degree of blackness β cautiously.

Practical methods of calculation of losses of energy $\Delta Q_{f.pl}$ in arc channel for account of convective streams of plasma are absent. Therefore to define a part of energy dissipated by radiation ($\Delta Q_{rad} = \Delta Q_{ch} - \Delta Q_{f.pl}$), and, hence, effective temperature in arc channel it is not obviously possible. However the effective temperature can be defined, if average specific conductivity, structure of plasma and its pressure are known.

So, for example, at $i_{arc.\max} = 24{,}5\ \kappa A$, $u_{arc} = 44\ V$, $r_{arc} = 1{,}23\ cm$, $\delta = 0{,}67\ cm$ average value specific conductivity of plasma in arc channel is equal:

$$\sigma_{av} = \frac{i_{arc.\max} \cdot \delta}{u_{arc} \cdot S_{bs}} = \frac{24500A \cdot 0{,}67cm}{44V \cdot 4{,}75cm^2} = 78{,}5\ (Ohm \cdot cm)^{-1},$$

where $S_{bs} = \pi \cdot r_{arc}^2 = 3{,}14 \cdot (1{,}23\ cm)^2 = 4{,}75\ cm^2$ –area of base spot of arc.

In that case pressure in arc channel is:

$$P_{arc} = P_{atm} + 9{,}87 \cdot 10^{-9} \cdot j_{arc} \cdot i_{arc.\max} = 1\ atm + 9{,}87 \cdot 10^{-9} \times$$
$$\times 5{,}158 \cdot 10^3\ A/cm^2 \cdot 24500\ A = 2{,}25\ atm,$$

where $j_{arc} = i_{arc.\max} / S_{bs} = 24500A / 4{,}75cm^2 = 5{,}158 \cdot 10^3 A / cm^2$ – current intensity in base spot of arc.

In this experiment arc burnt on argentiferous contacts. Therefore with help of fig. 2.12 [2.4, p.I. Add. 3, fig. П.3.1, p. 334] we will define effective temperature of channel of short constricted arc which are on contacts in motionless position. At $\sigma = 78{,}5(Ohm \cdot cm)^{-1}$ and $P_{arc} = 2{,}25atm$ effective temperature in arc channel is equal to $T_{ef} \sim 11 \cdot 10^3 K$. This value T_{ef} essentially differs from defined one earlier:

$$T_{ef}^{'} = 14758K > 11000K \sim T_{ef}.$$

Knowing now that $T_{ýô} \sim 11 \cdot 10^3 \hat{E}$, we will define a part of energy which dissipates in environment by radiation. Surface density of energy flux of radiation is [2.8, p. 189]:

$$q_{rad} = \sigma \cdot \beta \cdot T_{ef}^4 = \sigma^{'} \cdot \beta \cdot \left(\frac{T_{ef}}{100} \right)^4 =$$

$$= 5{,}67 \cdot 10^3 \frac{erg}{s \cdot cm^2 \cdot K^4} \cdot 0{,}6 \cdot \left(\frac{11000K}{100} \right)^4 = 4{,}98 \cdot 10^{11} \frac{erg}{s \cdot cm^2},$$

where $\sigma = 5{,}67 \cdot 10^{-5} \frac{erg}{s \cdot cm^2 \cdot K^4}$ – Stefan-Boltzmann constant, $\sigma^{'} = 5{,}67 \cdot 10^3 \frac{erg}{s \cdot cm^2 \cdot K^4}$, $\beta = 0{,}6$ – blackness degree, and a dimensionless divider 100 it is entered for simplification of calculations.

Quantity of heat ΔQ_{rad}, radiated with surface S_{rad} of arc channel in environment during $\Delta t = 0{,}167 \cdot 10^{-3} s$, will be equal:

$$\Delta Q_{rad} = q_{rad} \cdot S_{rad} \cdot \Delta t =$$

$$= 4{,}98 \cdot 10^{11} erg / (s \cdot cm^2) \cdot 3{,}623 cm^2 \times$$

$$\times 0{,}167 \cdot 10^{-3} s = 3{,}01 \cdot 10^8 erg = 30{,}1 W \cdot s,$$

where $S_{rad} = 4{,}396 \cdot r_{arc} \cdot \delta = 4{,}296 \cdot 1{,}23cm \cdot 0{,}67cm = 3{,}623\ cm^2$ – area of radiations

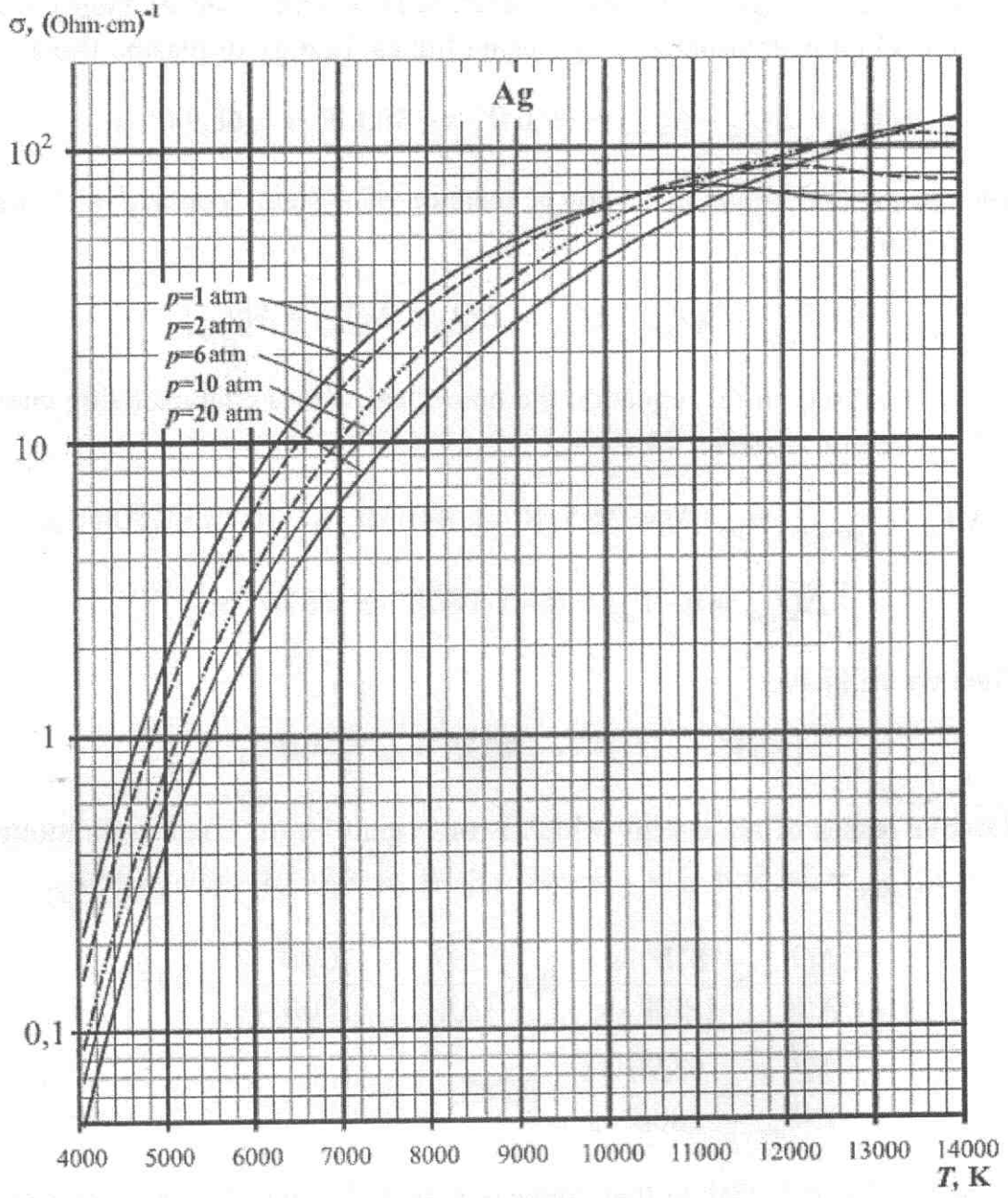

Fig. 2.12. Specific conductivity of steams of silver depending on temperature at different pressures

of arc channel.

Earlier it has been defined that energy of arc channel $Q_{ch} = 99{,}0W \cdot s$. Hence, at $T_{ef} \sim 11 \cdot 10^3 K$ in this case relative part η_{rad} of energy dissipated by radiation, is:

$$\eta_{rad} = \frac{\Delta Q_{rad}}{\Delta Q_{ch}} = \frac{30{,}1W \cdot s}{99{,}0W \cdot s} = 0{,}304,$$

that is 30,4 % of all energy dissipates by radiation only. Other part of energy from arc channel is taken out in environment by plasma fluxes. Energy of plasma fluxes is:

$$\Delta Q_{f.pl} = \Delta Q_{ch} - \Delta Q_{rad} = 99{,}0\,W \cdot s - 30{,}1\,W \cdot s = 68{,}9\,W \cdot s.$$

Thus, a general equation of power balance of system "contacts-arc" assumes the following kind:

$$\Delta W_{arc} = \Delta Q_{con} + \Delta Q_{ch} = \Delta Q_{ch} + \Delta Q_{rad} + \Delta Q_{f.pl}.$$

Let us substitute in this equation the numerical values characterising energy of arc during exposition of a shot 24:

$$\Delta W_{arc} = i_{arc.\max} \cdot u_{arc} \cdot \Delta t = 24{,}5 \cdot 10^3\,A \cdot 44V \cdot 0{,}167 \cdot 10^{-3}\,s = 180W \cdot s.$$

$$\Delta Q_{con} = \eta \cdot W_{arc} = 0{,}45 \cdot 180W \cdot s = 81W \cdot s.$$

Then we will have:

$$180W \cdot s = 81W \cdot s + 30{,}1W \cdot s + 68{,}9W \cdot s.$$

Relative losses of arc energy which is on argentiferous contacts in motionless position, at $i_{arc.\max} = 24{,}5\kappa A$ и $u_{arc} = 44V$ (short 24, fig. 2.4) are equal to:

$$\frac{\Delta Q_{con}}{\Delta W_{arc}} = \frac{81W \cdot s}{180W \cdot s} = 0{,}45; \frac{\Delta Q_{rad}}{\Delta W_{arc}} = \frac{30{,}1W \cdot s}{180W \cdot s} = 0{,}167;$$

$$\frac{\Delta Q_{f.pl}}{\Delta W_{arc}} = \frac{68{,}9W \cdot s}{180W \cdot s} = 0{,}383.$$

From fig. 2.4 it is visible that contacts gap at filming of shot 24 was 6,7 *mm* and plasma flux was stretched from contact gap on 80 *mm*. However on shot 4 a plasma flux does not leave limits of a zone of contacts at their gap 2,1 *mm*. Therefore energy of plasma fluxes remains in the channel. At the same time the effective temperature of arc channel T_{ef} reaches almost $17 \cdot 10^3\,K$ [2.4, part II, p. 114, table 4.29] and the base losses of energy of arc channel will form energy losses on radiation [2.4, part II, p. 118, fig. 4.62]. In that case an equation of power balance of system «contacts - arc» will look like:

$$\Delta W_{arc} = \Delta Q_{con} + \Delta Q_{rad},$$

where $\Delta W_{arc} = i_{arc} \cdot u_{arc} \cdot \Delta t = 15 \cdot 10^3 A \cdot 34V \cdot 0{,}167 \cdot 10^{-3} s = 85{,}2W \cdot s;$

$$\Delta Q_{con} = \eta \cdot W_{arc} = \frac{20V}{34V} \cdot 85{,}2W \cdot s = 50{,}1W \cdot s.$$

Losses of energy of arc channel for radiation is:

$$\Delta Q_{rad} = \Delta W_{arc} - \Delta Q_{con} = 85{,}2W \cdot s - 50{,}1W \cdot s = 35{,}1W \cdot s.$$

Relative losses of energy of arc which is on argentiferous contacts in motionless position, at i_{arc}=15,0 *кА*, u_{arc}=34 *V* and contacts gap δ=2,1 *mm* are equal to:

$$\frac{\Delta Q_{con}}{\Delta W_{arc}} = \frac{50{,}1W \cdot s}{82{,}5W \cdot s} = 0{,}59; \frac{\Delta Q_{rad}}{\Delta W_{arc}} = \frac{35{,}1W \cdot s}{82{,}5W \cdot s} = 0{,}41.$$

The resulted examples show that losses of energy of arc on opening contacts depend on their gap.

For estimation of the thermal phenomena on base spots of short constricted arc with a continuous core on opening argentiferous contacts we will define a superficial thermal flux (power density), coming on them. Power density q_{bs}, coming on a base spot of arc, is defined by formula:

$$q_{bs} = \frac{\eta \cdot i_{arc} \cdot u_{arc}}{2 \cdot S_{bs}},$$

where $\eta = 20 / u_{arc}$ – the factor taking into account a part of energy of arc absorbed by argentiferous contacts; i_{arc} and u_{arc} – average values of a current and voltage of arc for time interval $\Delta t = 0{,}167 \cdot 10^{-3} s$, equal to exposition of one shot of high-speed filming, S_{bs} – an area of a base spot and the figure 2 means that power density q_{bs} comes on one contact and is average value both for the cathode and for the anode.

In table 2.5 numerical values of power density q_{bs}, coming on one contact at switching-off of current by a breaker in a test loop 16,0 *кА* are given.

At enough high currents and long time of arc delay on contacts there is a running off of liquid metal from a surface of contacts. In fig. 2.4 we can see a running

off of jet of liquid metal from mobile contact during 4,0 *ms* from 8-th to 32-nd shots. After experience on the bottom part of contact support a thin layer of hardened metal has been found out.

Table 2.5. Elektro - and thermophysical properties of a motionless arc on opening contacts of a breaker at current switching-off in loop 16,0 *кА*

t_{arc}, ms	0,334	0,668	1,34	2,00	2,67	4,00	5,34	6,68
$i_{arc}, кА$	13,0	15,0	18,2	21,5	23,2	24,5	21,9	14,6
u_{arc}, V	27	34	36	44	44	44	44	48
η	0,74	0,59	0,56	0,45	0,45	0,45	0,45	0,42
S_{bs}, cm^2	0,14	0,62	1,65	2,74	3,02	3,46	3,46	2,38
$q_{bs}, 10^5, W/cm^2$	9,29	2,42	1,10	0,78	0,76	0,70	0,62	0,62
Bi_{melt}	47,7	12,4	5,6	4,0	3,9	3,6	3,2	3,2
Bi_{boil}	50,0	13,1	5,9	4,2	4,1	4,8	3,4	3,4

According to classical theory of heat conductivity, uniformity of distribution of temperature between external and internal layers of a body is defined by Biot number [2.6, p. 12]:

$$Bi = \frac{q \cdot h}{\lambda \cdot T_d},$$

where q – superficial density of a thermal flux, h – body`s thickness, $\lambda$ – heat conductivity factor, $T_d$ – destruction temperature. For a body`s thickness we will accept thickness of a contact plate equal $h = 2{,}5\ mm$. We will analyse, as a number Biot changes during arc burning on contacts if to accept that in one case destruction temperature is metal fusion temperature, and in other - boiling temperature of contact metal.

The factor of heat conductivity λ of liquid Ag at $T_{melt} = 1285\ K$ is equal to $379 \cdot 10^5\ erg/(s \cdot cm \cdot K)$ [2.4, table 1.23, p. 110], at $T_{boil} = 2485\ K - 186 \cdot 10^5\ erg/(s \cdot cm \cdot K)$ [2.4, part I, p. 112]. Results of calculation of Biot number are given in table 2.5.

During all time of standing of arc for contacts when a liquid-melt on a base spot achieves both as a temperature of fusion as a boiling temperature, Biot number $Bi >> 1{,}0$. It means that heat supplied by arc to contacts warms up only their top

layer and does not get in a body of contact. An internal part of a body of contact is heated up only for by means of Joule heat generated at flowing of current in a body of contact ($i^2 \cdot r$).

Now we will estimate time when a facial layerof achieves a temperature of fusion and boiling temperature on a base spot of arc with help of available experimental data and will compare it with actual time of arc burning. Time of achievement of temperature of fusion T_{melt} and boiling temperature T_{boil} of a surface of base spot under influence of superficial thermal flux q_{bs} can be calculated by the formula [2.6, p. 54].:

$$\tau_d = \frac{\pi \cdot \lambda \cdot c \cdot \rho \cdot (T_d - T_i)^2}{4 \cdot q_{bs}^2},$$

where q_{bs} will be taken from table 2.5 and will be constant during time of exposition of one shot $\Delta t = 0{,}167 \cdot 10^{-3} s$; temperature of destruction T_d will be equaled to T_{melt} or T_{boil}, T_i – initial temperature of contact for which at definition of time of achievement of temperature of fusion τ_{melt}, we will accept $T_i = 400\ K$, equal to temperature of contact originally warmed up by rated current, and at definition of time of achievement of boiling temperature τ_{boil} – temperature of fusion T_{melt}, λ – heat conductivity factor, c - specific heat capacity и ρ – density of a material of contacts at corresponding temperatures.

For Ag at temperature $T_{melt} = 1285\ K$: $\lambda = 379 \cdot 10^5 \frac{erg}{s \cdot cm \cdot K}$ [2.4. table 1.23, p. 110], $c_{sp} = 0{,}275 \cdot 10^7 \frac{эрг}{g \cdot K}$ [2.4, table 1.20, p. 106] и $\rho = 9{,}32 \frac{g}{cm^3}$ [2.7, p. 175]. At temperature $T_{boil} = 2485\ K$ we will accept for Ag: $\lambda = 186 \cdot 10^5 \frac{erg}{s \cdot cm \cdot K}$ [2.4, p. 112], $c_{sp} = 0{,}29 \cdot 10^7 \frac{erg}{g \cdot K}$ [2.7, p. 180] and $\rho = 9{,}0 \frac{g}{cm^3}$ [2.7, p. 175].

At an initial moment of time of contacts opening at $q_{bs} = 9{,}29 \cdot 10^5 W / cm^2$ time of achievement of fusion temperature τ_{melt} or boiling temperature τ_{boil} by metal facial layer on base spot of arc is equal:

$$\tau_{melt} = \frac{\pi \cdot 379 \cdot 10^5 erg/(s \cdot cm \cdot K) \cdot 0{,}275 \cdot 10^7 erg/(g \cdot K)}{4(9{,}29 \cdot 10^{12} erg/(s \cdot cm^2))^2} \times$$

$$\times 9{,}32 g/cm^3 \cdot (1285K - 400K)^2 = 6{,}9 \cdot 10^{-6} s;$$

$$\tau_{boil} = \frac{\pi \cdot 186 \cdot 10^5 erg/(s \cdot cm \cdot K) \cdot 0{,}29 \cdot 10^7 erg/(g \cdot K)}{4(9{,}29 \cdot 10^{12} erg/(s \cdot cm^2))^2} \times$$

$$\times 9{,}0 g/cm^3 \cdot (2485K - 1285K)^2 = 6{,}4 \cdot 10^{-6} s;$$

$$\tau_{melt} + \tau_{boil} = (6{,}9 + 6{,}4) \cdot 10^{-6} s = 13{,}3 \cdot 10^{-6} s.$$

As $\tau_{melt} + \tau_{boil} = 0{,}0133 \cdot 10^{-3} s << 0{,}334 \cdot 10^{-3} = t_{arc}$, that is obvious at an initial stage of contacts opening while power density, coming on a base spot, exceeds $10^5 W/cm^2$, on its surface a layer of liquid metal and its temperature can reach a boiling temperature. Further, in process of arc burning a power density q_{bs} decreases and accordingly time of warming up of metal on a base spot upto fusion temperature T_{melt} and boiling temperature T_{melt} increases. Power density can be insufficient for fusion of all surface of base spot. In that case on its surface the separate centres of liquid-melt are formed only.

The analysis electro- and thermophysical characteristics of short constricted arc, which are in motionless state on opening argentiferous contacts, received as a result of researches of arc of switching-off of high power in low-voltage breakers [2.4] and as a result of calculation method with use of theory of simplified channel model of arc with a continuous core shows that power density q_{bs} coming on a surface of base spot of arc is equal to $(10^5 \div 10^4) W/cm^2$. Power density exceeding $10^5 W/cm^2$, leads to formation of liquid-melt of contacts metal on a surface of base spot. Its temperature reaches boiling temperature. It is necessary to underline especially that power densities coming on the cathode and the anode have equal values. In that case the cathode and the anode will be subjected by electric erosion equally. Besides, power density equal $10^4 W/cm^2$ is capable to melt only a part of a surface of base spot.

2.3. Model of short constricted arc with a discrete core

2.3.1. Effective electrode potentials and power density coming on the cathode and the anode

In channel model of arc with a continuous core at definition of power density coming on base spot of arc, concepts of electrode voltage drops have been used. For *Ag* U_c = (12,5÷17) *V*, U_a = (4÷6) *V* and U_c+U_a=20 *V* - average value of sum of electrode voltage drops.

In [2.10] effective potential $U_{эф}$ of the cathode for electrodes from various metals has been measured. It was defined from expression:

$$U_{ef} = \frac{Ð_{el}}{i_{arc}},$$

where P_{el} – power taken away in electrode, i_{arc} – arc current [2.8, p. 397]. Energy taken away in the cathode was defined from change of enthalpy its metal in process of arc burning. In table 2.6 values $U_{ef.c}$ of the cathode and voltage of arc U_{arc} are given at its current intensity 100 *A*.

Table 2.6. Voltage of arc U_{arc} and effective potential of cathode $U_{ef.c}$ for a number of metals at current of arc 100 *A* [2.10]

Metal	*Cd*	*Zn*	*Sn*	*Ag*	*Ni*	*Cu*	*W*	*Mo*	
U_{arc}, *V*	11,0	12,0	13,5	17,5	18	20	28	26,5 (200 A)	28 (600 A)
$U_{ef.c}$, *V*	2,7	3,0	3,9	5,25	5,35	6,2	9,5	8,7	9,25
$U_{ef.c}/U_{arc}$	0,25	0,25	0,29	0,30	0,30	0,31	0,34	0,33	0,33

It is necessary to notice that value U_{ef} depends on a current intensity. Unfortunately, the similar data for other values of a current in the published works is absent.

Contact gap in [2.10] changed from 0,5 to 10,0 *mm*. That is arc was enough short. Therefore voltage on arc can be accepted equal to sum of effective electrode potentials:

$$U_{arc} = U_{ef.c} + U_{ef.à},$$

where $U_{ef.a}$ – effective potential of the anode.

From here, for example, for electrodes from *Ag* we will have effective potential of the anode:

$$U_{ef.à} = U_{arc} - U_{ef.c} = 17{,}5\,V - 5.25\,V = 12{,}25\,V\,.$$

Taking into account values of effective potentials for cathode $U_{ef.c}$ and anode $U_{ef.a}$, proceeding from balances of powers in electrode areas of the channel of arc, it is possible to define power density coming on the cathode $q_{bs.c}$ and the anode $q_{bs.a}$ separately. The formulas defining $q_{bs.c}$ and $q_{bs.a}$ look like:

$$q_{bs.c} = \frac{\eta_c \cdot (1-\eta_{loss}) \cdot i_{arc} \cdot U_{ef.c}}{S_{bs.c}};\ q_{bs.à} = \frac{\eta_à \cdot (1-\eta_{loss}) \cdot i_{arc} \cdot U_{ef.à}}{S_{bs.à}}\,.$$

Here $\eta_c = \frac{U_{ef.c}}{u_{arc}}$ и $\eta_à = \frac{U_{ef.à}}{u_{arc}}$ – the factors taking into account the parts of power taken away from electrode areas of the channel of arc in the cathode and the anode respectively; η_{loss} – the factor taking into account all losses of energy by the channel of arc, including losses of energy by radiation and convection streams of plasma taken out in environment. The values η_{loss} are given in [2.4, part II, table 4.27, p. 112]. $(1-\eta_{loss}) \cdot i_{arc} \cdot U_{ef}$ – a part of power of electrode area of the channel of arc. The values i_{arc} and u_{arc} are given in table 2.1 and $S_{bs.c}$ and $S_{bs.à}$ – in table 2.3. Numerical values η_c and $q_{bs.c}$, $\eta_à$ and $q_{bs.à}$ and η_{loss} are given in table 2.7.

From data of table 2.7 it is visible that power densities, coming on cathodic and anode base spots of arc, have different values and at a current 16 *кА* on the cathode they change from ~10^4 *W/cm*^{2} to ~10^3 *W/cm*^{2}, and on the anode - from ~10^5 *W/cm*^{2} to ~10^4 *W/cm*^{2}. Power densities $q_{bs.c}$ and $q_{bs.à}$ on a surface of base spots cause the thermal phenomena which initiate the emission processes providing current flowing of in arc discharge.

According to data [2.4, part I, p. 293, table 3.10] a density of thermionic current on the cathode from *Ag* at temperature of its boiling can be equal to 1,5 *A/cm*^{2}. With the account of amplification of thermionic current by means of local intensity of electric field in a cathodic area of arc discharge of low-voltage arc a density of current will not exceed 5,0 *A/cm*^{2} [2.4, part I, p. 295].

Table 2.7. Elektro - and thermophysical parametres of electrode areas of arc on opening argentiferous contacts of a breaker at current switching-off in test loop I=16,0 κA, U_{ph}=420 V and $cos\ \varphi = 0{,}2$

t_{arc}, ms	0,334	0,668	1,34	2,0	2,67	4,0	5,34	6,68
i_{arc}, κA	13,0	15,0	18,2	21,5	23,2	24,5	21,9	14,6
u_{arc}, V	27	34	36	44	44	44	44	48
η_{loss}	0,65	0,56	0,47	0,388	0,350	0,309	0,330	0,436
η_c	0,194	0,154	0,146	0,119	0,119	0,119	0,119	0,109
$S_{bs.c}$, cm^2	0,18	0,51	1,63	2,95	4,05	4,75	4,9	3,53
$q_{bs.c}$, 10^4, W/cm^2	2,57	1,05	0,454	0,279	0,233	0,223	0,187	0,133
$\eta_{à}$	0,454	0,630	0,340	0,278	0,278	0,278	0,278	0,255
$S_{bs.à}$, cm^2	0,14	0,62	1,65	2,74	3,02	3,46	3,46	2,38
$q_{bs.à}$, 10^4, W/cm^2	18,07	4,690	2,435	1,635	1,700	1,666	1,444	1,080

According to table 2.1 an average density of a current on the cathode of argentiferous contact changes from $71{,}9 \cdot 10^3\ À/cm^2$ to $4{,}14 \cdot 10^3\ À/cm^2$ during time of immovability of arc on contacts. Obviously, on base spots of ultra-high arc of switching-off of low voltage some fundamental physical processes should proceed which provide so high values of current intensity.

Let us analyse as number Biot changes during arc burning on contacts if to accept that in one case a destruction temperature is a fusion temperature, and in other case - boiling temperature of contacts metal. Results of calculations of number Biot for the cathode and the anode are given in table 2.8. From data of table 2.8 it is visible that on the cathode number Biot is less than 1. Hence, at power density ~ 10^4 W/cm^2 and less and Bi <1,0 a liquid-melt of contacts metal can not be formed on all area of base spot on the cathode.

For confirmation of this conclusion we will define time of warming up Ag for a base spot on the cathode under influence of power density $q_{bs.c} = 2{,}57 \cdot 10^4\ W/cm^2$ to temperature of its fusion $T_{melt} = 1285\ K$:

Table 2.8. Value of number Biot on the cathode and the anode

t_{arc}, ms	0,334	0,668	1,34	2,0	2,67	4,0	5,34	6,68
$q_{bs.c}$, $10^{11}, \frac{erg}{s \cdot cm^2}$	2,57	1,05	0,454	0,279	0,233	0,223	0,187	0,133
$Bi_{c.melt}$	1,32	0,54	0,23	0,14	0,12	0,11	0,1	0,07
$Bi_{c.boil}$	1,4	0,57	0,25	0,15	0,13	0,12	0,1	0,07
$q_{bs.a}$, $10^{11}, \frac{erg}{s \cdot cm^2}$	18,07	4,690	2,435	1,635	1,70	1,666	1,444	1,080
$Bi_{a.melt}$	9,28	2,41	1,25	0,84	0,87	0,86	0,74	0,55
$Bi_{a.boil}$	9,77	2,54	1,32	0,88	0,92	0,9	0,78	0,58

$$\tau_{melt} = \frac{\pi \cdot \lambda \cdot c \cdot \rho \cdot (T_{melt} - T_{in})^2}{4 \cdot q_{bs.c}^2} =$$

$$= \frac{\pi \cdot 379 \cdot 10^5 \frac{erg}{s \cdot cm \cdot K} \cdot 0{,}275 \cdot 10^7 \frac{erg}{g \cdot K} \cdot 9{,}32 \frac{g}{cm^3} \cdot (1285K - 400K)^2}{4 \cdot (2{,}57 \cdot 10^{11} erg/(s \cdot cm^2))^2} = = 9{,}0 \cdot 10^{-3}\ s.$$

Really, at initial stage of contacts opening during arc burning $t_{arc} = 0{,}334 \cdot 10^{-3}\ s$ on the area of base spot $S_{bs.c} = 0{,}18\ cm^2$ under the influence of power density $q_{bs.c} = 2{,}57 \cdot 10^4\ W/cm^2$ a liquid-melt Ag can not be formed:

$$\tau_{melt} = 9 \cdot 10^{-3}\ s >> 0{,}334 \cdot 10^{-3}\ s = t_{arc}.$$

On the anode according to table 2.7 a base spot is subjected by influence of power density $q_{bs.a} \geq (10^5 \div 10^4)\ W/cm^2$. In that case the number $Bi \geq 1{,}0$ (see table 2.8). It is possible to admit that on all surface of a base spot on the anode under influence of power density $q_{bs.a} \geq (10^5 \div 10^4) W/cm^2$ and at $Bi \geq 1{,}0$ a liquid-melt Ag will be formed.

Let us define time of warming up Ag on anode base spot upto fusion temperature T_{melt}=1285 K, and then to boiling temperature T_{melt}= 2485 K at an initial stage of opening of contacts under influence of power density $q_{bs.a} = 1{,}807 \cdot 10^5\ W/cm^2$:

$$\tau_{melt} = \pi \cdot \lambda \cdot c \cdot \rho \cdot (T_{melt} - T_{in})^2 / (4 \cdot q_{bs.a}^2) =$$

$$= \frac{\pi \cdot 379 \cdot 10^5 \frac{erg}{s \cdot cm \cdot K} \cdot 0{,}275 \cdot 10^7 \frac{erg}{g \cdot K} \cdot 9{,}32 \frac{g}{cm^3} \cdot (1285K - 400K)^2}{4 \cdot (1{,}807 \cdot 10^{12} erg/(s \cdot cm^2))^2} = 0{,}183 \cdot 10^{-3}\ s;$$

$$\tau_{boil} = \pi \cdot \lambda \cdot c \cdot \rho \cdot (T_{boil} - T_{melt})^2 / (4 \cdot q_{bs.a}^2) =$$

$$= \frac{\pi \cdot 186 \cdot 10^5 \frac{erg}{s \cdot cm \cdot K} \cdot 0{,}29 \cdot 10^7 \frac{erg}{g \cdot K} \cdot 0{,}9 \frac{g}{cm^3} \cdot (2485K - 1285K)^2}{4 \cdot (1{,}807 \cdot 10^{12} erg/(s \cdot cm^2))^2} = 0{,}168 \cdot 10^{-3}\ s;$$

$$\tau_{melt} + \tau_{boil} = (0{,}183 + 0{,}168) \cdot 10^{-3}\ s = 0{,}351 \cdot 10^{-3}\ s.$$

Hence, at an initial stage of opening of argentiferous contacts during arc burning $t_{arc} = 0{,}334 \cdot 10^{-3}$ *s* on an area of base spot on anode $S_{bs.a}$=0,14 cm^2 under influence of power density $q_{bs.a} = 1{,}807 \cdot 10^5\ W/cm^2$ a liquid-melt *Ag* can be formed. Its temperature reaches a temperature of its boiling T_{boil}= 2485 *K*:

$$\tau_{melt} + \tau_{boil} = 0{,}351 \cdot 10^{-3} s \sim 0{,}334 \cdot 10^{-3}\ s = t_{arc}.$$

Correctness of calculations is confirmed with the photos of high-speed filming given in fig. 2.4 on which we can see a running-off of a jet of liquid metal from the mobile contact from 8 to 32 shots during 4,0 *ms*. This mobile contact is the anode.

2.3.2. Erosion traces on high-current contacts

For the purpose of model building of short constricted arc with discrete core and theoretical methods of calculation of its parametres let us turn to microelectronic photos of a surface of argentiferous contacts after switching-off of short-circuit currents. In fig. 2.13 photos of erosion traces of contacts КМК-А10м (content: *Ag* - 85 % and *CdO* - 15 %) and КМК-А30мд (content: Ag - 70 % and *Ni* - 30 %) are given.

The structure of a surface of contacts after switching-off of short-circuit currents has a chaotic appearance with difficult topology. The surface of contacts is spotted by numerous deepenings of a various kind with the cross-section sizes from 0,3 to 100 *μm*. In some cases the surface of contacts looks like "the streams" which have a step (0,2÷0,3) *mm* and depth (10÷80) *μm*. Numerous macro- and microledges have the pointed tops. In the central part of contacts there are many supersmall droplets with the sizes from 0,3 to 1,0 *μm* (fig. 2.14).

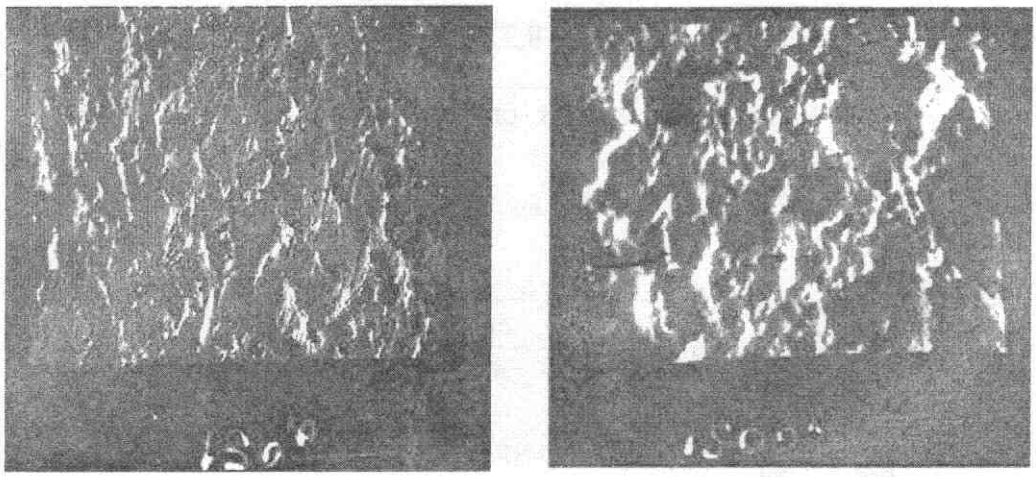

КМК-А30мд, 150^{x} КМК-А10м, 1500^{x}

a) b)

Fig. 2.13. View of a surface of argentiferous contacts after switching-off of short-circuit currents: a - ×150; b - ×1500.

On periphery of contacts rather large drops settle down with diameters (0,2÷0,5) *mm*. More detailed view of craters on a surface of contacts КМК-А10м after switching-off of short-circuit currents is shown in fig. 2.15. Diameters of craters on erosion surface of contacts КМК-А10м after switching-off of short-circuit currents change from 3,0 to 10 *μm*. The internal surface of craters is covered by numerous microwaves. The parapets and flows of metal on the edges of craters are absent.

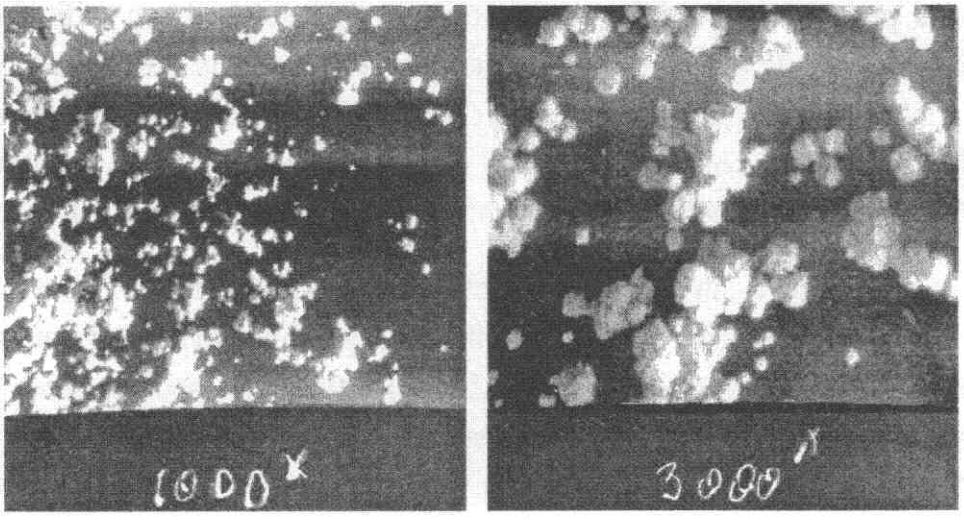

a) b)

Fig. 2.14. Fragments of a surface of contacts КМК-А30мд after switching-off of short-circuit currents covered with drop particles: a - ×1000; b - ×3000

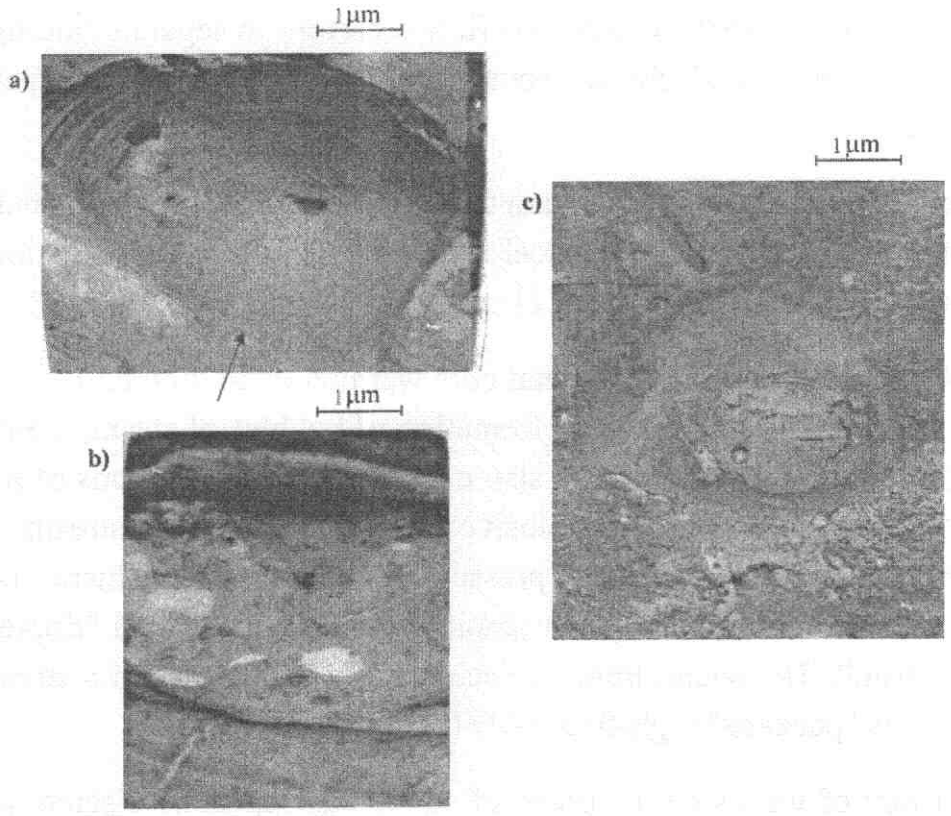

Fig. 2.15. Craters on a surface of contacts КМК-А10м after switching-off of short-circuit currents

From analysis of the microelectronic photos given in fig. 2.13, 2.14 and 2.15, it is followed that prominent features of erosion traces on argentiferous contacts after switching-off of short-circuit currents by low-voltage breakers are their difficult relief with the numerous pointed microledges, deep hollows and the craters in which internal surface is covered by microwaves, and presence of set of microdrops.

It is represented to us that craters on contacts of low-voltage breakers at switching-off of short-circuit currents are formed as a result of superficial bubble boilings of a thin layer of liquid metal on base spots of arc which leads to cyclic formation of numerous microbubbles with their subsequent explosion. At explosion of microbubbles there is an eruption of microjets of plasma and emission of microdrops from contacts metal. Eruption of microjets of plasma is accompanied by generation of portions of electrons. A portion of electrons, generated at their explosive emission in vacuum arc discharge, was named **ectons** (from the first letters of words Explosive Centre - centre of explosion) by academician G.A.Mesjats [2.8]. We are represented pertinent to use concept "ecton" in the description of physical processes in low-voltage arc of switching-off of high power.

Each portion of electrons and ions flow a current in separate microjets of plasma. A sum of currents of all simultaneously functioning microjets of plasma provides a flow of arc current.

In favour of the come out assumption the materials of experimental and theoretical researches of thermomechanical mechanisms of a fragmentation of liquid drops at steam explosion can serve [2.11, p. 491, 2.12, p. 100, 2.13, p. 913].

In the specified researches a metal core warmed up to 400÷850 ^{o}C was lowered in distilled water and it was observed formation of bubbles of steam, their explosions and expiration of steam streams, and also oscillograms of pulsations of pressure and sound fluctuations were made at explosive emission of a steam stream. Researches have shown that a pulsation of steam pressure in a bubble and influence of a superficial tension lead to formation of short (capillary) waves (so-called "ripples") on border "liquid-steam". The sound impulse accompanying emission of a stream of water steam represents "package" high-frequency (~ 3 *kHz*) fluctuations.

Frequency of waves on a surface of anode base spots of discrete jets of plasmaof diffuse arc at switching-off of short-circuit is equal to ~ 10^4 *Hz* [2.4, part I, p. 252]. This frequency corresponds to a sound range perceived by a person.

Hence, presence of capillary microwaves on a surface of craters is cofirmation of their formation as a result of an explosive mechanism of microbubbles destruction and expiration of steam streams from them.

Thus, at switching-off of short-circuit currents by low-volage breakers on their opening contacts there is a short constricted arc with a discrete core. In this arc a continuity of current flow is provided by the numerous ectons which discrete both in space and in time [2.8].

2.4. Current flow in short constricted arc with a discrete core by means of evaporation of contacts metal

Current flowing in arc discharge of high power is provided with emission processes of a different kind. In [2.4. part I] it is shown that in the low-voltage arc discharge high power thermo- and autoelectronic emissions can not provide a current flow. In the previous paragraph possibility of current flow in short constricted arc with a discrete core of high power is shown for the account of explosive emission of elecrons. However it is necessary to take into account thermal processes on base spotss of arc which can lead to evaporation of contacts metal.

In [2.9, appendix 3, p. 238] velosity of evaporation Zn, Cu and W in $g/(cm^2 \cdot s)$ is given depending on power density q coming on a metal surface in W/cm^2.

In the investigated breakers as it was already specified, as explosive contacts the composite argentiferous ceramic-metal materials on the basis of Ni and W were applied. In such contacts in process of arc burning a silver Ag will be subjected to evaporation basically.

According to [2.5, p. 204], evaporation of substance from its free surface in adiabatic mode is defined by the formula:

$$j_{ev} = \frac{q_{ev}}{W_{ev}},$$

where j_{ev} – density of a stream of steam mass on evaporation surface, $g/(cm^2 \cdot s)$; q_{ev} – power density spent for evaporation, W/cm^2 and W_{ev} – specific heat of evaporation of substance $W \cdot s/g$.

For power density q_{ev} spent for evaporation, we will accept power density coming on a base spot of cathode $q_{bs.c}$ and of the anode – $q_{bs.a}$ (table 2.7). Specific heat of evaporation Ag at boiling temperature: $W_{av}^{Ag} = 2{,}36 \cdot 10^3 W \cdot s/g$ (table 1.1).

For an example we will calculate a flux density of steam mass of Ag and value of a current intensity, flowing in arc for the account of steams evaporation of Ag from a surface of base spots, at the initial stage of contacts opening, using data given in table 2.7 corresponding to the shot 2 in fig. 2.4.

Shot 2.

The cathode: stream density of steam mass of Ag:

$$j_{ev} = \frac{q_{bs.c}}{W_{ev}^{Ag}} = \frac{2{,}57 \cdot 10^4 W/cm^2}{2{,}36 \cdot 10^3 W \cdot s/g} = 10{,}89 g/(cm^2 \cdot s).$$

Mass of steam which has evaporated from a surface of base spot on the cathode with area $S_{bs.c}$ during filming of one shot $\Delta t = 0{,}167 \cdot 10^{-3} s$:

$$m_{st.c} = j_{ev.c} \cdot S_{bs.c} \cdot \Delta t =$$

$$= 10{,}89 g/(cm^2 \cdot s) \cdot 0{,}18 cm^2 \cdot 0{,}167 \cdot 10^{-3} s = 0{,}327 \cdot 10^{-3} g.$$

Quantity of atoms Ag in steam mass:

$$N_{o.c} = \frac{m_{st.c}}{m_o} = \frac{0{,}327 \cdot 10^{-3}\, g}{179{,}1 \cdot 10^{-24}\, g} = 1{,}826 \cdot 10^{18},$$

where $m_o = 179{,}1 \cdot 10^{-24}\, g$ – atom mass Ag.

The anode: stream density of steam mass of Ag:

$$j_{ev.a} = \frac{q_{bs.a}}{W_{ev}^{Ag}} = \frac{18{,}07 \cdot 10^4 W/cm^2}{2{,}36 \cdot 10^3 W \cdot s/g} = 76{,}57 g/(cm^2 \cdot s).$$

Mass of steam which has evaporated from a surface of a base spot on the anode:

$$m_{st.a} = j_{ev.a} \cdot S_{bs.a} \cdot \Delta t =$$

$$= 76{,}57 g/(cm^2 \cdot s) \cdot 0{,}14 cm^2 \cdot 0{,}167 \cdot 10^{-3} s = 1{,}79 \cdot 10^{-3} g.$$

Quantity of atoms Ag in mass of steam:

$$N_{o.a} = \frac{m_{ev.a}}{m_o} = \frac{1{,}79 \cdot 10^{-3}\, g}{179{,}1 \cdot 10^{-24}\, g} = 9{,}99 \cdot 10^{18}.$$

Total quantity of atoms Ag which has arrived in the arc channel for the account of evaporation from a surface of base spots on the cathode and the anode:

$$\sum N_o = N_{o.c} + N_{o.a} = (1{,}826 + 9{,}99) \cdot 10^{18} = 1{,}182 \cdot 10^{19}.$$

According to the data [2.4, table 4.21, p. 104] in considered experience degree of plasma ionization x_e in arc channel is ~1,0 during filming of a shot 2. Hence, quantity of electrons in mass of evaporated steam Ag in arc channel is equal to a quantity of atoms, that is:

$$\sum N_e = \sum N_i .$$

In that case during filming time of one shot electrons having a charge $1{,}6 \cdot 10^{-19}$ Coulomb, transfer a current intensity equal to:

$$i_{ev.arc} = \frac{e \cdot \sum N_e}{\Delta t} = \frac{1{,}6 \cdot 10^{-19} Coulomb \cdot 1{,}182 \cdot 10^{19}}{0{,}167 \cdot 10^{-3} s} = 11{,}32 \cdot 10^3 A.$$

During filming of a shot 2 according to experimental data an average instant

value of a current is equal to $i_{arc} = 13{,}0 \cdot 10^3\ A$. Deficiency of a current intensity is:

$$\Delta i_{arc} = i_{arc} - i_{ev.arc} = (13{,}0 - 11{,}32) \cdot 10^3\ A = 1680 A.$$

In table 2.9 the results of calculations of stream density of steams weight and values of current flowing in arc channel for the account of evaporation Ag from a surface of base spots of arc at current switching-off in a test loop 16,0 *кА* (r.m.s), phase voltage 420 *V* and $cos\ \varphi = 0{,}2$ are given.

In fig. 2.16 the graphs of change of current i_{arc} and current $i_{ev.arc}$ in the process of arc burning are given. They were built according to table 2.9.

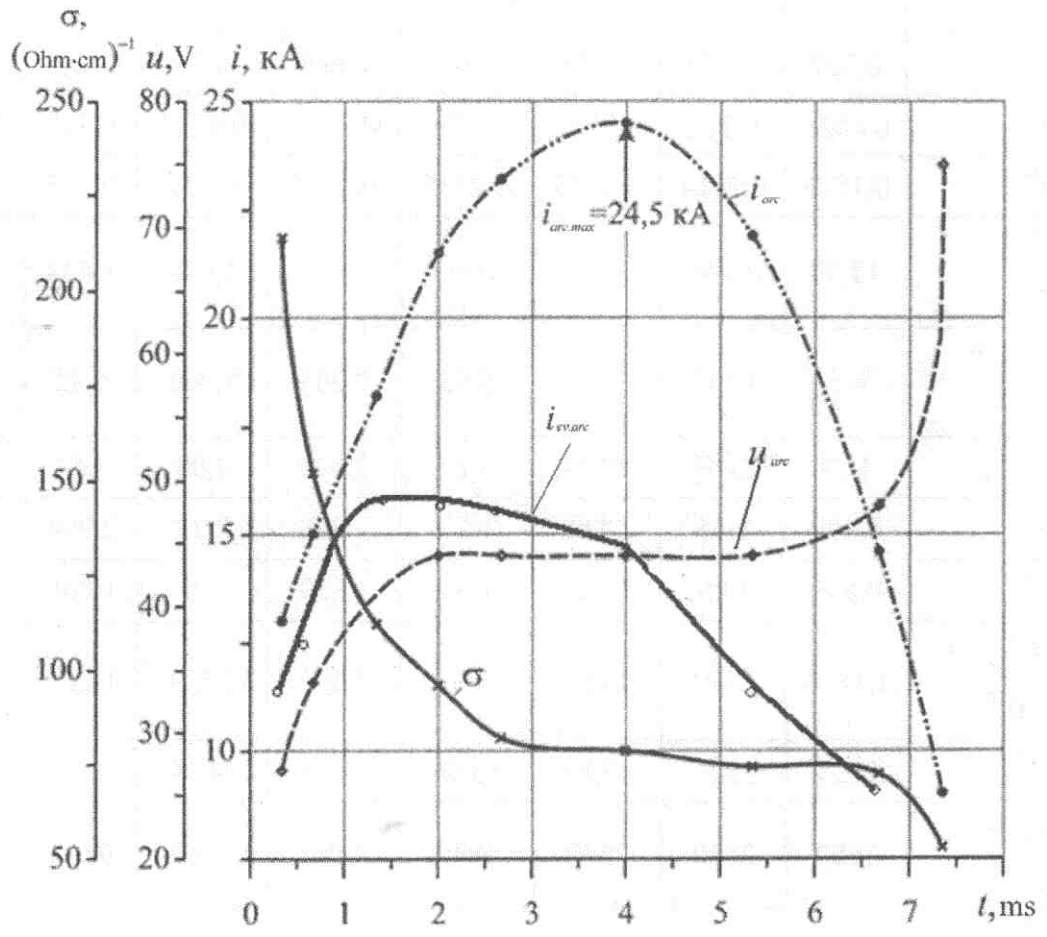

Fig. 2.16. An arc current i_{arc}, current $i_{ev.arc}$ and specific conductivity of plasma on opening argentiferous contacts at switching-off of current 16 *кА*

Obviously, deficiency of a current should fill by the ectons arising in the result of explosive emission of electrons.

Table 2.9. Density of steam mass stream Ag j_{arc} and current i_{arc} flowing in arc channel for the account of evaporation at current switching-off 16,0 κA, $U_{ph} = 420V$ and $\cos\varphi = 0{,}2$

t_{arc}, ms	0,334	0,668	1,34	2,0	2,67	4,0	5,34	6,68
$i_{arc}, \kappa A$	13,0	15,0	18,2	21,5	23,2	24,5	21,9	14,6
$X_{å}$	~1,0	~0,95	~0,88	0,78	0,67	0,57	0,54	0,55
$q_{bs.c}, 10^4$, W/cm^2	2,57	1,05	0,454	0,279	0,233	0,223	0,287	0,133
$j_{ev.c}$, $g/(cm^2 \cdot s)$	10,89	4,45	1,924	1,182	0,997	0,945	0,792	0,564
$m_{ev.c}, 10^{-3}, g$	0,327	0,379	0,542	0,582	0,668	0,75	0,648	0,332
$N_{o.c}, 10^{19}$	0,1826	0,212	0,2926	0,325	0,3727	0,4185	0,362	0,1856
$N_{e.c}, 10^{19}$	0,1826	0,2014	0,2575	0,2535	0,2497	0,239	0,195	0,102
$q_{bs.a}, 10^4$, W/cm^2	18,07	4,690	2,435	1,635	1,7	1,666	1,444	1,08
$j_{ev.a}$, $g/(cm^2 \cdot s)$	76,57	19,87	10,32	6,93	7,203	7,060	6,12	4,58
$m_{ev.a}, 10^{-3}, g$	1,79	2,057	2,844	3,17	3,633	4,08	3,54	1,82
$N_{o.a}, 10^{19}$	0,999	1,15	1,588	1,77	2,028	2,28	2,974	1,016
$N_{e.a}, 10^{19}$	0,999	1,09	1,397	1,39	1,359	1,3	1,066	0,559
$\sum N_e = (N_{e.c} + + N_{e.a}), 10^{19}$	1,1816	1,291	1,655	1,634	1,609	1,539	1,261	0,661
$i_{ev.arc}, 10^3, A$	11,32	12,37	15,86	15,66	15,41	14,74	12,08	6,33
$\Delta i_{arc} = i_{arc} - - i_{ev.arc}, A$	1680	2630	2340	5840	7790	9760	9820	8270

2.5. Centres of concentration of charges

As a result of technological processes of manufacture the surface of contacts has a non-uniform form. As it has been shown earlier the erosion surface of contacts has rather difficult relief. Moreover, presence of drops on contacts complicates its relief. Microroughness on a surface of contacts can be presented in the form of various simple geometrical figures [2.8]. In that case the surface of contacts can be

represented as chaotically covered with hemispherical craters, deepenings in the form of cones, microledges in the form of hemispheres, cones with various corners and radiuses of rounding in their top and microdrops.

Microledges locally concentrate on themselves electric field in which they are. Thus there are centres of concentration of charges and there is a local amplification of average intensity of a field in contact gap which is defined by expression:

$$E_{av} = \frac{u_{arc}}{\delta},$$

where u_{arc} – arc voltage in V and δ – contact gap in cm.

Microledges of a different configuration amplify a field in different degree:

$$E_{top} = \beta_E \cdot E_{av},$$

where E_{top} – local field intensity at top of a microledge and β_E – factor of amplification of a field.

In [2.8, p. 19] it was considered an amplification of field on the microledges, located on a surface of electrodes in the conditions of the vacuum, having a view of geometrical figures: ellipsoid, a cylinder with spherical top, a cone with spherical top and sphere on the thin basis. Fig. 2.17 shows the graphs of change of factors of amplification of field β_E on microledges depending on the relation of their height h to rounding radius r_{top} of microledges tops [2.8, p. 20].

On fig. 2.18 configurations of microledges on the cathode in the conditions of vacuum are schematically shown for definition of factors of amplification of field β_E [2.8, p. 56].

On erosion surface of contacts of low-voltage breakers working in the conditions of atmospheric air, as the microledges can settle down shown in fig. 2.18, and the microledges schematically represented in fig. 2.19.

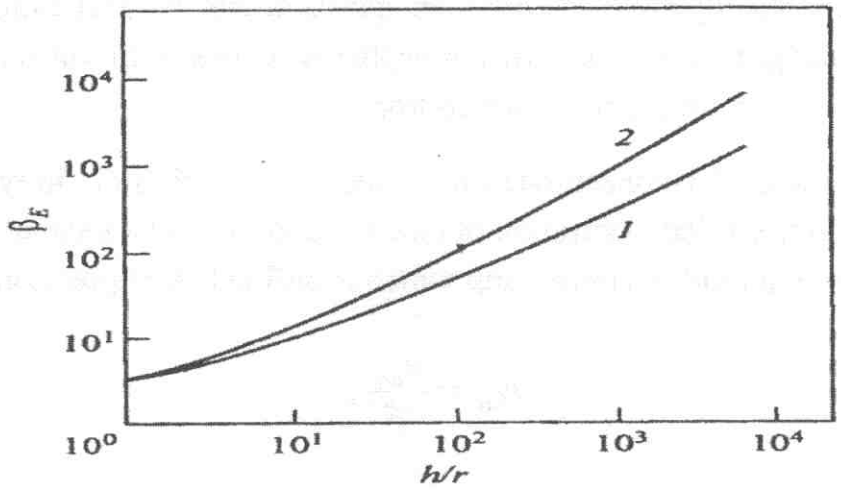

Fig. 2.17. Field amplification factor on a microledge depending on the relation of height of a ledge to tip radius: ellipsoidal form of a ledge (1); the cylinder with spherical top, sphere on the thin basis (2)

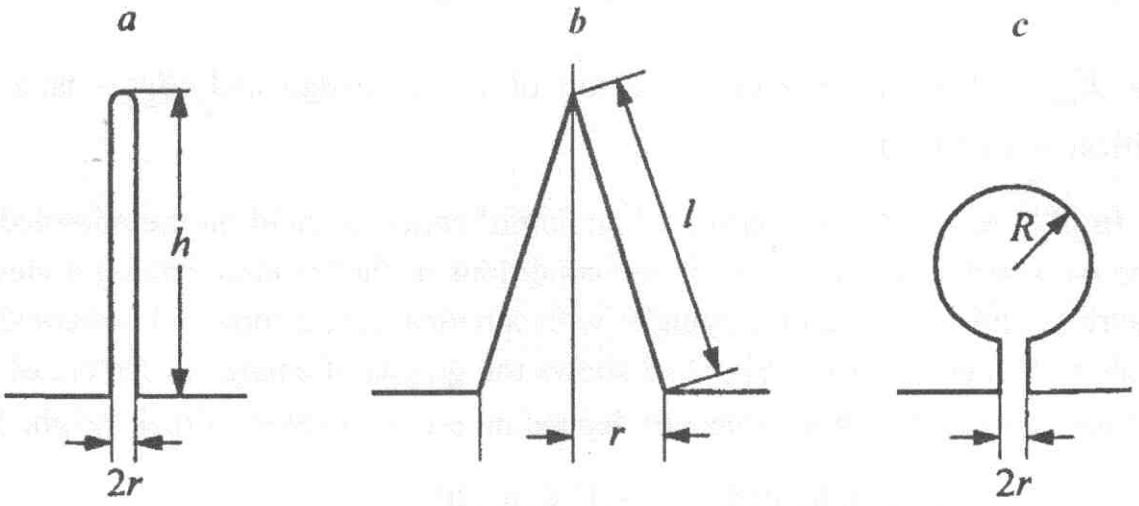

Fig. 2.18. A configuration of nonuniformities on the cathode for definition of field factor β_E and current density β_j: the cylinder (a); a cone (b); sphere (c)

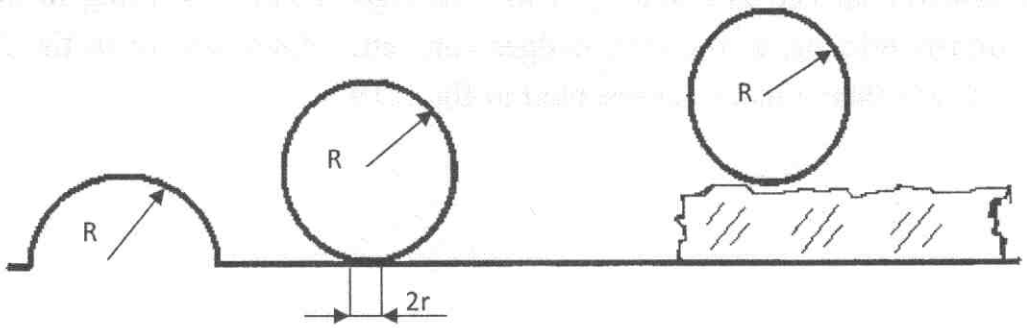

Fig. 2.19. A microledge in the form of a hemisphere and a drop on a contacts surface

In the previous paragraph it has been shown that on base spots of arc can proceed superficial bubble boiling of a liquid-melt Ag. Formed in a liquid-melt microbubbles either burst or blow up. At their explosion there is a scattering of microdrops and perturbance in the form of dispersing waves. Then microbubbles collapse and on their place the splashes of liquid metal in the form of columns with microdrops at their tops and dispersing waves arise. Those microbubbles which do not blow up, collapse also. Process of collapse is schematically shown in fig. 2.20 [2.15, p. 94].

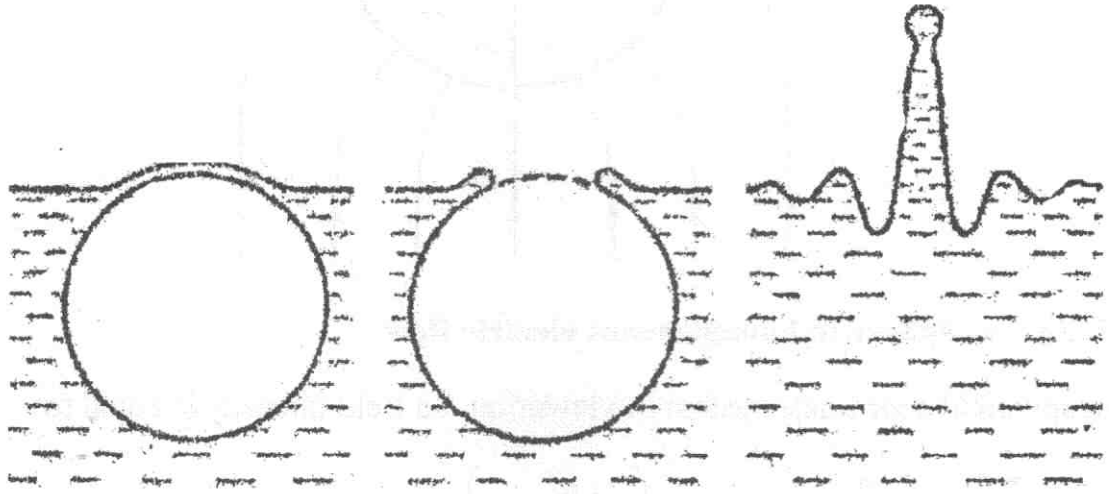

Fig. 2.20. Collapsed bubble on a surface of liquid forms a water column and a circular wave. Consecutive stages of process

Similar perturbances are well observed in fig. 3.31 (colour insert) and fig. 3.32 on p. 228 given in [2.4, part I]. In points of intersection of diverging waves there are splashes of a liquid-melt with droplets at their tops. Splashes of a liquid-melt in the form of columns and cones with small corners in their top and microdrops on base spots of arc become the centres of concentration of charges which lead to amplification of field.

According to classical theory of electric field, a metal sphere brought in a homogeneous field leads to its distortion (fig. 2.21).

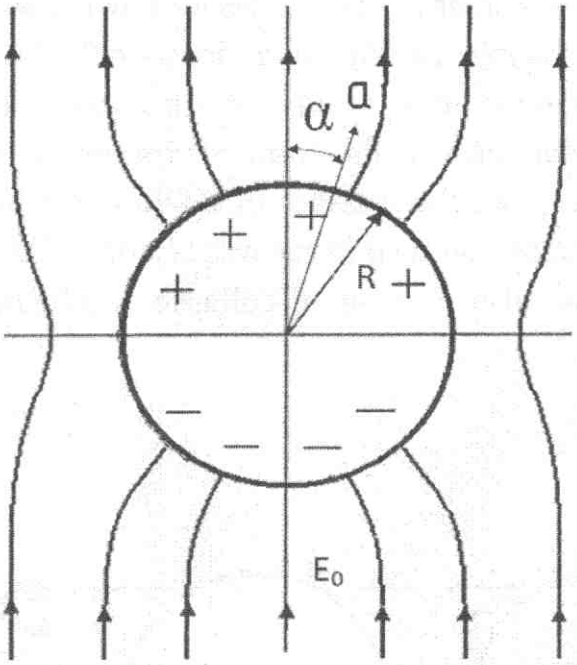

Fig. 2.21. Metal sphere in homogeneous electric field

In spherical coordinate system in viewpoint *a* a field intensity is equal to:

$$E_a = E_0\left(\frac{2\cdot R^3}{a^3}+1\right)cos\,\alpha;$$

$$E_\alpha = E_0\left(\frac{2\cdot R^3}{a^3}+1\right)sin\,\alpha.$$

The total field is equal to:

$$E=\sqrt{E_{\grave{a}}^2+E_\alpha^2}.$$

On a sphere surface, that is at $a=R$, we will have:

- $E_a = 3E_0\cos\alpha$ and $E_\alpha = 3\mathring{A}_0\sin\alpha$;
- at $\alpha = 0^\circ$ $E_a = 3E_0 = E_{\max}$ and $E_\alpha = 0$.

Hence, the amplification factor of field in the centre of sphere top is $\beta_E = 3$.

In [2.8, p. 20] there are given the formulas defining value of amplification factors of field on spherical top of radius r_{top}:

- of cylinder – $\beta_E = \dfrac{h}{r_{top}} + 2;$
- of cone – $\beta_E = \dfrac{h}{2r_{top}} + 5;$ at angle in top $2\alpha = 5 \div 10^\circ$.

Here h – height of cylinder or cone.

Amplification factors of field calculated according to these formulas can reach value 100 and more.

The superficial density of the induced electric charge on spherical top of a microledge is equal in a general view:

$$\sigma = \beta_E \cdot \varepsilon_0 \cdot E_{av} \cdot \cos\alpha,$$

where $\varepsilon_0 = 8{,}86 \cdot 10^{-12} F/m$ – electric constant in measurement system SI ($1 F/m = 9 \cdot 10^9$ *CGS*).

On a sphere surface a superficial density of a charge is equal:

$$\sigma = 3 \cdot \varepsilon_0 \cdot E_0 \cdot \cos\alpha.$$

At:

$$\alpha = 0 \quad \sigma = 3\varepsilon_0 \cdot E_0;$$

$$\alpha = 90^\circ \quad \sigma = 0.$$

A quantity of the induced charge in a top centre on a hemisphere is equal to:

$$q_{ch} = 3\pi \cdot \varepsilon_0 \cdot E_0 \cdot R^2.$$

In the centre of spherical top with radius r_{top} of any microledge on surfaces of contacts a charge increases up to value:

$$q_{ch} = \beta_E \cdot \pi \cdot \varepsilon_0 \cdot E_{av} \cdot r_{top}^2.$$

Thus, the centre of concentration of charges, formed on a microledge, gets a charge q_{ch} which exceeds average value of a charge in contact gap, transferred by arc current, in β_A times.

As a charge q is equal to product $i \cdot t$ for the same time a current flowing through the microledge centre, having a square of base $\pi \cdot r^2$, will increase by value β_E. Hence, a power density, coming on the centre of concentration of charges, increases also.

In [2.8, p. 56] a current density on a microledge, located on the cathode, is defined by the formula:

$$j_{cyl} = j_{av} \cdot \frac{S}{\pi \cdot r^2},$$

where $S_{cyl} = 2\pi \cdot r \cdot h$ – square of cylinder, $S_{cone} = \pi \cdot r \cdot l$ – square of cone, $S_{sph} = 4\pi \cdot r^2$ – square of sphere (see fig. 2.18).

According to table 2.7 power density $q_{bs.c}$ coming on base spot of arc on the cathode during the first moment of time of contacts opening, is equal $2{,}57 \cdot 10^4\ W/cm^2$. It was shown earlier that power density equal $2{,}57 \cdot 10^4\ W/cm^2$ can not lead to melting of all area of base spot equal $0{,}18\ cm^2$.

For example we will define an amplification of current density on a microledge in the form of a cone with radius of the base equal to average radius of a crater on cathode $r_{cr.c} = 10^{-4} cm$ and angle in top $2\alpha = 10°$. In that case density of current, flowing through a cone, will increase in:

$$\beta_j = \frac{S_{cone}}{\pi \cdot r_{cr.c}^2} = \frac{\pi \cdot r_{cr/c} \cdot l}{\pi \cdot r_{cr.c}^2} = \frac{11{,}5 \cdot 10^{-4} cm}{10^{-4} cm} = 11{,}5,$$

where $l = \frac{r_{cr.c}}{\sin\alpha} = \frac{10^{-4} cm}{\sin 5°} = \frac{10^{-4} cm}{0{,}0872} = 11{,}5 \cdot 10^{-4} cm.$

As a density of current, flowing through a cone, will increase in β_j=11,5 times then power density, coming on a cone, will also increase in β_j=11,5 times in comparison with power density $q_{bs.c}$, coming on the cathode. For example, at initial stage of contacts opening a power density on a cone will be equal:

$$q_{cone} = \beta_j \cdot q_{bs.c} = 11{,}5 \cdot 2{,}57 \cdot 10^4\ W/cm^2 = 2{,}96 \cdot 10^5 W/cm^2.$$

Value of power density $q_{cone} = 2{,}96 \cdot 10^5\ W/cm^2$ is average value. At top of a cone with rounding radius a maximum value of power density can reach values of

tens-hundreds sizes of atoms [2.8, p. 24]. Radiuses of atoms Ni, Fe, Cu, W and Ag change from $1{,}24\cdot10^{-8}\,cm$ to $1{,}44\cdot10^{-8}\,cm$. For estimated calculations rounding radius in cone top we will accept equal $r_{top}=5\cdot10^{-6}\,cm$. In that case amplification factor of field β_E:

$$\beta_E=\frac{h}{2r_{top}}+5=\frac{11{,}4\cdot10^{-4}\,cm}{2\cdot5\cdot10^{-6}\,cm}+5=119,$$

where $h=\frac{r_{cr.c}}{tg5^\circ}=\frac{10^{-4}\,cm}{0{,}0875}=11{,}4\cdot10^{-4}\,cm$ – height of cone.

On erosion surfaces of contacts there will be sufficiently large quantity of microledges in the form of a cone with sizes accepted in the example. Power density at initial stage of contacts opening on such cones, located on the cathode, will reach values:

$$q_{cyl.\max.c}=\beta_E\cdot q_{bs.c}=119\cdot2{,}57\cdot10^4 W/cm^2=3{,}06\cdot10^6 W/cm^2.$$

A result of calculations of values of power density on the centres of concentration of charges in process of arc burning on contacts is given in table 2.10 at switching-off of short-circuit currents equal 16,0 κA.

Obviously, power density equal $3{,}06\cdot10^6 W/cm^2$ and less cannot lead to explosive destruction of microledges in the form of cones.

For explosive destruction of microledges of contacts metal a power density equal not less $10^8\ W/cm^2$ is needed. Moreover, density of current, flowing through a cone, equal:

$$j_{cyl}=j_{av}\cdot\beta_j=71{,}9\cdot10^3\,A/cm^2\cdot11{,}5=8{,}27\cdot10^5\,A/cm^2-$$

is obviously insufficient for explosive destruction of microledges also. For explosive destruction of a current conductor a current density should be not less $10^8\ A/cm^2$.

However under influence of power density $q_{cyl.\max.c}=30{,}6\cdot10^5 W/cm^2$ and less the drops on a base spot of arc can be subjected to explosive destruction as a result of action of mechanocaloric forces [2.11, 2.12 and 2.13].

Table 2.10. Values $q_{cyl.\max.c}$ running on microledges on the cathode in process of contact opening at switching-off of current 16,0 κA and phase voltage 420 V

t_{arc}, ms	0,334	0,668	1,34	2,0	2,67	4,0	5,34	6,68
$i_{arc}, \kappa A$	13,0	15,0	18,2	21,5	23,2	24,5	21,9	14,6
$q_{bs.c}, 10^4$, W/cm^2	2,57	1,05	0,454	0,279	0,233	0,223	0,187	0,133
$q_{cyl.\max.c}, 10^5$, W/cm^2	30,6	12,5	5,4	3,32	2,77	2,65	2,23	1,58

At explosion the drop are split up for small parts with minimum critical radius $r_{c.crit}$ which for drops from Ag is defined by the formula [2.4, part II, p. 81]:

$$r_{c.crit} \sim 122\sqrt{\frac{1}{q_c}},$$

where q_c – power density running on a drop. For example we will define $r_{c.crit}$ for drops from Ag under influence of maximal and minimal values of power density $q_{cyl.max.c}$, which are given in table 2.10:

$$r_{c.crit} \sim 122\sqrt{\frac{1}{q_{cyl.\max.c}}} = 122\sqrt{\frac{1}{30{,}6\cdot 10^{12}\, erg/(s\cdot cm^2)}} = 0{,}22\cdot 10^{-4}\, cm;$$

$$r_{c.crit} \sim 122\sqrt{\frac{1}{1{,}58\cdot 10^{12}\, erg/(s\cdot cm^2)}} = 0{,}97\cdot 10^{-4}\, cm.$$

The obtained results of calculations $r_{c.crit}$ coincide well enough with the sizes of the drops shown in fig. 2.14. Their radiuses change from $0{,}15\cdot 10^{-4}\, cm$ to $0{,}5\cdot 10^{-4}\, cm$.

The mentioned values $r_{c.crit}$ mean that drops Ag will be subjected to destruction only which have a radius not exceeding $r_{c.crit}$ on two orders.

The drops, in which radius exceeds top limit of splitting, can have a break a shell without their destruction and steam flow, leading to formation of hollow drops.

Each explosion of the drop, which is in arc channel, is accompanied by emission of the ionised portion of metal steam which contains certain quantity of electrons

and ions. Thus, explosive emission of electrons, accompanying explosion of the drops, raises their concentration in arc channel and, thereby, promotes self-maintenance of its burning.

The mentioned calculations of thermomechanical splitting of drops at switching-off of short-circuit currents by low-voltage breakers prove conformity of presence in arc chutes as a microbubbles so large drops including the hollow ones.

2.6. Current conduct by ectons in short constricted arc with a discrete core

In the previous paragraphs two fundamental physical processes were shown which provide a current flowing in short constricted arc with a discrete core on opening contacts of low-voltage breakers: evaporation of a contacts material and explosive emission of electrons on basy spots of arc. In table 2.9 we can see the values of a current intensity flowing in arc at switching-off of short-circuit current equal 16,0 κA by means of evaporation of contacts material i_{ev} and deficiency of a current Δi_{arc} which, obviously, should be filled for the account of explosive emission of electrons.

In low-voltage arc of switching-off of high power ectons can appear due to explosions of microbubbles formed at superficial bubble boiling of a liquid-melt on base spot.

We will be convinced that on base spot both on the cathode and on the anode at switching-off of current equal 16,0 κA, superficial bubble boiling can arise in a thin layer of a liquid-melt.

2.6.1. Current conduct by ectons on the cathode

Earlier an impossibility of formation of a liquid-melt was been shown on all area of a cathodic base spot under influence of power density $q_{bs.c} = 2{,}57 \cdot 10^4\ W/cm^2$. However due to increasing of power density $q_{cyl.max}$ up to a value running on the centres of charges concentration which reach value $10^5\ W/cm^2$ and more (see table 2.10), it is possible to expect a formation of a liquid-melt of metal on a place of the centres of charges concentration. For example we will define a fusion time τ_{melt} Ag under influence of power density $q_{cyl.max.c} = 30{,}6 \cdot 10^5\ W/cm^2 = 30{,}6 \cdot 10^{12}\ erg/\left(s \cdot cm^2\right)$, and then a time when a liquid-melt reach a boiling temperature:

$$\tau_{melt} = \frac{\pi \cdot \lambda \cdot c \cdot \rho \cdot (T_{melt} - T_0)^2}{4 \cdot q_{cyl.max.c}^2} =$$

$$= \frac{\pi \cdot 379 \cdot 10^5 \frac{erg}{s \cdot cm \cdot K} \cdot 0{,}275 \cdot 10^7 \frac{erg}{g \cdot K} \cdot 9{,}32 \frac{g}{cm^3} \cdot (1285K - 400K)^2}{4 \cdot (30{,}6 \cdot 10^{12} erg/(s \cdot cm^2))^2} = 6{,}38 \cdot 10^{-7}\ s;$$

$$\tau_{boil} = \frac{\pi \cdot \lambda \cdot c \cdot \rho \cdot (T_{boil} - T_{melt})^2}{4 \cdot q_{cyl.max.c}^2} =$$

$$= \frac{\pi \cdot 186 \cdot 10^5 \frac{erg}{s \cdot cm \cdot K} \cdot 0{,}29 \cdot 10^7 \frac{erg}{g \cdot K} \cdot 9{,}0 \frac{g}{cm^3} \cdot (2485K - 1285K)^2}{4 \cdot (30{,}6 \cdot 10^{12} erg/(s \cdot cm^2))^2} = 5{,}86 \cdot 10^{-7}\ s;$$

$$\tau_{melt} + \tau_{boil} = (6{,}38 + 5{,}86) \cdot 10^{-7}\ s = 12{,}24 \cdot 10^{-7}\ s.$$

Really, under influence of power density $q_{cyl.max.c} = 30{,}6 \cdot 10^5\ W/cm^2$ on a place of microledge located on a cathodic base spot during $\tau_{melt} + \tau_{boil} = 12{,}24 \cdot 10^{-7}\ s$ a liquid-melt of *Ag* arises in which temperature reaches temperatures of its boiling.

Forming time of craters, according to [2.8, p. 354], is defined by the formula:

$$t_{cyl} = \frac{r_{cr}^2}{4 \cdot a},$$

where r_{cr} – radius of a crater and a – temperature conductivity coefficient.

As well as earlier, for estimated calculations we will accept an average radius of craters on the cathode equal 10^{-4} *cm*. Then a forming time of a crater on a liquid-melt *Ag* will be equal:

$$t_{cyl} = \frac{(10^{-4}\ cm)^2}{4 \cdot 0{,}55\ cm^2/s} = 4{,}5 \cdot 10^{-9}\ s.$$

Forming time of a crater, which can be accepted as forming time of microbubble, practically is less on three orders than time when a liquid-melt reach a temperature of its boiling:

$$\tau_{melt} + \tau_{boil} = 1{,}224 \cdot 10^{-6}\ s >> 4{,}5 \cdot 10^{-9}\ s.$$

Moreover, time when a liquid-melt reaches a boiling temperature *Ag* is much less than time of arc burning at its initial stage:

$$\tau_{melt} + \tau_{boil} = 1{,}224 \cdot 10^{-6}\ s << 0{,}334 \cdot 10^{-3}\ s = t_{arc}.$$

In process of arc burning on opening contacts a power density $q_{cyl.max.c}$ coming on the centres of concentration of charges, decreases. But, as the calculations show, time when a liquid-melt reaches a boiling temperature *Ag* still does not exceed time of arc burning. That is superficial bubble boiling of a liquid-melt on a cathodic base spot is **discrete** and also it proceeds during all time of a finding of arc on contacts. In that case, in a thin layer of boiling liquid-melt there are microbubbles which, blowing up, flow out microjets of plasma and form craters.

In fig. 2.22 a bubble is schematically shown in a thin layer of liquid metal.

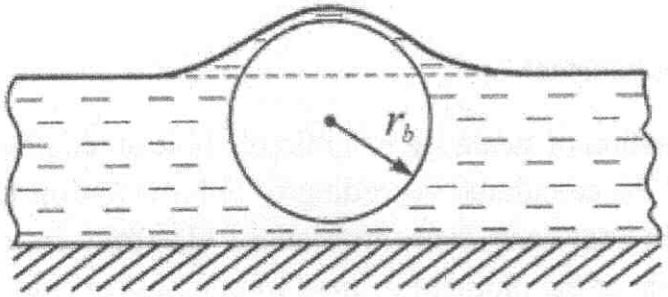

Fig. 2.22. A bubble in a thin layer of liquid metal

Pressure in a bubble P_b having a form of sphere makes a pressure of environment P_{av} in which it is, and the pressure P_L created by forces of a superficial tension, named by Laplace pressure [2.15, p. 21]:

$$P_b = P_{av} + P_L = \frac{\mu_0 \cdot i_{arc}^2}{8 \cdot \pi^2 \cdot r_{bs}^2} + \frac{4 \cdot \sigma}{r_b},$$

where P_{av}=P_m we accept for electromagnetic pressure on base spot arising in a place of transition of current from electrode in arc channel [2.2, p. 22], i_{arc} – arc current, r_{bs} – radius of a base spot, σ – factor of a superficial tension of a liquid and r_b – radius of bubbble.

Steam pressure of in a microbubble located on the cathode during the initial moment of conact opening (table 2.1, a shot 2):

$$P_b = \frac{\mu_0 \cdot i_{arc}^2}{8 \cdot \pi^2 \cdot r_{bs.c}^2} + \frac{4 \cdot \sigma}{r_b} = \frac{1{,}26 \cdot 10^{-6} \frac{H}{m} \cdot \left(13 \cdot 10^3\ A\right)^2}{8 \cdot \pi^2 \cdot \left(2{,}4 \cdot 10^{-3}\ m\right)^2} + \frac{4 \cdot 0{,}98 \frac{N}{m}}{1 \cdot 10^{-6}\ m} =$$

$$= 0{,}469 \cdot 10^6\ Pa + 3{,}92 \cdot 10^6\ Pa = 4{,}39 \cdot 10^6\ Pa = 43{,}9 \cdot 10^6 \frac{dynes}{cm^2}.$$

Steam in a microbubble is in a condition of saturation. According to [2.7] a calculated value of temperature of steam saturation of *Ag* is equal to ~ 3510 *K* at pressure of $43{,}9 \cdot 10^6$ *dynes/cm*^{2}. If to accept a steam in a microbubble for ideal gas, we will define concentration of atoms *Ag* n_0 in it which is equal:

$$n_0 = \frac{Ð_b}{k \cdot Ò_{sat}} = \frac{43{,}9 \cdot 10^6\ dynes/cm^2}{1{,}38 \cdot 10^{-16}\ erg/Ê \cdot 3510\,Ê} = 9{,}06 \cdot 10^{19}\,cm^{-3},$$

where *k* – Boltzmann constant.

Degree of ionisation of steam *Ag* in a microbubble at temperature T_{sat}=3510 *K* and pressure P_b=$4{,}39 \cdot 10^6$ *Pa* calculated according to Saha equation [2.4, part I, p. 96], is equal to x_e=$1 \cdot 10^{-7}$. In that case concentration of electrons in a microbubble which apeared on the cathode at the moment of time of contacts opening is equal:

$$n_å = n_0 \cdot \tilde{o}_å = 9{,}06 \cdot 10^{19} \cdot 1 \cdot 10^{-7} = 9{,}06 \cdot 10^{12}\ cm^{-3}.$$

A quantity of primary electrons in a microbubble having volume V_b is equal:

$$N_å = n_å \cdot V_b = 9{,}06 \cdot 10^{12}\ cm^{-3} \cdot \frac{4}{3} \cdot \pi \cdot \left(10^{-4}\right)^3\ cm^3 = 38,$$

where r_b=10^{-4} *cm* – average radius of a microbubble on the cathode.

At explosion of a microbubble under pressure of P_b=$4{,}39 \cdot 10^6$ *Pa* (44,3 *atm*) primary electrons in a cathodic zone get speed [2.4, part II, p. 46] under influence of cathodic effective potential $U_{ef.c}$=5,25 *V*:

$$\upsilon_å = 0{,}593 \cdot 10^8 \cdot \sqrt{U_{ef.c}} = 0{,}593 \cdot 10^8 \cdot \sqrt{5{,}25\,V} = 1{,}36 \cdot 10^8\ cm/s.$$

Velocity of electrons $1{,}36 \cdot 10^8$ *cm/s* is almost equal to velocity $1{,}63 \cdot 10^8$ *cm/s* which causes ionisation of atoms *Ag* at their unitary not elastic mutual impact. And it leads to avalanche ionisation of steams *Ag* in a microbubble [2.4, part I, p.130]. Thus, degree of ionisation of steams *Ag* in a microvial gets higher value.

As a first approximation let us accept a degree of ionisation of steams *Ag* in microbubbles on the cathode, apearing during the filming of a shot 2 equal $x_e = 0{,}18$. In that case concentration of electrons will be:

$$n_{å} = n_0 \cdot \frac{\tilde{o}_{å}}{1+\tilde{o}_{å}} = 9{,}06 \cdot 10^{19}\ cm^{-3} \cdot \frac{0{,}18}{1+0{,}18} = 1{,}38 \cdot 10^{19}\, cm^{-3}.$$

Let us estimate a density of current flowing in a microbubble which is equal to:

$$j_{ec} = 3{,}34 \cdot 10^{-10} \cdot å \cdot n_{å} \cdot \upsilon_{å} =$$

$$= 3{,}34 \cdot 10^{-10} \cdot 4{,}8 \cdot 10^{-10} \cdot 1{,}38 \cdot 10^{19}\ cm^{-3} \cdot 1{,}36 \cdot 10^{8}\ cm/s =$$

$$= 3{,}0 \cdot 10^{8}\ \frac{À}{cm^2}.$$

Average value of an ecton current, flowing in a microbubble on the cathode during filming of a shot 2, is:

$$i_{ec} = j_{ec} \cdot S_{cr.c} = 3{,}0 \cdot 10^{8}\ \frac{À}{cm^2} \cdot 3{,}14 \cdot 10^{-8}\ cm^2 = 9{,}4\ À,$$

where $S_{cr.c} = \pi \cdot r_c^2 = \pi \cdot \left(10^{-4}\ cm\right)^2 = 3{,}14 \cdot 10^{-8}\ cm^2$ – average value of square a crater on the cathode.

As

$$i_{ec} = \frac{q_{ch}}{t_{ec}},$$

where q_{ch} – a charge transferred by an ecton current. Then it is possible to define functioning time of ecton:

$$t_{ec} = \frac{q_{ch}}{i_{ec}} = \frac{e \cdot N_{e.ec}}{i_{ec}} = \frac{1{,}6 \cdot 10^{-19}\ \text{Coulomb} \cdot 5{,}8 \cdot 10^{7}}{9{,}4\ A} = 9{,}8 \cdot 10^{-13}\ s.$$

Here $N_{e.ec} = n_e \cdot V_n = 1{,}38 \cdot 10^{19}\ cm^{-3} \cdot \frac{4}{3} \cdot \pi \cdot \left(10^{-4}\ cm\right)^3 = 5{,}8 \cdot 10^{7}$ – quantity of electrons in ecton.

Average time of a functioning cycle of a crater and ecton on the cathode is equal to:

$$t_{cyc} = t_{cr} + t_{ec} = 4{,}5 \cdot 10^{-9}\ s + 9{,}8 \cdot 10^{-13}\ s \simeq 4{,}51 \cdot 10^{-9}\ s.$$

A quantity of cycles repeating consistently one after another during filming of one shot, equal $\Delta t = 0{,}167 \cdot 10^{-3}\ s$, will be equal:

$$n_{cyc} = \frac{\Delta t}{t_{cyc}} = \frac{0{,}167 \cdot 10^{-3}\ s}{4{,}51 \cdot 10^{-9}\ s} = 3{,}7 \cdot 10^{4}.$$

A quantity of craters apearing on the cathode simultaneously during a cycle, at the initial stage of opening contacts, corresponding to filming of a shot 2, is equal:

$$n_{cr} = \frac{\Delta i_{arc}}{i_{ec}} = \frac{1680A}{9{,}4A} \simeq 180,$$

wher $\Delta i_{\partial} = 1680\ A$ – deficiency of a current (table 2.9).

A quantity of ectons which provide a flow of current deficiency Δi_{arc} on the cathode during filming of a shot 2 is equal to:

$$\Delta N_{ec.c} = n_{cr} \cdot n_{cyc} = 180 \cdot 3{,}7 \cdot 10^{4} = 6{,}66 \cdot 10^{6}.$$

Results of calculations of quantity of ectons on a cathodic base spot of arc in process of its burning on argentiferous contacts at switching-off of current equal 16,0 κA, at phase voltage 420 V and $\cos\varphi$ = 0,2 are given in table 2.11. The values of arc current i_{arc} given in table 2.11 were taken from table 2.1, deficiency of current Δi_{arc} - from table 2.9.

Total quantity of ectons on the cathode, providing flowing of arc current in the considered test, during its finding on argentiferous contacts was equal according to result of numerical integration of function $\Delta N_{ec.c}(t_{arc})$:

$$\Sigma \Delta N_{ec.c}(t_{arc}) = 1{,}177 \cdot 10^{9}.$$

Table 2.11. Values of current intensity of ecton $i_{эс.с}$ and quantity of ectons $\Delta N_{эс.с}$ on the cathode base spot at switching-off of short-circuit current equal 16,0 *кА* and phase voltage 420 *V* and $cos\varphi$=0,2

t_{arc}, *ms*	0,334	0,668	1,34	2,0	2,67	4,2	5,34	6,68
i_{arc}, *кА*	13,0	15,0	18,2	21,5	23,2	24,5	21,9	14,6
P_m, 10^6, *dynes/cm*^{2}	4,69	2,19	1,02	0,78	0,67	0,63	0,49	0,3
P_L, 10^6, *dynes/cm*^{2}	39,2							
P_b, 10^6, *dynes/cm*^{2}	43,9	41,4	40,2	40	39,9	39,8	39,7	39,5
T_{sat}, *K*	3510	3500	3495	3493	3492	3490	3490	3488
n_0, 10^{19}, *cm*$^{-3}$	9,06	8,57	8,3	8,29	8,28	8,26	8,24	8,21
x_e	0,18	0,183	0,185	0,185	0,185	0,185	0,187	0,187
n_e, 10^{19}, *cm* $^{-3}$	1,38	1,326	1,296	1,294	1,293	1,289	1,298	1,293
j_{ec}, 10^8, *A/cm*^{2}	3,0	2,89	2,825	2,821	2,819	2,81	2,83	2,819
i_{ec}, *A*	9,4	9,07	8,87	8,86	8,85	8,82	8,89	8,85
$n_{cr}= \Delta i_{arc}/ i_{ec}$	180	290	264	659	880	1106	1105	934
$\Delta N_{ec.c}=n_{cr}\cdot n_{cyc}$, 10^6	6,66	10,73	9,77	24,38	32,56	40,22	40,88	34,56
$\Sigma \Delta N_{ec.c}$ (t_{arc})	$1{,}117\cdot10^9$							

2.6.2. Current conduct by ectons on the anode

The physical mechanism of flowing of current of arc charge on the anode differs essentially from physical mechanism of flowing of current on the cathode. Electrons, formed on the cathode as a result both evaporations of contact material and explosive emission, direct to the anode. Ions, generated on the cathode, come back and bombard its surface. Thus ions promote self-maintenance of emission processes on the cathode.

On the anode the same as and on the cathode, processes of evaporation and superficial bubble boilings of contact material proceed. Generated ions on the anode are partially transferred on the cathode warming up its additionally. They are partially taken out by convectional plasma fluxes for limits of contact gap. Emitted electrons from the anode partially recombine with ions, and partially come back and bombard an anode surface. As a result, at more intensive bombardment of the anode by electrons than of cathode by ions, heat is generated on the anode more than on the cath-

ode. Therefore on the anode thermal processes proceed violently, and the craters, formed as a result of superficial bubble boiling, have bigger size than on the cathode.

Earlier it was been shown that power density, running on the anode, to leads mel of all area of base spot. Its liquid-melt can reach temperature of boiling of contact material. In process of violent boiling of liquid-melt on its surface splashes of liquid metal of different height can be formed. On tops of these splashes drops will be formed under influence of forces of a superficial tension. According to data given in [2.8, p. 20], a factor of amplification of a field on sphere with radius R on thin base with height h is defined by the formula:

$$\beta_E = \frac{h}{R} + 2.$$

If for estimated calculations to accept that a radius of drop R is equal to minimum value of radiuses of drops shown on fig. 2.14 and $h=5\cdot10^{-4}$ *cm* the factor of amplification of field will be equal:

$$\beta_E = \frac{5\cdot10^{-4}\,см}{0{,}15\cdot10^{-4}\,см} + 2 = 35.$$

Let us notice that the factor of amplification of field equal to 35 can be and at other values h and R. For example: $h=7\cdot10^{-4}$ *cm* and $R=0{,}2\cdot10^{-4}$ *cm*, $h=10\cdot10^{-4}$ *cm* and $R=0{,}3\cdot10^{-4}$ *cm* .That is, it is quite probable that the factor of amplification of field on the anode can be equal to $\beta_E=35$.

Hence, at initial stage of opening of contacts on the centres of concentration of the charges located on the anode, power density can reach values:

$$q_{c.max.a} = \beta_E \cdot q_{bs.a} = 35\cdot18{,}07\cdot10^4\ W/cm^2 = 6{,}32\cdot10^6\ W/cm^2,$$

where $q_{bs.a} = 18{,}07\cdot10^4\ W/cm^2$ – table 2.7.

A value of power density $q_{c.max.a}$ exceed a value $q_{c.max.c}$:

$$q_{c.max.a} = 6{,}32\cdot10^6\ W/cm^2 > 3{,}06\cdot10^6\ W/cm^2 = q_{c.max.c},$$

where $q_{c.max.c} = 3{,}06\cdot10^6\ W/cm^2$ – table 2.10.

Calculated values of power density $q_{c.max.a}$ running on the centres of concentration of charges, being on the anode, in process of arc burning on opening contacts at switching-off of current 16,0 *кА* and phase voltage 420 *V* are given in table 2.12.

According to the results of the previous calculations a liquid-melt *Ag* on anode base spot under influence of power density $q_{c.max.a}$=3,24·10^5 *W/cm*^{2} and more will obviously reach a boiling temperature.

Under influence of power density on the anode $q_{c.max.a}$ which has the larger value than $q_{c.max.c}$ on the cathode, microbubbles and, hence, craters in a layer of liquid-melt *Ag* on the anode will get bigger sizes than on the cathode. Earlier for estimated calculations it was accepted that an average diameter of craters on the anode has a value: $d_{a.av}$ = 7,0·10^{-4} *cm*.

Table 2.12. Values $q_{c.max.a}$, running on microledges on the anode, in process of opening of contacts at switching-off of a current 16,0 *кА*

t_{arc}, *ms*	0,334	0,668	1,34	2,0	2,67	4,0	5,34	6,68
i_{arc}, *кА*	13,0	15,0	18,2	21,5	23,2	24,5	21,9	14,6
$q_{bs.a}$, 10^4, *W/cm*^{2}	18,07	4,69	2,435	1,635	1,70	1,666	1,444	1,080
$q_{c.max.a}$, 10^5, *W/cm*^{2}	63,2	16,42	8,52	5,42	5,95	5,83	5,05	3,24

At initial stage of opening of contacts a pressure in a microbubble on the anode is equal to:

$$P_b = P_m + P_L = \frac{\mu_0 \cdot i_{arc}^2}{8 \cdot \pi^2 \cdot r_{bs.a}^2} + \frac{4 \cdot \sigma}{r_{b.a.av}} =$$

$$= \frac{1{,}26 \cdot 10^{-6}\ G/m \cdot \left(13 \cdot 10^3\ A\right)^2}{8 \cdot \pi^2 \cdot \left(2{,}1 \cdot 10^{-3}\ m\right)^2} + \frac{4 \cdot 0{,}98 \cdot N/m}{3{,}5 \cdot 10^{-6}\ m} =$$

$$= 0{,}61 \cdot 10^6\ Pa + 1{,}12 \cdot 10^6\ Pa = 1{,}73 \cdot 10^6\ Pa = 17{,}3 \cdot 10^6\ \frac{dynes}{cm^2}.$$

A temperature of steam saturation *Ag* in a microbubble at pressure of 17,3·10^6 *dynes/cm*^{2} is: T_{sat}=3200 *K*.

Concentration of atoms *Ag* n_0 in a microbubble is equal to:

$$n_0 = \frac{P_b}{\kappa \cdot T_{sat}} = \frac{17{,}3 \cdot 10^6 \ dynes/cm^2}{1{,}38 \cdot 10^{-16} \ erg/K \cdot 3200 \ K} = 3{,}92 \cdot 10^{19} \ cm^{-3}.$$

In a microbubble on the anode the same as on the cathode, there is a quantity of free electrons. At explosion of microbubbles under influence of anode effective potential electrons get a velocity:

$$\upsilon_e = 0{,}593 \cdot 10^8 \cdot \sqrt{U_{ef.a}} = 0{,}593 \cdot 10^8 \cdot \sqrt{12{,}25 \ V} = 2{,}08 \cdot 10^8 \ \frac{cm}{s}.$$

A velocity of electrons $2{,}08 \cdot 10^8$ *cm/s* is sufficient for ionisation of atoms *Ag* at their unitary not elastic impact. Therefore steams *Ag* in a microbubble at its explosion are subjected by avalanche ionisation.

As a first approximation let us accept that degree of ionisation of steams *Ag* in a microbubble on the anode is equal to x_e=0,138 at initial stage of opening of contacts (a shot 2).

Concentration of electrons in a microbubble will be:

$$n_e = n_0 \cdot \frac{x_e}{1 + x_e} = 3{,}92 \cdot 10^{19} \ cm^{-3} \cdot \frac{0{,}138}{1 + 0{,}138} = 0{,}475 \cdot 10^{19} \ cm^{-3}.$$

In that case current density in a microbubble will be equal to:

$$j_{ec} = 3{,}34 \cdot 10^{-10} \cdot e \cdot n_e \cdot \upsilon_e =$$

$$= 3{,}34 \cdot 10^{-10} \cdot 4{,}8 \cdot 10^{-10} \cdot 0{,}475 \cdot 10^{19} \ cm^{-3} \cdot 2{,}08 \cdot 10^8 \ \frac{cm}{s} =$$

$$= 1{,}584 \cdot 10^8 \ A/cm^2.$$

Ecton current, flowing in a microbubble on the anode with average square $S_{cr.a}$, is equal to:

$$i_{ec} = j_{ec} \cdot S_{cr.a} = 1{,}584 \cdot 10^8 \ \frac{A}{cm^2} \cdot 38{,}5 \cdot 10^{-8} \ cm^2 = 61 \ A,$$

where $S_{cr.a} = \pi \cdot r_{cr.a}^2 = \pi \cdot \left(3{,}5 \cdot 10^{-4} \ cm\right)^2 = 38{,}5 \cdot 10^{-8} \ cm^2$.

Functioning time of ecton on the anode:

$$t_{ec} = \frac{q_{ch}}{i_{ec}} = \frac{e \cdot N_{e.ec}}{i_{ec}} = \frac{1{,}6 \cdot 10^{-19}\ Coulomb \cdot 8{,}526 \cdot 10^{8}}{61\ A} = 2{,}236 \cdot 10^{-12}\ s,$$

where $N_{e.ec} = V_b \cdot n_e = \frac{4}{3} \cdot \pi \cdot r_{cr.a}^3 \cdot n_e = \frac{4}{3} \cdot \pi \cdot \left(3{,}5 \cdot 10^{-4}\ cm\right)^3 \cdot 0{,}475 \cdot 10^{19}\ cm^{-3} = 8{,}526 \cdot 10^{8}$

– quantity of ecton`s electrons.

Forming time of a crater:

$$t_{cr} = \frac{r_{cr.a}^2}{4 \cdot a} = \frac{\left(3{,}5 \cdot 10^{-4}\ cm\right)^2}{4 \cdot 0{,}55\ cm^2/s} = 5{,}57 \cdot 10^{-8}\ s.$$

Here $a = 0{,}55\ cm^2/s$ – temperature conductivity coefficient of liquid *Ag*.

Average time of a cycle of functioning of a crater and ecton on the anode is equal to:

$$t_{cyc} = t_{cr} + t_{ec} = 5{,}57 \cdot 10^{-8}\ s + 2{,}23 \cdot 10^{-12}\ s \simeq 5{,}57 \cdot 10^{-8}\ c.$$

Quantity of cycles, repeating consistently one after another during filming of one shot is equal to $\Delta t = 0{,}167 \cdot 10^{-3}\ s$, is equal:

$$n_{cyc} = \frac{\Delta t}{t_{cyc}} = \frac{0{,}167 \cdot 10^{-3}\ s}{5{,}57 \cdot 10^{-8}\ s} = 3 \cdot 10^{3}.$$

Quantity of craters, arising simultaneously during a cycle at initial stage of opening of contacts, corresponding filming of a shot 2, is equal to:

$$n_{cr} = \frac{\Delta i_d}{i_{ec}} = \frac{1680\ A}{61\ A} = 28,$$

where Δi_d – deficiency of current (table 2.9).

Quantity of ectons, providing flowing of current deficiency Δi_d on the anode during filming of a shot 2, is equal:

$$\Delta N_{ec.a} = n_{cr} \cdot n_{cyc} = 28 \cdot 3 \cdot 10^{3} = 8{,}4 \cdot 10^{4}.$$

Table 2.13. Values of current intensity of ectons $i_{ec.a}$ and quantity of ectons $N_{ec.a}$ on anode base spot of arc at switching-off of short-circuit current equal 16,0 κA and phase voltage 420 V and $cos\ \varphi = 0{,}2$

t_{arc}, ms	0,334	0,668	1,34	2,0	2,67	4,2	5,34	6,68
i_{arc}, κA	13,0	15,0	18,2	21,5	23,2	24,5	21,9	14,6
P_m, 10^6, $dynes/cm^2$	6,1	1,8	1,0	0,8	0,9	0,9	0,7	0,5
P_L, 10^6, $dynes/cm^2$	11,2							
P_b, 10^6, $dynes/cm^2$	17,3	13,0	12,2	12,0	12,1	12,1	11,9	11,7
T_{sat}, K	3200	3120	3100	3100	3100	3100	3090	3080
$n_0, 10^{19}$, cm^{-3}	3,92	3,02	2,86	2,85	2,85	2,85	2,83	2,75
x_e	0,138	0,155	0,16	0,158	0,155	0,155	0,153	0,155
$n_e, 10^{19}$, cm^{-3}	0,475	0,405	0,394	0,389	0,382	0,382	0,375	0,369
$j_{ec}, 10^8$, A/cm^2	1,584	1,35	1,314	1,297	1,274	1,274	1,251	1,231
$i_{ec.a}$, A	61	52	50,6	49,9	49	49	48,2	47,4
$n_{cr} = \Delta i_d / i_{ec.a}$	28	51	46	117	159	199	204	174
$\Delta N_{ec.a} = n_{cr} \cdot n_{cyc}$, 10^4	8,4	15,3	13,8	35,1	47,7	59,7	61,2	52,2
$\Sigma\, \Delta N_{ec.a}\ (t_{arc})$	$1{,}378 \cdot 10^7$							

Results of calculations of quantity of ectons on an anode base spot of arc in process of its burning on argentiferous contacts at switching-off of short-circuit current equal 16,0 κA, at phase voltage 420 V and $cos\ \varphi = 0{,}2$ are given in table 2.13. The values of arc current i_{arc} indicated in table 2.13 were taken from table 2.1 and deficiency of current Δi_d - from table 2.9.

Total quantity of ectons providing flowing of arc current on the anode during its standing on argentiferous contacts at switching-off of short-circuit current equal 16,0 κA, phase voltage 420 V and $cos\ \varphi = 0{,}2$ according to the result of numerical integration of function $\Delta N_{ec.a}\ (t_{arc})$ is equal to:

$$\Sigma \Delta N_{ec.a}(t_{arc}) = 1{,}378 \cdot 10^7.$$

2.7. Microplasmoids on base spots of arc

At microbubble explosion it is meant that microjet of plasma which effuses from it has some length. Existence time of microjet of plasma is equal to functioning time of ecton t_{ec}. At switching-off of short-circuit current equal 16,0 κA, functioning time of ectons, for example, on the cathode is $t_{ec} = 9{,}8 \cdot 10^{-13} s$. Electrons in the cathode area, having velocity $\upsilon_e = 1{,}36 \cdot 10^8 cm/s$, fly a distance from a outfall of blown up microbubble:

$$l_e = \upsilon_e \cdot t_{ec} = 1{,}36 \cdot 10^8 cm/s \cdot 9{,}8 \cdot 10^{-13} s = 1{,}33 \cdot 10^{-4} cm.$$

General length of a microjet of electrons is:

$$l_{e.c} = d_{b.c} + l_e = 2 \cdot 10^{-4} cm + 1{,}33 \cdot 10^{-4} cm = 3{,}33 \cdot 10^{-4} cm,$$

where $d_{b.c} = 2 \cdot 10^{-4} cm$ – average value of diameter of microbubble on the cathode. Ions in microbubble do not leave its volume and come back in the cathode. Under influence of pressure in microbubble P_b neutral steams of Ag get velocity υ_{st} equal to several units of 10^4 cm/s [2.4, p. II, table 4.7, p.52]. During existence of ecton steams of Ag can fly a distance:

$$l_{st} = \upsilon_{st} \cdot t_{ec} = 7 \cdot 10^4 cm/s \cdot 9{,}8 \cdot 10^{-13} s = 6{,}7 \cdot 10^{-8} cm.$$

That is during functioning time of ecton on the cathode steams of Ag have not time to leave a volume of blowing up microbubble.

The presented results of calculations of length of plasma microjet, which is effused from blown up microbubble, lead to a conclusion that it represents a blob of plasma of limited volume in form of a kind of ellipsoid which it is possible to name **microplasmoid**. The schematic image of plasmoid in a boiling layer of a liquid-melt on the cathode is shown in fig. 2.23.

Ions escape from blown up microbubble on the anode with velocity [2.4. part II, p. 45]:

$$\upsilon_i = 0{,}134 \cdot 10^6 \sqrt{U_{ef.a}} = 0{,}134 \cdot 10^6 \sqrt{12{,}25\,V} = 0{,}469 \cdot 10^6 cm/s.$$

During functioning time of ecton on anode $t_{ec} = 2{,}2 \cdot 10^{-12} s$ ions will fly a distance

from a outfall of blown up microbubble:

$$l_i = v_i \cdot t_{ec} = 0{,}469 \cdot 10^6 cm/s \cdot 2{,}2 \cdot 10^{-12} s = 1{,}03 \cdot 10^{-6} s.$$

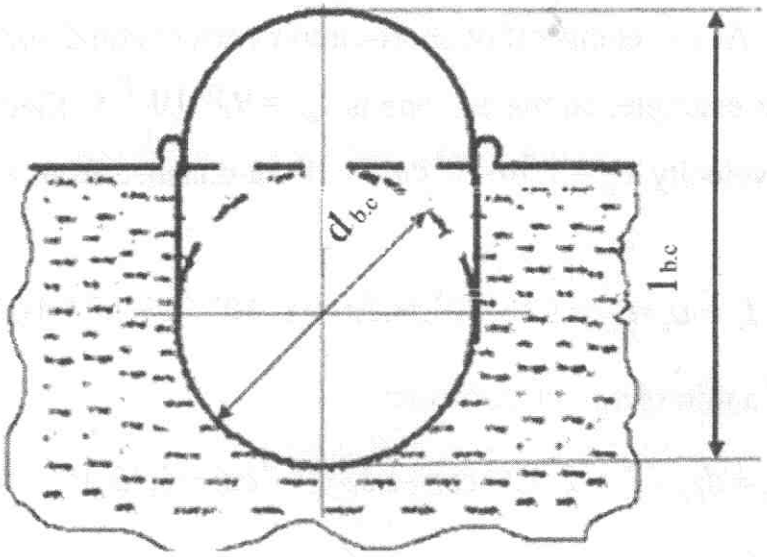

Fig. 2.23. Schematic drawing of microplasmoid in a boiling layer of a liquid-melt Ag on the cathode

That is during functioning time of ecton on the anode ions practically have not time to leave a volume of microbubble. Electrons do not leave a volume of a microbubble and come back in the anode.

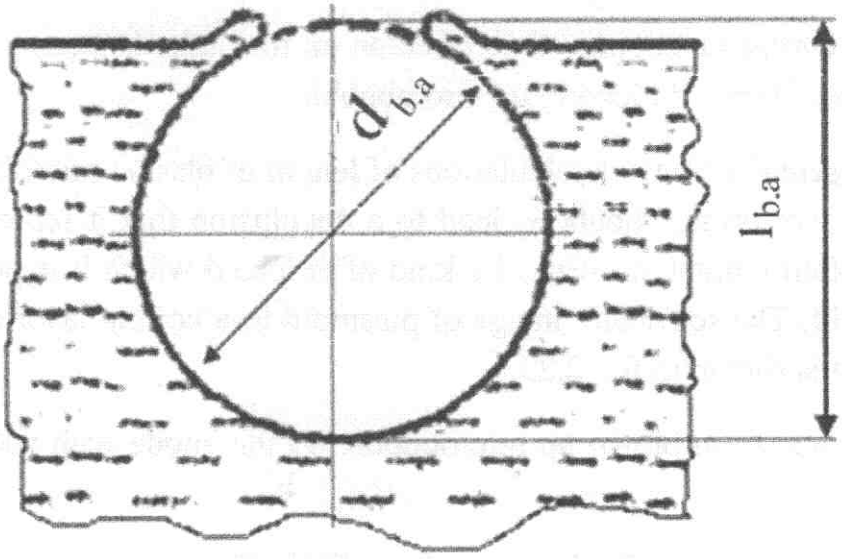

Fig. 2.24. Schematic drawing of microplasmoid in a boiling layer of a liquid-melt Ag on the anode

Hence, it is possible to present a plasma microjet in a microbubble on the anode in a form of microplasmoid of spherical form with size equal to diameter of a microbubble (see fig. 2.24):

$$l_{b.a} = d_{b.a} = 7 \cdot 10^{-4}\ cm.$$

Let us estimate thermophysical parametres of microplasmoids. Power density, coming on a bottom of craters on the cathode and the anode, is defined by formulas:

$$q_{mpl.c} = \frac{\eta_c \cdot i_{ec.c} \cdot U_{ef.c}}{S_{cr.c}}; q_{mpl.a} = \frac{\eta_a \cdot i_{ec.a} \cdot U_{ef.a}}{S_{cr.a}}.$$

Values η_c and η_a are given in table 2.7, $i_{ec.c}$ – in table 2.11, $i_{ec.a}$ – in table 2.13, $U_{ef.c} = 5{,}25\,V$, $U_{ef.a} = 12{,}25\,V$, $S_{cr.c} = 3{,}14 \cdot 10^{-8} cm^2$, $S_{cr.a} = 38{,}5 \cdot 10^{-8} cm^2$.

Calculation data $q_{mpl.c}$ and $q_{mpl.a}$ are given in table 2.14.

Table 2.14. Values $q_{mpl.c}$ and $q_{mpl.a}$ in process of arc burning on opening argentiferous contacts at switching-off of short-circuit currents equal 16,0 κA, at phase pressure 420 V and $\cos\varphi = 0{,}2$

t_{arc}, ms	0,334	0,668	1,34	2,0	2,67	4,0	5,34	6,68
$i_{arc}, \kappa A$	13,0	15,0	18,2	21,5	23,2	24,5	21,9	14,6
$q_{mpl.c}, 10^8, \frac{W}{cm^2}$	3,02	2,33	2,16	1,76	1,76	1,75	1,77	1,61
$q_{mpl.a}, 10^8, \frac{W}{cm^2}$	8,81	5,96	5,47	4,41	4,33	4,35	4,26	3,85

Electromagnetic pressure, compressing microplasmoids on the cathode and the anode as a result of flowing of ecton currents, can be defined by formulas:

$$P_{mpl.c} = 9{,}87 \cdot 10^{-9} \cdot i_{ec.c} \cdot j_{ec.c}, atm;$$

$$P_{mpl.a} = 9{,}87 \cdot 10^{-9} \cdot i_{ec.a} \cdot j_{ec.a}, atm.$$

Here $i_{ec.c}$ in A and $j_{ec.c}$ in A/cm^2 are given in table 2.11 and $i_{ec.a}$ in A and $j_{ec.a}$ in A/cm^2 are given in table 2.13. Calculation data $P_{mpl.c}$ and $P_{mpl.a}$ are given in table 2.15.

In fig. 2.25 a crater is schematically shown which is similar to shown craters on microelectronic photos in fig. 2.15. Energy of microplasmoid, being in such crater, will dissipate through its internal surface, forming by a liquid metal, and opened one, adjoining to plasma of arc channel. Obviously, quantity of dissipated energy through the internal and opened surfaces of a crater will be proportional to their areas. Hence, energy dissipation factor of microplasmoid can be expressed by a geometrical factor defining a relation of area, through which energy dissipates, to full area of a crater. For example, a geometrical factor of energy losses, defining a part of energy of microplasmoid, absorbed by a liquid-melt through internal surface of a crater, is equal:

$$\eta_g = \frac{S_{cr}/2 + S_{cyl.lat}}{S_{cr}/2 + S_{cyl.lat} + S_{cyl}} = \frac{4\pi \cdot r^2/2 + 2\pi \cdot r \cdot r}{4\pi \cdot r^2/2 + 2\pi \cdot r \cdot r + \pi \cdot r^2} = \frac{4}{5} = 0{,}8,$$

where $S_{cr}/2$ – an area of bottom hemisphere of a crater, $S_{cyl.lat}$ – a lateral area of cylinder forming a top part of a crater and S_{cyl} – an area of open surface of a crater (cylinder).

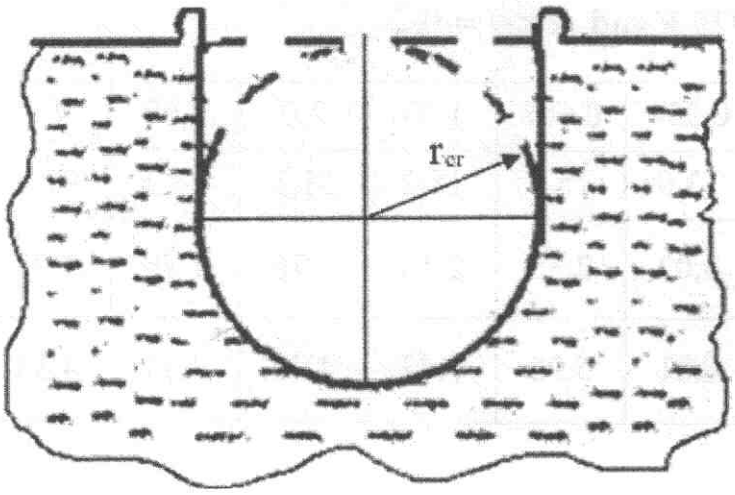

Fig. 2.25. Schematic drawing of a crater

That is 80 % of energy of microplasmoid will be absorbed by a liquid-melt through an internal surface of a crater. In that case, power of microplasmoid which

dissipate in volume of arc channel, will be defined by the formula:

$$\Delta P_{mpl} = (1-\eta_g)\cdot i_{ec}\cdot U_{ef}.$$

If an effective temperature of plasma microplasmoid will be enough high then its power will dissipate in arc channel by radiation basically. Proceeding from such representation we will define effective temperature of microplasmoid plasma by means of the formula [2.4, part I, p. 277]:

$$T_{ef} = 447\left(\frac{(1-\eta_g)\cdot i_{ec}\cdot U_{ef}}{\beta\cdot r_{cr}\cdot l_{mpl}}\right)^{1/4}.$$

At initial stage of contacts opening (a short 2), for example, an effective temperature of microplasmoid plasma on the cathode will be equal to:

$$T_{ef} = 447\left(\frac{(1-\eta_g)\cdot i_{ec.c}\cdot U_{ef.c}}{\beta\cdot r_{cr.c}\cdot l_{e.c}}\right)^{1/4} =$$

$$= 447\left(\frac{(1-0{,}8)\cdot 9{,}4\ A\cdot 5{,}25\ V}{0{,}6\cdot 10^{-4}\ cm\cdot 3{,}33\cdot 10^{-4}\ cm}\right)^{1/4} = 66450\ K.$$

Really, an effective temperature of microplasmoid plasma is very high and it allows to accept dissipation of its energy in volume of arc channel by radiation only.

Degree of ionization x_e of microplasmoid plasma on the cathode at pressure $P_{mpl.c}$, created by a current of ecton, and effective temperature will be defined by means of Saha equation:

$$\lg\frac{P_{mpl.c}\cdot \mathrm{x}_e^2}{1-\mathrm{x}_e^2} = \lg\frac{g_e\cdot g_i}{g_a} + 2{,}5\cdot\lg\cdot T_{ef} - \frac{5040\cdot U_i}{T_{ef}} - 6{,}5.$$

Numerical value of proportion of quantum statistical weigths of electron, ion and atom for steams of Ag is equal to:

$$\frac{g_e\cdot g_i}{g_a} = a^2 = 1.$$

Potential of ionisation Ag $U_i = 7{,}54\ B$ [2.4, part I, p. 327]. We will substitute

numerical values $P_{mpl.c}$ and T_{ef} in Saha equation, their corresponding values for the cathode at filming of a shot 2:

$$\lg\frac{27{,}58\cdot10^5 Pa\cdot x_e^2}{1-x_e^2}=2{,}5\lg 66450K-\frac{5040\cdot 7{,}54V}{66450K}-6{,}5.$$

After the numerical calculation of last expression we will get a degree of ionisation of microplasmoid plasma on the cathode equal $x_e = 0{,}183$. Comparing obtained value x_e with a value accepted as a first approximation and presented in table 2.11, it is visible that they coincide well enough for practical engineering calculations:

$$x_e = 0{,}18 \simeq 0{,}183 = x_e.$$

From here it is possible to make a conclusion that concentration of electrons n_e in microplasmoid, current density j_{ec} and current i_{ec}, given in table 2.11, were calculated precisely enough for engineering practice.

Table 2.15 gives the results of calculations of pressure created by currents of ectons, temperatures and degrees of plasma ionisation in microplasmoids on the cathode and the anode at switching-off of short-circuit currents equal 16,0 *кА*.

Table 2.15. Values $P_{mpl.c}, P_{mpl.a}, T_{ef.mpl.c}, T_{ef.mpl.a}$ and degrees of ionisation of microplasmoids plasma at switching-off of short-circui currents equal 16,0 *кА*, at phase voltage 420 *V* and $\cos\varphi = 0{,}2$.

t_{arc}, ms	0,334	0,668	1,34	2,0	2,67	4,0	5,34	6,68
$i_{arc}, кА$	13,0	15,0	18,2	21,5	23,2	24,5	21,9	14,6
$P_{mpl.c}, 10^5, Pa$	27,58	26,21	25,06	25,0	25,86	24,79	25,15	24,95
$T_{ef.mpl.c}, K$	66450	66030	65660	65650	65200	65570	65700	65630
$x_{e.mpl.c}$	0,183	0,185	0,188	0,188	0,187	0,189	0,189	0,188
$P_{mpl.a}, 10^5, Pa$	96,6	70,2	66,47	64,72	62,43	62,43	60,3	58,35
$T_{ef.mpl.a}, K$	79860	76730	76210	75950	75600	75600	75290	74980
$x_{e.mpl.a}$	0,139	0,152	0,157	0,155	0,156	0,156	0,158	0,159

Let us pay attention to that according to tables 2.11, 2.13 and 2.15 parametres of microplasmoids j_{ec}, i_{ec}, P_{mpl}, $T_{ef.mpl}$ on the cathode and the anode considerably differ from each other. At the same time, in process of arc burning on contacts both on the cathode and on the anode they change slightly and practically do not depend on change of arc current i_{arc}.

However a quantity of microplasmoids, formed in process of arc burning on contacts, essentially depends on change of arc current. Quantity of microplasmoids, formed on the cathode, surpasses their quantity on the anode in two orders:

$$\sum \Delta N_{ec.c}(t_{arc}) = 1{,}177 \cdot 10^{9} >> 1{,}38 \cdot 10^{7} = \sum \Delta N_{ec.a}(t_{arc}).$$

Considering a geometrical configuration microplasmoids, it is possible to accept them for the dot sources radiating energy in volume of arc channel.

Energy of electric network comes in arc discharge through the centres of concentration of charges located on its base spots. Under influence of amplified power density coming on the centres of concentration of charges, on their place there are the microbubbles repeatedly alternating on base spots. At explosion of microbubbles the microplasmoids are formed which radiate their energy in volume of arc discharge channel partially. Partially energy of arc discharge dissipates in environment and partially comes on base spots. Under influence of power density coming on base spots, from their surface there is evaporation of contacts metal. Evaporated steams of metal of contacts come in volume of arc discharge channel in which they are subjected to thermal ionisation. At the same time, metal steams lead to some cooling of plasma in volume of arc discharge channel. Ionised steams of metal provide for flowing of a part of current of arc discharge. Flowing of other part of current is provideв by ectons in microplasmoids apearing at explosion of microbubbles.

As a result of electro- and thermophysical processes on opening contacts at switching-off of short-circuit currents by low-voltage breakers their erosion is taken place. Quantity of eroded masses of contacts consists of mass of steam of evaporated metal of contacts from a surface of base spots and mass of steam and droplets of metal of contacts, formed at explosion of microjets.

Conclusions to chapter 2

2.1. A form and structure of arc discharge is directly connected with a form and structure of its traces on base spots.

2.2. Two models of a low-voltage arc of switching-off of high power are considered:

- simplified channel model of short constricted arc with a continuous core;
- model of short constricted arc with a descrete core;

2.3. Qualitative and quantitative estimations of both models differ from each other essentially. The substantive provisions, accepted by theoretical consideration of models, are:

2.3.1. For simplified channel model of arc with a continuous core:

- electrode voltage drops U_c and U_a;
- average value of power density coming on all area of base stpot, is equal to for the cathode and the anode.

2.3.2. For arc with a discrete core:

- electrode effective potensials $U_{ef.c}$ and $U_{ef.a}$;
- descrete power densities on centres of concentration of charges, which are on base spots as on the cathode and the anode, have values.

2.4. Form and structure of arc discharge, structure of its plasma and mobility are defined by its geometrical characteristic:

$$S_{lat} / \left(S_{bs.c} + S_{bs.a}\right) = l_{arc} / r_{bs} \lesssim 1{,}0.$$

2.5. Traces of arc of high power on base spots have a chaotic appearance with a difficult relief. It is possible to represent microledges in the form of simple geometrical figures: columns, cones and drops of the spherical form.

2.6. Columns, cones and spheres deform electric field and by that on their tops the centres of concentration of charges are formed.

2.7. As a result of amplification of power density on a place of the centres of concentration of charges the layer of boiling liquid-melt of metal and microbubbles are formed. At explosion of microbubbles the microplasmoids arise in which currents of ectons flow.

2.8. The microbubbles, formed in a thin layer liquid-melt, collapse after functioning end of microplasmoids. On their place the splashes of liquid metal arise in the form of columns with microdrops at their tops and divergent disturbance waves. Columns with microdrops at their tops become new centres of concentration of charges and functioning cycle of microplasmoids renews.

2.9. Parametres of microplasmoids j_{ec}, i_{ec}, q_{mpl}, P_{mpl} and T_{ef} on the cathode and the anode differ from each other considerably. A quantity of microplasmoids on the cathode and the anode differs from each other in two orders and considerably depends on value of a current intensity of arc. Parametres of microplasmoids in process of arc burning change slightly and practically do not depend on change of arc current.

2.10. Energy of electric network comes in arc discharge through the centres of concentration of charges. On their place the microplasmoids are formed repeatedly alternating on all area of base spots. Energy of microplasmoids, from which the most part is absorbed by a liquid-melt, is partially radiated in volume of arc channel of the arc discharge. Energy of arc discharge partially dissipates in environment and is partially absorbed by a liquid-melt on base spot. From a surface of base spot under influence of power density q_{bs} an evaporation of contacts metal is taket place. Evaporated steams of metal, getting to a channel of arc discharge, are subjected to thermal ionisation.

2.11. Carrying out of current in short constricted arc with a discrete core is provided with two fundamental physical processes, proceeding on base spots:

- evaporation of contacts metal of from their surface;
- explosive emission of electrons.

2.12. Energy of arc, arising on opening contacts and being on them in motionless position, dissipates by:

- radiation from 16 to 40 %;
- convective of plasma fluxes upto 40 %;
- absorbation of contacts body from 40 to 60 %.

Reference index to chapter 2

2.1 *Bron O.B.* Electric arc in control switches. – M.; L.: GEI, 1954 [rus].

2.2 *Bron O.B., Sushkov L.K.* Plasma fluxes in electric arc of sitching devices. – L.: Energy, 1975 [rus].

2.3 *Leskov G.I.* Electric welding arc. – M.: Mashinostroenie, 1970 [rus].

2.4 *Mestcheryakov V.P.* Electric arc of high power in circuit breakers. – Ulyanovsk; part I, 2006; part II, 2008 [rus].

2.5 Thermotechnical catalogue. Vol. 2. – M.: Energy, 1976 [rus].

2.6 *Polezhaev Y.V., Yurevich F.B.*. Thermal protection. – M.: Energy, 1976 [rus].

2.7 *Gerasimov Y.I., Krestavnikov A.N., Shakhov A.S.* Chemical thermodynamics in nonferrous metallurgy. Reference manual 8 vol. Vol.2. Thermodynamics of copper, plumb, tin, silver and their compounds. – M.: Metallurgizdat, 1961 [rus].

2.8 *Mesyats G.A.* Ectons in vacuum discharge: breakdown, spark, arc. – M.: Science, 2000 [rus].

2.9 *Butkevich G.V., Belkin G.S., Vedeshenkov N.A., Zhavoronkov M.A.* Electric erosion of high-current of contacts and electrodes. – M.: Energy, 1978 [rus].

2.10 *J. E. Daalder.* Energy dissipation in the cathode of a vacuum arc. I. Phys. D: Appl. Phys., Vol. 10.1977. 2225.

2.11 Thermodynamic mechanism of thin fragmentation of liquid drops at steam explosion./ *Y.A. Zeigarnik, Y.P. Ivochkin, E.Z. Korol //* Thermophysics of high temperatures. 2004. – Vol. 42. – №3. – p. 491-492 [rus].

2.12 Behavior of steam film on high overheated surface drowned in underheated water / *V.S. Grigoriev, V.G. Zhilin, Y.A. Zeigarnik, Y.P. Ivochkin, V.V. Glazkov, O.A. Sinkevich //* Thermophysics of high temperatures. – 2005. – Vol. 43. – №1. – p. 100-114 [rus].

2.13 About one possible mechanism of initiation (triggering) of steam explosion. / *V.V. Glazkov, V.S. Grigoriev, V.G. Zhilin, Y.A. Zeigarnik, Y.P. Ivochkin, K.G. Kubrikov, N.V. Medvetskaya, A.A. Oksman, O.A. Sinkevich //* Thermophysics of high temperatures. – 2006. – Vol. 44. – № 6. – p. 913-917 [rus].

2.14 *Mitskevich M.K., Bushkin A.I., Bakuto I.A., Shikhov V.A., Devoino I.G.*. Electroerosion machining of metals. – Minsk: Science and technics, 1988 [rus].

2.15 *Geguzin Y.E.*. Bubbles. – M.: Science, 1985 [rus].

2.16 *Bazarov Y.B., Dolotov A.S., Ignatiev V.Y., Meshkov E.E., Sladkov A.* Method development of stream visualization near air bubble floating up on surface. // РФЯЦ-ВНИИЭФ, Lyceum №15, SarFTI [rus].

Chapter 3

Explosive erosion of high-current contacts and electrodes

The large quantity of works is devoted research of erosion of contacts and electrodes in various experimental conditions. Works on erosion research of high-current contacts and electrodes were carried out the limited quantity [3.1, 3.2, 3.3, 3.4, 3.5, etc.].

The review of theoretical and experimental works on erosion of contacts and construction of techniques of its quantitative account shows that the behaviour of electric arc on opening contacts, and, hence, and their erosion are rather variously and depend on many factors and in each case has the features. All researches can be divided on a way of arc initiation, current value, voltage value, duration of current flowing, a kind of arc-quenching environments, material of contacts, designs of experimental devices, velocity of contacts movement and a gap between them.

The analysis of the published materials about electroerosive processes in various conditions leads to following conclusions.

1. It is impossible to transfer the results of experimental and theoretical researches of erosion of fixed electrodes at breakdowns by pulse discharges with limited time of action in conditions of opening contacts of breakers at switching-off of short-circuit currents.

2. Results of researches of erosion of contacts, disconnecting in vacuum, can extend on erosion of contacts in atmospheric air at initial stage of their opening:

- at formation of liquid bridge and its destruction;

- in a transition period from a bridge to arc discharge and during arc immovability under a condition $\delta_{con} < r_{bs}$ (δ_{con} - gap of contacts, r_{bs} - radius of base spot of arc). That is when a square of a lateral surface of intercontact gap S_{lat} is less than sum of squares of base spots ΣS_{bs} ($S_{lat} < \Sigma S_{bs}$). Under these conditions an environment gas cannot get into arc volume.

3. The most intensive erosion of contacts both in air and in vacuum occurs at formation of a macrobath and intensive emission of fused metal for limits of contacts.

4. At currents in some kiloamperes an wear of both contacts occcurs as a result of evaporation and metal emission in a vaporous phase in the form of plasma flux and fusion and sputtering in a liquid phase under influence of various forces (thermodynamic, electrodynamic and electromagnetic (pressure)).

5. Coefficient of emission of a liquid-melt on fixed electrodes depending on a current intensity, in a range from 13 to 26 κA and its duration 10 ms, was equal:

- on copper – 0,3÷0,38;
- on AgW – 0,21÷0,41.

Data on division of thrown out metal on phases on opening contacts in air atmosphere at switching-off of short-circuit current is not given.

6. Early calculation methods of erosion were based on drawing up of balance of energy with account of importance of those or other phenomena, allocation of the main members of balance and application of various approximations. This approach is close to engineering one and was comprehensible at uncertainty for the most parts of parametres of arc discharge.

7. It was accepted that contacts get energy of arc to relation of sum of electrode voltage drops to full voltage of arc proportionally.

8. Other group of calculation methods of erosion both at pulse discharges and at current switching-off, is based on a solution of equation of energy conservation with the account of phase transformations and material ablation.

In the present work the concrete examples will be considered about quantitative estimation of erosion of argentiferous contacts at switching-off of short-circuit currents by low-voltage breakers. Also it will be considered a bridge erosion, ablation of steam mass of contacts metal from a surface of base spots of arc by evaporation, emission of steam mass of metal at explosion of microbubbles in a boiling layer of a liquid-melt on base spots and sputtering of contacts metal at explosion of erosion cones.

For acceptance of effectual measures on decrease in electric erosion of contacts and electrodes of disconnecting devices, being the basic means of increase of a resource of breakers and their service life, it is necessary to study physical mechanisms of their erosion in details.

3.1. Bridge erosion of contacts

Opening of contacts of breakers at switching-off of currents at any values of a current intensity in the electric circuits, containing inductance, is accompanied by formation of liquid-metal bridge from a liquid-melt in a contacting spot in which

aconstriction of current occurs. A mechanism of formation of bridge and its destruction is distinguished at different values of a current intensity.

A mechanism of destruction of bridge at switching-off of short-circuit currents has the features [3.1, 3.6, part I, p. 196, part II, p. 14]. According to experimental data existence time of a bridge is equal upto 0,5 *ms* at switching-off of short-circuit currents by argentiferous contacts. As a rule a velocity of opening of contacts of automatic circuit breakers does not exceed 2,0 *m/s*. At such velocity of opening of contacts in time equal 0,5 *ms* a gap between them will be equal ~ 1,0 *mm*. In these conditions in dependence on value of a current intensity a bridge either will easy evaporate, or will be subjected to destruction by electric (thermal) explosion.

In chapter 1 it was considered in detail under what conditions a quiet destruction of bridge occurs and under what conditions - explosive. We will remind that explosive destruction of bridge occurs at [3.7]:

- at entering energy in its mass exceeding energy of sublimation of a material of contacts in several times;
- power density coming on its surface, not less than 10^8 W/cm^2;
- current density ~ $(10^8 \div 10^9)$ A/cm^2;
- rate of current rise > 10^8 A/s;
- at pressure in its channel ~ $(10^8 \div 10^9)$ Pa.

From the given critical parametres at which the bridge collapses with a burst, it follows that explosion of bridge can occur at considerable short-circuit currents. For example, as it is shown in chapter 1, a bridge from liquid Ag has blown up at instantaneous short-ciruit current equal 52,0 κA.

In the second chapter a geometrical characteristic of short consricted arc is given on opening contacts $S_{lat}/(S_{bs.c}+S_{bs.a})=l_{arc}/r_{bs}$, which has appeared enough ustful. The characteristic comport well with electrophysical characteristics of arc and proves its form, structure, content of plasma and mobility. In this case, in respect to liquid-metal bridge pertinently to enter the relation $\Delta Q_{bs.br}/\Sigma S_{bs.br}$. Here $\Delta Q_{bs.br}$ - quantity of heat absorbed by contacts, and $\Sigma S_{bs.br}=S_{bs.c}+S_{bs.a}$ - sum of areas of the bases of bridge on the cathode and the anode.

For estimation of a part of energy generated in the bridge ΔW_{br}, as a result of current flowing through it, absorbed by contacts $\Delta Q_{bs.br}$, we will make use of geometrical factor of distribution of arc energy [3.6, part II,p. 325]:

$$\eta_g = 1 - \frac{\delta}{r_{bs} + \delta},$$

where r_{bs} – radius of base spot, δ – contact gap and proportion $\frac{\delta}{r_{bs} + \delta}$ – defines a part of energy ΔW, generated in its channel ΔQ_{ch}. In the context of a bridge $r_{bs} = r_{bs.br}$ and δ_{br} its length.

Let us consider the concrete examples. According to data [3.6, part II, p. 27, table 4.2] at opening of contacts instantaneous current intensity was equal 7,5 κA, δ_{br}=0,16 cm and average value of radius of bridge bases:

$$r_{bs.br} = \frac{d_{bs.c} + d_{bs.a}}{4} = \frac{0{,}35\ cm + 0{,}28 cm}{4} = 0{,}158\ cm.$$

In this case coefficient η_g is equal to:

$$\eta_g = 1 - \frac{\delta_{br}}{r_{bs} + \delta_{br}} = 1 - \frac{0{,}16\ cm}{0{,}158\ cm + 0{,}16\ cm} = 1 - 0{,}503 = 0{,}497.$$

The energy, generated in bridge, was defined in chapter 1 and is equal ΔW_{br}=60$W \cdot s$. The sum of squares of bridge bases is equal according to data [3.6, part II, p. 27, table 4.2]:

$$\Sigma S_{bs.br} = S_{bs.c} + S_{bs.à} = 0{,}096\ cm^2 + 0{,}062\ cm^2 = 0{,}158\ cm^2.$$

A ratio $\Delta Q_{bs.br}/\Sigma S_{bs.br}$ is equal:

$$\frac{\Delta Q_{bs.br}}{\Sigma S_{bs.br}} = \frac{\eta_g \cdot \Delta W_{br}}{\Sigma S_{bs.br}} = \frac{0{,}497 \cdot 60\ W \cdot s}{0{,}158\ cm^2} = 188{,}7\ \frac{W \cdot s}{cm^2}.$$

Further we will define a ratio of energy of bridge channel to square of its lateral surface:

$$\frac{\Delta Q_{ch}}{S_{lat.br}} = \frac{(1-\eta_g)\cdot \Delta W_{br}}{2\cdot\pi\cdot r_{bs.br}\cdot\delta_{br}} = \frac{(1-0{,}497)\cdot 60\, W\cdot s}{2\cdot\pi\cdot 0{,}158\, cm\cdot 0{,}16\, cm} = 190{,}1\,\frac{W\cdot s}{cm^2}.$$

It appears that the ratios $\Delta Q_{bs.br}/\Sigma S_{bs.br}$ and $\Delta Q_{ch}/S_{lat.br}$ are almost equal each other:

$$\frac{\Delta Q_{bs.br}}{\Sigma S_{bs.br}} = 188{,}7\,\frac{W\cdot s}{cm^2} \simeq 190{,}1\,\frac{W\cdot s}{cm^2} = \frac{\Delta Q_{ch}}{S_{lat.br}}.$$

Let us notice that at instantaneous current equal 7,5 κA a bridge has collapsed easy by evaporation (see chapter 1).

Now we will define these ratios in case of opening of contacts at instantaneous current intensity equal 13,0 κA [3, part II, p. 26, table 4.1]:

1. $r_{bs.br} = \dfrac{d_{bs.c} + d_{bs.a}}{4} = \dfrac{0{,}48\, cm + 0{,}42\, cm}{4} = 0{,}225\, cm$

2. $\eta_g = 1 - \dfrac{\delta_{br}}{r_{bs} + \delta_{br}} = 1 - \dfrac{0{,}08\, cm}{0{,}225\, cm + 0{,}08\, cm} = 1 - 0{,}262 = 0{,}738;$

3. $\Sigma S_{bs.br} = S_{bs.c} + S_{bs.à} = 0{,}18\ ñm^2 + 0{,}14\ ñm^2 = 0{,}32\ ñm^2;$

4. $S_{lat.br} = 2\cdot\pi\cdot r_{bs.br}\cdot\delta_{br} = 2\cdot\pi\cdot 0{,}225\, cm\cdot 0{,}08\, cm = 0{,}113\, cm^2;$

5. $\Delta Q_{bs.br} = \eta_g\cdot\Delta W_{br} = 0{,}738\cdot 117\, W\cdot s = 86{,}3\, W\cdot s;$

6. $\Delta Q_{ch} = (1-\eta_g)\cdot\Delta W_{br} = (1-0{,}738)\cdot 117\, W\cdot s = 30{,}7\, W\cdot s;$

7. $\dfrac{\Delta Q_{bs.br}}{\Sigma S_{bs.br}} = \dfrac{86{,}3\, W\cdot s}{0{,}32\, cm^2} = 269{,}7\,\dfrac{W\cdot s}{cm^2};$

8. $\dfrac{\Delta Q_{ch}}{S_{lat.br}} = \dfrac{30{,}7\, W\cdot s}{0{,}113\, cm^2} = 271{,}7\,\dfrac{W\cdot s}{cm^2};$

9. $\dfrac{\Delta Q_{bs.br}}{\Sigma S_{bs.br}} = 269{,}7\,\dfrac{W\cdot s}{cm^2} \simeq 271{,}7\,\dfrac{W\cdot s}{cm^2} = \dfrac{\Delta Q_{ch}}{S_{lat.br}}.$

Let us remind that at instantaneous current intensity equal 13,0 κA a bridge has collapsed easy by evaporation also (see chapter 1).

At instantaneous current intensity equal 52,0 κA a bridge at opening of argentiferous contacts has collapsed as a result of electric explosion. What values do the ratios $\Delta Q_{bs.br}/\Sigma S_{bs.br}$ and $\Delta Q_{ch}/S_{lat.br}$ have in case of bridge explosion? The necessary initial data for a considered example are given in chapter 1.

1. $r_{bs.br} = \frac{d_{br}}{2} = \frac{0{,}25\ cm}{2} = 0{,}125\ cm$.

2. $\delta_{br} = 0{,}05\ cm$.

3. $\eta_g = 1 - \frac{\delta_{br}}{r_{bs.br} + \delta_{br}} = 1 - \frac{0{,}05\ cm}{0{,}125\ cm + 0{,}05\ cm} = 1 - 0{,}286 = 0{,}714$.

4. $\Sigma S_{bs.br} = 2 \cdot S_{bs.br} = 2 \cdot \pi \cdot r_{bs.br}^2 = 2 \cdot \pi \cdot (0{,}125\ cm)^2 = 0{,}0981\ cm^2$.

5. $S_{lat.br} = 2 \cdot \pi \cdot r_{bs.br} \cdot \delta_{br} = 2 \cdot \pi \cdot 0{,}125\ cm \cdot 0{,}05\ cm = 0{,}0392\ cm^2$.

6. $\Delta Q_{bs.br} = \eta_g \cdot \Delta W_{br} = 0{,}714 \cdot 429\ W \cdot s = 306{,}3\ W \cdot s$.

7. $\Delta Q_{ch} = (1 - \eta_g) \cdot \Delta W_{br} = (1 - 0{,}714) \cdot 429\ W \cdot s = 122{,}7\ W \cdot s$.

8. $\frac{\Delta Q_{bs.br}}{\Sigma S_{bs.br}} = \frac{306{,}3\ W \cdot s}{0{,}0981\ cm^2} = 3122{,}3\ \frac{W \cdot s}{cm^2}$.

9. $\frac{\Delta Q_{ch}}{S_{lat.br}} = \frac{122{,}7\ W \cdot s}{0{,}0392\ cm^2} = 3130{,}1\ \frac{W \cdot s}{cm^2}$.

10. $\frac{\Delta Q_{bs.br}}{\Sigma S_{bs.br}} = 3122{,}3\ \frac{W \cdot s}{cm^2} \simeq 3130{,}1\ \frac{W \cdot s}{cm^2} = \frac{\Delta Q_{ch}}{S_{lat.br}}$.

Thus, as a result of given calculations the interesting phenomenon is revealed which consists in equality of superficial densities of energy dissipating through a surface of bases and a lateral surface of metal-liquid bridge at its destruction both by quiet evaporation and by explosion. It is possible to assert that at superficial density of energy $\Delta Q / S < 300\ W \cdot s / cm^2$ a liquid metal of bridge from Ag is steady thermodynamically and collapses by quiet evaporation, and at $\Delta Q / S \geq 3000\ W \cdot s / cm^2$ - a bridge is not steady thermodynamically and is subjected to explosive destruction. Numerical values of bridge erosion of argentiferous contacts are specified in table 3.1 at

various instantaneous current intensities at which contacts were opened, according to the calculations given in chapter 1.

Table 3.1. A bridge erosion of argentiferous contacts at different values of a current

I_{arc}, κA	7,5	13,0	52,0
M_{br}, g	0,117	0,14	0,0228

3.2. Erosion of contacts by evaporation of their metal

In paragraph 2.4 current flowing in arc on opening contacts is considered due to evaporation of their metal from a surface of base spots. In table 2.9 values of steams mass of Ag which has evaporated from a surface of base spots on the cathode and the anode during high-speed filming of separate shots at current switching-off in a test loop equal 16 κA, $U_{ph} = 420V$ and $\cos\varphi = 0{,}2$. According to table 2.9 in fig. 3.1 one can see graphes of change of mass of steams Ag which has evaporated from cathode $m_{st.c}$ and anode $m_{st.a}$ depending on time of arc burning. As a result of numerical integration of functions $m_{st.c}(t_{arc})$ and $m_{st.a}(t_{arc})$ in table 3.2 there are values of mass of steams Ag which has evaporated from a surface of base spots on cathode $\sum m_{st.c}(t_{arc})$ and on anode $\sum m_{st.a}(t_{arc})$ during arc burning on opening contacts.

Table 3.2. Erosion of contacts by means of evaporation Ag from a surface of base spots on the cathode and the anode at switching-off of a current 16 κA, $U_{ph} = 420V$ and $cos\,\varphi = 0{,}2$

t_{arc}, ms	0,334	0,668	1,34	2,0	2,67	4,0	5,34	6,68
i_{arc}, κA	13,0	15,0	18,2	21,5	23,2	24,5	21,9	14,6
u_{arc}, V	27,0	34,0	36,0	44,0	44,0	44,0	44,0	48,0
$m_{st.c}$, 10^{-3}, g	0,327	0,379	0,524	0,582	0,668	0,750	0,648	0,332
$\sum m_{st.c}$, g	$21{,}0\cdot10^{-3}$							
$m_{st.a}$, 10^{-3}, g	1,790	2,057	2,844	3,170	3,633	4,080	3,540	1,820
$\sum m_{st.a}$, g	$115{,}0\cdot10^{-3}$							
$M_{st} = \sum m_{st.c} + \sum m_{st.a}$, g	$136{,}0\cdot10^{-3}$							

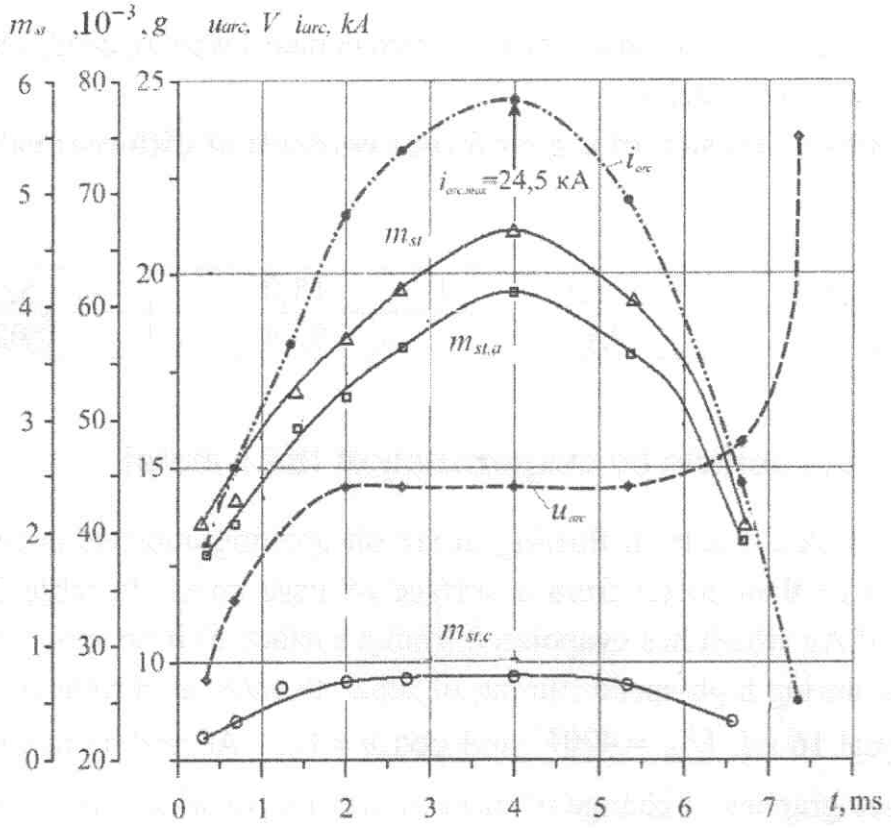

Fig. 3.1. Erosion of contacts by evaporation of their metal at current switching-off in loop equal 16 *кА*, $U_{ph} = 420V$ and $cos\,\varphi = 0{,}2$

Total mass of steams Ag which has evaporated from contacts at switching-off of a current 16 *кА* at $U_{ph} = 420V$ and $\cos\varphi = 0{,}2$, is equal to:

$$M_{st} = \sum m_{st.c} + \sum m_{st.a} = (21{,}0 + 115{,}0)\cdot 10^{-3} g = 136{,}0 \cdot 10^{-3} g.$$

3.3. Cathode erosion at switching-off of short-circuit current

In the previous sections it was shown that erosion of opening contacts is consisted of bridge erosion and mass of steams of contact metal evaporated with a surface of base spots of arc.

In paragraph 2.5 a formation of columns from liquid metal is shown in the form of cones with drops at their tops after collapse of microbubbles. Power density, coming on a cone with radius of base equal $r_{cone} = 10^{-4} cm$ and an angle in top $2\alpha = 10°$, can not lead to explosive destruction of contacts at initial stage of their disconnection $q_{c.max.c} = 3{,}06 \cdot 10^{6} W / cm^2$. That is a cone on the cathode should be

subjected to evaporation. Average mass $m_{cone.c}$ of liquid Ag is equal at temperature close to temperature of its boiling in a cone on the cathode:

$$m_{cone.c} = \rho_{boil}^{Ag} \cdot V_{cone.c} = 9{,}0 g/cm^3 \cdot 11{,}9 \cdot 10^{-12} cm^3 = 1{,}07 \cdot 10^{-10} g,$$

where $\rho_{boil}^{Ag} = 9{,}0 g/cm^3$ (table 1.1);

$V_{cone.c} = \frac{1}{3} \cdot \pi \cdot r_c^2 \cdot h = \frac{1}{3} \cdot \pi \cdot (10^{-4} cm)^2 \cdot 11{,}4 \cdot 10^{-4} cm = 11{,}9 \cdot 10^{-12} cm^3$ – average volume of a cone on the cathode; $h = \frac{r_c}{tg\alpha} = \frac{10^{-4} cm}{tg5^\circ} = \frac{10^{-4} cm}{0{,}08749} = 11{,}4 \cdot 10^{-4} cm$ – height of a cone.

At initial stage of opening of contacts a density of stream of mass of steams Ag at evaporation of cone metal at coming on it power density equal $q_{c.\max.c} = 3{,}06 \cdot 10^6 W/cm^2$ is equal:

$$j_{ev} = \frac{q_{c.\max.c}}{W_{ev}^{Ag}} = \frac{3{,}06 \cdot 10^6 W/cm^2}{2{,}36 \cdot 10^3 W \cdot s/g} = 1{,}3 \cdot 10^3 g/(cm^2 \cdot s),$$

where $W_{ev}^{Ag} = 2{,}36 \cdot 10^3 W \cdot s/g$ – table 1.1.

In that case a metal-liquid cone on the cathode can evaporate in time:

$$t_{cone.c} = \frac{m_{cone.c}}{j_{ev} \cdot S_{cone.c}} = \frac{1{,}07 \cdot 10^{-10} g}{1{,}3 \cdot 10^3 g/(cm^2 \cdot s) \cdot 36{,}1 \cdot 10^{-4} cm^2} = 2{,}28 \cdot 10^{-11} s,$$

where $S_{cone.c} = \pi \cdot r_c \cdot l_{cone.c} = \pi \cdot 10^{-4} cm \cdot 11{,}5 \cdot 10^{-4} cm = 36{,}1 \cdot 10^{-4} cm^2$ – square of cone surface;

$l_{cone.c} = \frac{r_c}{\sin 5^\circ} = \frac{10^{-4} cm}{0{,}08716} = 11{,}5 \cdot 10^{-4} cm$ – length of cone generatrix.

Time of evaporation of a cone on the cathode is less on two orders than time of crater formation, but is more than functioning time of ecton:

$$t_{cr} = 4{,}5 \cdot 10^{-9} s > t_{cone.c} = 2{,}28 \cdot 10^{-11} s > 9{,}8 \cdot 10^{-13} s = t_{ec}.$$

Therefore cycle time of functioning of a cone, a crater and ecton is almost equal to time of crater formation:

$$t_{cyc} = 4{,}52 \cdot 10^{-9} s \simeq 4{,}5 \cdot 10^{-9} s = t_{cr}.$$

According to data of table 2.11, total quantity of cones which we will accept equal to total quantity of ectons $\sum \Delta N_{ec}(t_{arc})$ on the cathode, is equal $1{,}177 \cdot 10^9$. Therefore, loss of mass by the cathode due to evaporation of cones is:

$$\sum m_{cone.c} = m_{cone.c} \cdot \sum \Delta N_{ec}(t_{arc}) = 1{,}07 \cdot 10^{-10} g \cdot 1{,}177 \cdot 10^9 = 0{,}126 g.$$

At microbubble explosion in a layer of a liquid-melt on the cathode the portion of steams Ag is generated which also is a part of steam fraction of erosion of the cathode.

Average volume of a microbubble on the cathode is equal:

$$V_b = \frac{4}{3}\pi \cdot r_c^3 = \frac{4}{3}\pi \cdot (10^{-4})^3 = 4{,}19 \cdot 10^{-12} cm^3.$$

At initial stage of opening of contacts a quantity of atoms Ag in a microbubble is:

$$N_0 = n_0 \cdot V_n = 8{,}92 \cdot 10^{19} cm^{-3} \cdot 4{,}19 \cdot 10^{-12} cm^3 = 3{,}47 \cdot 10^8,$$

where $n_0 = 8{,}92 \cdot 10^{19} cm^{-3}$ – concentration of atoms in a microbubble (table 2.11). Mass of steam Ag in a microbubble has a value:

$$m_{st.b} = m_0^{Ag} \cdot N_0 = 179{,}1 \cdot 10^{-24} g \cdot 3{,}74 \cdot 10^8 = 6{,}7 \cdot 10^{-14} g,$$

where $m_0^{Ag} = 179{,}1 \cdot 10^{-24} g -$ mass of atom Ag (table 1.1).

Total quantity of steam mass Ag, lost by the cathode in the results of microbubbles explosion during arc burning on the contacts, is equal:

$$\sum m_{st.b} = m_{st.b} \cdot \sum \Delta N_{ec}(t_{arc}) = 6{,}7 \cdot 10^{-14} g \cdot 1{,}177 \cdot 10^9 = 7{,}9 \cdot 10^{-5} g.$$

Thus, total mass of steam fraction of erosion of the cathode at switching-off of current in loop 16 κA at $U_{ph} = 420V$ and $\cos\varphi = 0{,}2$ argentiferous contacts is equal:

$$M_{st.c} = \sum m_{st.c} + \sum m_{cone.c} + \sum m_{st.b} =$$

$$= 21 \cdot 10^{-3} g + 126 \cdot 10^{-3} g + 7{,}9 \cdot 10^{-5} g = 147{,}1 \cdot 10^{-3} g.$$

Liquid-drop fraction of erosion of the cathode consists of mass of drops come

off from tops of metal-liquid of columns in the form of cones and formed as a result of crushing of external cover of microbubbles at their explosion.

In fig. 2.14 we can see microelectronic photos of supersmall drops with sizes from 0,3 to 1,0 μm on a surface of argentiferous contacts after switching-off of short-circuit currents. As drops at standing in arc channel are subjected to partial evaporation that for calculation of liquid-drop erosion of contacts we will accept that average diameter of drops is equal to their greatest value 1,0 μm. Volume of drop is equal to:

$$V_d = \frac{4}{3}\pi \cdot r_d^3 = \frac{4}{3}\pi \cdot (0{,}5 \cdot 10^{-4} cm)^3 = 0{,}52 \cdot 10^{-12} cm^3.$$

Mass of such drop from Ag is equal at temperature close to its boiling temperature:

$$m_d = \rho_{boil}^{Ag} \cdot V_d = 9{,}0 g/cm^3 \cdot 0{,}52 \cdot 10^{-12} cm^3 = 4{,}68 \cdot 10^{-12} g.$$

Quantity of the drops, which have come off from metal-liquid columns in the form of cones, is equal to quantity of ectons on the cathode, which functioned in process of arc burning on contacts. In that case total mass of drops will be equal:

$$\sum m_{d.cone} = m_d \cdot \sum \Delta N_{ec}(t_{arc}) = 4{,}68 \cdot 10^{-12} g \cdot 1{,}177 \cdot 10^9 = 5{,}5 \cdot 10^{-3} g.$$

The drops are as the second component of liquid-drop erosion of the cathode. They are formed as a result of microbubble explosion in a boiling layer of liquid-melt.

Microbubble explosion in a liquid-melt on a base spot of high arc of switching-off consists of two phases. In the first phase explosion of microbubble, located at a surface of a liquid-melt, occurs from influence of pressure P_b in which basic component is Laplace pressure. Pressure in microbubble P_b acts in all directions and aspires to expand it. However a close arrangement of a microbubble to a surface of a liquid-melt leads to explosion of its external shell and its splitting on microdrops.

In a considered example according to data of table 2.11 during arc burning on contacts a pressure in a microbubble on the cathode is equal to:

$$P_b = (43{,}9 \div 39{,}5) \cdot 10^6 dynes/cm^2 (P_L = 39{,}2 \cdot 10^6 dynes/cm^2).$$

Such high value of pressure can quite lead to explosion of microbubble.

From fig. 2.15 and the figures given in [3.6, part II, fig. 3.36, p. 234 and fig. 3.46, p. 242], we can see a form of craters on the cathode at switching-off of short-circuit currents. Schematically it is possible to present a crater how it is shown in fig.

3.2. In that case cathode erosion at explosion of microbubble will be consisted of volume of a liquid melt, being over its surface. Volume of eroded liquid-melt V_{er} is equal:

$$V_{er} = V_{cyl} - \frac{1}{2}V_b = \pi \cdot r_c^2 \cdot r_c - \frac{1}{2} \cdot \frac{4}{3} \cdot \pi \cdot r_c^3 =$$

$$= \pi(10^{-4} cm)^3 - \frac{2}{3}\pi(10^{-4} cm)^3 = 1{,}05 \cdot 10^{-12} cm^3,$$

где V_{cyl} и V_b – volumes of cylinder and microbubble respectevely.

At temperature close to boiling temperature Ag a mass of eroded unit volume of a liquid-melt is equal to:

$$m_{d.b} = \rho_{boil}^{Ag} \cdot V_{er} = 9{,}0\ g/cm^3 \cdot 1{,}05 \cdot 10^{-12} cm^3 = 9{,}45 \cdot 10^{-12} g.$$

Total mass of liquid-drop erosion of the cathode at explosion of microbubbles during arc burning on the contacts is:

$$\sum m_{d.b} = m_{d.b} \cdot \sum \Delta N_{ec}(t_{arc}) = 9{,}45 \cdot 10^{-12} g \cdot 1{,}177 \cdot 10^9 = 11{,}1 \cdot 10^{-3} g.$$

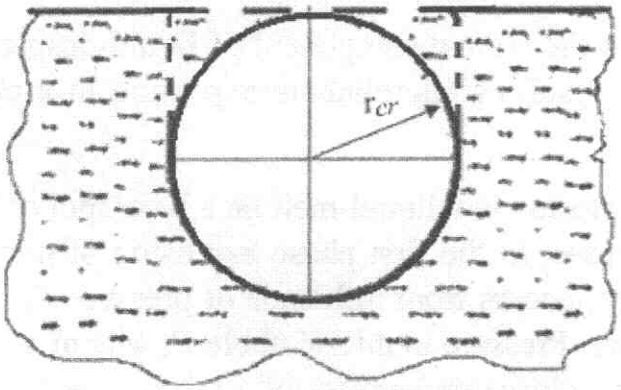

Fig. 3.2. Schematic image of a crater on the cathode

As a result of microbubble explosion in its volume microplasmoid is formed in which a current of ecton flows i_{ec}. According to data of table 2.11 a current of ecton on the cathode changes in process of arc burning on contacts from 9,4 to 8,85 *A*. As a result of flowing of current of ecton in microplasmoid electromagnetic pressure arises $P_{mpl.c}$, which constricts it.

After the first phase of explosion of microbubble under influence of Laplace

pressure there comes the second phase of its explosion under influence of electromagnetic pressure.

According data of table 2.15, pressure in microplasmoids on the cathode during arc burning on opening contacts changes in an interval $(27{,}58 \div 24{,}95) \cdot 10^5 Pa$. This pressure causes jet force $F_{mpl.c}$, acting on crater bottom. Its square is $S_{cr.c} = 3{,}14 \cdot 10^{-8} cm^2$.

Jet force F_{cr}, acting on a crater bottom on the cathode, at initial stage of opening of contacts is equal:

$$F_{mpl.c} = P_{mpl.c} \cdot S_{cr.c} =$$

$$= 27{,}58 \cdot 10^6 dynes/cm^2 \cdot 3{,}14 \cdot 10^{-8} cm^2 = 0{,}87 dynes = 0{,}88 \cdot 10^{-3} g.$$

In appearance of the craters shown, for example, in microelectronic photos (fig. 2.15), it is visible that craters are not subjected to explosive destruction. Therefore it is possible to draw a conclusion about insufficiency of jet force F_{cr} equal less than one milligramme for the crater destruction. The crater`s diameter is two microns.

It is rather indicative a kinetic energy of a mass flux of microparticles can serve. These microparticles are thrown up from a crater in the second phase of its explosion. In process of microplazmoid functioning ions are absorbed by the cathode, and elecrons are thrown up out of crater limits. Singular electron on the cathode gets kinetic energy which equal:

$$w_e^c = \frac{m_e \cdot \upsilon_e^2}{2} = \frac{9{,}11 \cdot 10^{-28} g \cdot (1{,}36 \cdot 10^8 cm/s)^2}{2} = 8{,}42 \cdot 10^{-12} erg,$$

where $9{,}11 \cdot 10^{-28} g$ – electron mass and $1{,}36 \cdot 10^8 cm/s$ – oriented velocity on cathode (see 2.6.1).

Total quantity of electrons N_e in microplasmoid on the cathode is equal $5{,}8 \cdot 10^7$ (see 2.6.1). Hence, kinetic energy of mass flux of electrons in microplasmoid on the cathode is equal to:

$$W_{ec.e}^{c} = w_e^c \cdot N_e = 8{,}42 \cdot 10^{-12} erg \cdot 5{,}8 \cdot 10^7 =$$
$$= 4{,}8 \cdot 10^{-4} erg = 4{,}8 \cdot 10^{-11} J.$$

Probably, a flux of electrons, flowing out from opened crater and possessing kinetic energy, equal to order $10^{-11} J$, can not lead to crater destruction on the cathode in the second phase of explosion of a microbubble.

Total mass of liquid-drop of fraction of erosion on the cathode at switching-off of a current 16 κA by argentiferous contacts at $U_{ph} = 420V$ and $\cos\varphi = 0{,}2$ is equal to:

$$M_{ld.c} = \sum m_{d.cone} + \sum m_{d.b} =$$

$$= 5{,}5 \cdot 10^{-3} g + 11{,}1 \cdot 10^{-3} g = 16{,}6 \cdot 10^{-3} g.$$

Thus, in the given example of calculation of erosion of the cathode its general mass is equal:

$$M_{эr.c} = M_{st.c} + M_{ld.c} = 147{,}1 \cdot 10^{-3} g + 16{,}6 \cdot 10^{-3} g = 163{,}7 \cdot 10^{-3} g.$$

A part of a liquid-drop of fractions of erosion of the cathode at switching-off of a current in a contour 16 κA at $U_{ph} = 420V$ and $cos\,\varphi = 0{,}2$ is equal to:

$$\frac{M_{ld.c}}{M_{er.c}} \cdot 100\% = \frac{16{,}6 \cdot 10^{-3} g}{163{,}7 \cdot 10^{-3} g} \cdot 100\% = 10{,}14\%.$$

Hence, the bulk of mass of erosion of argentiferous cathode in a low-voltage arc at switching-off of a current 16 κA consists of steam fraction.

3.4. Explosive erosion of the anode at switching-off of short-circuit current

Electric erosion of the anode on opening contacts at switching-off of short-circuit current consists of steam and metal-liquid fractions as well as for the cathode. An estimation of bridge erosion of contacts and their erosion for the account of evaporation of metal from a surface of base spot of arcdischarge is given in the previous paragraphs.

Average value of power density coming on the anode at switching-off of current equal 16,0 *кА* by argentiferous contacts, according to data of table 2.7,is equal $q_{bs.a} \geq (10^5 \div 10^4)$ W/cm^2. At this value of power density and criterion $Bi \geq 1{,}0$ all square of anode base spot is subjected to melting and a thin layer of a liquid-melt *Ag* reaches temperature of its boiling. In a thin layer of a liquid-melt *Ag* superficial bubble boiling takes place. At increase of volume of a microbubble and its achievement of a surface of a liquid-melt a break of its outer shell occurs under influence of pressure P_b (table 2.13). Steams *Ag* in a microbubble ionized like an avalanche and microplazmoid forms in which current of ecton flows. As a result of ecton current flowing in microplazmoid electromagnetic pressure $P_{mpl.a}$ (table 2.15) takes place which changes during arc burning on contacts from 96,6 to 58,35 *atm*. This pressure causes a jet force $F_{cr.a}$ influencing a bottom of a crater, being on the anode:

$$F_{cr.à} = Ð_{mpl.à} \cdot S_{cr.à} = 96{,}6\ kgf/cm^2 \cdot 38{,}5 \cdot 10^{-8} cm^2 = 37{,}2 \cdot 10^{-3}\ g,$$

where $S_{cr.a} = 38{,}5 \cdot 10^{-8}$ $см^2$ – average value of crater square on the anode. Jet force on anode $F_{mpl.a}$ more on two orders than on the cathode:

$$F_{mpl.à} = 37{,}2 \cdot 10^{-3}\ g >> 0{,}88 \cdot 10^{-3}\ g = F_{mpl.c}\ .$$

Moreover, ions in microplasmoid on the anode, unlike ions on the cathode, are directed to environment. As pressure in a microbubble P_b on the anode is rather insignificant (table 2.13) its external shell is subjected to destruction not completely. In it a break occurs only (see fig. 2.24). Therefore ions and neutral atoms at the movement can mechanically influence walls of a half-closed microbubble. We will estimate this influence.

Kinetic energy of singular ion *Ag* is equal:

$$\omega_i^a = \frac{m_i^{Ag} \cdot \upsilon_i^2}{2} = \frac{179{,}1 \cdot 10^{-24}\ g \cdot \left(0{,}469 \cdot 10^6 \frac{cm}{s}\right)^2}{2} = 1{,}97 \cdot 10^{11}\ erg,$$

where $m_i^{Ag} = 179{,}1 \cdot 10^{-24}$ g – mass of atom (ion) *Ag*, and average speed of ions in anode zone of electrode from *Ag* [3.6, part II, p. 45]:

$$\upsilon_i = 0{,}134 \cdot 10^6 \cdot \sqrt{U_{ef.a}} = 0{,}134 \cdot 10^6 \cdot \sqrt{12{,}25\ V} = 0{,}469 \cdot 10^6\ cm/s.$$

Total number of ions N_u in microplasmoid on the anode is equal N_i=$N_{e.ec}$=$8{,}526 \cdot 10^8$ (see the item 2.6.2 see) N_i=$N_{e.ec}$=$8{,}526 \cdot 10^8$ (see item 2.6.2).

Kinetic energy of mass flux of ions in microplasmoid on the anode is equal to:

$$W^a_{ec.i} = \omega^a_i \cdot N_i =$$

$$= 1{,}97 \cdot 10^{-11}\ erg \cdot 8{,}526 \cdot 10^8 = 1{,}68 \cdot 10^{-2}\ erg = 1{,}68 \cdot 10^{-9}\ J.$$

Kinetic energy of flux of ions in microplasmoid on the anode is more in two orders than kinetic energy of flux of electrons on the cathode:

$$W^a_{ec.i} = 1{,}68 \cdot 10^{-9}\ J >> 4{,}8 \cdot 10^{-11}\ J = W^c_{ec.e}.$$

Numerical calculations of values of electromagnetic pressure in microplasmoid on the anode created by ecton`s current, jet force acting on a crater bottom and kinetic energy of flux of ions in microplasmoid prove a presence of cavities with a diameter up to $100 \cdot 10^{-4}$ *cm* (see fig. 2.13) on eroded surface of argentiferous contacts, numerous supersmall drops with a diameter $(0{,}3 \div 1{,}0) \cdot 10^{-4}$ *cm* in the central part of contacts (see fig. 2.14) and relatively large drops which diameters (0,2 ÷ 0,5) *mm* on their periphery. Moreover, fragments of a material of contacts (see fig. 3.3) have been found out on their surface. In [3.6, part II, paragraph 4.4] numerous drops are shown from arc chambers of automatic circuit breaker after current switching-off in a test loop equal 65,0 *кА*.

All presented experimental supervision of products of erosion of high-current contacts and results of calculations are proofs of intensive explosive processes on their surface at switching-off of short-circuit currents..

According to Daalder`s data given in [3.7, p. 379], at switching-off of currents in a range from 52 to 210 *A* the drops scattered at angle 10° ÷ 20° concerning a surface of copper contacts.

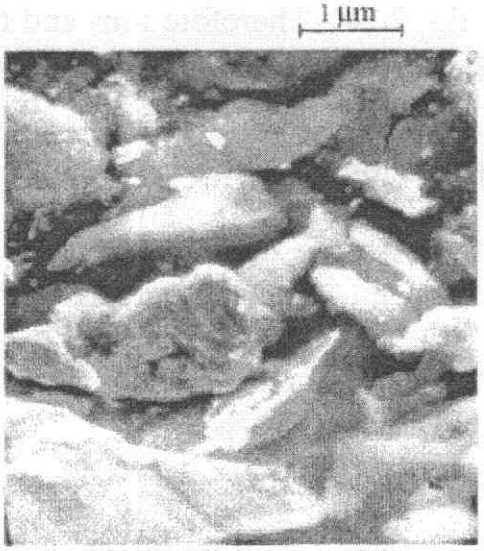

Fig. 3.3. Fragments of metal of contacts on their surface after switching-off of short-circuit current

Thus, at the second phase of explosion of microplasmoid on a microbubble place there are formed erosion cone (it is schematically shown in fig. 3.4 c) and emission of drops and solid particles of contacts metal.

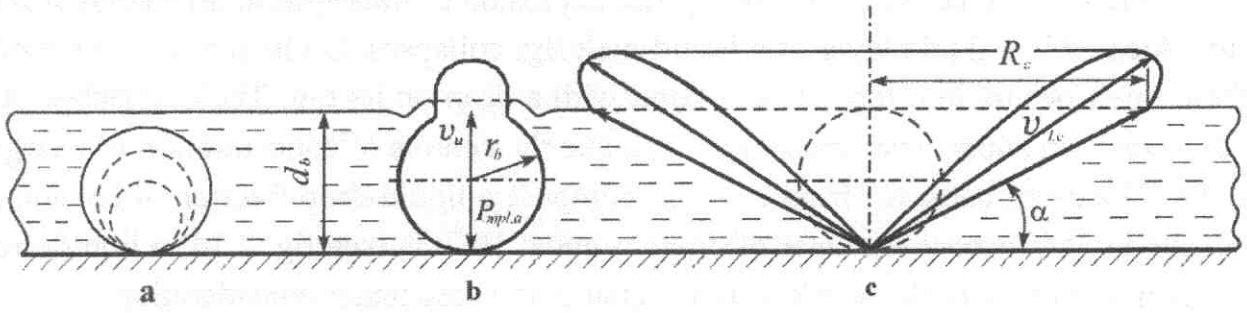

Fig. 3.4. Schematic drawing: a – formation of microbubble; b - break of shell of a microbubble and formation of microplasmoid; c - formation of a cone of erosion as a result of crater explosion

Volume of a cone:

$$V_{cone} = \frac{1}{3} \cdot \pi \cdot R_{cone}^2 \cdot h,$$

where R_{cone} – radius of a base of cone and h – its height. We will accept a cone height is average diameter of a microbubble, that is $h = d_b = 7 \cdot 10^{-4}$ *cm*. Radius of cone is defined from expression:

$$R_{cone} = \frac{d_b}{tg\alpha}.$$

We will accept that corner of scattering of drops α is 10° that corresponds to a corner of scattering of copper drops. In that case, a radius of cone and its volume will be equal:

$$R_{cone} = \frac{d_b}{tg\alpha} = \frac{7 \cdot 10^{-4}\ cm}{tg10°} = \frac{7 \cdot 10^{-4}\ cm}{0{,}1763} = 39{,}7 \cdot 10^{-4}\ cm,$$

$$V_{cone} = \frac{1}{3} \cdot \pi \cdot \left(39{,}7 \cdot 10^{-4}\ cm\right)^2 \cdot 7 \cdot 10^{-4}\ cm = 1{,}1 \cdot 10^{-8}\ cm^3.$$

Average mass of liquid *Ag*, contained in an erosion cone, will be equal at temperature of its boiling:

$$m_{cone.er} = \rho \cdot V_{cone} = 9{,}0\ g/cm^3 \cdot 1{,}1 \cdot 10^{-8}\ cm^3 = 9{,}9 \cdot 10^{-8}\ g.$$

Total mass of contact erosion, lost for the account of scattering of particles from erosion cone on the anode at switching-off of current 16,0 *кА* ($i_{arc.max}$=24,5 *кА*) in process of arc burning on contacts:

$$\sum m_{er.cont} = m_{cone.er} \cdot \sum N_{ec.a}(t_{arc}) = 9{,}9 \cdot 10^{-8}\ g \cdot 1{,}378 \cdot 10^7 = 1{,}364\ g,$$

where $\sum N_{ec.a}(t_{arc})$ – total quantity of ectons, functioning on the anode during arc burning on contacts at switching-off of current 16,0 κA (see table 2.13).

After end of ecton`s functioning and explosion of microplasmoid a cone of erosion, located in a liquid layer of a liquid-melt Ag, collapses. On its place a splash of a liquid-melt occurs in a form of a column with a drop on its top. These splashes of a liquid-melt on anode base spots of arc become the centres of concentration of charges again. The drops came off from columns compose a liquid-drop fraction of erosion of the anode. If to accept diameter of drops is equal 10^{-4} cm (see fig. 2.14) a liquid-drop fraction of erosion of the anode will be equal in the case under consideration:

$$\sum m_d = m_d \cdot \sum N_{ec.a}(t_{arc}) = 4{,}68 \cdot 10^{-12}\ g \cdot 1{,}378 \cdot 10^{7} = 6{,}45 \cdot 10^{-5}\ g.$$

According to data of table 2.12, power density $q_{c.max.a}$, coming on the centres of concentration of charges in the form of columns on the anode during arc burning on contacts, changes in a range from $6{,}32 \cdot 10^{6}$ W/cm^2 to $5 \cdot 10^{5}$ W/cm^2 which cannot lead to their explosive destruction. Hence, a metal-liquid fraction of erosion of the anode at current switching-off in a loop 16,0 κA at $U_{ph} = 420$ V and $cos\ \varphi = 0{,}2$ is equal to:

$$M_{d.k.a} = \sum m_{er.cont} + \sum m_d = 1{,}364\ g + 6{,}45 \cdot 10^{-5}\ g = 1{,}365\ g.$$

Splash of liquid Ag in form of a column, formed at collapse of a cone of erosion, height $h = 5 \cdot 10^{-4}$ cm under influence of power density 10^{5} W/cm^2, should evaporate and compose a part of steam fraction of erosion of the anode. At explosion of a cone of erosion steams of Ag, contained in a microbubble, should also compose a part of steam fraction of erosion of the anode. However, as calculations show, their total mass in anode erosion composes only units $(10^{-5} \div 10^{-6})$ g [3.6, part II, p. 137]. Therefore it is no necessity to take into account the specified components of steam fraction of erosion of the anode in total mass of erosion of contacts.

Thus, in the resulted example of calculation of erosion of the anode its general mass is equal:

$$M_{er.a} = M_{st.a} + M_{ld.a} = 115 \cdot 10^{-3}\ g + 1{,}365\ g = 1{,}48\ g,$$

where $M_{st.a} = \Sigma m_{st.a}$ – table 3.2.

A part of metal-liquid fractions in erosion of the anode from argentiferous contacts at current switching-off in a loop 16,0 κA is equal:

$$\frac{M_{ld.a}}{M_{er.a}} \cdot 100\% = \frac{1{,}365\ g}{1{,}48\ g} \cdot 100\% = 92{,}2\%.$$

Total mass of erosion of argentiferous contacts at switching-off of a current equal 16,0 κA by the low-voltage breaker at $U_{ph} = 420$ V and $cos\ \varphi = 0{,}2$ is equal:

$$M_{er} = M_{er.c} + M_{er.a} = 163{,}7 \cdot 10^{-3}\ g + 1{,}48\ g = 1{,}644\ g.$$

In a considered example anode erosion surpasses cathode erosion in $\frac{M_{er.a}}{M_{er.c}} = \frac{1{,}48\ g}{0{,}1637\ g} = 9$ times, that is practically an order of magnitude increase. A part of steam fraction of erosion of contacts at switching-off of current 16,0 *кА* is equal:

$$\frac{M_{st.c} + M_{st.a}}{M_{er}} \cdot 100\% = \frac{147{,}1 \cdot 10^{-3}\ g + 115 \cdot 10^{-3}\ g}{1{,}644\ g} \cdot 100\% = 15{,}9\%.$$

Let us notice that in [3.6, part II, p. 138] erosion of both argentiferous contacts at current switching-off in a loop 16,0 *кА* ($i_{arc.max}$ = 24,5 *кА*), calculated by the simplified technique, was equal:

$$M'_{er} = 2 \cdot M_{er.c} = 2 \cdot 0{,}89\ g = 1{,}78\ g.$$

That is difference in the results of calculations according to the simplified and specified techniques is:

$$\frac{M'_{er}}{M_{er}} \cdot 100\% = \frac{1{,}78\ g}{1{,}644\ g} \cdot 100\% = 108\%.$$

Hence, in practical engineering calculations for estimation of expected erosion of contacts at switching-off of short-circuit currents it is possible to use the simplified technique of its calculation.

3.5. The erosion mechanism of deion plates of arc chute

Service life of breakers and reliability of repeated switching-off of rated currents and short-circuit currents depend on erosion resistance of deion plates of arc chute, arc horns and other details of arc devices of breakers. Decrease in their erosion can be reached only as a result of in-depth study of the mechanism of their electric erosion. Mechanisms of electric erosion of electrodes and erosive traces of arc discharge are varied. It is connected with a large quantity of versions of arc discharges and conditions of their occurrence. Obviously, in each specific case the mechanism of erosion of electrodes will depend on electric and geometrical characteristics of arc discharge, heat- and electrophysical properties of metals of electrodes and their steams and duration of influence of arc discharge on electrodes.

In [3.6, paragraph 3.4] the basic features of the form and structure of base spots of arc of switching-off of high power on deion plates with various kinds of coverings of arc chutes of low-voltage breakers are considered.

Erosion of deion plates depending on value of force of a opened current and geometry of arc chute can be or in the form of the explosive mechanism with ablation of considerable mass of their metal, or discrete practically without metal loss.

3.5.1. Explosive erosion of deion plates

In fig. 3.5 we can see a photo of plate of arc chamber after switching-off of short-circuit current. For clarity of degree of its erosion from below a new plate was laid under it. In fig. 3.5 b a drawing of plate in section is shown, on which black part – a cross-section of entrained metal.

In fig. 3.6 we can see oscillogramm of a current and voltage in process of arc extinguishing at switching-off of short-circuit currents by highspeed circuit breaker. On the breaker a chamber with deion plate was mounted which is shown in fig. 3.5. Maximal instantaneous current of arc in phase A reached $i_{arc.max}$=79,3 κA. Average of current intensity, coming on a square of one side of deion plate $S_{d.pl}$=2000 mm^2, is equal to:

$$j_{av.d.pl} = \frac{i_{arc.max}}{S_{d.pl}} = \frac{79300\ A}{2000\ mm^2} = 39{,}6\ A/mm^2.$$

As the distance between deion plates was 3 and 5 mm arc in arc chute can be only short consricted with the characteristic relation l/r_{bs} <<1. Arc has not entered completely in arc chute, and a square of its base spot on a plate was equal made 900 mm^2 only. Therefore, actually, average value of current density is equal:

$$j_{act.av.d.pl} = \frac{i_{arc.max}}{S_{bs.act}} = \frac{79300\ A}{900\ mm^2} = 88\ A/mm^2.$$

Power density coming on all surface of deion plate and on the actual square of base spot of arc, is equal respectively:

$$q_{d.pl} = \frac{\eta \cdot i_{arc.max} \cdot \Delta U_{arc}}{2 \cdot S_{d.pl}} = \frac{0{,}66 \cdot 79300\ A \cdot 36\ V}{2 \cdot 20\ cm^2} = 4{,}71 \cdot 10^4\ \frac{W}{cm^2}.$$

$$q_{bs.act} = \frac{\eta \cdot i_{arc.max} \cdot \Delta U_{arc}}{2 \cdot S_{bs.act}} = \frac{0{,}66 \cdot 79300\ A \cdot 36\ V}{2 \cdot 9\ cm^2} = 1{,}05 \cdot 10^5\ \frac{W}{cm^2}.$$

Here:

$$\eta = \frac{U_c + U_a}{U_{arc}} = \frac{(15{,}5 \div 17)V + (6 \div 9)V}{2 \cdot 36\ V} = 0{,}66\ \_$$

a factor considering a part of arc power, coming on a surface of electrode

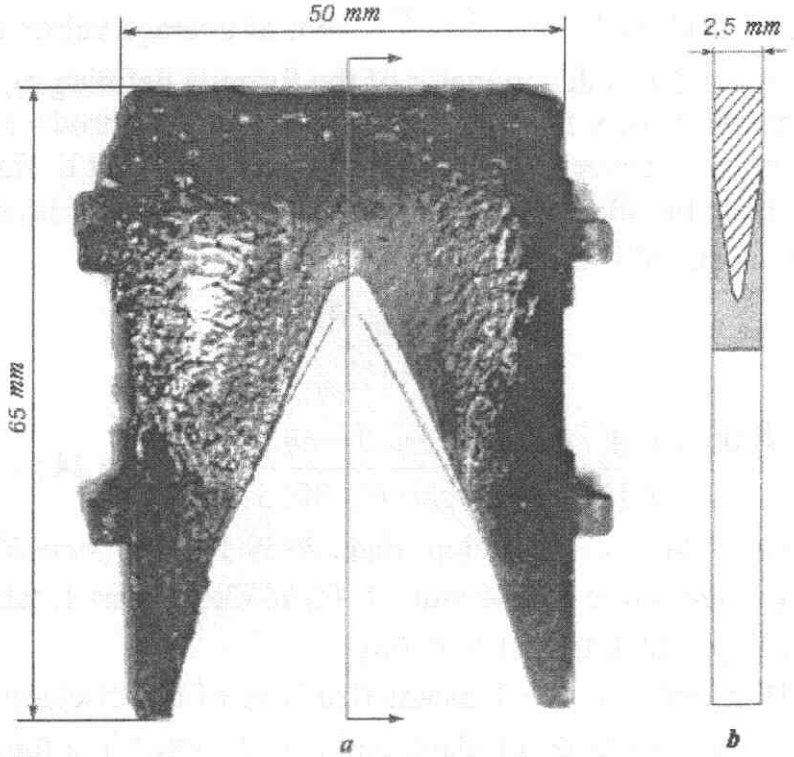

Fig. 3.5. Partially burnt out deion plate after switching-off of short-circuit current. From below the new plate is laid

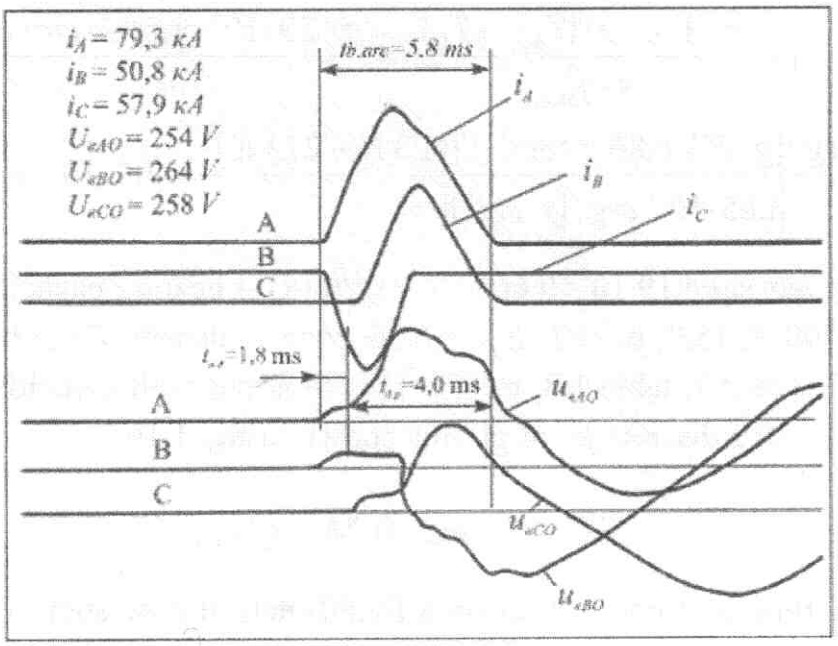

Fig. 3.6. Oscillogram of current and voltage at switching-off of short-circuit current by a high-speed circuit breaker

$U_c = (15{,}5 \div 17)\,V$ - cathodic and $U_a = (6 \div 9)\,V$ - anode drops of voltage *Fe* [2.6, part I, table 3.7, p. 281]; $U^{Fe}_{av.(c+a)} = 23{,}75\,V$ - sum of average values of electrode voltage drops *Fe*; number 2 in a denominator of the formula defining $q_{bs.act}$, takes into account a part of power density falling on a surface of one electrode, and ΔU_{arc}=36 *V* – arc pressure in one gap between deion plates from *Fe* [2.6, part II, fig. 5.47].

Let us estimate possibility of penetration of heat in inside layers of a body of a plate from *Fe* by means of Biot criterion:

$$Bi = \frac{q_{bs.act} \cdot \delta_{d.pl}}{\lambda \cdot T_{boil}} =$$

$$= \frac{(1{,}05 \cdot 10^5\ W/cm^2) \cdot 10^7\ erg/(s \cdot cm^2) \cdot 0{,}2\ cm}{29 \cdot 10^5\ erg/(s \cdot cm \cdot K) \cdot 3023\ K} = 24 >> 1,$$

where $\delta_{d.pl}$=0,2 *cm* – thickness of deion plate, λ=29·10^5 *erg/(s·cm·K)* – heat conduction coefficient of steel 08 at temperature 1200 *K* [3.6, part I, table 1.23, p. 110], T_{boil}= 3023 *K Fe* [3.6, part I, table 1.5, p. 68].

Value of Biot criterion >> 1 means that heat of arc discharge does not penetrate into inside layers of a body of plate, and is distributed in a thin layer of boiling metal on a surface of base spot.

Time of warming up of a facial layer of metal on base spot under influence of power density $q_{bs.act}$ up to boiling temperature is equal to:

$$\tau_{bs.boil} = \frac{\pi \cdot \lambda \cdot c \cdot \rho \cdot (T_{boil} - T_0)^2}{4 \cdot q^2_{bs.act}} = \frac{\pi \cdot 29 \cdot 10^5\ erg/(s \cdot cm \cdot K)}{4} \times$$

$$\times \frac{0{,}666 \cdot 10^7\ erg/(g \cdot K) \cdot 6{,}86\ g/cm^3 \cdot (3023\ K - 273\ K)^2}{[1{,}05 \cdot 10^{12}\ erg/(s \cdot cm^2)]^2} = 7{,}4 \cdot 10^{-4}\ s,$$ where c =

= 0,159 *cal/(g·degree)*·4,19·10^7=0,666·10^7 *erg/(g·K)* – heating capacity of steel 08 at temperature 1300 °C [3.9, p. 162] и ρ = 6,86 *g/cm*^{3} – density *Fe* at boiling temperature 3023 *K* [3.6, part I, table 1.8, p. 69]. This time has well coincided with binding time of base spot of a discrete jet of plasma shown in fig. 1.16.

$$T_{arc} \sim 0{,}7\ ms \simeq 0{,}74 = t_{bs.boil}.$$

Forming time of a microcrater on a liquid-melt of base spot of arc burning on deion plate from *Fe*, is equal [3.7, p. 354]:

$$t_{cr} = \frac{r^2_{cr}}{4 \cdot a_l} = \frac{(10 \cdot 10^{-4}\ cm)^2}{4 \cdot 0{,}07\ cm^2/s} = 3{,}57 \cdot 10^{-6}\ s,$$

where $r_{cr} = 10 \cdot 10^{-4}$ *cm* – the greatest value of radius of microcraters on a surface of plate from steel 08 and $a_l = 0{,}07$ cm^2/s – temperature conductivity coefficient of liquid *Fe* [3.7, table 7.2, p. 123].

From the presented results of calculations follows that under influence of power density on a base spot of arc $q_{bs.act} \simeq 10^5$ W/cm^2, a thin layer of liquid metal are formed on it, and process of superficial bubble boilings with formation of craters is quite possible. In fig. 3.7 one can see the electron-microscopic photos of fragments of erosion of deion plates from fig. 3.5. After triple influence of arc discharge erosion of plate is characterised by deep damage in a form of the truncated ***cones of erosion*** with difficult topology with diameters 90 μs, microcraters with diameters upto 20 μs and presence of a great number of microdrops on their surface.

Presence of microwaves on internal surfaces of erosion cones and craters and numerous spherical particles of products of erosion with diameters $1 \div 5$ μm, confirms their formation as a result of explosive processes in microbubbles on boiling liquid-melt and is their specific feature.

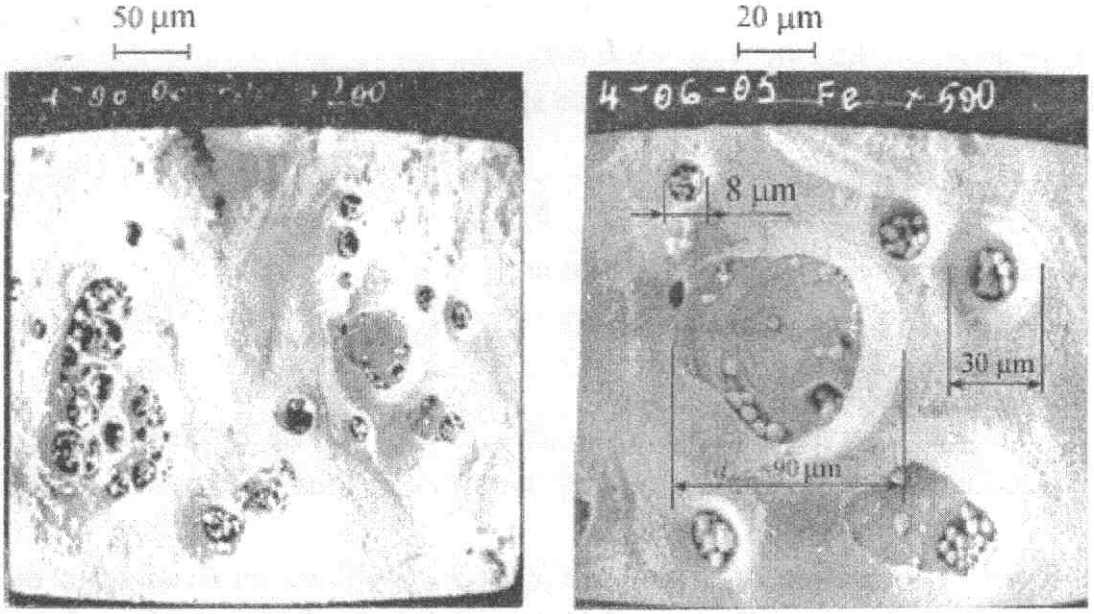

Fig. 3.7. Fragments of erosion of deion plate from fig. 3.5: a – ×200; b – ×500. $I_{arc.max}$=79,3 кА

A mass of new plate $M_{d.pl}$, shown in fig. 3.5, is equal 51,6 *g*. After triple switching-off of short-circuit current a mass of deion plate $M_{d.pl.er}$ was equal to 47,7 *g*. Hence, ablation of metal mass of deion plate after single switching-off of short-circuit current was equal to:

$$\Delta M_{er.d.pl} = \frac{M_{d.pl} - M_{d.pl.er}}{3} = \frac{51{,}6\ g - 47{,}7\ g}{3} = 1{,}3\ g.$$

Let us define electro- and thermophysical properties of short constricted arc in one gap of arc chute with distance between deion plates 5 *mm* at current switching-off $i_{arc.max}$=79,3 *кА*. In fig. 3.6 it is shown that time of arc quenching $t_{arc.ext}$ in a phase A is equal to 5,8 *ms*. This time is combined from time of arc immobility on contacts $t_{im.arc}$=1,8 *ms* and time of arc standing in arc chute $t_{arc.ch}$=4,0 *ms*. As a current in process of arc extinguishing was changed, we will divide $t_{arc.ch}$ into intervals Δt=0,5·10^{-3} *s* and we will define an average value of arc current i_{∂} for each interval Δt (table 3.3). We will accept that voltage in electrode area for Fe is equal to [3.6, part II, fig. 5.47]:

$$\Delta U_{el} = \frac{U_{av.(c+a)}}{2} = \frac{23{,}75V}{2} = 11{,}87\ V.$$

Approximately we will define that specific conductivity of plasma is equal to by the formula:

$$\sigma = \frac{i_{arc} \cdot l}{S_{bs.act} \cdot \Delta U_{el}},$$

where i_{arc} – in *A*; l = 0,5 *cm*, $S_{bs.act}$ = 9,0 *cm*^{2}.

Average density of current in a base spot:

$$j_{bs} = \frac{i_{arc}}{S_{bs.act}}.$$

Excess pressure in electrode area of arc:

$$P_{arc} = 9{,}87 \cdot 10^{-9} \cdot j_{bs} \cdot i_{arc}\ , atm,$$

where $j_{bs} - A/cm^2$ and $i_{arc} - A$.

Effective temperature in electrode area of arc will be estimated according to specific conductivity σ at pressure P_{arc} by means of graphs [3.6, part I, fig. П.3.2, p. 335].

Degree of ionisation of steams *Fe* x_e at P_{arc} will be received from data presented in [3.6, part I, Appendix 1, p. 325]. We will define concentration of neutral atoms in steams *Fe* n_0 by the formula:

$$n_0 = n_{boil} \cdot \frac{T_{boil} \cdot P_{arc}}{T_{ef} \cdot P_0}$$

with using of pressure-temperature saturation curve [3.6, part I, fig. 1.5, p. 71, table 1.8, p. 69]. Concentration of electrons is equal:

$$n_e = n_0 \frac{\tilde{o}_{\mathring{a}}}{1 + \tilde{o}_{\mathring{a}}}.$$

The directed velocity of electrons:

$$\upsilon_e = 0{,}593 \cdot 10^8 \cdot \sqrt{\Delta U} = 0{,}593 \cdot 10^8 \cdot \sqrt{36\,V} = 3{,}56 \cdot 10^8\ cm/s,$$

where $\Delta U = 36\ V$ – voltage on arc at gap between electrodes 5 *mm* [3.6, part I, fig. 5.47].

Results of calculations of plasma parametres in a channel of short constricted arc in one interval of deion chute at current switching-off $i_{arc.max}$ = 79,3 *кА* are given in table 3.3.

Let us estimate electric parametres of microjets of plasma flowing out from craters which are formed on a liquid-melt of base spot of arc.

The current arising as a result of explosion of microbubble and flowing through a crater i_{cr}:

$$i_{cr} = j_b \cdot S_{cr},$$

where we will accept an initial average square of microcraters $S_{cr} = \pi \cdot r_{cr}^2 = \pi \cdot (4 \cdot 10^{-4}\ cm)^2 = 50{,}2 \cdot 10^{-8}\ cm^2$ from which the erosion cones are formed as a result of explosions of microbubbles (fig. 3.7, b).

Current density in a plasma microjet:

$$j_{pl} = 3{,}34 \cdot 10^{-10} \cdot e \cdot n_e \cdot \upsilon_e\ A/cm^2,$$

where $e = 4{,}8 \cdot 10^{-10}$ CGS units – a charge of electron; n_e – concentration of electrons, cm $^{-3}$ and $\upsilon_å$ – their velocity, *cm/s.*

Power density coming on one crater:

$$q_{cr} = \frac{i_{cr} \cdot \Delta U_{el}}{S_{cr}} W/cm^2,$$

where $i_{cr} - A$, $\Delta U_{el} - V$, $S_{cr} - cm^2$.

Excess pressure in a microjet of plasma, which are thrown up from a blowing up microbubble:

$$P_{mpl} = 9{,}87 \cdot 10^{-9} \cdot j_b \cdot i_c\ atm.$$

On a base spot of arc n_{cr} craters functions simultaneously:

$$n_{cr} = \frac{i_{arc}}{i_{cr}}.$$

Time of functioning cycle of a microbubble will be accepted equal to:

$$t_{cyc} \simeq \frac{r_{cr}^2}{4 \cdot a} = \frac{(4 \cdot 10^{-4})^2}{4 \cdot 0{,}07\ cm^2/s} = 5{,}71 \cdot 10^{-7}\ s,$$

where $r_{cr} = 4 \cdot 10^{-4}\ cm$ – average value of initial radius of a microcrater, a = 0,07 cm^2/s - temperature conductivity coefficient of liquid *Fe*. For time interval $\Delta t = 0{,}5 \cdot 10^{-3}\ s$ on one place n_{cyc} functioning cycles of microbubbles can repeat:

$$n_{cyc} = \frac{\Delta t}{t_{cyc}} = \frac{0{,}5 \cdot 10^{-3}\ s}{5{,}71 \cdot 10^{-7}\ s} = 876.$$

Number $N_{\Delta t}$ of the blown up microbubbles on a base spot of arc during time $\Delta t = 0{,}5 \cdot 10^{-3}\ s$ is equal to:

$$N_{\Delta t} = n_{cyc} \cdot n_{cr} = 876 \cdot n_{cr}.$$

Table 3.3. Electro - and thermophysical characteristics of short constricted arc in one gap of a chute with distance between deion plates 5 *mm* at current switching-off $i_{arc.max}$=79,3 кА and plasma microjets

Δt, 10^{-3}, s	0,5	1,0	1,5	2,0	2,5	3,0	3,5	4,0
I_{arc}, кА	68	79,3	68	62	54	44	24	8
σ, $(Ohm \cdot cm)^{-1}$	102	119	102	93	81	66	36	12
J_{bs}, 10^3, A/cm^2	7,56	8,81	7,56	6,89	6,0	4,89	2,67	0,89
P_{arc}, atm	5,07	6,90	5,07	4,22	3,2	2,12	0,63	0,07
T_{ef}, K	14000	14500	14000	12800	11400	9800	7600	6000
x_e	0,9	0,9	0,9	0,84	0,72	0,43	0,13	0,024
n_0, 10^{18}, cm^{-3}	4,61	5,8	4,61	4,34	3,92	3,38	2,28	1,9
n_e, 10^{18}, cm^{-3}	2,18	2,75	2,18	1,98	1,64	1,02	0,26	0,045
J_{pl}, 10^8, A/cm^2	1,092	1,377	1,092	0,991	0,821	0,511	0,130	0,023
i_c, A	54,8	69,1	54,8	49,7	41,2	25,6	0,65	0,11
q_{cr}, 10^8, W/cm^2	12,9	16,3	12,0	11,7	9,7	6,0	0,15	0,026
P_{mpl}, atm	58,7	93,9	58,7	48,3	33,2	12,8	0,08	0,002
n_{cr}	1241	1147	1241	1247	1311	1719	-	-
$N_{\Delta t}$, 10^4	108,71	100,48	108,71	109,24	114,84	150,58	-	-
$\Sigma N_{\Delta t}$, 10^4	692						-	-

Results of calculations are summarized in the table 3.3. From data of table 3.3 it is visible that, for example, power density q_{cr}, coming on a crater and exceeding 10^8 W/cm^2, may lead to explosion of microbubble a crater.

At definition of total number of erosion cones which are formed in process of arc extinguishing on one deion plate, only those cones in which power density q_{cr} excessed 10^8 W/cm^2.

Total number of erosion cones on both sides of deion plate is equal to:

$$2\sum N_{\Delta t} = 2 \cdot 692 \cdot 10^4 = 1384 \cdot 10^4.$$

Volume of a cone is equal:

$$V_{cone} = \frac{1}{3} \cdot \pi \cdot R_{cone}^2 \cdot h = \frac{1}{3} \cdot \pi \cdot \left(45 \cdot 10^{-4}\ cm\right)^2 \cdot 8 \cdot 10^{-4}\ cm = 1{,}7 \cdot 10^{-8}\ cm^3,$$

where $R_{cone} = 45 \cdot 10^{-4}$ cm and $h = d_{cone} = 8 \cdot 10^{-4}$ cm (fig. 3.7).

Mass of singular erosion cone of liquid Fe at temperature of its boiling is equal:

$$m_{er.cone} = \rho_l \cdot V_{cone} = 6{,}863\ g/cm^3 \cdot 1{,}7 \cdot 10^{-8}\ cm^3 = 11{,}67 \cdot 10^{-8}\ g,$$

where $\rho_l = 6{,}863$ g/cm^3 – density of liquid iron at boiling temperature [3.6, part I, table 1.8, p. 69 and fig. 1.5, p. 71].

Mass of entrained metal from a surface of deion plate at single switching-off of short-circuit current is equal:

$$M_{d.pl.er} = m_{er,cone} \cdot 2 \cdot \sum N_{\Delta t} = 11{,}67 \cdot 10^{-8}\ g \cdot 1384 \cdot 10^4 = 1{,}61\ g.$$

According to experimental data, mass of entrained metal of deion plate at single switching-off of a current $i_{arc.max} = 79{,}3$ κA is equal to 1,3 g. Calculated value of mass of entrained metal coincide with experimental data well adequately. Calculating error is quite comprehensible to engineering practice.

Repeated tests of breakers of different types and manufacturers for short-circuit breaking capacity, equipped with arc chutes in which gaps between plates are accepted equal 3÷5 mm, have shown that plates are subjected to strong melting with their partial burning out (fig. 3.5) and distortion. On a surface of deion plates the flows of liquid metal are formed which quite often lead to their shorting.

3.5.2. Discrete damage of plates

In [3.6, part I, fig. 21, p. 40] arc chamber of breakers rated current 4000 and 6300A is shown in which short-circuit breaking capacity at rated voltage 380 V is equal to 65 and 115 κA (r.m.s.) respectively. In fig. 1.18 oscillogram of current and voltage is given at current switching-off in loop 65 κA at operation "OPEN". Maximal instantaneous current of arc appeared in phase B and was equal $i_{arc.max} = 79{,}4$ κA.

In fig. 1.19 deion plates are shown after switching-off of current 65 κA in a mode O-CO-CO. A gap between deion plates in a chute was 17 mm, arc completely entered into a chute and got a diffuse form with a split core. Discrete erosive traces of arc are distributed in regular intervals on all area of plates. Erosion of plates has appeared superficial and insignificant, practically without loss of its mass.

In a case of diffuse arc with a split core the discrete traces of erosion settle down enough uniformly on all surface of deion plates. Their similar distribution causes electric field which is enough homogeneous in a gap between deion plates, having a squared shape and rather big square. In that case electric field promotes uniform distribution of lines of a current on all area of electrode, and its edge distortions practically do not influence their distribution. If deion plates have rather small area and, especially, if they have cuts the edge distortions of a field concentrate current lines on their edges, raising local density of a current. The increase of current density on the edges of deion plates leads to their more intensive erosion.

In fig. 1.21 we can see electron-microscopic photos of separate zones of erosion from fig. 1.19.

Comparing images of erosive traces of arc in fig. 3.27,b and in fig. 1.21,b and c at the same increase ($\times 500$) and value of current $i_{arc.max} \simeq 79{,}0$ κA, essential differences are visible between them. First, at distances between deion plates $l = 3 \div 5$ *mm* (short constricted arc) a deep depth of damage and erosion cones are observed, and at distances $l = 17$ *mm* (diffuse arc with split core) - superficial damage and craters. Secondly, at $l = 3 \div 5$ *mm* diameter of erosion cones reaches 90 μm, and at $l = 17$ *mm* diameters of craters do not exceed 15 μm. Thirdly, at $l = 17$ *mm* on a surface of erosion the drops of erosion products are absent practically, and at $l = 3 \div 5$ *mm* a considerable quantity of drop-shaped particles are observed.

By the results of calculations of parametres of plasma microjets flowing out from craters on a base spot of a plasma discrete jet on the anode of diffuse arc with a split core, a current density is equal to $j_a = 9{,}63 \cdot 10^6$ A/cm^2, a current $i_a = 3{,}7$ A and exsess pressure $P_{cone} = 0{,}35$ *atm* (see paragraph 1.4).

Obviously, exsess pressure in plasma microjet, flowing out from a microbubble, equal 0,35 *atm* cannot lead to formation of erosion cone on a base spot at explosion of a microbubble and, hence, to considerable damage of a surface of deion plates.

Thus, a short constricted arc causes deep erosive damage of deion plates with continuous melt of their surface and ablation of considerable mass of metal. On a surface of base spot of arc the craters are formed in the form of cones with a diameter up to 90 μm and mass of metal particles of a spherical form with diameters ~ 1,0 ÷ 5,0 μm.

A diffuse arc with a split core causes superficial discrete erosive damage of deion plates. On a surface of base spots of plasma discrete jets the craters are observed with a diameter up to 15 μm with equal oval edges. Metal particles of erosion of deion plates are absent on their surface.

Conclusions to chapter 3

The carried out experimental and theoretical researches of erosion of argentiferous contacts and deion plates of arc chutes of low-voltage automatic circuit breakers at switching-off of short-circuit currents and the published works of some authors give a possibility to draw following conclusions.

3.1. Erosion of opening contacts is compose from bridge, steam and metal-liquid fractions.

3.2. A metal-liquid bridge can be destroyed or by quiet evaporation, or with a burst:

- at $\frac{\Delta Q_{bs.br}}{S_{bs.br}} = \frac{\Delta Q_{ch}}{S_{lat}} \leq 300 W \cdot s / cm^2$ – a bridge evaporates;
- at $\frac{\Delta Q_{bs.br}}{S_{bs.br}} = \frac{\Delta Q_{ch}}{S_{lat}} \geq 3000 W \cdot s / cm^2$ – a bridge blows up.

3.3. A steam fraction of erosion of contacts is equal $n \cdot 10^{-3} g$:

- for the cathode n – tens of units;
- for the anode n – hundreds of units.

3.4. The metal-liquid fraction of erosion of contacts is equal to units of grammes.

3.5. A steam fraction of erosion of contacts can be equal up to 15% of total mass of its erosion.

3.6. Base part of erosion of the cathode is composed by steam fraction which can reach 90 % of total mass of its erosion.

3.7. Basic form of erosion of the anode is composed by erosion cones and its metal-liquid fraction can reach 92 % of total mass of anode erosion.

3.8. Short constricted arc causes deep erosive damage of deion plates of arc chute in the form of erosion cones with ablation of considerable part of its mass.

3.9. Diffuse arc with a split core causes superficial discrete insignificant erosive damage of deion plates.

Reference index to chapter 3

3.1. *Rahovski V.I., Levchenko G.V., Teodorovich O.K.* Arcing tips of electrical devices. – M.; L.: Energy, 1966 [rus].

3.2. *Ryvkin A.M.* Wear of high-current contacts under influence of rupturing arc of alternating current // Electricity. – 1971. – №8 [rus].

3.3. *Belkin G.S.* Calculation methods of value of erosion of high-current contacts under influence of electric arc // Electricity. – 1972. – №1 [rus].

3.4. *Butkevich G.V., Belkin G.S., Vedeshenkov N.A., Zhavoronkov M.A.* Electric erosion of high-current of contacts and electrodes. – M.: Energy, 1978 [rus].

3.5. *Zhavoronkov M.A., Nesterov G.G., Taiver E.I.* Estimation of coefficient of emission at calculation of erosion of high-current contacts. // Izvestia vuzov. Electromechanics. – 1981. – №10 [rus].

3.6. *Mestcheryakov V.P.* Electric arc of high power in circuit breakers. – Ulyanovsk; part I, 2006; part II, 2008 [rus].

3.7. *Mesyats G.A.* Ectons in vacuum discharge: breakdown, spark, arc. – M.: Science, 2000 [rus].

3.8. *Polezhaev Y.V., Yurevich F.B..* Thermal protection. – M.: Energy, 1976 [rus].

3.9. Physical quantities: reference book / *Edited by I.S. Grigorieva, E.Z. Meilikhova* – M.: Energoatomizdat, 1991 [rus].

Addendam

To a question about choice of silver-containing contacts for automatic circuit breakers

The choice of the necessary contact material for circuit breakers with the set electric and mechanical characteristics is a difficult task. For estimation of possibility and frontiers of application of the chosen material as electric contact, at first, certain knowledge of bases of physics of solid body, metallurgical science and arc discharge are required. Secondly, a solving of this task is complicated by absence of the exhaustive data about characteristics of these materials in catalogues and specifications for contacts, and also in the published works on influence research on contact materials of mechanical and thermal loads of arc discharge of different power. For example, at definition of time of achievement of a liquid-melt on a base spot of arc of switching-off of temperature of fusion and boiling it is necessary to know a data about values for contact materials: $\lambda -$ factor of heat conductivity, $c -$ specific thermal capacity and $\rho -$ density at these temperatures. This data is absent at temperature of boiling for Ag, Cu, Ni, Fe and other metals. For Ag and Ni, for example, PT - diagrammes with the account of their condition in a steam phase are absent also.

For ceramic-metal composite contacts in specification a data of density and specific electric resistance only for normal conditions of atmosphthere are given. Such data as factor of heat conductivity and hardness on Brinellju in specification are not given practically.

Now there is enough great number of modifications of the composite contacts consisting of two, three and more components. Their properties have been studied experimentally. According to these the recommendations about their application were developed. Existing composite contacts are applied in a wide range of rated currents of breakers, up to 10 000 A.

However investigations of processes of arc extinguishing of many authors in a wide range of currents have shown two their lacks at least:

- long arc immovability on opening contacts;
- graphite application leads to decreasing of erosion resistance of contacts, recovery rate of electric strength of intercontact gap after arc extinction in no-

- current condition at current transition through a zero and electric resistance of isolation of circuit breaker poles at its opened contacts after repeated switching-off of rated currents and short-circuit currents.

Contact materials for automatic circuit breakers should possess:

- high electric conductivity;
- high erosion resistance;
- low hardness;
- high heat conductivity;
- low temperature of fusion and boiling;
- high voltage to welding;
- low electronic work function;
- ability to fast recovery of electrical strength of intercontact gap;
- ability to provide with a great velocity of expansion of arc base spots and its moving on contacts.

However mechanical and heat- and electrophysical properties of components of contacts and their steams are often included into contradictions that essentially complicates a choice of existing contact materials and analytical search of their combinations in projected composite contacts with defined properties. The general laws of mutual influence of components are looked through more or less for the composite contacts consisting of two components which, as a rule, have opposite properties.

A.1 Contact transition resistance

Summarily let us state the substantive provisions defining contact transition resistance.

Inclusion of contact connection of a breaker in electric circuit causes introduction of additional transition resistance R_{cont} in it, on which, as a result of current flow, a voltage drop arires u_{cont} equal [1]:

$$u_{cont} = I \cdot R_{cont} = \frac{I \cdot \rho}{2 \cdot a},$$

where $R_{cont} = \frac{\rho}{2a}$ – contact transition resistance, *Ohm*; ρ – specific resistance of contacts metal, *Ohm ·cm*; a – radius of a circular spot of contacting, *cm*.

Current density of spot of contacting is distributed non-uniformly on its area and defined under a law:

$$j(r) = \frac{I}{2 \cdot \pi \cdot \grave{a} \cdot \sqrt{a^2 - r^2}}.$$

Here r – distance from the centre of spot. According to this law a maximum density of current is observed on spot`s periphery.

For contacts, having a form of hemispheres and a hemisphere-plane, value of radius of contacting spot it is possible to define precisely enough under the formula:

$$a = \sqrt[3]{\frac{3}{4} \cdot P_{cont} \cdot \left(\frac{1-\sigma_1^2}{E_1} + \frac{1-\sigma_2^2}{E_2} \right) \cdot \left(\frac{1}{r_1} + \frac{1}{r_2} \right)^{-1}},$$

where P_{cont} – contact force, *kg*; $\sigma_{1,2}$ – Poisson's constant of both contacts; $E_{1,2}$ – Young's modulus of both contacts, *kg/cm²*; $r_{1,2}$ – contacts curve radius, *cm*.

For pair contacts Ni - Ni and Cu - Cu, for which Poisson's constant ≈ 0,3, having a form sphere-plane:

$$a = 1{,}11 \cdot \sqrt[3]{\frac{P_{cont} \cdot r}{E}}.$$

For pair contacts Ag – Ag, for which $r_1 = r, r_2 = \infty$, (plane), $E_1 = E_2 = E$ and $\sigma_1 = \sigma_2 = 0{,}4$ formula, defining transition resistance, becomes:

$$R_{cont} = 0{,}58\rho \cdot \sqrt[3]{\frac{E}{P_{cont} \cdot r}}.$$

As a result of increasing of temperature in a field of current constriction an increasing of transition resistance R_{cont} is defined from ratio:

$$\frac{R_{cont}(T_0)}{R_{cont}(T_{\max})} = \frac{\alpha}{\varepsilon} \cdot \frac{2}{u_{cont}} \cdot \sqrt{\frac{\rho_0 \cdot \lambda_0}{\varepsilon}} \cdot arctg\left(\frac{u_{cont}}{2} \cdot \sqrt{\frac{\varepsilon}{\rho_0 \cdot \lambda_0}} \right) + \frac{\beta}{\varepsilon},$$

where $R_{cont}(T_0)$ – transition resistance without heating, *Ohm*; $R_{cont}(T_{\max})$ – transition resistance at hot test, *Ohm*; u_{cont} – contact voltage, *V*; ρ_0 – specific resistance of contact metal at temperature T_0, *Ohm·cm*; λ_0 – factor of heat conductivity of contact metal at temperature T_0, *W/(cm·K)*; α – temperature factor of specific resistance at temperature T_0, *1/K*; β – temperature factor of heat conductivity at temperature T_0, *1/K*; ε – it is defined from expression:

$$\rho \cdot \lambda = \rho_0 \cdot \lambda_0 [1 + \varepsilon (T_{\max} - T_0)] \approx \alpha + \beta.$$

Processes of deformation of contacts are very difficult, as plastic metal not only spreads in sides but deforms also in depth. After repeated mechanical impacts of contacts their surface is strengthened and it occurs so-called «hardening». In that case a facial layer of contacts gets higher hardness H.

Relation of contact force with an area of a contact spot is expressed by formula:

$$P_{cont} = \pi \cdot a^2 \cdot H,$$

где H – «contact hardness» of metal contacts, *kg/cm²*. From the last formula it follows that $a = \sqrt{\frac{P_{cont}}{\pi \cdot H}}$.

«Contact hardness» is not equivalent the technological one. But it differs a little from Brinnel hardness H_B. Therefore in practical engineering calculations it is possible to use values H_B. Transition resistance of contacts, having the same metal, can be defined with help of formula received experimentally:

$$R_{cont} = 0{,}89\rho \cdot \sqrt{\frac{H_B}{P_{cont}}}. \qquad (1.1)$$

If contacts are made from diverse metals with sufficient accuracy for calculations it is possible to accept the formula:

$$R_{cont} = \frac{\rho_1 + \rho_2}{2} \cdot \sqrt{\frac{H_B}{P_{cont}}},$$

where $\rho_{1,2}$ – specific resistance of contact metals, *Ohm·cm* and H_B – hardness of more soft contact metal, *kg/cm²*.

Dependence of maximum temperature of area of current constriction and voltage drop u_{cont} is expressed by equality:

$$L \cdot (T_{\max}^2 - T_0^2) = \frac{u_{cont}^2}{4},$$

where $L \approx 3 \cdot 10^{-8} (B/K)^2$ – Lorentz coefficient for Ag, not dependent on temperature up to temperature of its boiling.

For liquid Ag a maximum temperature in the field of current consriction can be defined with accuracy ±10 % from the formula:

$$T_{\max} \approx 3100 \cdot u_{cont}.$$

Thus, ultimate value of transition voltage drop, at which fusion Ag occurs, equals:

$$u_{cont} = \frac{T_{melt}}{3100} = \frac{1285K}{3100} = 0{,}41V.$$

This voltage defines the tendency of contacts to welding. Basically welding of contacts of circuit breakers it is observed at flowing of short-circuit current through them. In that case it is necessary to define u_{cont} from the formula:

$$u_{cont} = i_{ic} \cdot R_{cont} = i_{ic} \cdot \frac{\rho}{2a} = i_{ic} \cdot \frac{\rho}{2} \cdot \sqrt{\frac{P_{cont}}{\pi \cdot H_B}}. \qquad (1.2)$$

where $i_{ic} = K\sqrt{2} \cdot I$ – initial fault current at presence of aperiodic component, *A*; K – impact factor, which depends on $\cos\varphi$ of electrical circuit, and I – r.m.s. value of steady-state short-circuit current, *A*.

Table 1. Dependance of coefficient $\sqrt{2}$ K on $\cos\varphi$

$\cos\varphi$	0	0,10	0,15	0,2	0,25	0,30	0,40	0,50	0,60	0,80	1,0
$\sqrt{2}K$	2,83	2,44	2,30	2,17	2,06	1,96	1,80	1,68	1,58	1,45	1,41

Welding of argentiferous contacts, for example, at $i_{ic} = 100\kappa A$ can occur if transition resistance in one a-spot will equal to:

$$R_{cont} = \frac{u_{cont}}{i_{ic}} = \frac{0.41V}{10^5 A} = 4{,}1 \cdot 10^{-6} Ohm = 4{,}1\ \mu Ohm. \qquad (1.3)$$

Here it is necessary to have in mind that transition resistance in a current carrying chain of breaker`s pole makes only its part. In table 2 one can see resistances of poles depending on rated current of breakers of different manufacturers.

For decreasing of transition resistance R_{cont} (formula 1.1) and voltage u_{cont} (formula 1.2) in one a-spot it is obviously necessary to reduce specific resistance ρ and contact hardness H_B of contacts material and to create sufficient contact force P_{cont}.

For purpose of decreasing of influence of transition resistance R_{cont} in one a-spot on resistance of a pole it is necessary to divide one contact into several parallel ones.

Thus it is necessary to have in mind that at switching-on of contacts their vibration (bouncing) occurs. At that contact rebound can occur. Experimentally it has been established that for elimination of bouncing of contacts with their rebound it is necessary to create contact force $P_{cont} \geq 5 \div 7\ kgf$ on each contact.

In zone of a-spot a current constriction occurs. At that electrodynamic force of rebound of contacts arises which is equal to [2]:

$$F = 1{,}08 \cdot 10^{-8} \cdot i^2 \ln\left(\frac{S_{cont}}{S_a}\right)^{\frac{1}{2}}, kgf, \qquad (1.4)$$

where i – instantaneous current, A; $S_{cont} = \pi R^2$ – area of contact, cm^2; $S_a = \pi a^2$ – effective area of contacting, cm^2.

Table 2. Resistance of poles in μOhm depending on rated current of breaker

Rated current, A	100	160	250	400	600	1000	1600	2500	4000	6300
Circuit breaker XS of standard series. Terasaki	1030	720	420	180	190	53				
Circuit breakers Masterpact NT and NW. Merlin Gerin							26		8	5
Circuit breakers AE of standard series SS. Mitsubishi Electric						26	16	8	9	8,5

By means of calculations from formulas (1.3) and (1.4) it is necessary to exclude possibility thermal welding and electrodynamic rebounds of closed contacts at flowing of initial fault current i_{ic} through them.

A.2 Power balance of arc on contacts and their erosion

An equation of power balance of system "contacts-arc" during arc immovability on opening contacts looks like [3]:

$$\Delta W_{arc} = \Delta Q_{cont} + \Delta Q_{ch},$$

where $\Delta Q_{con} = \eta_{el} \cdot \Delta W_{arc} = \frac{U_c + U_a}{u_{arc}} \cdot \Delta W_{arc}$ – energy of arc absorbed by contacts for the account of electrode phenomena, and ΔQ_{ch} – energy of arc channel.

A part of energy of short constricted arc, which are on opening contacts in motionless position and absorbed by them, can be equal from 75 to 45 %. This part of energy can be estimated by means of geometrical factor of arc energy distribution for the account of heat dissipation between contacts and arc channel:

$$\eta_g = 1 - \frac{\delta}{r_{bs} + \delta},$$

where r_{bs} – radius of arc base spot on contacts and δ – contact gap. Ratio $\frac{\delta}{r_{bs} + \delta}$ defines energy of arc channel which are in motionless position.

Energy of channel ΔQ_{ch} of short constricted arc dissipates in environment by fluxes of plasma and radiation.

According to classical theory of heat conductivity, uniformity of temperature distribution between external and inside layers of a body of contact is defined by Biot criterion:

$$Bi = \frac{q \cdot h}{\lambda \cdot T_d},$$

where $q = \frac{\eta \cdot i_{arc} \cdot u_{arc}}{2S_{bs}}$ – surface density of a thermal flux (power density), W/cm^2; coming on a base spot of arc area S_{bs}, $см^2$; h – thickness of contact tip, cm; λ – factor of heat conductivity of metal, $erg/(s \cdot cm \cdot K)$; T_d – the temperature of destruction equal to temperature of fusion or boiling of a fusible component of contact, K.

As calculations show, at standing of arc on opening contacts in motionless position criterion of Bio $Bi >> 1$. It means that heat, applied to contacts, warms up only their top layer and does not get into a body of contacts. At switching-off of short-circuit currents a power density, coming on a base spot, equals $10^4 \div 10^5$ W/cm^2. At power density 10^5 W/cm^2 on a base spot surface bubble boiling proceeds. At explosion of microbubbles erosion cones are formed. Sum of their elementary weights is a basic component of contacts erosion. The internal part of a body of contact gets warm only due to Joule heat generated in a body of contact at current flowing ($i^2 \cdot r$).

Experimental data and calculations of arc current i_{arc} during its extinguishing show that during arc standing on opening contacts in motionless position because of its low voltage u_{arc} as regard to voltage of circuit $U_{\tilde{n}}$, arc current i_{arc} differs a little from an expected current of circuit $i_{\exp}$. Therefore, for preliminary estimation of possible erosion of contacts, at working out of new designs of circuit breakers, it is possible to take advantage of the simplified design procedure of contacts erosion. A current half wave during opening contacts can be divided into intervals of time Δt and to define:

- i_{arc} – average value of a current during interval of time Δt;
- $n_{cr} = i_{arc} / i_{cr}$ – number of simultaneously functioning craters (cones of erosion) on arc base spot; $i_{cr} = 280$ A –average current of plasma jet flowing through one crater on base spot of short constricted arc at switching-off of short-circuit current;
- $n_{cyc} = \Delta t / t_{cyc}$ – number of cycles of functioning craters on base spot which can arise on one place during interval of time Δt, $t_{cyc} = 5{,}6 \cdot 10^{-8} s$ – duration of functioning of one crater on a surface of contact from Ag;
- $N_{\Delta t} = n_{cr} \cdot n_{cyc}$ – number of erosion cones on arc base spot arising during Δt;

- $\sum N_{\Delta t} = \dfrac{N_{\Delta t} \cdot t_{st}}{\Delta t}$ – total number of erosion cones on base spot during arc standing on contacts t_{st} which can be defined from oscillogram of a current and voltage of arc or to accept its value equal 5,45 ms - average time of arc immovability on contacts;

- $M_{er.cont} = m_{c.er} \sum N_{\Delta t}$ – mass of contact erosion at one switching-off of short-circuit current; $m_{c.er} = 9{,}9 \cdot 10^{-8} g$ – average elementary mass of liquid Ag in erosion cone;

- $\Delta = M_{er.cont} / (\rho \cdot S_{bs})$ – thickness of a layer of solid Ag carried away from area of arc base spot: $S_{bs} = i_{arc} / j_{bs}$ – average area of arc base spot; $j_{bs} = 10^4 A / cm^2$ – average density of current in arc base spot on contacts at flowing of short-circuit current; $\rho = 10{,}5 g / cm^3$ – density of solid Ag at normal conditions.

Values: $i_{cr} = 280 A$; $t_{cyc} = 5{,}6 \cdot 10^{-8} s$; $m_{c.er} = 9{,}9 \cdot 10^{-8} g$; $j_{bs} = 10^4 A$ are received by or calculated path or experimentally [3].

For decreasing erosion of contacts it is necessary to give them velocity of opening not less than 6,5 *m/s*. At such velocity of contact opening a time of arc immovability will equal $t_{im} \simeq 1{,}0$ ms, instead of 5,45 ms, equal to average time of arc immovability at contacts opening with velocity 1,5 – 2,0 m/s.

A part of metal steams of contacts at switching-off of short-circuit currents is small at their electric wear. Therefore there is no necessity to accept it at calculation of erosion of contacts.

Inclusion of components in composite contacts, which have a temperature of boiling and ionisation potential higher and factor of heat conductivity lower than Ag has, will lead to more high temperature on base spot and in arc channel. It, in turn, will cause increasing in electric erosion of contacts. For example, current density in freely burning arc on electrodes Cu - Cu equals (1,0 – 1,6) · 10^3 A/cm^2, Ni – Ni – (1,6 -2,0) · 10^3 A/cm^2 , Zn – Zn- (3,3 – 3,8) · 10^3 A/cm^2.

It is necessary to have in mind also that decreasing of density (increasing of porosity) ceramic-metal contacts can lead to considerable decreasing of heat conductivity factor.

Inclusion of ≈ 5 % Cs in copper contacts reduces a voltage drop on arc by ≈ 25 %. It leads to decreasing of power density on base spot and reduces erosion of contacts [4] correspondingly.

A.3 Recovery electric strength of arc gap

Heat- and electrophysical properties of contacts metal and their steams influence recovery electric strength of arc channel essentially.

As a result of electric breakdowns between contacts repeated ignitions of arc arise at no-current condition at free transition of a current through a zero, at exit of arc on horns and at input in arc chute.

In the published works recovery electric strength is considered in short and long disconnecting intervals. At short intervals recovery electric strength after current transition through a zero in disconnecting gap occurs in thin gas layer adjoining a surface of the cathode and on its surface. Thus it means that emission of electrons can occur as under influence of high temperature of a surface of the cathode (thermoionic emission) and as under influence of high field density (autoelectronic emission). Only thermionic emission is possible in a low-voltage arc of switching-off.

In fig. A.1 change of voltage of breakdown at two values of gap between electrodes and of recovering voltage in time is schematically shown [5].

From fig. A.1 it is visible that at a short gap ($\delta_1 < \delta_2$) electric strength of a disconnecting interval grows faster than at more long one at which breakdown occurs (point *a*).

It is recognised that more high electric strength of short arc intervals than long ones is provided for due to rejection of greater quantity of energy generated in a gap between contacts in electrodes than in arc channel. A part of energy, taken away in electrodes due to heat dissipation, is defined by the formula [3]:

$$\eta_g = 1 - \frac{\delta}{r_{bs} + \delta},$$

where η_g – geometrical factor defining a part of energy, generated in arc interval, taken away in both electrodes, δ – contact gap, r_{bs} – radius of base spot of arc or re-

sidual plasma of its channel and the ratio $\delta/(r_{bs}+\delta)$ – a part of energy which composes energy of arc channel or its residual plasma.

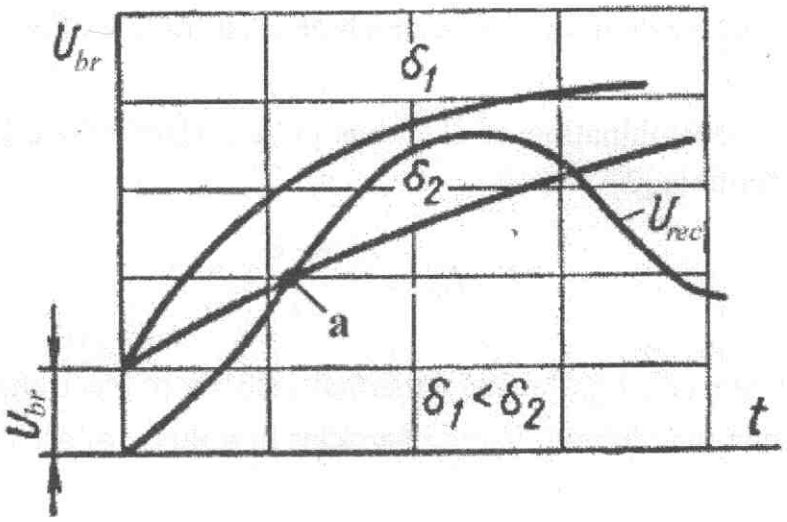

Fig. A.1. [5] Growth of electric strength in short gaps at various distances between electrodes

If, for example, to accept r_{bs} = 3,0 *mm* and for one case – δ = 1,0 *mm* and for other one – δ = 7,0 mm. than we get:

$$1)\ \eta_g = 1 - \frac{1{,}0\ mm}{3{,}0\ mm + 1{,}0\ mm} = 0{,}75;$$

$$2)\ \eta_g = 1 - \frac{7{,}0\ mm}{3{,}0\ mm + 7{,}0\ mm} = 0{,}3.$$

That is in the first case both contacts would absorb 75 % of the energy generated by arc, and in the second - only 30 %.

Really, the more gap between electrodes is, the more quantity of energy is absorbed by them. However it is necessary to notice that, the more energy will be absorbed by electrodes, the more there temperature of their surface will be. Ultimate temperature of heating of metal on base spot of arc is its temperature of boiling. At achievement by a layer of a liquid melt on base spot of temperature of boiling at continuation of energy income a base spot will extend and mass of its liquid melt will increase.

It is obvious that after a stopping of energy income process of plasma deionization proceeds for shorter time than its cooling. And cooling of liquid melt of metal on arc base spot after its extinction occurs for longer time than plasma cooling.

Therefore it is possible to accept that temperature of plasma in procces of its deionization is constant and equal to those which was before a stopping of energy income [6].

Process of plasma deionization occurs both on a surface of arc base spot and in its volume.

Time of full recombination of electrons on a surface of arc base spot can be defined from the formula [3]:

$$t_{rec.bs} = \frac{4 \cdot \delta}{\upsilon_e},$$

where δ – contact gap, *cm*; $\upsilon_{å}$ – average thermal velocity of electrons, *cm/s*.

Time of recombination of charged particles in volume of arc channel equals to [6]:

$$t_{rec.vol} \simeq \frac{1}{\beta \cdot n_{e.vol}},$$

where β – coefficient of recombination of steams of contact metal, cm^3/s; $n_{e.vol}$ – initial concentration of electrons in arc channel, cm^{-3}.

From the mentioned formulas it follows that time of recombination of electrons in both cases depends on temperature of steams of contacts metal of, as:

$$\upsilon_{å} = \left(\frac{3 \cdot \hat{E} \cdot \grave{O}}{m_{å}} \right)^{1/2}; \; n_{e.vol}(T, P) \text{ and } \beta(\grave{O}, Ð).$$

That is time of deionization of residual plasma in intercontact gap in no-current condition entirely depends on heat- and electrophysical properties of contacts metal and their steams. Therefore at a choice of contacts it is necessary to consider ability of their metals to recover electric strenghth of intercontact gap after arc extinction.

For an example we will accept that temperature of residual plasma, consisting of ionised steams *Ag*, equal 6800 *K* and its pressure *P* = 1,0 *atm*. In that case average thermal velocity of electronsis is equal to:

$$\upsilon_e = \left(\frac{3 \cdot 1{,}38 \cdot 10^{-16} \; erg/K \cdot 6800 \; K}{9{,}11 \cdot 10^{-28} \; g} \right)^{1/2} = 55{,}6 \cdot 10^6 \; cm/s.$$

Time of recombination of electrons on arc base spot at contact gap δ = 1,0 *mm* is equal to:

$$t_{r.bs} = \frac{4 \cdot 0{,}1\ cm}{55{,}6 \cdot 10^6\ cm/s} = 7{,}2 \cdot 10^{-9}\ s.$$

Time of recombination of charged particles in volume of channel of residual plasma is equal to:

$$t_{r.vol} \simeq \frac{1}{1{,}7 \cdot 10^{-9}\ cm^3/s \cdot 5{,}82 \cdot 10^{16}\ cm^{-3}} = 1{,}0 \cdot 10^{-8}\ s,$$

where $\beta = 1{,}7 \cdot 10^{-9}\ cm^3/s$ – coefficient of recombination of ionisied steams Ag [3] and $n_{eo} = 5{,}82 \cdot 10^{16}\ cm^3$ – initial concentration of electrons in ionisied steams Ag at $T =$ 6800 K and $P = 1{,}0\ atm$.

If contact gap equals to $\delta = 7{,}0\ mm$, we will have:

$$t_{r.bs} = \frac{4 \cdot 0{,}7\ cm}{55{,}6 \cdot 10^6\ cm/s} = 5{,}0 \cdot 10^{-8}\ s.$$

The mentioned results of calculations show that in discharge gap equaled 1,0 *mm* after stopping of energy supply a decay of residual plasma occurs at temperature 6800 K and pressure $P = 1{,}0\ atm$ as due to recombination of the charged particles on a surface of base spot as in its volume.

$$t_{r.bs} = 7{,}2 \cdot 10^{-9}\ s \simeq 1{,}0 \cdot 10^{-8}\ s = t_{r.vol}.$$

At simultaneous course of processes of recombination of the charged particles in a short disconnecting gap on arc base spot and in its volume of residual plasma time of its deionization will be $<5 \cdot 10^{-9}\ s$.

In rather long arc a decay of residual plasma occurs basically after stopping of energy supply at current transition through a zero due to recombination of the charged particles in plasma volume ($t_{r.vol} = 0{,}87 \cdot 10^{-8}\ s < 5{,}0 \cdot 10^{-8}\ s = t_{r.bs}$ [3, part II, p. 307]) and can be more long than after short arc extinction. Deionization time of relatively short disconnecting gap can be 10 times as less than relatively long one.

Hence, it is necessary to believe that higher electric strength of a short discharge gap is provided for higher velocity of its deionization instead of extraction of large quantity of energy by contacts.

However comparing calculated values of deionization time of residual plasma with recovering time of electric strength in contacts gap, received experimentally and shown in fig. A.2 [7], one can see their difference of values by severel digits. Such difference of deionization time of residual plasma in arc channel at current transition through a zero and recovering time of strength of contacts gap can be explained only

by rather long process of cooling of liquid melt on base spot from surface of which steams of metal of contacts continue to arrive.

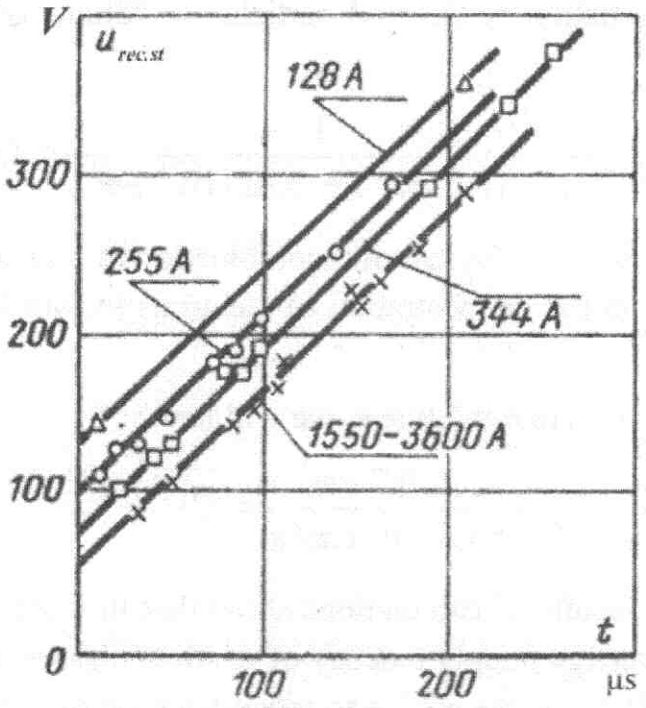

Fig. A.2. [7] Growth of recovering strength at high currents (free arc)

Recovery rate of electric strength of contacts gap after arc extinction at current transition through a zero or exit of arc from contacts on arc horns is an important parameter characterising a material of contacts. However in the published literature there are rather poor data about influence of contacts materials on recovery rate of electric strength of contacts gap.

Heat- and electrophysical properties of contacts metals influence on recovery rate of electric strength of arc gap essentialy. Various combinations of components in ceramic-metal contacts influence on recovering electric strength of arc gap differently. In fig. A.3 dependences of electric strength on values of current intensity for various contacts [7] are given.

Combination of ability of contacts metal to transmit heat well, low temperature of its boiling and susceptibility of ionisation with a smaller consumption of energy of their steams leads to higher electric strength of arc gap between contacts after arc extinction. Therefore in a gap between contacts from *Ag* electric strength is the highest and from *AgC* - the lowest.

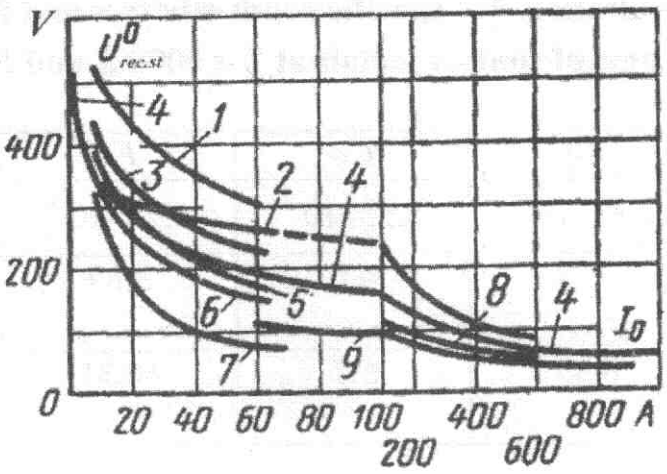

Fig. A.3 [7] Initial strength as function of current for different contact materials. 1 – silver; 2 – brass; 3 – *Ag* – *Ni*(40%); 4 – copper; 5 – Ag – *W*(50%); 6 – *Ag* – *CdO*(15%); 7 – *Ag* – C(3%); 8 – aluminium; 9 – iron

It would seem, low voltage of ionization (table 3) should facilitate arc ignition between contacts. But decreasing of ionisation voltage and temperature of boiling of contacts metal reduces a temperature on base spot of arc and plasma in its channel. Decreasing of temperature of plasma in arc channel, in turn, reduces degree of its ionization and electric conductivity.

Table 3. Heat- and electrophysical properties of metals

Parameter	*Ag*	*Cu*	*Ni*	*W*	*Fe*	*Zn*	*Cd*	*Sn*	*C*	*Cs*
T_{melt}, *K*	1285	1357	1728	3863	1808	692	594	505	3650	301,5
T_{boil}, *K*	2485	2840	3003	5933	3023	1179	1038	2543	Eva-po-ration	978
λ, $\frac{W}{cm \cdot K}$	4,18	3,8	0,7	1,9	0,6	1,1	0,9	0,64	0,15-1,6	0,18
U_i, *V*	7,54	7,72	7,63	7,98	7,83	9,39	8,99	7,33	11,22	3,87

For example in table 4 their values are given at $T = 5000$ *K* and pressure $P = 1$ *atm*.

Table 4. Degree of ionisation x_e, specific conductivity σ and factor volume recombination β of steams of contact metals at $T = 5000\ K$ and $P = 1\ atm$

Parameter	*Ag*	*Cu*	*Fe*	*Cs*
x_e	$3{,}84 \cdot 10^{-3}$	$5{,}53 \cdot 10^{-3}$	$4{,}25 \cdot 10^{-3}$	$2{,}61 \cdot 10^{-1}$
σ, $(Ohm \cdot cm)^{-1}$	1,79	4,0	3,89	5,65
β, 10^{-10}, cm^3/s	6,39	5,7	10,31	345,4

Inclusion of additives to *Ag* with low values of temperature of boiling and voltage of ionisation, and also with high values of factors of heat conductivity and volume recombination promotes to increase recovering electric strength of arc gap between contacts after arc extinction. Additives with higher values of ionisation voltage and temperature of boiling, than at *Ag*, especially graphite, reduce electric strength of contact gap. The same materials have values of factor of heat conductivity lower than value of silver.

As a rule, one component of composite contacts possesses increased refractoriness and mechanical durability, and another - high electric conductivity. Components should not give among themselves solid solutions and chemical compounds. As refractory components there are applied pure metals and their chemical compounds: oxides, carbides and nonmetals: graphite, boron.

Pure *Cs* possesses low potential of ionisation and its compounds essentially decrease a temperature on arc base spot and plasma in its channel even with small amounts. Lanthanides and other elements, having low electronic work function, lead to diffuse expansion of base spot and dispersal of thermal load on a surface of contacts [4].

Under influence of arc additives of oxides of metals and fluoric compounds (CdF_2, AlF_3) to Ag generate fluorine and oxygen which are capable to capture electrons and to generate negative ions. Heavy negative ions decrease electric conductivity of plasma [4].

Oxides *CdO* and Ta_2O_5 have an impact on wear resistance of contacts favorably because of under influence of arc they decay with absorption of a considerable quantity of energy: $(2 \div 4) \cdot 10^3\ W/g$ [4].

A.4 Route selection for creation of new contacts

Long immovability of arc on opening contacts (average time of immovability of arc at switching-off of short-circuit current, established experimentally, is equal to 5,45 *ms*) leads to their considerable erosion [3, part II].

Decreasing of recovery rate of electric strength of intercontact gap leads to repeated ignitions of arc not only at free transition of a current through a zero, but also at its exit on arc horns and input in arc chute. Repeated ignitions of arc delay time of its extinction and thus increase thermal and mechanical damages in a place of occurrence of short-circuit and electric wear of circuit breaker [3, part. II].

Decreasing of electric resistance of isolation of circuit breaker causes necessity of carrying out of off-schedule preventive repair.

Proceeding from the above-stated it is expedient to search of new compositions of components of contacts with the aim of:

- reductions of immovability time of arc on opening contacts at switching-off of small critical and rated currents and short-circuit currents;
- replacement of graphite in composite contacts.

On immovability time of arc on opening contacts essential influence renders its inertial properties caused by relatively big mass of steams of contacts metal and their viscosity in channel of short constricted arc being in motionless position [3, part. II].

Mass of metal steams in arc channel consists of a sum of mass of atoms and ions of the elements which are a part of steams of contacts and their density, depending on temperature and pressure of plasma in its channel.

Also obviously immovability time of arc is influenced by ability of base spot enough quickly to move on a surface of contacts. It is known that on oxidised surface of electrode a base spot moves with greater speed than on cleared homogeneous metal [8]. Moving of base spot of arc on a surface of ceramic-metal contacts is essentially complicated because of a difference of temperatures of fusion and boiling of the components composing contact [9].

Also it is necessary to pay attention to energy of a superficial tension of separate components of contact under action of which the superficial relief of liquid melt on contact can be very non-uniform.

If for a base composition of contacts to accept AgNi, average time of arc immovability is equal to 5,45 *ms* at velocity of contacts opening 2,0 *m/s* then additive to them should have mass of atom m_o much less than mass of atoms Ag and Ni [3, part I]:

$$m_0^{Ag} = 179{,}1 \cdot 10^{-24}\, g; m_0^{Ni} = 97{,}5 \cdot 10^{-24}\, g.$$

From analysis of the table of periodic system of elements of D.Mendeleyev follows that to one of the first applicants as an additive to composite contacts AgNi can serve Li with nuclear mass $m_\mu = 6{,}94$, and its compounds.

Mass of atom Li is equal:

$$m_0^{Li} = m_\mu \cdot 1{,}66 \cdot 10^{-24}\, g = 6{,}94 \cdot 1{,}66 \cdot 10^{-24}\, g = 11{,}52 \cdot 10^{-24}\, g.$$

That is mass of atom Li is more than 10 times less than mass of atom Ag which composes 70 % of ceramic-metal contacts, as a rule.

However the temperature of fusion Li is equal $180{,}5^0\, C$ only. At disconnection of contacts it can lead to its fast smelting. Therefore it is expedient to use compaund Li - LiF to argentiferous contacts as an additive. Mass of molecule LiF is equal $m_0 = 43{,}06 \cdot 10^{-24}\, g$ under normal conditions and is commensurable with average mass of a molecule of air which is equal $m_{0.air} = 48{,}09 \cdot 10^{-24}\, g$.

At plasma temperature in arc channel equal, for example, 8000 K mass of a molecule of air will be equal to:

$$m_{0.air} = m_\mu \cdot 1{,}66 \cdot 10^{-24}\, g = 15{,}394 \cdot 1{,}66 \cdot 10^{-24}\, g = 25{,}55 \cdot 10^{-24}\, g.$$

Molecules LiF at temperature 8000 K will be subjected by dissotiation, and their atoms – by ionization. Therefore, depending on percentage LiF by mass of content of composite contacts AgNi, mass of plasma in arc channel will be much less than if plasma consists only of atoms and ions of Ag and Ni. Thus, the response rate of plasma in channel of short constricted arc on opening contacts will be essentially lowered and it can get mobility.

Electronic work function φ at Li is less almost twice than one at Ag and Ni. Therefore a arc base spot can faster extend and power density q W/cm^2, coming on its surface, will be essentially decreased [4]. It, in turn, will lead to decreasing of erosion of contacts [4]. It is established that at $q \geq 10^5$ W/cm^2 on a base spot at switching-off of short-circuit currents the cones of erosion are formed which lead to considerable erosion of contacts. At $q < 10^5$ W/cm^2 erosion cones can not be formed and it will lead to decreasing of contacts erosion [3, part II].

Atoms of fluorine, generated at dissociation of molecules LiF, possess ability to attract electrons and form negative ions. Affinity of electrons with atoms of fluorine is estimated 3,62 eV. Rather heavy negative ions F can considerably decrease electric conductivity of residual plasma in arc channel after its extinction at no-current condi-

tion at free transition of current through a zero [4], or in intercontact gap at exit of arc from contacts on arc horns, or at its input in arc chute. Considerable decreasing of electric conductivity of residual plasma can lead to enough fast deionization of arc gap and prevent repeated ignition of arc.

In the published works there is data which point to fast diffuse expansion of base spot of arc and decreasing of its voltage at inclusion of additives Cs and La into contacts [4]. That and another reduce power density q W/cm^2 on a basic stain and thereby reduce electric erosion of contacts at currents switching-off. However masses of atoms Cs and La surpass masses of atoms Ag and Ni considerably.

$$m_0^{Cs} = 220{,}6 \cdot 10^{-24}\, g \text{ and } m_0^{La} = 230{,}6 \cdot 10^{-24}\, g.$$

Hence, application of Cs and La as additives to ceramic-metal contacts can increase a response rate of plasma steams in arc channel and its delay time on opening contacts. Taking into consideration that arc on opening contacts gets mobility under a condition $l_{arc} / r_{bs} > 1$ (l_{arc} - length of arc, r_{bs} - radius of base spot) than at application of Cs and La optimum result can not succeed for decreasing of contact erosion.

The most intensive process of erosion of contacts occurs at initial stage of their opening which proceeds ~ 1,0 *ms*. Therefore, in order to essentially reduce erosion of contacts, it is necessary to reduce delay time of arc on opening contacts from average time equal 5,45 *ms* to 0,15 ÷ 0,2 *ms*. For decreasing of immovability time of arc to the specified value it will be insufficiently to reduce only the response rate of plasma in arc channel. As well as arc mobility occurs at condition $l_{arc} / r_{bs} > 1$ it is necessary to increase velocity of contacts opening from 2,0 *m/s* to 6,5 ÷ 8,0 *m/s*. At such velocity of contacts opening an increasing of contact gap l_{arc} will advance growth of radius of base spot of arc r_{bs} [3].

Replacement of graphite, which is a part of ceramic-metal contacts AgNC, causes great difficulties.

Graphite is entered into ceramic-metal contacts for prevention of welding of contacts at flowing of short-circuit currents through them. Strictly speaking, their welding occurs always at flowing of short-circuit currents. But thanks to a structure of crystal lattice of graphite a welding place breaks down at contacts opening enough easily. Therefore for searching of substances which could replace graphite, it is necessary to search among those substances which would have properties of crystal lattices approached to properties of crystal lattices of graphite. At that electric conductivity and heat conductivity will be preferably more than graphite`s ones. It would be desirable that ionisation potential of new substance will be lower than graphite`s one as well as it would reduce plasma temperature in arc channel a little.

It is preferable to consider boron B having mass of atom equal:

$$m_0^B = \mu \cdot 1{,}66 \cdot 10^{-24}\, g = 10{,}81 \cdot 1{,}66 \cdot 10^{-24}\, g = 17{,}95 \cdot 10^{-24}\, g,$$

which is less whole degree than at Ag and Ni and it is slightly less than at graphite:

$$m_0^C = \mu \cdot 1{,}66 \cdot 10^{-24}\, g = 12{,}001 \cdot 1{,}66 \cdot 10^{-24}\, g = 19{,}94 \cdot 10^{-24}\, g.$$

Application of boron as a part of contacts with composition AgNi would not lead to increasing of delay time of arc on opening contacts.

However boron is a substance with semi-conductor properties and, hence, with difficult dependences of its parametres on temperature.

Boron can be in a crystal and amorphous kind. The pure crystal boron represents a substance of grayish-black colour with density $2{,}34\ g/cm^3$, $t^\circ_{melt} = 2300^\circ$, $t^\circ_{boil} = 2550^\circ$. Atomic heat capacity 3,3 *cal/g – atom, degree* (from 0° to 100°). Heat of sublimation 95 *kcal/g – atom* (at 25°). Ionization voltage of boron 8,3 *V*, which is less than graphite`s one (11,22 *V*).

Amorphous boron has structure of the fine-grained powder with density $\sim 1{,}73\ \ g/cm^3$.

Pure boron carries electric current very badly [11].

In [12] results of experimental researches of electric conductivity of boron depending on its temperature (see fig. A.4) are given.

Taking into account very low electric conductivity and very high hardness of boron its application in the pure state in contacts is not obviously possible.

Boron is a part of some chemical compounds. Nitride *BN* attracts attention - the white powder with crystal structure corresponding to graphite type. But it possesses high insulating properties.

Compounds of boron with metals (borides) can compose a number of various structures: Me_4B, Me_3B, Me_2B, Me_3B_2, MeB, Me_3B_4, MeB_2, Me_2B_5, MeB_4 and MeB_6. At surplus of atoms of metal in a lattice the atoms of boron are usually isolated from each other. If on the contrary atoms of boron form chains, grids, skeletons.

In table 5 some parametres of the pure metals applied in contacts and their borides are given.

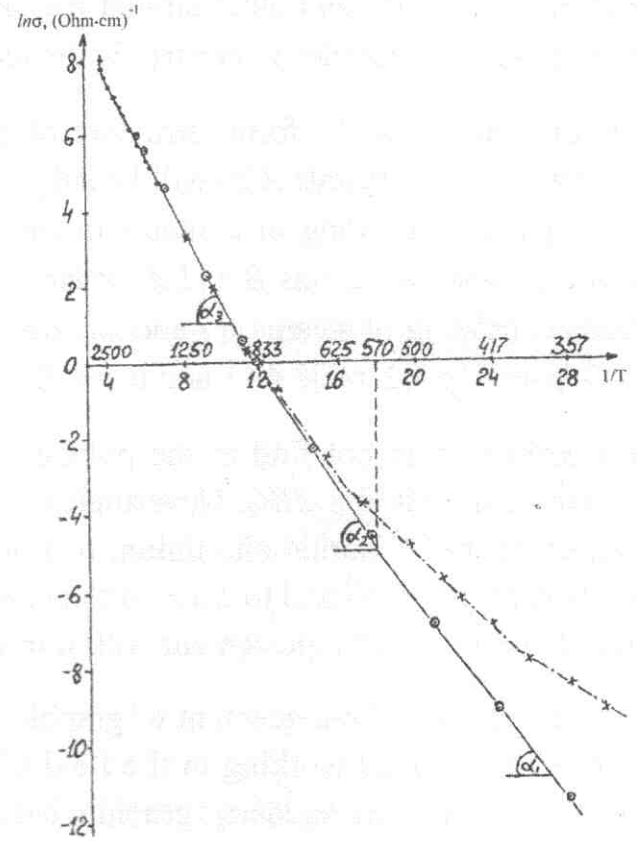

Fig. A4. Dependence diagram $\sigma(T)$, where o – crystal boron [13], x – amorphous boron [13], measured data [12]

Table 5. Parametres of pure metals and their borides

For-mula	Mass of atom, m_o, 10^{-24} g	Den-sity ρ, g/cm^3	Electrical resistivity 10^{-6} *Ohm·cm*	Boiling tem-perature, *K*	heat con-ductivity, *W/(cm·K)*	Heating capac-ity, *kJ/(kg·K)*
B	17,95	2,34	п/п	2573	0,015	11,09 = C_p, *J/(mole·K)*
W	305,1	19,3	5,5	3670	1,9	0,134
W_2B_5	-	11	21	2573	0,318	
Mo	159,3	10	5,8	2900	1,4	0,264
Mo_2B_5	410	8,6	25	2373	0,268	0,3
Al	44,8	2,7	2,9	873	2,1	
AlB_2	80,68 (molecule)	3,19	2,35	1928		
C	19,94	1,8	700	3973	1,14	0,71

Compounds of boron with *W*, *Mo* and other similar metals form refractory materials. Some of them are applied as cathodes in electronic devices.

Compounds of boron with *Al* (AlB_2) forms structure of a crystal lattice in the form of a grid. The scaly structure of crystals AlB_2 will be subjected, from our point of view, to easier break of a place of welding of contacts in case of flowing of short-circuit currents through them. Besides, steams *B* and *Al* in arc channel will reduce the response rate of its plasma consisting of steams *Ag* and *Ni*, and, thereby, will provide its mobility on contacts [3, part II, p. 62, table 4.11 and p. 63, fig. 4.29].

Unfortunately, the author could not find in the published works a number of physical properties of diboride aluminium AlB_2. Nevertheless, it is represented to us that it is expedient to enter crushed diboride aluminium to fine-grained structure of small doses into composite contacts *AgNi* and to carry out necessary research tests for the purpose of definition of possibility of replacement with it in graphite contacts.

Certainly, considered example of replacement of graphite in contacts is one of variants. The author invokes the experts working in the field of creation of contacts, to strengthen searches of the components replacing graphite because its application in contacts **is extremely undesirable.**

Conclusions to Addendam

At a choice of contact materials for automatic circuit breakers it is necessary to consider heat- and electrophysical properties of the components entering into composite contacts and their steams.

1. ρ – specific resistance, H_B – Brinnel hardness, heat conduction coefficient λ_0 of contact materials, contact force P_{cont} and maximal instantaneous current (i_{in}) influence values of transitive resistance R_{cont} and transient voltage u_{cont}.

2. Transient voltage u_{cont}, at which argentiferous contacts are welded under thermal influence of flowing current, is equal $u_{cont} = 0{,}41$ *V*.

3. Electrodynamic forces, arising in closed contacts in area of current constriction, can lead to rebound of contacts and or to their welding, or to their burning out.

4. Mechanism of contacts erosion at switching-off of short-circuit currents represents superficial bubble boiling accompanied by explosive processes on arc base spots which lead to formation of erosion cones. Sum of elementary masses of func-

tioning erosion cones on base spots of short constricted arc, which are in motionless position on contacts, composes total mass of their erosion.

5. Heat- and electrophysical properties of contact metals and their steams influence recovering electric strength of arc gap essentially. At contacts metal the more high factor of heat conductivity λ, factor of volume recombination β are and the more low a temperature of boiling T_{boil} and potential of ionisation U_i are the faster electric strength of arc gap recovers.

6. Inclusion of ≈ 5 % Cs in contacts reduce voltage on arc by ≈ 25 % and it leads to decreasing of power density on base spot and to reduction of erosion of contacts accordingly.

7. Lanthanides and other elements, having low electronic work function, lead to fast diffuse expansion of base spot and dispersal of thermal load on a surface of contacts and to reduction of contacts erosion.

8. Oxides CdO and Ta_2O_5 lead to decreasing of contacts erosion as well as under influence of arc they decay with absorption of a considerable quantity of energy.

9. Under influence of arc additives of fluoric compounds CdF_2 or AlF_3 to Ag generate fluorine which is capable to capture electrons to generate negative ions. Heavy negative ions decrease electric conductivity of plasma.

10. As may be supposed graphite in composite contacts can be replaced by diboride aluminium AlB_2.

Reference index to Addendam

1. *Merl Vilgelm.* Electrical contacts. // GEN. – M., L., 1962 [rus].

2. *Holm P.* Electrical contacts. – M.: И.Л., 1961.

3. *Mestcheryakov V.P.* Electric arc of high power in circuit breakers. – Ulyanovsk; part I, 2006; part II, 2008 [rus].

4. *Namitokov K.K.* Electroerosion phenomena. – M.: Energy, 1978 [rus].

5. *Butkevich G.V.* Arc processes at commutation of electric circuits. – M.: Vysshaya schkola, 1967 [rus].

6. *Namitokov K.K., Pakhonov P.L., Kharin S.N.* Mathematic simulation of processes in gas-discharge plasma. – Alma-Ata: Science, 1988 [rus].

7. *Taev I.S.* Elecrical contacts and arc quenching devices of low-voltage devices. – M.: Energy, 1973 [rus].

8. *Mitskevich M.K., Bushkin A.I., Bakuto I.A., Shikhov V.A., Devoino I.G..* Electroerosion machining of metals. – Minsk: Science and technics, 1988 [rus].

9. *Bron O.B., Sushkov L.K.* Plasma fluxes in electric arc of sitching devices. – L.: Energy, 1975 [rus].

10. *Radtsit A.A., Smirnov B.M.* Reference book about atom and molecular physics. – M.: Atomizdat, 1980.

11. Brief chemical encyclopedia. Vol. 1 // GNI «Sovetskaya encyclopedia». – M., 1961 [rus].

12. Optical and electrical properties of boron at firing temperatures. / *L.A. Koval, A.V. Florka* // The Mechnikov Odesski national University [rus].

13. *Berezin A.A., Golikov O.A., Zaitsev V.K.* Electrical properties of betarhombohedral boron and amorphous boron. – M.: Mir, 1988 [rus].

14. Physical quantities: reference book / *Edited by I.S. Grigorieva, E.Z. Meilikhova* – M.: Energoatomizdat, 1991 [rus].

15. *Polezhaev Y.V., Yurevich F.B..* Thermal protection. – M.: Energy, 1976 [rus].

16. Physical encyclopedic dictionary // GNI «Sovetskaya encyclopedia». – M., 1960 – 1966 [rus].

17. *Samsonov G.V., Serebryakova T.N., Neronov V.A.* Borides. – M., 1975 [rus].

18. Silicides, borides, intermaterialides and other refractory compounds. *J. H. Westibrook.* Researches at high temperatures. – M.: I.L., 1962 [rus].

19. Catalogue. Production of metal nanopowders. Advanced Powder Technologies LLC. APT. – Tomsk, 2008 [rus].

20. On the electronic and structural properties of aluminum diboride $Al_{0.9}B_2$. *Ulrich Burkhard, Vladimir Gurin, Frank Haarman, Horst Borrmann, Walter Schnelle, Alexander Yaresko and Yuri Grin.* Available online 27 October 2003.

Scientific publication

MESTCHERYAKOV Valentin Petrovich

EXPLOSIVE EROSION OF HIGH-CURRENT CONTACTS AND ELECRODES

Typesetting and composition – S.A. Akachev
E-mail: stanislav.akachev@gmail.com

Passed for printing 24.04.2012. Format 60x84/8.
Printer's sheet 22,32. Number of copies 25 pcs. Order 463 .

Printing office USTU. 432027, Ulyanovsk, Sev. Venets Str., 32.

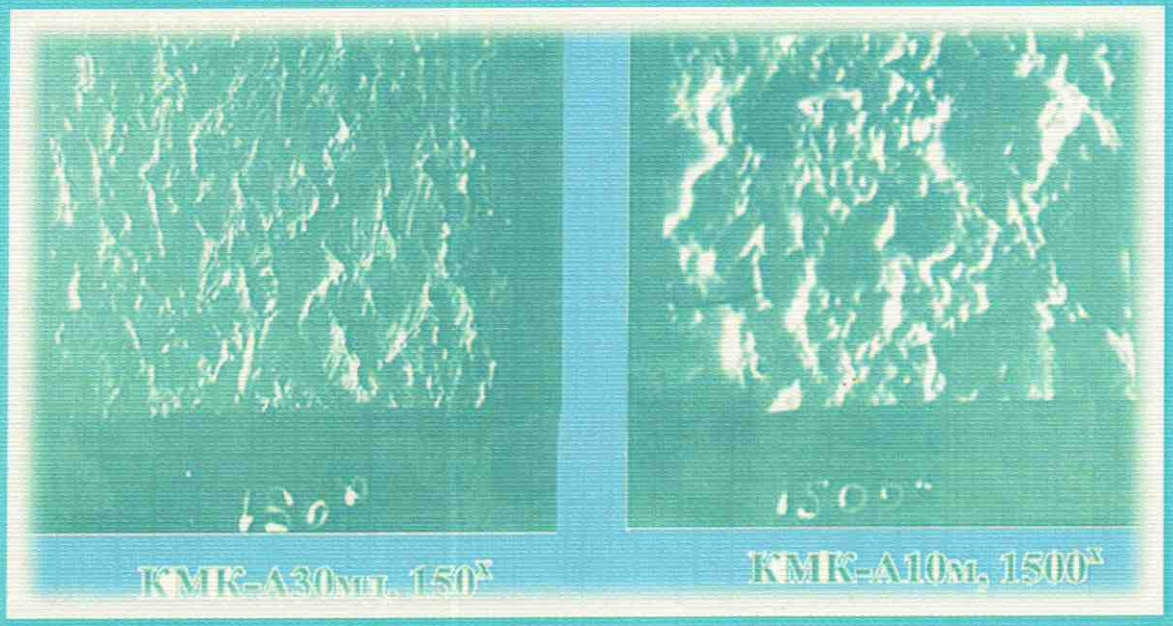

КМК-А30мц, 150^{x} КМК-А10м, 1500^{x}